

# **Report No. 6**

## **The ECHAM3 Atmospheric General Circulation Model**

Edited by:  
Deutsches Klimarechenzentrum,  
Modellbetreuungsgruppe,  
Hamburg, September 1993  
**Revision 2**



# Contents

|  |           |
|--|-----------|
| <b>1. SUMMARY PAGE</b>   | <b>1</b>  |
| 1.1 SHORT DESCRIPTION AND MAIN AUTHORS   | 1         |
| 1.1.1 Numerical solution   | 1         |
| 1.1.2 Surface boundary conditions.   | 1         |
| 1.1.3 Physical parameterization  | 2         |
| 1.2 ACKNOWLEDGEMENTS.  | 4         |
| <b>2. MODEL DYNAMICS</b>   | <b>5</b>  |
| 2.1 INTRODUCTION   | 5         |
| 2.2 THE CONTINUOUS EQUATIONS   | 6         |
| 2.3 HORIZONTAL DISCRETIZATION  | 9         |
| 2.3.1 Spectral representation  | 9         |
| 2.3.2 Spectral /grid-point transforms, and the evaluation of spectral tendencies | 13        |
| 2.4 VERTICAL DISCRETIZATION  | 16        |
| 2.4.1 The hybrid vertical representation.  | 16        |
| 2.4.2 The vertical finite-difference scheme                                      | 19        |
| 2.5 TIME INTEGRATION SCHEME  | 23        |
| 2.6 HORIZONTAL DIFFUSION   | 29        |
| 2.6.1 Basic scheme.  | 29        |
| <b>3. MODEL PHYSICS</b>  | <b>33</b> |
| 3.1 INTRODUCTION   | 33        |
| 3.2 RADIATION  | 36        |
| 3.2.1 Radiative heating  | 36        |
| 3.2.2 The radiative transfer model   | 36        |
| 3.2.3 Input to the radiation scheme  | 40        |
| 3.3 VERTICAL DIFFUSION   | 43        |
| 3.3.1 Basic equations  | 43        |
| 3.3.2 Surface fluxes   | 45        |
| 3.3.3 Definition of the drag coefficients  | 48        |

|           |   |           |
|-----------|---|-----------|
| 3.3.4     | Definition of the exchange coefficients . . . . .     | 52        |
| 3.3.5     | Moisture and cloud effects . . . . .                  | 53        |
| 3.3.6     | Definition of the top of the boundary layer . . . . . | 54        |
| 3.3.7     | Roughness length . . . . .                            | 54        |
| 3.3.8     | Vegetation . . . . .                                  | 55        |
| 3.3.9     | Kinetic energy dissipation. . . . .                   | 55        |
| 3.3.10    | Vertical diffusion at higher levels . . . . .         | 55        |
| 3.4       | GRAVITY WAVE DRAG . . . . .                           | 56        |
| 3.4.1     | Theory . . . . .                                      | 56        |
| 3.4.2     | The formulation of the scheme . . . . .               | 56        |
| 3.5       | CUMULUS CONVECTION . . . . .                          | 59        |
| 3.5.1     | Large-scale budget equations . . . . .                | 59        |
| 3.5.2     | Cloud model equations . . . . .                       | 60        |
| 3.5.3     | Discretization of the model equations . . . . .       | 66        |
| 3.5.4     | Melting of snow . . . . .                             | 67        |
| 3.5.5     | Evaporation of rain . . . . .                         | 67        |
| 3.5.6     | Stratocumulus . . . . .                               | 68        |
| 3.6       | STRATIFORM CLOUDS . . . . .                           | 70        |
| 3.6.1     | Sub-grid scale cloud formation. . . . .               | 70        |
| 3.6.2     | Condensation and evaporation . . . . .                | 71        |
| 3.6.3     | Precipitation formation . . . . .                     | 72        |
| 3.6.4     | Evaporation of precipitation . . . . .                | 74        |
| 3.6.5     | Melting of snow . . . . .                             | 74        |
| 3.7       | SOIL PROCESSES . . . . .                              | 75        |
| 3.7.1     | General . . . . .                                     | 75        |
| 3.7.2     | Soil temperature . . . . .                            | 76        |
| 3.7.3     | Snow pack temperature. . . . .                        | 77        |
| 3.7.4     | Snow melt . . . . .                                   | 78        |
| 3.7.5     | Sea-ice temperature . . . . .                         | 78        |
| 3.7.6     | Soil hydrology . . . . .                              | 79        |
| <b>4.</b> | <b>SYSTEM DESCRIPTION . . . . .</b>                   | <b>83</b> |
| 4.1       | OVERVIEW AND THE CONTROL ROUTINES. . . . .            | 83        |
| 4.2       | FLOW DIAGRAM . . . . .                                | 85        |

|                   |   |            |
|-------------------|---|------------|
| 4.3               | COMPUTER CODE ORGANIZATION . . . . .                              | 92         |
| 4.3.1             | The two scans . . . . .   | 92         |
| 4.3.2             | Dynamic subroutines. . . . .                                      | 93         |
| 4.4               | SUBROUTINES IN ALPHABETICAL ORDER . . . . .                       | 97         |
| 4.5               | TECHNICAL DETAILS . . . . .                                       | 103        |
| 4.5.1             | Internal data flow of the model . . . . .                         | 103        |
| 4.5.2             | Connection between buffers, work- and history-files . . . . .     | 105        |
| <b>5.</b>         | <b>USER'S MANUAL . . . . .</b>                                    | <b>107</b> |
| 5.1               | MODIFICATION OF THE SOURCE CODE. . . . .                          | 107        |
| 5.1.1             | General . . . . .   | 107        |
| 5.1.2             | Modification tree . . . . .                                       | 107        |
| 5.1.3             | Location of libraries . . . . .                                   | 108        |
| 5.1.4             | Example script for model modification. . . . .                    | 109        |
| 5.2               | I/O . . . . .   | 110        |
| 5.2.1             | Diagnostic output . . . . .                                       | 110        |
| 5.2.2             | Newstart . . . . .  | 110        |
| 5.2.3             | Rerun . . . . .   | 111        |
| 5.2.4             | Input of sea surface temperature . . . . .                        | 111        |
| 5.2.5             | Files used for a model run. . . . .                               | 112        |
| 5.2.6             | Location of initial files . . . . .                               | 113        |
| 5.3               | RUNNING THE MODEL . . . . .                                       | 114        |
| 5.3.1             | Example script for running the T21-model (Bourne shell) . . . . . | 114        |
| 5.3.2             | Selectable model parameters. . . . .                              | 117        |
| 5.3.3             | Output examples . . . . .   | 119        |
| 5.4               | STRUCTURE OF DATASETS . . . . .                                   | 120        |
| <b>6.</b>         | <b>REFERENCES . . . . .</b>                                       | <b>123</b> |
| <b>Appendix A</b> | <b>THE UNPARAMETRIZED EQUATIONS . . . . .</b>                     | <b>133</b> |
| A.1               | INTRODUCTION . . . . .  | 133        |
| A.2               | THE ADVECTIVE FORM OF THE UNPARAMETRIZED EQUATIONS . . . . .      | 134        |
| A.2.1             | The material derivative. . . . .                                  | 134        |
| A.2.2             | The equation of state . . . . .                                   | 134        |
| A.2.3             | Mass conservation . . . . .                                       | 135        |
| A.2.4             | The velocity equation . . . . .                                   | 135        |

|   |            |
|---|------------|
| A.2.5 The thermodynamic equation . . . . .                            | 136        |
| A.3 THE FLUX FORMS OF THE EQUATIONS . . . . .                         | 137        |
| A.4 THE INTRODUCTION OF DIFFUSIVE FLUXES . . . . .                    | 138        |
| A.5 APPROXIMATIONS AND DEFINITIONS . . . . .                          | 139        |
| A.6 RETURN TO THE ADVECTIVE FORM. . . . .                             | 140        |
| A.7 THE MODEL EQUATIONS . . . . .                                     | 140        |
| <b>Appendix B LISTS OF CONSTANTS AND SYMBOLS. . . . .</b>             | <b>143</b> |
| <b>Appendix C GAUSSIAN LATITUDES FOR ECHAM3-TRUNCATIONS . . . . .</b> | <b>147</b> |
| C.1 THE "GAUSSIAN" LATITUDES FOR T21-TRUNCATION . . . . .             | 147        |
| C.2 THE "GAUSSIAN" LATITUDES FOR T42-TRUNCATION . . . . .             | 148        |
| C.3 THE "GAUSSIAN" LATITUDES FOR T63-TRUNCATION . . . . .             | 149        |
| C.4 THE "GAUSSIAN" LATITUDES FOR T106-TRUNCATION . . . . .            | 150        |
| <b>Appendix D LAND-SEA MASKS FOR ECHAM3-TRUNCATIONS . . . . .</b>     | <b>153</b> |
| <b>Appendix E PROGRAMMING CONVENTIONS . . . . .</b>                   | <b>157</b> |
| E.1 INTRODUCTION . . . . .  | 157        |
| E.2 PROGRAM STRUCTURE. . . . .  | 157        |
| E.2.1 Subtasks . . . . .  | 157        |
| E.2.2 Utility routines . . . . .                                      | 157        |
| E.3 SUBROUTINE STRUCTURE . . . . .                                    | 159        |
| E.4 COMMON BLOCK STRUCTURE . . . . .                                  | 160        |
| E.5 FORMAT STATEMENTS . . . . .                                       | 160        |
| E.6 BLOCK STRUCTURE . . . . .   | 161        |
| E.7 VARIABLE NAMES . . . . .  | 162        |
| E.8 MEMORY MANAGEMENT. . . . .  | 163        |
| E.8.1 General . . . . .   | 163        |
| E.8.2 Method of use . . . . .   | 163        |
| E.8.3 Example . . . . .   | 163        |
| E.8.4 Managed arrays. . . . .   | 166        |
| <b>Appendix F ECHAM3 CODE-LIST OF VARIABLES . . . . .</b>             | <b>179</b> |

## 1. SUMMARY PAGE

### 1.1 SHORT DESCRIPTION AND MAIN AUTHORS

The ECHAM model has been developed from the ECMWF model (cycle 31, November 1988). It contains several changes, mostly in the parameterization, in order to adjust the model for climate simulations.

The reference resolution is T42, but the model is set up to use resolutions in the range T21 to T106. Long term integrations have so far only been done for T21, T42 and T63. The lay-out is as follows

(⊕ indicates changes from the original ECMWF model):

#### 1.1.1 Numerical solution

- prognostic variables:
  - vorticity, divergence, temperature,
  - log surface pressure, water vapour,
  - ⊕ cloud water
- horizontal representation:
  - spectral transform, triangular truncation (T21/T42/T63/T106)
- vertical representation:
  - hybrid coordinate system, second order finite differences, 19 layers
- time integration:
  - semi-implicit; leap frog with time filter,
  - ⊕  $\Delta t = 40$  min (T21),  $\Delta t = 24$  min (T42),  $\Delta t = 15$  min (T63),  $\Delta t = 12$  min (T106)

#### 1.1.2 Surface boundary conditions

- SST and sea-ice:
  - blended data set (Reynolds, 1988) and Alexander and Mobley (1976) (ECHAM1,ECHAM2)
  - COLA/CAC AMIP SST and Sea-Ice Dataset (ECHAM3)
- orography:
  - mean terrain heights computed from high resolution US Navy data set
  - land-sea mask: from US Navy data set
- roughness length
  - sea: Charnock formula, modified after Miller et al. (1992)
  - sea-ice: constant (0.01 m)
  - land: function of vegetation and orography (variance)
- vegetation:
  - fraction of grid area covered by vegetation based on
  - Wilson and Henderson - Sellers(1985) data

- albedo:
  - ⊕ sea: function of solar zenith angle
  - bare land: satellite data (Geleyn and Preuss (1983))
  - ⊕ sea ice: function of temperature (Robock, 1980)
  - ⊕ land ice: function of temperature (Robock, 1980; Kukla and Robinson, 1980)
  - ⊕ snow: function of temperature and fractional forest area (Robock, 1980; Matthews, 1983)

### 1.1.3 Physical parameterization

- ⊕ radiation (Hense et al., 1982; Rockel et al, 1991; Eickerling, 1989)
  - two-stream approximation
  - six spectral intervals in the terrestrial part
  - four spectral intervals in the solar part
  - gaseous absorbers: H<sub>2</sub>O, CO<sub>2</sub> and O<sub>3</sub> (CO<sub>2</sub> and O<sub>3</sub> prescribed)
  - aerosols: prescribed
  - clouds: computed cloud optical depth and cloud cover
  - emissivity: function of cloud water path (Stephens, 1978)
  - continuum absorption: included
  - cloud overlap: maximum for contiguous clouds layer and random otherwise
  - diurnal cycle: included
  - radiation time step: 2 hours
- ⊕ clouds (Sundquist, 1978; Roeckner and Schlese, 1985; Roeckner et al, 1991)
  - cloud water transport equation
  - subgrid-scale condensation and cloud formation with different thresholds for convective and stratiform clouds (Xu and Krueger, 1991)
  - temperature dependent partitioning of liquid/ice phase (Matveev, 1984)
  - rain formation by auto-conversion of cloud droplets (Sundquist, 1978)
  - sedimentation of ice crystals (Heymsfield, 1977)
  - evaporation of cloud water
  - evaporation of precipitation
- convection (Tiedtke, 1989)
  - mass flux scheme for deep, shallow and mid-level convection
  - clouds are represented by a bulk model and include updraft and downdraft mass fluxes
  - convective momentum transport is parameterized according to Schneider and Lindzen (1976)
  - Evaporation of rain is parameterized according to Kessler (1969)
  - stratocumulus convection is parameterized as a vertical diffusion process with enhanced eddy diffusion coefficients (Tiedtke et al., 1988)



- planetary boundary layer (Louis, 1979)
  - surface fluxes of momentum, heat, moisture and cloud water are calculated from Monin-Obukhov similarity theory with transfer coefficients depending on roughness length and Richardson number
  - above the surface layer: eddy diffusivity approach with coefficients depending on wind shear, thermal stability and mixing length
  - above the PBL: vertical diffusion only for unstable stratification
  - ⊕ cloud water
  - ⊕ “moist” Richardson number (Brinkop, 1991; 1992)
- ⊕ land-surface processes (Sellers et al., 1986; Blondin, 1989; Dümenil and Todini, 1992)
  - heat transfer: diffusion equation solved in a 5-layer model with zero heat flux at the bottom (10 m )
  - water budget equation for three reservoirs: soil moisture, interception reservoir (vegetation), snow
  - vegetation effects: stomatal control on evapotranspiration and interception of rain and snow
  - run-off scheme: based on catchment considerations including sub-grid scale variations of field capacity over inhomogeneous terrain
  - sea-ice temperature calculated from surface energy budget
- ⊕ horizontal diffusion (Laursen and Eliassen, 1989)
  - scale selective operator applied beyond a threshold wave number
- gravity wave drag (Palmer et al, 1986; Miller et al, 1989)
  - surface stress due to gravity waves, which are excited by stably stratified flow over irregular terrain is calculated from linear theory and dimensional considerations
  - orographic forcing prescribed as a directionally dependent sub-grid scale orographic variance computed from the high resolution US Navy data set
  - vertical structure of momentum flux induced by gravity waves calculated from a local wave Richardson number, which describes the onset of turbulence due to convective instability and the turbulent breakdown approaching a critical level
  - the GWD scheme is not used at T21 resolution

## 1.2 ACKNOWLEDGEMENTS

The ECHAM climate model has been developed from the ECMWF model (therefore the first part of its name: EC) and a comprehensive parametrisation package developed at Hamburg (therefore the abbreviation HAM). This documentation has been written in a similar fashion: A substantial part is based on the ECMWF documentation, which then had been modified to describe the newly implemented subroutines and the changes necessary for climate experiments.

## 2. MODEL DYNAMICS

### 2.1 INTRODUCTION

In this section the technical details of the adiabatic part of the ECHAM operational model are described. The first two sections describe the governing equations, the coordinates and the discretization schemes used in the operational ECHAM model. Attention is concentrated on the representation of the explicitly resolved adiabatic processes, but a derivation of the equations including terms requiring parametrization is included in Appendix A.

Detailed descriptions of the parametrizations themselves are given in section 3.

The ECHAM model is formulated in spherical harmonics. After the inter-model comparisons by Jarraud et al. (1981) and Girard and Jarraud (1982) truncated expansions in terms of spherical harmonics were adopted for the representation of dynamical fields. The transform technique developed by Elisassen et al. (1970), Orszag (1970) and Machenhauer and Rasmussen (1972) is used such that non-linear terms, including parameterizations, are evaluated at a set of almost regularly distributed grid points (Gaussian grid).

In the vertical, a flexible coordinate is used, enabling the model to use either the usual terrain-following sigma coordinate (Phillips, 1957), or a hybrid coordinate for which upper-level model surfaces “flatten” over steep terrain, becoming surfaces of constant pressure in the stratosphere (Simmons and Burridge, 1981, Simmons and Strüfing, 1981). Moist processes are treated in a consistent way in both the dynamical equations and parameterization schemes.

Section 2.2 presents the continuous form of the governing equations. Sections 2.3 and 2.4 give details of the spectral discretization and of the vertical coordinate and its associated vertical finite difference scheme. The temporal finite-difference scheme, which includes not only a conventional semi-implicit treatment of gravity-wave terms (Robert et al., 1972) but also a semi-implicit treatment of the advection of vorticity and moisture (Jarraud et al., 1982), is also described (section 2.5), as is the formulation chosen for horizontal diffusion (section 2.6).

## 2.2 THE CONTINUOUS EQUATIONS

Although the model has been programmed for one particular form of vertical coordinate, which is introduced in section 2.4, it is convenient to introduce the equations and their spectral discretization for a general pressure-based terrain-following vertical coordinate,  $\eta(p, p_S)$ . This must be a monotonic function of pressure,  $p$ , and depend also on surface pressure,  $p_S$ , in such a way that

$$\eta(0, p_S) = 0 \quad \text{and} \quad \eta(p_S, p_S) = 1$$

For such a coordinate, the continuous formulation of the primitive equations for a dry atmosphere may be directly derived from their basic height coordinate forms following Kasahara (1974).

During the design of the model, a detailed derivation of the corresponding equations for a moist atmosphere, including a separation into terms to be represented explicitly in the subsequent discretized form of the equations and terms to be parameterized, was carried out. It is shown in Appendix A that under certain approximations, the momentum, thermodynamic and moisture equations may be written:

$$\frac{\partial U}{\partial t} - (f + \xi) \cdot V + \dot{\eta} \frac{\partial U}{\partial \eta} + \frac{R_d T_v}{a} \frac{\partial}{\partial \lambda} \ln p + \frac{1}{a} \frac{\partial}{\partial \lambda} (\phi + E) = P_U + K_U \quad (2.2.1)$$

$$\frac{\partial V}{\partial t} + (f + \xi) \cdot U + \dot{\eta} \frac{\partial V}{\partial \eta} + \frac{R_d T_v}{a} (1 - \mu^2) \frac{\partial}{\partial \mu} \ln p + \frac{(1 - \mu^2)}{a} \frac{\partial}{\partial \mu} (\phi + E) = P_V + K_V \quad (2.2.2)$$

$$\frac{\partial T}{\partial t} + \frac{U}{a(1 - \mu^2)} \frac{\partial T}{\partial \lambda} + \frac{V}{a} \frac{\partial T}{\partial \mu} + \dot{\eta} \frac{\partial T}{\partial \eta} - \frac{\kappa T_v \omega}{(1 + (\delta - 1) q_v) p} = P_T + K_T \quad (2.2.3)$$

$$\frac{\partial q_v}{\partial t} + \frac{U}{a(1 - \mu^2)} \frac{\partial q_v}{\partial \lambda} + \frac{V}{a} \frac{\partial q_v}{\partial \mu} + \dot{\eta} \frac{\partial q_v}{\partial \eta} = P_{q_v} + K_{q_v} \quad (2.2.4)$$

$$\frac{\partial q_w}{\partial t} + \frac{U}{a(1 - \mu^2)} \frac{\partial q_w}{\partial \lambda} + \frac{V}{a} \frac{\partial q_w}{\partial \mu} + \dot{\eta} \frac{\partial q_w}{\partial \eta} = P_{q_w} + K_{q_w} \quad (2.2.5)$$

where  $q_v$  is the water vapour mixing ratio and  $q_w = q_l + q_i$  is the cloud water mixing ratio including the liquid  $q_l$  and the solid fraction  $q_i$ .

The continuity equation is

$$\frac{\partial}{\partial \eta} \left( \frac{\partial p}{\partial t} \right) + \nabla \cdot \left( y_h \frac{\partial p}{\partial \eta} \right) + \frac{\partial}{\partial \eta} \left( \dot{\eta} \frac{\partial p}{\partial \eta} \right) = 0 \quad (2.2.6)$$

and the hydrostatic equation takes the form

$$\frac{\partial \phi}{\partial \eta} = - \frac{R_d T_v}{p} \frac{\partial p}{\partial \eta} \quad (2.2.7)$$

The pressure coordinate vertical velocity is given by

$$\omega = y_h \nabla p - \int_0^\eta \nabla \cdot (y_h \frac{\partial p}{\partial \eta}) d\eta \quad (2.2.8)$$

and explicit expressions for the rate of change of surface pressure, and for  $\dot{\eta}$ , are obtained by integrating (2.2.6), using the boundary conditions  $\dot{\eta} = 0$  at  $\eta = 0$  and  $\eta = 1$ :

$$\frac{\partial p_S}{\partial t} = - \int_0^1 \nabla \cdot (y_h \frac{\partial p}{\partial \eta}) d\eta \quad (2.2.9)$$

and

$$\dot{\eta} \frac{\partial p}{\partial \eta} = - \frac{\partial p}{\partial t} - \int_0^\eta \nabla \cdot (y_h \frac{\partial p}{\partial \eta}) d\eta \quad (2.2.10)$$

(2.2.9) may also be written

$$\frac{\partial \ln p_S}{\partial t} = - \frac{1}{p_{S0}} \int_0^1 \nabla \cdot (y_h \frac{\partial p}{\partial \eta}) d\eta \quad (2.2.11)$$

Variables and constants are defined in Appendix B.2.

In the special case of sigma coordinates  $\eta = \sigma = p/p_S$ , the above equations are the same as those used in the first operational ECMWF model, apart from the factor  $(1 + (\delta - 1) \cdot q_v)$  in (2.2.3), which differs from unity by an amount of the same order as the difference between temperature and virtual temperature, and apart also from differences in the terms written symbolically on the right-hand sides of (2.2.1) - (2.2.5), which are those requiring parametrization. Following the derivation given in Appendix A, the terms  $P_U$ ,  $P_V$ ,  $P_T$ ,  $P_{q_v}$  and  $P_{q_w}$  are written:

$$P_U = -g \cos \theta \left( \frac{\partial p}{\partial \eta} \right)^{-1} \frac{\partial J_U}{\partial \eta} \quad (2.2.12)$$

$$P_V = -g \cos \theta \left( \frac{\partial p}{\partial \eta} \right)^{-1} \frac{\partial J_V}{\partial \eta} \quad (2.2.13)$$

$$P_T = \frac{1}{C_p} \left( Q_R + Q_L + Q_D - g \left( \frac{\partial p}{\partial \eta} \right)^{-1} \left[ \frac{\partial J_S}{\partial \eta} - C_{pd} T (\delta - 1) \frac{\partial J_{q_v}}{\partial \eta} \right] \right) \quad (2.2.14)$$

$$P_{q_v} = S_{q_v} - g \left( \frac{\partial p}{\partial \eta} \right)^{-1} \frac{\partial J_{q_v}}{\partial \eta} \quad (2.2.15)$$

$$P_{q_w} = S_{q_w} - g \left( \frac{\partial p}{\partial \eta} \right)^{-1} \frac{\partial J_{q_w}}{\partial \eta} \quad (2.2.16)$$

where

$$C_p = C_{pd} (1 + (\delta - 1) q_v)$$

In (2.2.12) - (2.2.16),  $J_U$ ,  $J_V$ ,  $J_S$ ,  $J_{q_v}$  and  $J_{q_w}$  represent net parametrized vertical fluxes of momen-

tum, dry static energy ( $C_p \cdot T + \phi$ ), moisture and cloud water. They include fluxes due to convection and boundary-layer turbulence.  $Q_R$ ,  $Q_L$  and  $Q_D$  represent heating due respectively to radiation, internal phase changes (including the evaporation of precipitation) and to internal dissipation of kinetic energy associated with the  $P_U$  and  $P_V$  terms.  $S_{q_v}$  and  $S_{q_w}$  denote the rates of change of  $q_v$  and  $q_w$  due to condensation, evaporation and precipitation formation. Details of the calculation of these terms are given in section 3.6.

The terms  $K_U$ ,  $K_V$ ,  $K_T$ ,  $K_{q_v}$  and  $K_{q_w}$  in (2.2.1) - (2.2.5) represent the influence of unresolved horizontal scales. Their treatment differs from that of the  $P_U$ ,  $P_V$ ,  $P_T$ ,  $P_{q_v}$  and  $P_{q_w}$  terms in that it does not involve a physical model of sub-grid scale processes, but rather a numerically convenient form of scale-selective diffusion of a magnitude determined empirically to ensure a realistic behaviour of resolved scales. These terms are specified in section 2.6.

In order to apply the spectral method, Eqs. (2.2.1) and (2.2.2) are written in vorticity and divergence form (Bourke, 1972). They become

$$\frac{\partial \xi}{\partial t} = \frac{1}{a(1-\mu^2)} \frac{\partial}{\partial \lambda} (F_V + P_V) - \frac{1}{a} \frac{\partial}{\partial \mu} (F_U + P_U) + K_\xi \quad (2.2.17)$$

$$\frac{\partial D}{\partial t} = \frac{1}{a(1-\mu^2)} \frac{\partial}{\partial \lambda} (F_U + P_U) + \frac{1}{a} \frac{\partial}{\partial \mu} (F_V + P_V) - \nabla^2 G + K_D \quad (2.2.18)$$

where

$$F_U = (f + \xi) V - \dot{\eta} \frac{\partial U}{\partial \eta} - \frac{R_d T_v}{a} \frac{\partial}{\partial \lambda} \ln p \quad (2.2.19)$$

$$F_V = - (f + \xi) U - \dot{\eta} \frac{\partial V}{\partial \eta} - \frac{R_d T_v}{a} (1 - \mu^2) \frac{\partial}{\partial \mu} \ln p \quad (2.2.20)$$

and

$$G = \phi + E \quad (2.2.21)$$

We also note that a streamfunction  $\psi$  and velocity potential  $\chi$  may be introduced such that

$$\left. \begin{aligned} U &= \frac{1}{a} \left[ - (1 - \mu^2) \frac{\partial \psi}{\partial \mu} + \frac{\partial \chi}{\partial \lambda} \right] \\ V &= \frac{1}{a} \left[ \frac{\partial \psi}{\partial \lambda} + (1 - \mu^2) \frac{\partial \chi}{\partial \mu} \right] \\ \xi &= \nabla^2 \psi \\ \text{and} \\ D &= \nabla^2 \chi \end{aligned} \right\} \quad (2.2.22)$$

## 2.3 HORIZONTAL DISCRETIZATION

### 2.3.1 Spectral representation

The basic prognostic variables of the model are  $\xi$ ,  $D$ ,  $T$ ,  $q_v$ ,  $q_w$  and  $\ln p_s$ . They, and the surface geopotential  $\phi_s$ , are represented in the horizontal by truncated series of spherical harmonics:

$$X(\lambda, \mu, \eta, t) = \sum_{m=-M}^M \sum_{n=m}^{N(M)} X_n^m(\eta, t) P_n^m(\mu) e^{im\lambda} \quad (2.3.1.1)$$

where  $X$  is any variable,  $m$  is the zonal wave number and  $n$  is the meridional index. The  $P_n^m(\mu)$  are the Associated Legendre Functions of the first kind, defined here by

$$P_n^m(\mu) = \sqrt{(2n+1) \frac{(n-m)!}{(n+m)!} \frac{1}{2^n n!}} (1-\mu^2)^{m/2} \frac{d^{(n+m)}}{d\mu^{(n+m)}} (\mu^2 - 1), \quad (m \geq 0) \quad (2.3.1.2)$$

and

$$P_n^{-m}(\mu) = P_n^m(\mu)$$

This definition is such that

$$\frac{1}{2} \int_{-1}^1 P_n^m(\mu) P_s^m(\mu) d\mu = \delta_{ns} \quad (2.3.1.3)$$

where  $\delta_{ns}$  is the Kronecker delta function.

The  $X_n^m$  are the complex-valued spectral coefficients of the field  $X$ , and they are given by

$$X_n^m(\eta, t) = \frac{1}{4\pi} \int_{-1}^1 \int_0^{2\pi} X(\lambda, \mu, \eta, t) P_n^m(\mu) e^{-im\lambda} d\lambda d\mu \quad (2.3.1.4)$$

Since  $X$  is real

$$X_n^{-m} = (X_n^m)^* \quad (2.3.1.5)$$

where  $( )^*$  denotes the complex conjugate. The model thus deals explicitly only with the  $X_n^m$  for  $m \geq 0$ .

The Fourier coefficients of  $X$ ,  $X_m(\mu, \eta, t)$  are defined by

$$X_m(\mu, \eta, t) = \frac{1}{2\pi} \int_0^{2\pi} X(\lambda, \mu, \eta, t) e^{-im\lambda} d\lambda \quad (2.3.1.6)$$

or using (2.3.1.1), by

$$X_m(\mu, \eta, t) = \sum_{n=m}^{N(m)} X_n^m(\eta, t) P_n^m(\mu) \quad (2.3.1.7)$$

with

$$X(\lambda, \mu, \eta, t) = \sum_{m=-M}^M X_m(\mu, \eta, t) e^{im\lambda} \quad (2.3.1.8)$$

Horizontal derivatives are given analytically by

$$\left(\frac{\partial X}{\partial \lambda}\right)_m = im X_m \quad (2.3.1.9)$$

and

$$\left(\frac{\partial X}{\partial \mu}\right)_m = \sum_{n=m}^{N(m)} X_n^m \frac{d}{d\mu} P_n^m \quad (2.3.1.10)$$

where the derivative of the Legendre Function is given by the recurrence relation:

$$(1 - \mu^2) \frac{d}{d\mu} P_n^m = -n \epsilon_{n+1}^m P_{n+1}^m + (n+1) \epsilon_n^m P_{n-1}^m \quad (2.3.1.11)$$

with

$$\epsilon_n^m = \left( \frac{n^2 - m^2}{4n^2 - 1} \right)^{1/2} \quad (2.3.1.12)$$

An important property of the spherical harmonics is:

$$\nabla^2 (P_n^m(\mu) e^{im\lambda}) = -\frac{n(n+1)}{a^2} P_n^m(\mu) e^{im\lambda} \quad (2.3.1.13)$$

Relationships (2.2.22) may thus be used to derive expressions for the Fourier velocity coefficients,  $U_m$  and  $V_m$ , in terms of the spectral coefficients  $\xi_n^m$  and  $D_n^m$ . It is convenient for later reference to write these expressions in the form

$$U_m = U_{\xi m} + U_{Dm} \quad (2.3.1.14)$$

$$V_m = V_{\xi m} + V_{Dm} \quad (2.3.1.15)$$

where

$$U_{\xi m} = -a \sum_{n=m}^{N(m)} \frac{1}{n(n+1)} \xi_n^m H_n^m(\mu) \quad (2.3.1.16)$$

$$U_{Dm} = -a \sum_{n=m}^{N(m)} \frac{im}{n(n+1)} D_n^m P_n^m(\mu) \quad (2.3.1.17)$$

$$V_{\xi m} = -a \sum_{n=m}^{N(m)} \frac{im}{n(n+1)} \xi_n^m P_n^m(\mu) \quad (2.3.1.18)$$

$$V_{Dm} = a \sum_{n=m}^{N(m)} \frac{1}{n(n+1)} D_n^m H_n^m(\mu) \quad (2.3.1.19)$$



and

$$H_n^m(\mu) = -(1 - \mu^2) \frac{d}{d\mu} P_n^m \quad (2.3.1.20)$$

The  $H_n^m$  can be computed from the recurrence relation (2.3.1.11).

The model is programmed to allow for a flexible pentagonal truncation, depicted in Figure 1 (Baede et al, 1979). This truncation is completely defined by the three parameters  $J$ ,  $K$  and  $M$  illustrated in the Figure. The common truncations are special cases of the pentagonal one:

|             |                |
|-------------|----------------|
| Triangular  | $M = J = K$    |
| Rhomboidal  | $K = J + M$    |
| Trapezoidal | $K = J, K > M$ |

The summation limit,  $N(m)$  is given by

$$N = J + |m| \quad \text{if } J + |m| \leq K,$$

and

$$N = K \quad \text{if } J + |m| > K.$$

The standard truncation is triangular (i.e.  $J = K = M = N$ ) at wave numbers 21, 42, 63 or 106 .

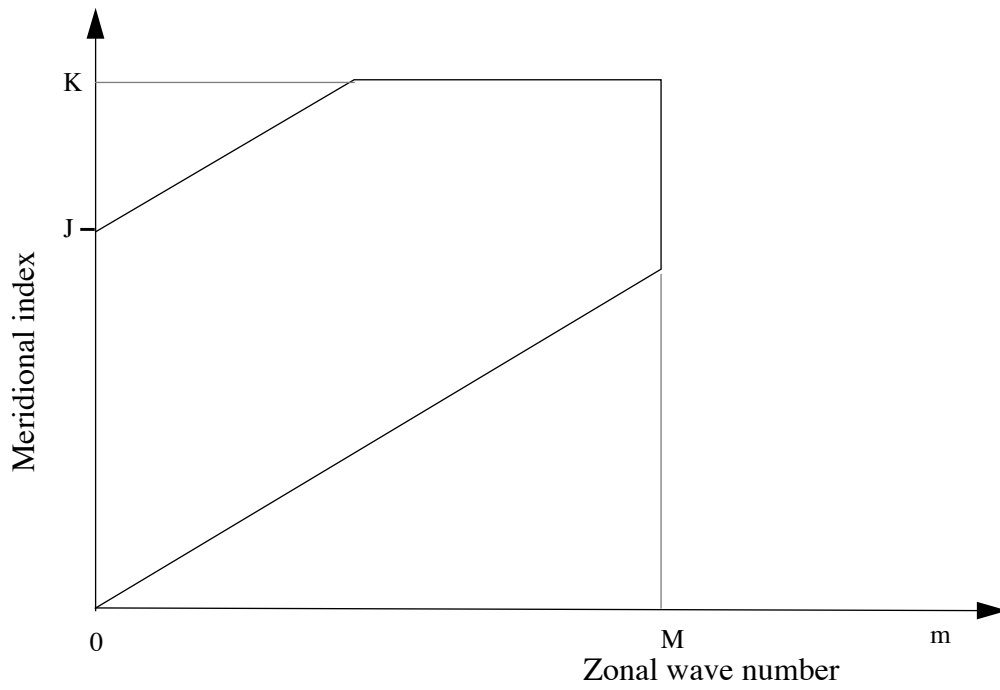


Figure 1 Pentagonal truncation

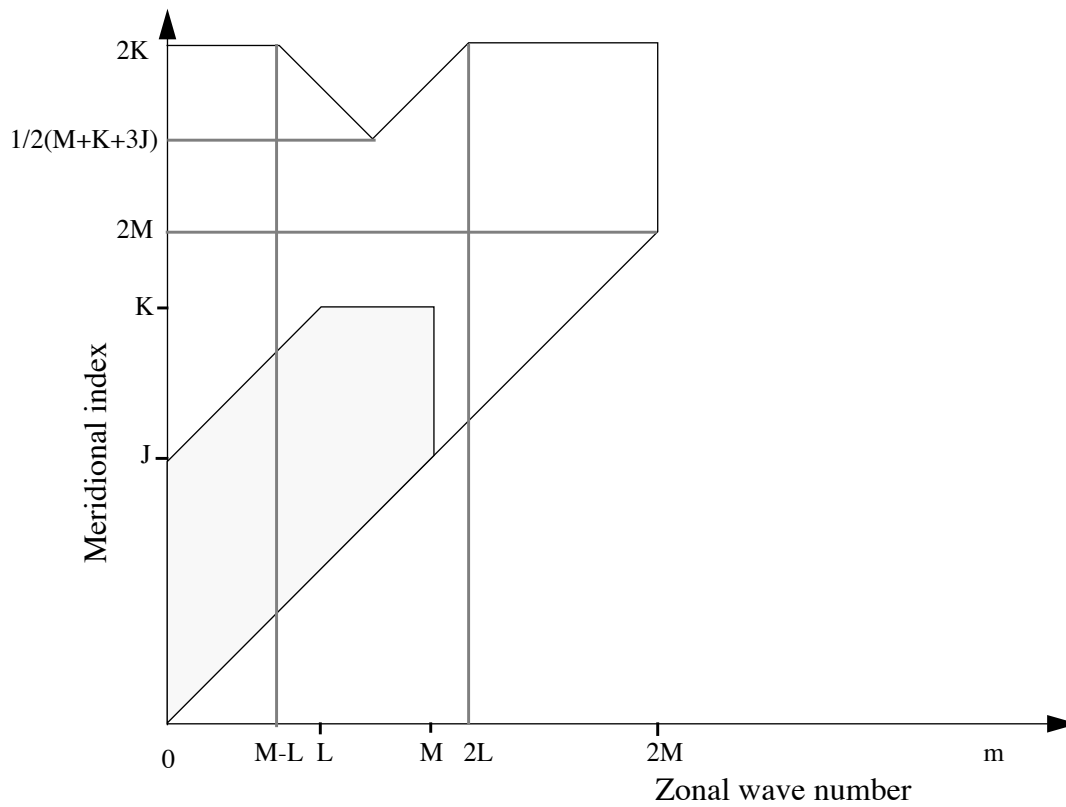


Figure 2 Product truncation

### 2.3.2 Spectral /grid-point transforms, and the evaluation of spectral tendencies

The general form of the calculations follows that of the early multi-level spectral models described by Bourke (1974) and Hoskins and Simmons (1975), although the present model differs in its use of an advective form for the temperature and moisture equations (2.2.17), (2.2.18), (2.2.3), (2.2.4), (2.2.5) and (2.2.11). Equations for the corresponding spectral coefficients are obtained by multiplying each side of these equations by  $P_n^m e^{-im\lambda}$ , and integrating over the sphere. This yields, from (2.3.1.4),

$$\frac{\partial \xi_n^m}{\partial t} = \frac{1}{4\pi a} \int_{-1}^1 \int_0^{2\pi} \left( \frac{1}{1-\mu^2} \frac{\partial}{\partial \lambda} (F_V + P_V) - \frac{\partial}{\partial \mu} (F_U + P_U) \right) P_n^m(\mu) e^{-im\lambda} d\lambda d\mu + (K_\xi)_n^m \quad (2.3.2.1)$$

$$\begin{aligned} \frac{\partial D_n^m}{\partial t} &= \frac{1}{4\pi a} \int_{-1}^1 \int_0^{2\pi} \left( \frac{1}{1-\mu^2} \frac{\partial}{\partial \lambda} (F_U + P_U) + \frac{\partial}{\partial \mu} (F_V + P_V) \right) P_n^m(\mu) e^{-im\lambda} d\lambda d\mu \\ &\quad - \frac{1}{4\pi} \int_{-1}^1 \int_0^{2\pi} (\nabla^2 G) P_n^m(\mu) e^{-im\lambda} d\lambda d\mu + (K_D)_n^m \end{aligned} \quad (2.3.2.2)$$

$$\frac{\partial T_n^m}{\partial t} = \frac{1}{4\pi} \int_{-1}^1 \int_0^{2\pi} (F_T + P_T) P_n^m(\mu) e^{-im\lambda} d\lambda d\mu + (K_T)_n^m \quad (2.3.2.3)$$

$$\frac{\partial (q_v)_n^m}{\partial t} = \frac{1}{4\pi} \int_{-1}^1 \int_0^{2\pi} (F_{q_v} + P_{q_v}) P_n^m(\mu) e^{-im\lambda} d\lambda d\mu + (K_{q_v})_n^m \quad (2.3.2.4)$$

$$\frac{\partial (q_w)_n^m}{\partial t} = \frac{1}{4\pi} \int_{-1}^1 \int_0^{2\pi} (F_{q_w} + P_{q_w}) P_n^m(\mu) e^{-im\lambda} d\lambda d\mu + (K_{q_w})_n^m \quad (2.3.2.5)$$

and

$$\frac{\partial (\ln p_s)_n^m}{\partial t} = \frac{1}{4\pi} \int_{-1}^1 \int_0^{2\pi} F_P P_n^m(\mu) e^{-im\lambda} d\lambda d\mu \quad (2.3.2.6)$$

where  $F_U$ ,  $F_V$  and  $G$  are given by (2.2.19) - (2.2.21), and

$$F_T = -\frac{U}{a(1-\mu^2)} \frac{\partial T}{\partial \lambda} - \frac{V}{a} \frac{\partial T}{\partial \mu} - \dot{\eta} \frac{\partial T}{\partial \eta} + \frac{\kappa T_v \omega}{(1 + (\delta - 1) q_v) p} \quad (2.3.2.7)$$

$$F_{q_v} = -\frac{U}{a(1-\mu^2)} \frac{\partial q_v}{\partial \lambda} - \frac{V}{a} \frac{\partial q_v}{\partial \mu} - \dot{\eta} \frac{\partial q_v}{\partial \eta} \quad (2.3.2.8)$$

$$F_{q_w} = -\frac{U}{a(1-\mu^2)} \frac{\partial q_w}{\partial \lambda} - \frac{V}{a} \frac{\partial q_w}{\partial \mu} - \dot{\eta} \frac{\partial q_w}{\partial \eta} \quad (2.3.2.9)$$

$$F_p = -\frac{1}{p_S} \int_0^1 \nabla \cdot (y_h \frac{\partial p}{\partial \eta}) d\eta \quad (2.3.2.10)$$

Equations (2.3.2.3) - (2.3.2.6) are in the form used in the model. The corresponding forms for the vorticity and divergence equations are obtained from (2.3.2.1) and (2.3.2.2) by integration by parts and use of (2.3.1.13):

$$\begin{aligned} \frac{\partial \xi_n^m}{\partial t} = & \frac{1}{4\pi a} \int_{-1}^1 \int_0^{2\pi} (1 - \mu^2)^{-1} [im (F_V + P_V) P_n^m(\mu) - (F_U + P_U) H_n^m(\mu)] e^{-im\lambda} d\lambda d\mu \\ & + (K_\xi)_n^m \end{aligned} \quad (2.3.2.11)$$

$$\begin{aligned} \frac{\partial D_n^m}{\partial t} = & \frac{1}{4\pi a} \int_{-1}^1 \int_0^{2\pi} (1 - \mu^2)^{-1} [im (F_U + P_U) P_n^m(\mu) + (F_V + P_V) H_n^m(\mu)] e^{-im\lambda} d\lambda d\mu \\ & + \frac{n(n+1)}{4\pi a^2} \int_{-1}^1 \int_0^{2\pi} G P_n^m(\mu) e^{-im\lambda} d\lambda d\mu + (K_D)_n^m \end{aligned} \quad (2.3.2.12)$$

where  $H_n^m(\mu)$  is given by (2.3.1.20).

An outline of the model's computation of spectral tendencies may now be given. First, a grid of points covering the sphere is defined. Using the basic definition of the spectral expansions (2.3.1.1) and equations (2.3.1.14) - (2.3.1.19), values of  $\xi$ ,  $D$ ,  $U$ ,  $V$ ,  $T$ ,  $q_v$ ,  $q_w$  and  $\ln p_S$  are calculated at the gridpoints, as also are the derivatives

$$\frac{\partial T}{\partial \lambda}, \frac{\partial T}{\partial \mu}, \frac{\partial q_v}{\partial \lambda}, \frac{\partial q_v}{\partial \mu}, \frac{\partial q_w}{\partial \lambda}, \frac{\partial q_w}{\partial \mu}, \frac{\partial \ln p_S}{\partial \lambda} \text{ and } \frac{\partial \ln p_S}{\partial \mu}$$

using (2.3.1.9) and (2.3.1.10). The resulting gridpoint values are sufficient to calculate gridpoint values of  $F_U$ ,  $F_V$ ,  $F_T$ ,  $F_{q_v}$ ,  $F_{q_w}$ ,  $F_p$  and  $G$ , together with the parametrized tendencies  $P_U$ ,  $P_V$ ,  $P_T$ ,  $P_{q_v}$  and  $P_{q_w}$ , since prognostic surface fields associated with the parametrization are defined and updated on the same grid. The integrands of the prognostic equations (2.3.2.11), (2.3.2.12), (2.3.2.3) - (2.3.2.6) are thus known at each gridpoint, and spectral tendencies are calculated by numerical quadrature.

The grid on which the calculations are performed is chosen to give an exact (given the spectral truncation of the fields, and within round-off error) contribution to spectral tendencies from quadratic non-linear terms. The integrals with respect to  $\lambda$  involve the product of three trigonometric functions, and as shown by Machenhauer and Rasmussen (1972) they may be evaluated exactly using a regularly-spaced grid of at least  $3 \cdot M + 1$  points. For the latitudinal integrals, Eliassen et al. (1970) showed that quadratic non-linear terms lead to integrands which are polynomials in  $\mu$  of a certain order.

They may thus be computed exactly using Gaussian quadrature (e.g. Krylov, 1962), with points located at the (approximately equally-spaced) latitudes which satisfy  $P_{N_G}^0(\mu) = 0$ , for sufficiently large integer  $N_G$ . These latitudes form what are referred to as the ‘‘Gaussian latitudes’’.

In order to find the necessary number of Gaussian latitudes for the triangular truncation, and from the exactness condition for the Gaussian integration it may be shown that the number of Gaussian latitudes  $N_G$  must fulfil the following condition:

$$N_G \geq \frac{3 \cdot K + 1}{2} .$$

An asymptotic property of the Legendre Functions which may be derived directly from the definition (2.3.1.2) is

$$P_n^m(\mu) \sim (1 - \mu^2)^{m/2} \text{ as } (\mu \rightarrow \pm 1) .$$

Thus for large  $m$  the functions become vanishingly small as the poles are approached, and the contributions to the integrals (2.3.2.1) - (2.3.2.6) from polar regions become less than the unavoidable round-off error for sufficiently large zonal wavenumbers.

## 2.4 VERTICAL DISCRETIZATION

### 2.4.1 The hybrid vertical representation

To represent the vertical variation of the dependent variables  $\xi$ ,  $D$ ,  $T$ ,  $q_v$  and  $q_w$  the atmosphere is divided into  $NLEV$  layers as illustrated in Figure 3. These layers are defined by the pressures of the interfaces between them (the "half levels"), and these pressures are given by

$$p_{k+1/2} = A_{k+1/2} + B_{k+1/2} p_S \quad (2.4.1.1)$$

for  $k = 0, 1, 2 \dots NLEV$ . The  $A_{k+1/2}$  and  $B_{k+1/2}$  are constants whose values effectively define the vertical coordinate. Necessary values are

$$A_{1/2} = B_{1/2} = A_{NLEV+1/2} = 0 \quad \text{and} \quad B_{NLEV+1/2} = 1 \quad (2.4.1.2)$$

The usual sigma coordinate is obtained as the special case

$$A_{k+1/2} = 0, \quad k = 0, 1, 2, \dots, NLEV \quad (2.4.1.3)$$

This form of hybrid coordinate has been chosen because it is particularly efficient from a computational viewpoint. It also allows a simple direct control over the "flattening" of coordinate surfaces as pressure decreases, since the  $A$ 's and  $B$ 's may be determined by specifying the distribution of half-level pressures for a typical sea-level surface pressure and for a surface pressure typical of the lowest expected to be attained in the model. Coordinate surfaces are surfaces of constant pressure at levels where  $B_{k+1/2} = 0$ .

The prognostic variables  $\xi$ ,  $D$ ,  $T$ ,  $q_v$  and  $q_w$  are represented by their values at intermediate ("full-level") pressures,  $p_k$ . Values for  $p_k$  are not explicitly required by the model's vertical finite-difference scheme, which is described in the following section, but they are required by parameterization schemes, in the creation of initial data, and in the interpolation to pressure levels that forms part of the post-processing. Alternative forms for  $p_k$  have been discussed by Simmons and Burridge (1981) and Simmons and Strüfing (1981). Little sensitivity has been found, and the simple form

$$p_k = \frac{1}{2} (p_{k+1/2} + p_{k-1/2}) \quad (2.4.1.4)$$

has been adopted, where half-level values are as given by (2.4.1.1).

The explicit relationship between  $p$  and  $p_S$  defined for model half levels implicitly determines a vertical coordinate  $\eta$ . The model formulation is in fact such that this coordinate need not be known explicitly, as demonstrated in the following section. However, it is computationally convenient to define  $\eta$  for the radiative parametrization and for the vertical interpolation used in the post-processing. The half-level values are given by

$$\eta_{k+1/2} = \frac{A_{k+1/2}}{p_0} + B_{k+1/2} \quad (2.4.1.5)$$

where  $p_0$  is constant pressure. From (2.4.1.1) it is seen that this coordinate is identical to the usual  $\sigma$  when  $A_{k+1/2} = 0$ , and in general equals  $\sigma$  when  $p_0 = p_S$ .  $\eta = p/p_0$  at levels where coordinate surfaces are surfaces of constant pressure. Values of  $\eta$  between half-levels are given by linear interpolation :

$$\eta = \eta_{k+1/2} + \frac{(p - p_{k+1/2}) (\eta_{k+1/2} - \eta_{k-1/2})}{(p_{k+1/2} - p_{k-1/2})} \quad \text{for } (p_{k-1/2} \leq p \leq p_{k+1/2}) \quad (2.4.1.6)$$

A 19-layer version is used operationally, and the corresponding values of the  $A_{k+1/2}$  and  $B_{k+1/2}$  are given in Table 1. The distribution of full-level pressures is shown in Figure 4. The top two layers are at constant pressures, and the lowest two layers are pure sigma layers. The value of  $p_0$  used for the definition of  $\eta$  is the reference sea-level pressure of 101325 Pa.

**Table 1 Vertical-coordinate parameters of the 19-layer ECHAM3 model**

| k  | $A_{k+1/2}$ (Pa) | $B_{k+1/2}$  |
|----|------------------|--------------|
| 0  | 0.000000         | 0.0000000000 |
| 1  | 2000.000000      | 0.0000000000 |
| 2  | 4000.000000      | 0.0000000000 |
| 3  | 6046.110595      | 0.0003389933 |
| 4  | 8267.927560      | 0.0033571866 |
| 5  | 10609.513232     | 0.0130700434 |
| 6  | 12851.100169     | 0.0340771467 |
| 7  | 14698.498086     | 0.0706498323 |
| 8  | 15861.125180     | 0.1259166826 |
| 9  | 16116.236610     | 0.2011954093 |
| 10 | 15356.924115     | 0.2955196487 |
| 11 | 13621.460403     | 0.4054091989 |
| 12 | 11101.561987     | 0.5249322235 |
| 13 | 8127.144155      | 0.6461079479 |
| 14 | 5125.141747      | 0.7596983769 |
| 15 | 2549.969411      | 0.8564375573 |
| 16 | 783.195032       | 0.9287469142 |
| 17 | 0.000000         | 0.9729851852 |
| 18 | 0.000000         | 0.9922814815 |
| 19 | 0.000000         | 1.0000000000 |

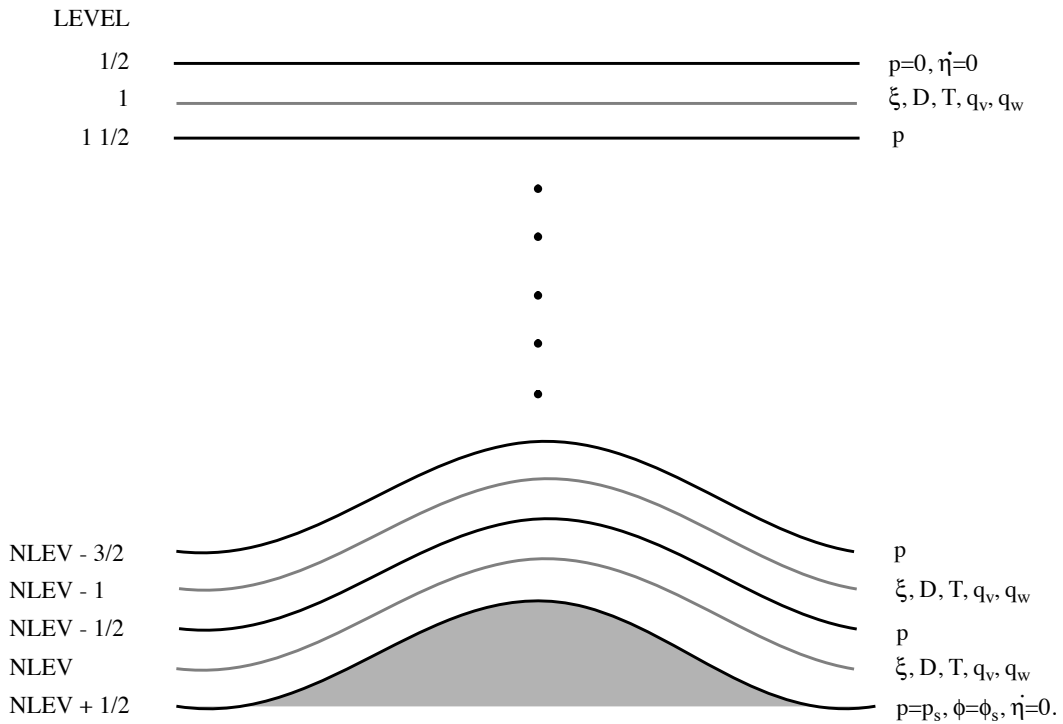


Figure 3 Vertical distribution of variables

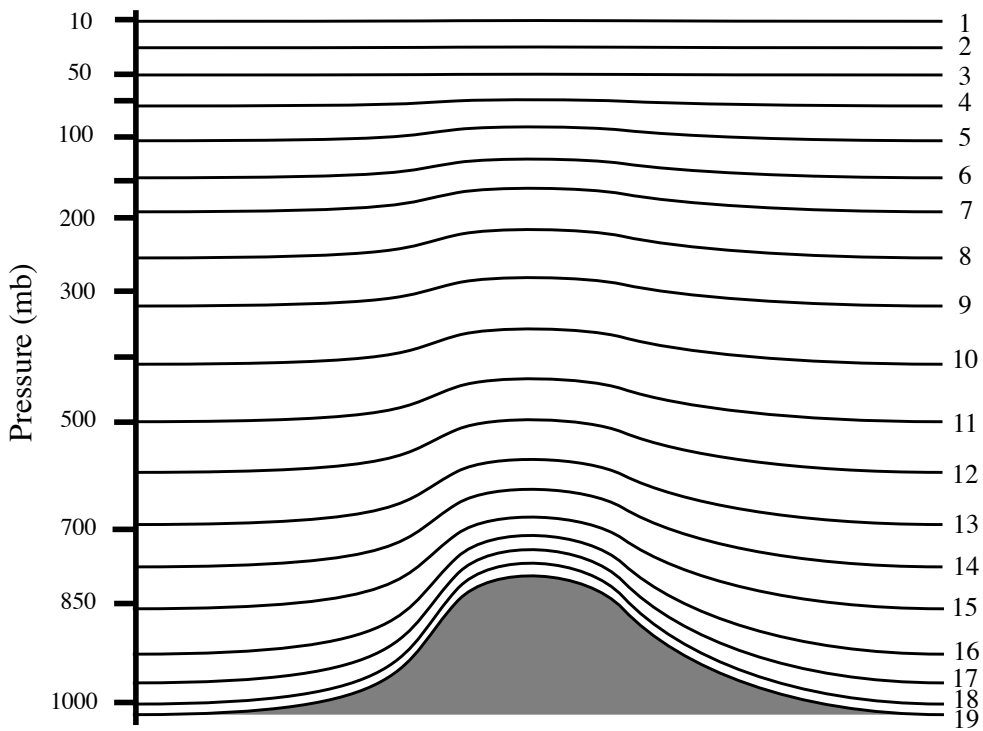


Figure 4 Distribution of full-level pressures in the 19-level ECHAM3 model



### 2.4.2 The vertical finite-difference scheme

The vertical finite-difference scheme is a generalization to the hybrid coordinate with form (2.4.1.1) of the scheme adopted in the first operational ECMWF model (Burrige and Haseler, 1977), apart from a small modification concerned with the conservation of angular momentum. The generalized scheme has been discussed by Simmons and Burrige (1981) and by Simmons and Strüfing (1981), and the presentation here is restricted to a prescription of the finite-difference forms of the various terms of the continuous equations that involve  $\eta$ .

#### a) The surface-pressure tendency

The finite-difference analogue of (2.2.11) is

$$\frac{\partial}{\partial t} \ln p_S = -\frac{1}{p_S} \sum_{k=1}^{NLEV} \nabla \cdot (v_k \Delta p_k) \quad (2.4.2.1)$$

where the subscript “ $k$ ” denotes a value for the  $k$ -th layer, and

$$\Delta p_k = p_{k+1/2} - p_{k-1/2} \quad (2.4.2.2)$$

From (2.4.1.1) we obtain

$$\frac{\partial}{\partial t} \ln p_S = -\sum_{k=1}^{NLEV} \left\{ \frac{1}{p_S} D_k \Delta p_k + (v_k \nabla \ln p_S) \Delta B_k \right\} \quad (2.4.2.3)$$

$$\text{where } \Delta B_k = B_{k+1/2} - B_{k-1/2} \quad (2.4.2.4)$$

#### b) The continuity equation

(2.2.10) gives

$$\left( \dot{\eta} \frac{\partial p}{\partial \eta} \right)_{k+1/2} = -\frac{\partial p_{k+1/2}}{\partial t} - \sum_{j=1}^k \nabla \cdot (v_j \Delta p_j) \quad (2.4.2.5)$$

and from (2.4.1.1)

$$\left( \dot{\eta} \frac{\partial p}{\partial \eta} \right)_{k+1/2} = -p_S \left[ B_{k+1/2} \frac{\partial}{\partial t} \ln p_S + \sum_{j=1}^k \left\{ \frac{1}{p_S} D_j \Delta p_j + (v_j \nabla \ln p_S) \Delta B_j \right\} \right] \quad (2.4.2.6)$$

where  $\frac{\partial}{\partial t} \ln p_S$  is given by (2.4.2.3).

c) Vertical advection

Given  $(\dot{\eta} \frac{\partial p}{\partial \eta})_{k+1/2}$  computed from (2.4.2.6), vertical advection of a variable  $X$  is given by

$$(\dot{\eta} \frac{\partial X}{\partial \eta})_k = \frac{1}{2\Delta p_k} \{ (\dot{\eta} \frac{\partial p}{\partial \eta})_{k+1/2} (X_{k+1} - X_k) + (\dot{\eta} \frac{\partial p}{\partial \eta})_{k-1/2} \cdot (X_k - X_{k-1}) \} \quad (2.4.2.7)$$

This form ensures that there is no spurious source or sink of kinetic energy, potential energy, moisture or cloud water due to the finite-difference representation of vertical advection.

d) The hydrostatic equation

The form chosen for the finite-difference analogue of (2.2.7) is

$$\phi_{k+1/2} - \phi_{k-1/2} = -R_d \cdot (T_v)_k \cdot \ln \left( \frac{p_{k+1/2}}{p_{k-1/2}} \right) \quad (2.4.2.8)$$

which gives

$$\phi_{k+1/2} = \phi_S + \sum_{j=k+1}^{NLEV} R_d \cdot (T_v)_j \cdot \ln \left( \frac{p_{j+1/2}}{p_{j-1/2}} \right) \quad (2.4.2.9)$$

Full level values of geopotential are given by

$$\phi_k = \phi_{k+1/2} + \alpha_k \cdot R_d \cdot (T_v)_k \quad , \quad (2.4.2.10)$$

$$\text{where } \alpha_1 = \ln 2 \quad (2.4.2.11)$$

and, for  $k > 1$ ,

$$\alpha_k = 1 - \frac{p_{k-1/2}}{\Delta p_k} \cdot \ln \left( \frac{p_{k+1/2}}{p_{k-1/2}} \right) \quad (2.4.2.12)$$

Reasons for this particular choice of the  $\alpha_k$  are given below.

e) The pressure gradient term

It is shown by Simmons and Strüfing (1981) that if the geopotential is given by (2.4.2.10), the form

$$R_d \cdot (T_v \cdot \nabla \ln p)_k = \frac{R_d \cdot (T_v)_k}{\Delta p_k} \left\{ \ln \frac{p_{k+1/2}}{p_{k-1/2}} \right\} \cdot \nabla p_{k-1/2} + \alpha_k \cdot \nabla (\Delta p_k) \quad (2.4.2.13)$$

for the pressure-gradient term ensures no spurious source or sink of angular momentum due to the vertical differencing. This expression is adopted in the model, but with the  $\alpha_k$  given by (2.4.2.12) for all  $k$ . This ensures that the pressure-gradient term reduces to the familiar form  $R_d (T_v)_k \nabla \ln p_S$  in the case of sigma coordinates, and the angular momentum conserving property of the scheme still holds in the case in which the first half-level below  $p = 0$  is a surface of constant pressure. The choice  $\alpha_1 = 1$  in the

hydrostatic equation would have given angular momentum conservation in general, but a geopotential  $\phi_1$  inappropriate to the pressure-level  $p = p_1 = \Delta p/2$ . If, alternatively,  $\phi_1$  were to be interpreted not as a value for a particular level, but rather the mass-weighted layer-mean value, then the choice  $\alpha_1 = 1$  would be appropriate.

It is shown by Simmons and Chen (1991) that the form (2.4.2.13) can be significantly improved, with benefit particularly in regions of steep terrain, if  $T_v$  is replaced by its deviation from a reference state,

$$\tilde{T}_v = T_v - T_{00} \left(\frac{p}{p_0}\right)^\beta \quad (2.4.2.14)$$

where  $\beta = \gamma \cdot R_d/g$ ,  $p_0 = 1013.25$  hPa,  $T_{00} = 288$  K and  $\gamma = 6.5$  K/km. The reference temperature (2.4.2.14) is based on the tropospheric part of the ICAO (1964) standard atmosphere with a uniform lapse rate  $\gamma$ .

Using the form (2.4.1.1) for the half-level pressures (2.4.2.13) may be written

$$R_d \cdot (\tilde{T}_v \cdot \nabla \ln p)_k = \frac{R_d \cdot (\tilde{T}_v)_k}{\Delta p_k} \left\{ \Delta B_k + C_k \cdot \frac{1}{\Delta p_k} \cdot \left( \ln \frac{p_{k+1/2}}{p_{k-1/2}} \right) \right\} \nabla p_S \quad (2.4.2.15)$$

where

$$C_k = A_{k+1/2} \cdot B_{k-1/2} - A_{k-1/2} \cdot B_{k+1/2} \quad (2.4.2.16)$$

The modified form (2.4.2.15) finally requires a reformulation of the surface geopotential according to

$$\phi_S = g \cdot z_S + \frac{R_d \cdot T_{00}}{\beta} \cdot \left(\frac{p_S}{p_0}\right)^\beta \quad (2.4.2.17)$$

#### f) Energy-conversion term

To obtain a form for the term  $\kappa \cdot T_v \cdot \omega / (1 + (\delta - 1) q_v)$  in (2.2.3) we use (2.2.8) to write

$$\left( \frac{\kappa \cdot T_v \cdot \omega}{(1 + (\delta - 1) q_v) p} \right)_k = \frac{\kappa \cdot (T_v)_k}{1 + (\delta - 1) (q_v)_k} \left( \frac{\omega}{p} \right)_k \quad (2.4.2.18)$$

where

$$\left( \frac{\omega}{p} \right)_k = -\frac{1}{p} \int_0^{\eta_k} \nabla \cdot \left( y \cdot \frac{\partial p}{\partial \eta} \right) d\eta + (y \cdot \nabla \ln p)_k \quad (2.4.2.19)$$

An expression for  $(\omega/p)_k$  is then determined by the requirement that the difference scheme conserves the total energy of the model atmosphere for adiabatic, frictionless motion. This is achieved by

(i) evaluating the first term on the right-hand side of (2.4.2.19) by

$$-\frac{1}{\Delta p_k} \left\{ \ln \frac{p_{k+1/2}}{p_{k-1/2}} \right\} \cdot \sum_{j=1}^{k-1} \nabla \cdot (y_j \cdot \Delta p_j) + \alpha_k \nabla \cdot (y_k \cdot \Delta p_k) \} \quad (2.4.2.20)$$

where the  $\alpha_k$  are as given by (2.4.2.11) and (2.4.2.12), and as in (2.4.2.3) and (2.4.2.5)

$$\nabla \cdot (y_k \cdot \Delta p_k) = D_k \cdot \Delta p_k + p_S \cdot (y_k \cdot \nabla \ln p_S) \cdot \Delta B_k \quad (2.4.2.21)$$

(ii) using the form of (2.4.2.15) to evaluate the second term on the right-hand side of (2.4.2.19)

$$(y \cdot \nabla \ln p)_k = \frac{p_S}{\Delta p_k} \cdot \{ \Delta B_k + C_k \cdot \frac{1}{\Delta p_k} \cdot \left( \ln \frac{p_{k+1/2}}{p_{k-1/2}} \right) \} \cdot y_k \cdot \nabla \ln p_S \quad (2.4.2.22)$$

## 2.5 TIME INTEGRATION SCHEME

A semi-implicit time scheme is used for equations of divergence, temperature and surface pressure, based on the work of Robert et al. (1972). The growth of spurious computational modes is inhibited by a time filter (Asselin, 1972). In addition, a semi-implicit method for the zonal advection terms in the vorticity and moisture equations is used, following results obtained by Robert (1981, 1982). He showed that in a semi-implicit shallow water equation model the time-step criterion was determined by the explicit treatment of the vorticity equation. Facilities also exist for selective damping of short model scales to allow use of longer timesteps. These are incorporated within the horizontal diffusion routines of the model, and are described in section 2.6.

The semi-implicit schemes are formally given by:

$$\delta_t \xi = ZT - \frac{1}{2a} \beta_{zQ} \frac{U_r(\mu)}{(1-\mu^2)} \frac{\partial}{\partial \lambda} \Delta_{tt} \xi \quad (2.5.1)$$

$$\delta_t q_v = Q_v T - \frac{1}{2a} \beta_{zQ} \frac{U_r(\mu)}{(1-\mu^2)} \frac{\partial}{\partial \lambda} \Delta_{tt} q_v \quad (2.5.2)$$

$$\delta_t q_w = Q_w T - \frac{1}{2a} \beta_{zQ} \frac{U_r(\mu)}{(1-\mu^2)} \frac{\partial}{\partial \lambda} \Delta_{tt} q_w \quad (2.5.3)$$

$$\delta_t D = DT - \nabla^2 G - \frac{1}{2} \beta_{DT} \nabla^2 \{ \gamma \Delta_{tt} T + R_d T_r \Delta_{tt} \ln p_s \} \quad (2.5.4)$$

$$\delta_t T = TT - \frac{1}{2} \beta_{DT} \tau \Delta_{tt} D \quad (2.5.5)$$

$$\delta_t \ln p_s = PT - \frac{1}{2} \beta_{DT} \nu \Delta_{tt} D \quad (2.5.6)$$

Here the terms  $ZT$ ,  $Q_v T$ ,  $Q_w T$ ,  $G$ ,  $TT$ ,  $PT$  represent those on the right-hand sides of equations (2.2.17), (2.2.4), (2.2.5), (2.2.18), (2.2.3) and (2.2.11), apart from the diffusion terms, which are neglected here. Adiabatic components are evaluated at the current time,  $t$ , and parametrized components are generally evaluated using values of fields at the previous timestep,  $t - \Delta t$ . The treatment of diffusion terms is described in the following section.

The remaining terms on the right-hand sides of (2.5.1) - (2.5.6) are corrections associated with the semi-implicit time schemes, and are discussed more fully below. The operators  $\delta_t$  and  $\Delta_{tt}$  are given by

$$\delta_t X = (X^+ - X_f^-) / (2\Delta t) \quad (2.5.7)$$

$$\Delta_{tt} X = (X^+ + X_f^- - 2X) \quad (2.5.8)$$

where  $X$  represents the value of a variable at time  $t$ ,  $X^+$  the value at time  $t + \Delta t$ , and  $X_f^-$  a filtered value at time  $t - \Delta t$ . A further operator that will be used is

$$\tilde{\Delta}_{tt}X = X_f^- - 2X \quad (2.5.9)$$

The time filtering is defined by

$$X_f = X + \varepsilon_f(X_f^- - 2X + X^+) \quad (2.5.10)$$

and it is computationally convenient to split it into two parts;

$$\tilde{X}_f = X + \varepsilon_f(X_f^- - 2X) \quad (2.5.11)$$

$$X_f = \tilde{X}_f + \varepsilon_f X^+ \quad (2.5.12)$$

The timestep  $\Delta t$  depends on the resolution and is specified as follows:

|      |                          |
|------|--------------------------|
| T21  | $\Delta t = 40$ minutes  |
| T42  | $\Delta t = 24$ minutes  |
| T63  | $\Delta t = 15$ minutes  |
| T106 | $\Delta t = 12$ minutes, |

and  $\varepsilon_f = 0.1$  independent of the resolution.

a) The semi-implicit treatment of vorticity and moisture (water vapour and cloud water)

Referring to equations (2.5.1), (2.5.2) and (2.5.3), an explicit treatment of the vorticity and moisture equations is obtained by setting  $\beta_{ZQ} = 0$ . Otherwise  $\beta_{ZQ} = 1$  and  $U_r(\mu)$  is a zonally-uniform reference zonal velocity, multiplied by  $\cos\theta$ . Terms describing advection by this reference velocity are represented implicitly by the arithmetic mean of values at times  $t + \Delta t$  and  $t - \Delta t$ , while the remainder of the tendencies are represented explicitly by values at time  $t$ .  $U_r(\mu)$  may vary in the vertical.

Because of the use of integration by parts in the derivation of the prognostic equation (2.3.2.11) for the spectral coefficients of vorticity, it is necessary to treat the vorticity and moisture equations separately. Considering first the moisture equations, we obtain from (2.5.2), (2.5.3) and (2.5.7) - (2.5.9):

$$(1 + 2\Delta t \alpha(\mu) \frac{\partial}{\partial \lambda}) q_v^+ = q_{vf}^- + 2\Delta t Q_v T - 2\Delta t \alpha(\mu) \frac{\partial}{\partial \lambda} \tilde{\Delta}_{tt} q_v \quad (2.5.13)$$

$$(1 + 2\Delta t \alpha(\mu) \frac{\partial}{\partial \lambda}) q_w^+ = q_{wf}^- + 2\Delta t Q_w T - 2\Delta t \alpha(\mu) \frac{\partial}{\partial \lambda} \tilde{\Delta}_{tt} q_w \quad (2.5.14)$$

where

$$\alpha(\mu) = \frac{1}{2a} \beta_{ZQ} \frac{U_r(\mu)}{(1 - \mu^2)} \quad (2.5.15)$$

Transforming to Fourier space then gives

$$q_{vm}^+ = b_m(\mu) \{ (q_{vf}^- + 2\Delta t Q_v T)_m - 2 im \Delta t \alpha(\mu) \tilde{\Delta}_{tt} q_{vm} \} \quad (2.5.16)$$

$$q_{wm}^+ = b_m(\mu) \{ (q_{wf}^- + 2\Delta t Q_w T)_m - 2 im \Delta t \alpha(\mu) \tilde{\Delta}_{tt} q_{wm} \} \quad (2.5.17)$$

where

$$b_m(\mu) = (1 + 2 im \Delta t \alpha(\mu))^{-1} \quad (2.5.18)$$

New values  $(q_n^m)_v^+$  and  $(q_n^m)_w^+$  of the spectral coefficients of  $q_v$  and  $q_w$  are then computed by Gaussian integration as described in 2.3.2 .

For the vorticity equation, (2.2.17) is used to write

$$ZT = \frac{1}{a(1-\mu^2)} \frac{\partial}{\partial \lambda} (F_V + P_V) - \frac{1}{a} \frac{\partial}{\partial \mu} (F_U + P_U) \quad (2.5.19)$$

where the horizontal diffusion term has for convenience been neglected, since as specified in the following section it merely modifies the value of vorticity computed for time  $t + \Delta t$ . Proceeding as for the moisture equations, we obtain

$$\xi_m^+ = b_m(\mu) \left[ \left( \xi_f^- + \frac{2 im \Delta t}{a(1-\mu^2)} (F_V + P_V) \right)_m - 2 im \Delta t \alpha(\mu) \tilde{\Delta}_{tt} \xi_m - \frac{2 \Delta t}{a} \frac{\partial}{\partial \mu} (F_U + P_U)_m \right] \quad (2.5.20)$$

The factor  $b_m(\mu)$  renders the right-hand side of this equation unsuitable for direct integration by parts, but a suitable form is found from the relation

$$b_m(\mu) \frac{\partial}{\partial \mu} (F_U + P_U) = \frac{\partial}{\partial \mu} \{ b_m(\mu) (F_U + P_U) \} - c_m(\mu) (F_U + P_U) \quad (2.5.21)$$

where

$$c_m(\mu) = \frac{\partial}{\partial \mu} b_m(\mu) \quad (2.5.22)$$

This gives

$$\xi_m^+ = \tilde{Z}_{\lambda m}(\mu) + \frac{\partial}{\partial \mu} \tilde{Z}_{\mu m}(\mu) \quad (2.5.23)$$

where

$$\begin{aligned} \tilde{Z}_{\lambda m}(\mu) &= b_m(\mu) (\xi_f^-)_m \\ &+ 2\Delta t \left( im b_m(\mu) \left[ \frac{(F_V + P_V)_m}{a(1-\mu^2)} - \alpha(\mu) \tilde{\Delta}_{tt} \xi_m \right] + \frac{1}{a} c_m(\mu) (F_U + P_U)_m \right) \end{aligned} \quad (2.5.24)$$

and

$$\tilde{Z}_{\mu m}(\mu) = -\frac{2\Delta t}{a} b_m(\mu) (F_U + P_U)_m \quad (2.5.25)$$

New values  $(\xi_n^m)^+$  are obtained from (2.5.23) by Gaussian quadrature, using integration by parts as illustrated by (2.3.2.1) and (2.3.2.11) for the continuous form of the equations.

In ECHAM3,  $\beta_{zQ} = 1$ .  $U_r(\mu)$  is the arithmetic mean of the maximum and minimum velocities multiplied by  $\cos\theta$ , as computed for each latitude and model level at timestep  $t-\Delta t$ . Different values are thus used for different levels.

b) The semi-implicit treatment of divergence, temperature and surface pressure

Referring to equations (2.5.4) - (2.5.6), an explicit treatment of the divergence, temperature and surface pressure equations is obtained by setting  $\beta_{DT} = 0$ . For  $\beta_{DT} = 1$ , the nature of the semi-implicit correction is such that gravity wave terms for small amplitude motion about a basic state with isothermal temperature  $T_r$  and surface pressure  $p_r$  are treated implicitly by the arithmetic mean of values at times  $t + \Delta t$  and  $t - \Delta t$ , while the remainder of tendencies are represented explicitly by values at time  $t$ . The choice of an isothermal reference temperature is governed by considerations of the stability of the semi-implicit time scheme (Simmons et al, 1978), while the appropriate choice of  $p_r$  for the hybrid vertical coordinate is discussed by Simmons and Burridge (1981) and Simmons and Strüfing (1981).

$\gamma$ ,  $\tau$  and  $\nu$  in equations (2.5.4) - (2.5.6) are operators obtained from linearizing the finite-difference forms specified in 2.3.2 about the reference state  $(T_r, p_r)$ . Their definitions are

$$(\gamma T)_k = \alpha_k^r R_d T_k + \sum_{j=k+1}^{NLEV} R_d T_j \ln \left( \frac{p_{j+1/2}^r}{p_{j-1/2}^r} \right) \quad (2.5.26)$$

$$(\tau D)_k = \kappa T_r \left\{ \frac{1}{\Delta p_k^r} \left( \ln \frac{p_{j+1/2}^r}{p_{j-1/2}^r} \right) S_{k-1/2}^r + \alpha_k^r D_k \right\} \quad (2.5.27)$$

and

$$\nu D = \frac{1}{p_r} S_{NLEV+1/2}^r \quad (2.5.28)$$

where

$$\begin{aligned} p_{k+1/2}^r &= A_{k+1/2} + p_r B_{k+1/2} \\ \Delta p_k^r &= p_{k+1/2}^r - p_{k-1/2}^r \\ S_{k+1/2}^r &= \sum_{j=1}^k D_j \Delta p_j^r \end{aligned} \quad (2.5.29)$$

and the  $\alpha_k^r$  are defined by (2.4.2.11) and (2.4.2.12), but with half-level pressures replaced by reference values  $p_{k+1/2}^r$ .

Expanding (2.5.4) - (2.5.6) using (2.5.7) and (2.5.8), and writing  $l$  to denote  $\ln p'_s$ , we obtain

$$D^+ = D_f^- + 2\Delta t (DT) - 2\Delta t \nabla^2 \left\{ G + \frac{1}{2} \beta_{DT} [\gamma(T^+ + T_f^- - 2T) + R_d T_r (l^+ + l_f^- - 2l)] \right\} \quad (2.5.30)$$



$$T^+ = T_1 - \Delta t \beta_{DT} \tau D^+ \quad (2.5.31)$$

and

$$l^+ = l_1 - \Delta t \beta_{DT} \nu D^+ \quad (2.5.32)$$

where

$$T_1 = T_f^- + 2\Delta t (TT) - \Delta t \beta_{DT} \tau \tilde{\Delta}_H D \quad (2.5.33)$$

and

$$l_1 = l_f^- + 2\Delta t (PT) - \Delta t \beta_{DT} \nu \tilde{\Delta}_H D \quad (2.5.34)$$

Substituting (2.5.31) and (2.5.32) into (2.5.30) then gives

$$(1 - \Gamma \nabla^2) D^+ = DT' \quad (2.5.35)$$

where

$$\Gamma = (\beta_{DT})^2 (\Delta t)^2 (\gamma \tau + R_d T_r \nu) \quad (2.5.36)$$

$$DT' = D_f^- + 2\Delta t (DT) + \nabla^2 R = \tilde{D}_\lambda + \tilde{D}_\mu + \nabla^2 R \quad (2.5.37)$$

with

$$\tilde{D}_\lambda = D_f^- + \frac{2\Delta t}{a(1-\mu^2)} \frac{\partial}{\partial \lambda} (F_U + P_U) \quad (2.5.38)$$

$$\tilde{D}_\mu = \frac{2\Delta t}{a} \frac{\partial}{\partial \mu} (F_V + P_V) \quad (2.5.39)$$

and

$$R = -2\Delta t \left\{ G + \frac{B_{DT}}{2} (\gamma T_2 + R_d T_r l_2) \right\} \quad (2.5.40)$$

Here

$$T_2 = T_1 + T_f^- - 2T \quad (2.5.41)$$

$$l_2 = l_1 + l_f^- - 2l \quad (2.5.42)$$

The sequence of these semi-implicit calculations in the model is thus as follows. The expressions (2.5.33), (2.5.34) and (2.5.40) - (2.5.42) are computed on the Gaussian grid to form the gridpoint values of  $R$ . The spectral expansion of  $DT'$  is then derived by Gaussian quadrature, using integration by parts as illustrated by (2.3.2.2) and (2.3.2.12) for the continuous form of the equations. Since

$$\left\{ (1 - \Gamma \nabla^2) D^+ \right\}_n^m = \left( 1 + \frac{n(n+1)}{a^2} \Gamma \right) (D^+)_n^m, \quad (2.5.43)$$

the spectral coefficients of divergence at time  $t + \Delta t$  are given from (2.3.32) by

$$(D^+)_n^m = \left(1 + \frac{n(n+1)}{a^2} \Gamma\right)^{-1} (DT')_n^m, \quad (2.5.44)$$

where this operation involves, for each  $(m, n)$ , multiplication of the vector of  $NLEV$  values of  $(DT')_n^m$  by a pre-computed  $NLEV \times NLEV$  matrix whose elements are independent of time and determined by writing the operators  $\gamma$ ,  $\tau$  and  $\nu$  in matrix and vector form. Finally, (2.5.31) and (2.5.32) are applied in spectral space to compute spectral coefficients of  $T$  and  $\ln p'_s$  at time  $t + \Delta t$  in terms of the spectral coefficients of  $T_1$  and  $l_1$  (again determined by Gaussian quadrature) and those of  $D^+$ . In ECHAM3,  $\beta_{DT} = 0.75$ ,  $T_r = 300$  K and  $p_r = 800$  hPa.

## 2.6 HORIZONTAL DIFFUSION

### 2.6.1 Basic scheme

While the original ECMWF model uses a  $\nabla^4$  horizontal diffusion, ECHAM3 uses a diffusion parameterization based on the ideas of Laursen and Eliassen (1989). The contribution to the spectral tendency of any prognostic variable  $X$  is

$$-k_X L_n X_n^m \quad (2.6.1.1)$$

With this term, calculated at the new time  $t + \Delta t$ , the diffusive contribution to the semi-implicit time stepping scheme is

$$X_n^m(t + \Delta t) = X_n^m(t - \Delta t) \cdot \{1 + 2\Delta t k_X L_n\}^{-1} \quad (2.6.1.2)$$

$L_n$  is chosen such that large scales are not damped, while short waves can be damped selectively,

$$L_n = \begin{cases} (n - n_*)^\alpha & \text{for } (n > n_*) \\ 0 & \text{for } (n \leq n_*) \end{cases} \quad (2.6.1.3)$$

with  $\alpha = 2$  for T21, and  $\alpha = 4$  for T42 truncation. For both resolutions, we chose a cut-off wave number  $n_* = 15$ , i.e. only modes with  $n \geq 16$  are damped.

The diffusion coefficient  $k_X$  varies for different variables and levels. While the lower levels (6 to 19) use the same  $k_X$ , the upper most levels are stronger damped,

$$k_X(l) = k_X \cdot fac(l) \quad (2.6.1.4)$$

where  $l$  denotes the vertical index. For  $fac = 1$  and T21 resolution the damping time  $1/(k_X \cdot L_n)$  of the shortest scale is 1.12 days for the vorticity, 0.22 days for the divergence and 5.59 days for temperature, humidity and cloud water, respectively. For T42 resolution the respective times are 0.30, 0.06 and 0.76 days. Figure 5 shows the damping times of the vorticity due to the horizontal diffusion as a function of the total wave number  $n$  and level  $l$ . Table 2 shows the amplification factors for the six uppermost levels.

**Table 2 Vertical amplification factor for the horizontal diffusion**

| level $l$ | factor $fac$ |
|-----------|--------------|
| 1         | 16           |
| 2         | 16           |
| 3         | 8            |
| 4         | 4            |
| 5         | 2            |
| 6         | 1            |

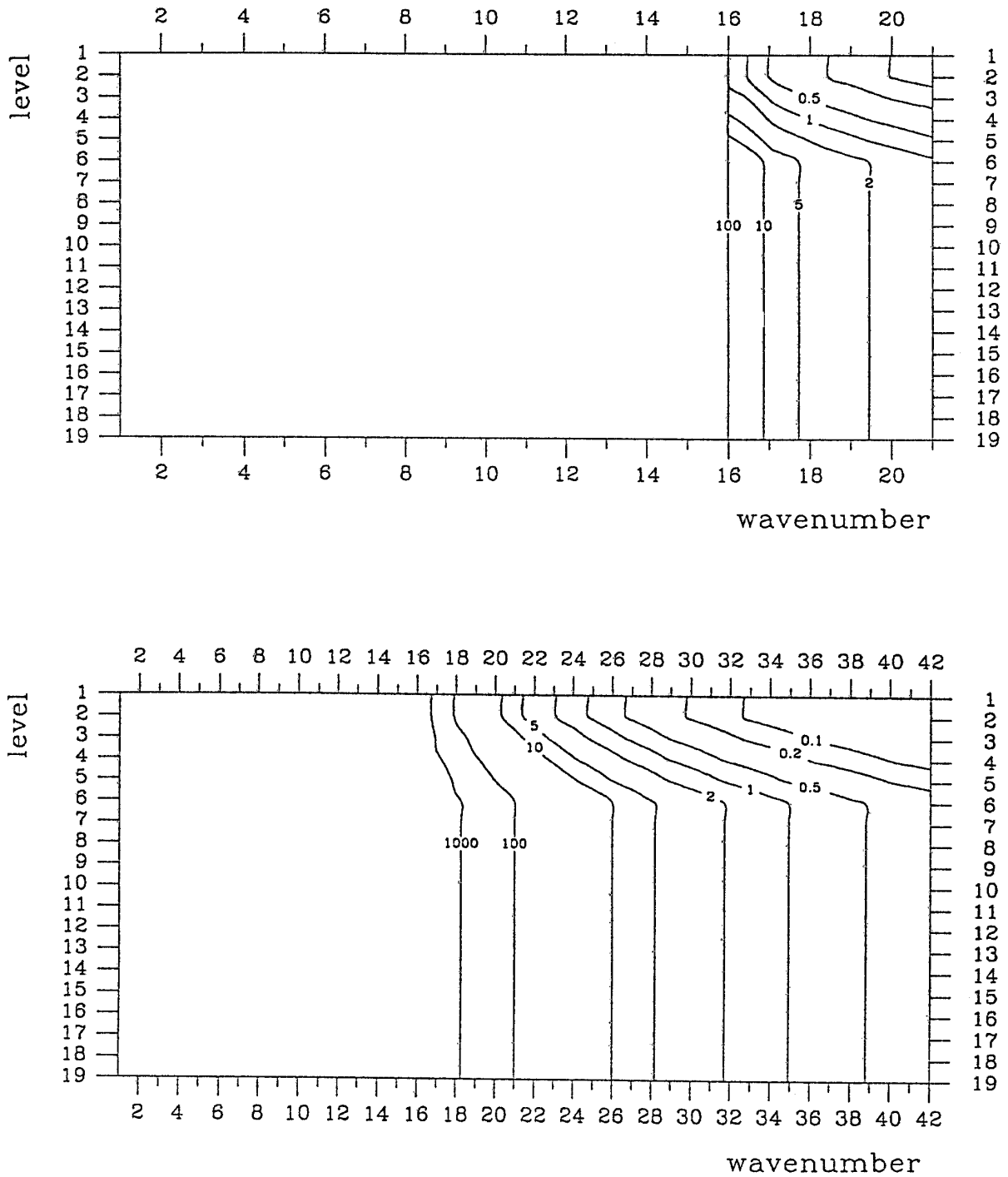
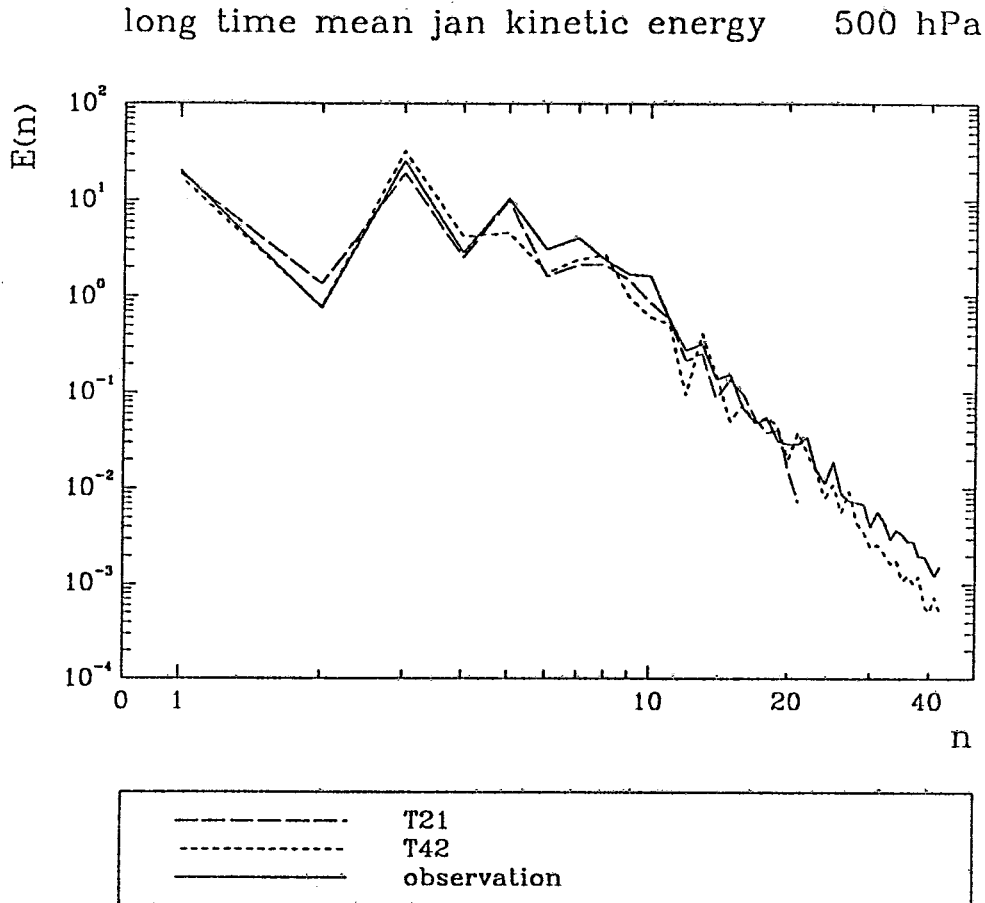


Figure 5 Damping times for the vorticity due to horizontal diffusion for T21 (upper panel) and T42 (lower panel) horizontal resolution. Contours for 0.1, 0.2, 0.5, 1, 2, 5, 10, 100, 1000 days.

A modified diffusion scheme is used for the temperature to avoid unrealistic warming of mountain tops and excessive summer precipitation associated with substantial mixing in the vicinity of steep mountain slopes. Only the deviation of the temperature field from the ICAO standard atmosphere is inserted into the diffusion procedure.

The diffusion coefficients were chosen such that the slope of the spectral kinetic energy is close to observations (see Figure 6). Moreover, as a result of the diffusion scheme together with a timestep of 40 /24/ 15/12 minutes for T21/T42/T63/T106 resolution, additional damping due to a violation of the CFL-criterion is considerably reduced as compared to the ECMWF model.



*Figure 6* Mean kinetic energy spectra at 500 hPa during January for observations (ECMWF, mean of 1980 - 1989), for T21 resolution (mean of a 20 year control run with prescribed climatological sea surface temperature) and for T42 resolution (mean of a 10 year simulation with the observed sea surface temperatures of the years 1979 - 1988).



### 3. MODEL PHYSICS

#### 3.1 INTRODUCTION

Processes associated with turbulent and convective transfer, condensation and radiation are important for the development of the atmospheric large-scale flow. Since these processes are related to spatially small or even molecular phenomena, they cannot be explicitly included in numerical models which only resolve scales larger than grid size in grid point models or the truncation wave number in spectral models.

Figure 7 shows the processes which are thought to be important for long term integrations. It shows how the different processes (printed within ellipses) depend on the variables given by the model (printed in rectangles). The thickness of the arrows represents qualitatively the importance of the interactions. For example, the effect of radiation on the ground temperature is very fast: It only takes a few hours for the sun to heat the ground. The relationship between radiation and the temperature of the air is much weaker: Condensation, diffusion and the flux of sensible heat from the ground change the air temperature more effectively. Any closed loop in the diagram (e.g. Temperature  $\rightarrow$  Evaporation  $\rightarrow$  Ground temperature  $\rightarrow$  Sensible heat flux  $\rightarrow$  Temperature) indicates a feed-back process. The reader can amuse himself by counting the number of closed loops in order to get a feeling for the complexity of the atmospheric system.

The effect of the sub-grid scale processes on the large-scale flow which we want to predict can only be considered by means of parameterisation, i.e. formulating the ensemble effect in terms of the resolved grid-scale variables.

Large efforts have been made in the recent past to design reliable parameterisation schemes for different processes. Based on a large amount of observational data the parameterisation of the turbulent fluxes in the planetary boundary layer has been considerably improved. A significant effort has been directed toward accounting for vegetation effects on the surface fluxes. Progress has also been made in calculating the radiative fluxes, and a hierarchy of schemes differing with respect to the degree of approximation of the equations of radiative transfer were developed.

However, the parameterisation of convection is still problematic since the interaction of cumulus clouds with the large scale circulation is not sufficiently understood to decide on one of the existing schemes. Finally, there are also processes which have only occasionally been the subject of parameterisation studies as, mesoscale circulations, topographically induced circulations, thin layer clouds, coastal effects.

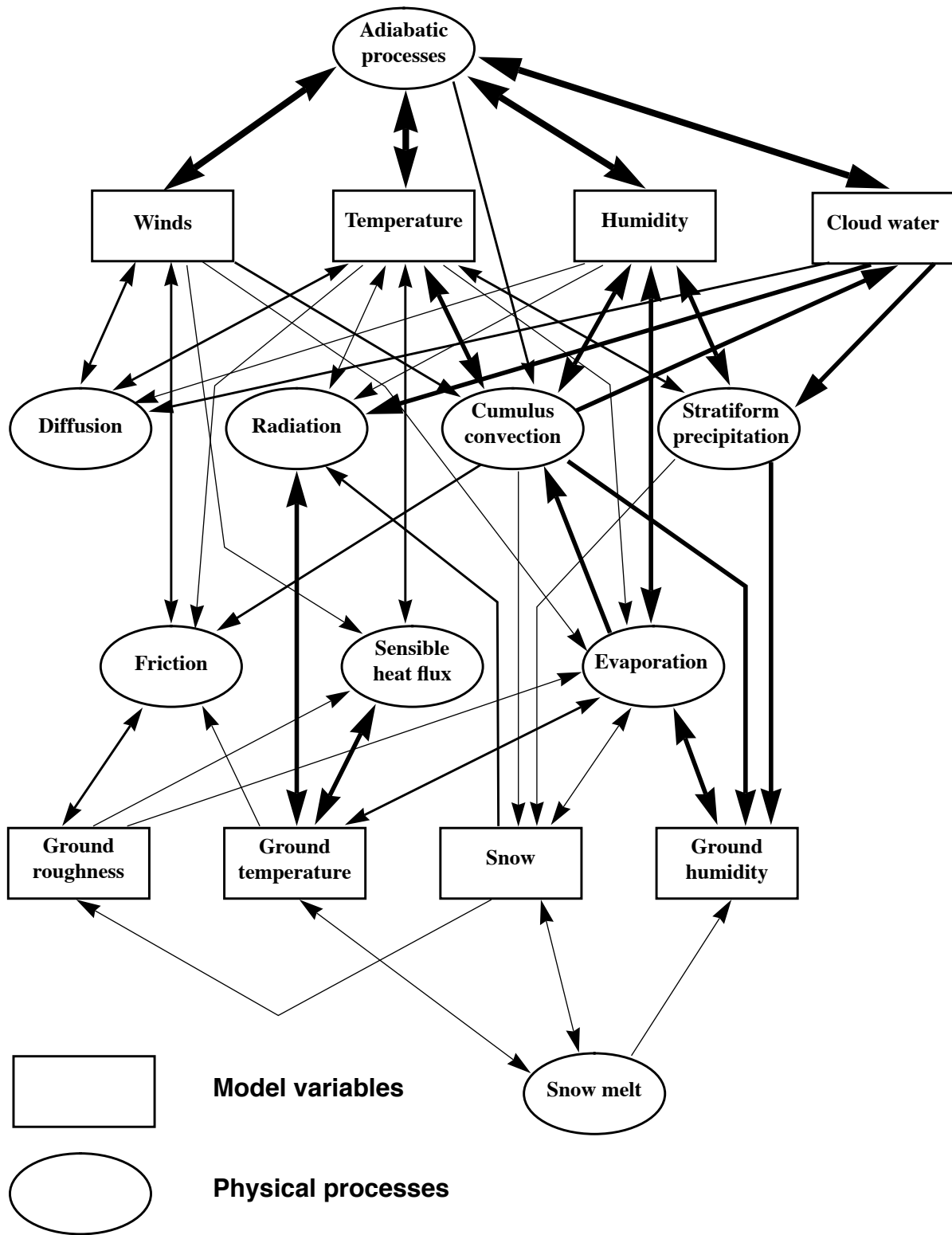


Figure 7 Schematic representation of the processes included in the ECHAM3 model.



The radiation scheme (section 3.2 ) is designed to take the cloud-radiation interaction into account in considerable detail. It allows partial cloud cover in any layer of the model, and considers multiple scattering. The effect of gases is subsequently taken into account. The reader can also refer to Hense et al. (1982), Rockel et al. (1991), and Eickerling (1989).

The dissipation processes are described in section 3.3 . The vertical eddy fluxes are simulated as a diffusive process. The dependence of the surface fluxes and diffusion coefficients on the stability of the atmosphere is based on the Monin-Obukhov similarity theory. The papers by Louis (1979) and Louis et al. (1982) may provide additional information.

An additional process by which momentum may be removed from the atmosphere is through the excitation of gravity waves when stably stratified flow interacts with the orography. This so-called "gravity-wave" drag (section 3.4 ) is parameterized using a modified version of a scheme developed by Boer et al. (1984) and Palmer et al. (1986), and which uses directionally dependent sub-grid scale orographic variances (Miller et al., 1989).

The moist processes are separated into convective precipitation and stratiform precipitation. The convective processes are simulated by a mass flux scheme, in which the convection is driven by the large-scale convergence of moisture (Tiedtke, 1989). The stratiform cloud scheme is based upon a transport equation for cloud water including the formation of sub-grid scale clouds and a simplified treatment of the microphysical processes such as condensation, evaporation and precipitation formation by coalescence of cloud droplets and sedimentation of ice crystals (Roeckner et al., 1991).

Based mainly on Sellers's ideas, (Sellers et al., 1986), the effect of vegetation on surface evapotranspiration has been accounted for. The dependence of sensible heat fluxes on snow coverage has been incorporated as well. The papers by Blondin and Böttger (1987) and Blondin (1989) give an overview of the surface parameterisation scheme.

Finally the ground processes include a prediction of the ground temperature, using a 5-level, finite-difference approximation of the diffusion equation. A prediction of soil moisture and snow cover is also included (Dümenil and Todini, 1992).

The horizontal diffusion, which is used in the operational model to keep the forecast from developing small scale noise, is included in the documentation of the adiabatic part (section 2.6).

## 3.2 RADIATION

### 3.2.1 Radiative heating

The radiative heating rate is computed as the divergence of net radiative fluxes  $F$  :

$$\left(\frac{\partial T}{\partial t}\right)_{rad} = -\frac{g}{C_{pd}} \cdot \frac{\partial F}{\partial p} \quad (3.2.1.1)$$

Section 3.2.2 describes the computation of the radiative fluxes. The solution of the radiative transfer equation to obtain the fluxes is unfortunately very expensive and is therefore performed only every two hours. To take into account the change in temperature and solar zenith angle between the times when the full radiation computation is performed, we define an effective emissivity  $\varepsilon_e$  and transmissivity  $\tau_e$  of the model levels such that

$$F_T = \varepsilon_e \cdot \sigma \cdot T^4 \quad (3.2.1.2)$$

and

$$F_S = \tau_e \cdot S_0 \quad (3.2.1.3)$$

where  $F_T$  and  $F_S$  are the net thermal (long wave) and solar (short wave) fluxes respectively.  $\sigma$  is the Stefan-Boltzmann constant and  $S_0$  is the solar flux at the top of the atmosphere. The values  $\varepsilon_e$  and  $\tau_e$  are kept constant between the full radiation time steps and the net fluxes are recomputed at every time step, using (3.2.1.2) and (3.2.1.3) with the correct temperature and solar zenith angle.

### 3.2.2 The radiative transfer model

#### 3.2.2.1 Introduction

The radiative transfer model is based on a two-stream approximation described by Kerschgens et al. (1978) and Zdunkowski et al. (1980). From the radiative transfer equations for the solar part of the spectrum, eqs. (3.2.2.1) and (3.2.2.2), and for the terrestrial part, eqs. (3.2.2.3) and (3.2.2.4), Hense et al. (1982) derived a broad-band formulation with spectral intervals listed in Table 3.

$$\frac{\partial}{\partial \delta} M^+ = [1 - \tilde{\omega}(1 - \beta)] \frac{M^+}{\bar{\mu}} - \tilde{\omega}\beta \frac{M^-}{\delta} - \beta_0 \tilde{\omega} S_0 e^{-\delta/\mu_0} \quad (3.2.2.1)$$

$$\frac{\partial}{\partial \delta} M^- = \tilde{\omega}\beta \frac{M^+}{\delta} - [1 - \tilde{\omega}(1 - \beta)] \frac{M^-}{\bar{\mu}} + (1 - \beta_0) \tilde{\omega} S_0 e^{-\delta/\mu_0} \quad (3.2.2.2)$$

$$\frac{d}{d\delta} M^+ = \frac{1}{\bar{\mu}} (M^+ - B) \quad (3.2.2.3)$$

$$\frac{d}{d\delta} M^- = \frac{1}{\bar{\mu}} (M^- - B) \quad (3.2.2.4)$$

where  $M^+$  and  $M^-$  are the upward and downward flux densities,  $\delta$  is the optical depth,  $\tilde{\omega}$  is the single scattering albedo,  $\beta$  and  $\beta_0$  are the backscattering parameters for diffuse and direct radiation respectively,  $1/\bar{\mu}$  is the diffusivity factor (2 for solar and 1.66 for terrestrial radiation),  $S_0$  is the solar irradiance,  $\mu_0$  is the cosine of the solar zenith angle, and  $B$  is the Planck function.

**Table 3 Spectral intervals and absorbers of the radiative transfer model**

| Terrestrial                        |                                   | Solar                              |                                   |
|------------------------------------|-----------------------------------|------------------------------------|-----------------------------------|
| Spectral Interval( $\mu\text{m}$ ) | Absorber                          | Spectral Interval( $\mu\text{m}$ ) | Absorber                          |
| 3.96 - 7.98                        | H <sub>2</sub> O                  | 0.215 - 0.685                      | O <sub>3</sub>                    |
| 7.98 - 8.89                        | H <sub>2</sub> O, dimer           | 0.685 - 0.891                      | H <sub>2</sub> O                  |
| 8.89 - 10.15                       | O <sub>3</sub> , dimer            | 0.891 - 1.273                      | H <sub>2</sub> O                  |
| 10.15 - 11.76                      | H <sub>2</sub> O, dimer           | 1.273 - 3.580                      | H <sub>2</sub> O, CO <sub>2</sub> |
| 11.76 - 20.10                      | H <sub>2</sub> O, CO <sub>2</sub> |                                    |                                   |
| 20.10 - 100.                       | H <sub>2</sub> O                  |                                    |                                   |

The optical parameters in a cloud-free atmosphere are taken from Hense et al. (1982) for the solar spectrum and from Eickerling (1989) for the terrestrial spectrum. In the terrestrial part scattering is neglected.

### 3.2.2.2 Terrestrial radiation

The optical depth  $\delta$  is defined as

$$\delta = \exp \left[ \sum_{j=0}^n a_j (\log u_i)^j \right] \quad (3.2.2.5)$$

with the effective absorber mass  $u_i$  of the  $i^{\text{th}}$  component,

$$u_i = \rho_i \left( \frac{p}{p_0} \right)^{\alpha_p} \left( \frac{T_0}{T} \right)^{\alpha_T} d \quad (3.2.2.6)$$

where  $a_j$ ,  $\alpha_p$ ,  $\alpha_T$  are coefficients derived by inverting the results of an "exact" reference radiation model,  $\rho_i$ ,  $p$  and  $T$  denote concentration of the  $i^{\text{th}}$  component, pressure and temperature, respectively, averaged over an atmospheric layer with geometrical thickness  $d$ ,  $p_0$  and  $T_0$  are reference values set to 1013 hPa and 273.15 °K, respectively.

With these definitions and assuming that the Planck function is a linear function of  $\delta$ , the radiative transfer equations can be solved as described by Hense et al. (1982).

### 3.2.2.3 Solar radiation

For the transfer of solar radiation, absorption (subscript  $a$ ) and multiple scattering (subscript  $s$ ) are taken into account. The relevant parameters are the optical thickness  $\delta$ , the single scattering albedo  $\tilde{\omega}$  and the backscattering coefficients  $\beta$ ,  $\beta_0$ . The backscattering coefficients  $\beta$  and  $\beta_0$  are derived from theory (Kerschgens et al., 1978). Scattering and absorption coefficients of stratospheric, urban and maritime aerosols are taken from a data set provided by Shettle and Fenn (1975). Multiplication by  $d$  gives the appropriate optical thicknesses  $\delta_a^{aerosol}$ ,  $\delta_s^{aerosol}$ .

The optical thickness  $\delta_a^{gas}$  for gas absorption is a function of the effective absorber amount and is defined similarly to the terrestrial radiation (see above). The optical thickness  $\delta_s^{gas}$  for Rayleigh scattering of gas molecules is given by

$$\delta_s^{gas} = \bar{N} \cdot A_R \cdot d \quad (3.2.2.7)$$

where  $\bar{N}$  is the mean number density and  $A_R$  is the scattering cross-section of molecules.

For diffuse radiation, the optical thickness  $\delta^{dif}$  is calculated from

$$\delta^{dif} = a_a (\delta_a^{gas} + \delta_a^{aerosol})^{b_a} + a_s (\delta_s^{gas} + \delta_s^{aerosol})^{b_s} \quad (3.2.2.8)$$

where  $a_a$ ,  $b_a$ ,  $a_s$  and  $b_s$  are coefficients derived by inverting results of an "exact" reference model.

The single scattering albedo is defined as

$$\tilde{\omega} = 1 - \frac{\delta_a^{dif}}{\delta_s^{dif}} \quad (3.2.2.9)$$

For direct radiation, the optical thickness  $\delta^{dir}$  at a level  $k$  is calculated by adding the optical thicknesses above this level

$$\delta^{dir} = \sum_{j=1}^k (\delta_{a_j}^{gas} + \delta_{a_j}^{aerosol} + \delta_{s_j}^{gas} + \delta_{s_j}^{aerosol}) \quad (3.2.2.10)$$

where  $\delta_a^{gas}$  depends on the zenith angle  $\theta$ .  $\delta_a^{gas}$  is parameterized for  $\theta = 35^\circ$  and  $\theta = 75^\circ$  only. Optical thicknesses for other zenith angles are calculated by linear interpolation.

### 3.2.2.4 Cloud optical properties

The emissivity  $\varepsilon$  of clouds in the terrestrial region is described by

$$\varepsilon = 1 - e^{-\left[\frac{k \cdot m \cdot d}{\bar{\mu}}\right]} \quad (3.2.2.11)$$

where  $k = 0.084 \text{ m}^2\text{g}^{-1}$  is the mass absorption coefficient (Stephens, 1978),  $d$  is the geometrical cloud thickness and  $m$  is the water or ice content in  $\text{gm}^{-3}$ .

Optical thickness  $\delta$ , single scattering albedo  $\tilde{\omega}$ , and back-scattering coefficient  $\beta$  are the optical parameters considered in transfer of solar radiation. For both cloud phases, the parameterization of Stephens (1978) is adopted:

$$\log(\delta) = \begin{cases} 0.2633 + 1.7095 \cdot \ln[\log(m \cdot d)] & (\lambda < 0.685 \text{ } \mu\text{m}) \\ 0.3492 + 1.6518 \cdot \ln[\log(m \cdot d)] & \text{otherwise} \end{cases} \quad (3.2.2.12)$$

Single scattering albedo and back-scattering coefficients are taken from Kerschgens et al. (1978).

### 3.2.3 Input to the radiation scheme

#### 3.2.3.1 Temperature

Temperature values are needed at the boundaries of the layers, where the fluxes are computed. They are derived from the full level temperatures using a pressure weighted interpolation:

$$T_{k+1/2} = T_k \cdot \frac{p_k (p_{k+1} - p_{k+1/2})}{p_{k+1/2} (p_{k+1} - p_k)} + T_{k+1} \cdot \frac{p_k (p_{k+1/2} - p_k)}{p_{k+1/2} (p_{k+1} - p_k)} \quad (3.2.3.1)$$

At the bottom of the atmosphere, the ground temperature  $T_S$  is used, while at the top the model's first full level temperature is used.

#### 3.2.3.2 Clouds

Cloud liquid water and cloud cover are provided by subroutine COND, which performs the stratiform cloud calculation. Cloud overlap is treated such that if two cloudy layers are contiguous, they are assumed to have maximum overlap of the cloudy parts. Otherwise random overlap is assumed.

#### 3.2.3.3 Aerosols

Provision is made to have various types of aerosols:

- oceanic
- desert
- urban

#### 3.2.3.4 Carbon dioxide and ozone

Carbon dioxide has a constant mass mixing ratio over the whole globe corresponding to a volume concentration of 345 ppm ( $\text{CO2FAC} = 1.045$ ). For ECHAM1 and ECHAM2 the concentration is 330 ppm ( $\text{CO2FAC} = 1.0$ ).

The ozone mixing ratio  $R_{03}$  depends on height, latitude, longitude and season. Its vertical distribution is assumed to be such that its integral from 0 to the pressure  $p$  is

$$\int_0^p R_{03} dp = \frac{a}{1 + (b/p)^{3/2}} \quad (3.2.3.2)$$

The constants  $a$  and  $b$  are related to the total amount of ozone and the height of its maximum mixing ratio. They are imposed in terms of a limited series of spherical harmonics for the geographical distribution and a Fourier series for the seasonal variation. The total amount of ozone was taken from London et al. (1976) and the altitude of the maximum concentration was derived from Wilcox and Belmont (1977).

### 3.2.3.5 Surface albedo

Over snow-free land areas an annual mean background albedo is specified from satellite data (Geleyn and Preuss, 1983). According to more recent analyses (e.g., Dorman and Sellers, 1989) the satellite-based estimates are too low in the tropics and at middle latitudes (North America, Eurasia). This bias has been removed by applying an empirical correction in those areas where the satellite data suggests values of less than 15 %. The minimum values thus obtained are around 12 % for tropical rain forests.

In snow-covered areas the surface albedo is modified according to

$$\alpha_{Surf} = \alpha_{Sb} + (\alpha_S - \alpha_{Sb}) \cdot \frac{Sn}{Sn + Sn^*} \quad (3.2.3.3)$$

where  $\alpha_S$  is the snow albedo (see below),  $\alpha_{Sb}$  is the background albedo,  $Sn$  is the simulated snow depth (in water equivalent) and  $Sn^* = 0.01$  m is a critical snow depth. For  $Sn \gg Sn^*$  the surface albedo approaches the albedo of snow.

The albedo of snow and ice surfaces ( $\alpha_S$ ) is a function of surface type ( $t_S$ ), surface temperature ( $T_S$ ) and fractional forest area ( $a_f$ ) over land. For  $T_S \geq T_m = 273.15$  K (i.e., for melting of snow or ice),  $\alpha_S$  is fixed at a relatively small value,  $\alpha_S = \alpha_{Smin}(t_S, a_f)$ , whereas  $\alpha_S$  is larger,  $\alpha_S = \alpha_{Smax}(t_S, a_f)$ , for cold surfaces ( $T_S \leq T_0 = 263.15$  K) according to Robock (1980). Over land, the respective snow albedos are assumed to depend on the fractional forest area ( $0 \leq a_f \leq 1$ ) according to

$$\begin{aligned} \alpha_{Smin}(a_f) &= a_f \cdot \alpha_{Smin}(a_f=1) + (1 - a_f) \cdot \alpha_{Smin}(a_f=0) \\ \alpha_{Smax}(a_f) &= a_f \cdot \alpha_{Smax}(a_f=1) + (1 - a_f) \cdot \alpha_{Smax}(a_f=0) \end{aligned} \quad (3.2.3.4)$$

In the temperature range  $T_0 < T_S < T_m$ ,  $\alpha_S = \alpha_S(T_S, t_S, a_f)$  is obtained by linear interpolation

$$\alpha_S = \alpha_{Smax} - (\alpha_{Smax} - \alpha_{Smin}) \cdot \frac{T_S - T_0}{T_m - T_0} \quad (3.2.3.5)$$

with  $\alpha_{Smax}$  and  $\alpha_{Smin}$  as specified in Table 4 according to the estimate of Robock (1980) for sea ice and snow (without the solar zenith angle correction, however) and according to Kukla and Robinson (1980) for land ice.

Over sea, the albedo is constant (0.065) for diffuse radiation but depends on the solar zenith angle  $\theta$  for the direct beam

$$\alpha_{S0} = \frac{0.05}{\cos\theta + 0.15} \quad (3.2.3.6)$$

with the limitation  $\alpha_{S0} \leq 0.15$ .

**Table 4** Minimum and maximum surface albedos (Robock, 1980; Kukla and Robinson, 1980) referring to the temperature ranges  $T_S \geq T_m = 273.15$  K and  $T_S \leq T_0 = 263.15$  K respectively. The fractional forest area ( $a_f$ ) is taken from a data set compiled by Matthews (1983).

| surface type |               | $\alpha_{Smin}$ | $\alpha_{Smax}$ |
|--------------|---------------|-----------------|-----------------|
| sea ice      |               | 0.5             | 0.75            |
| land ice     |               | 0.6             | 0.8             |
| snow on land | for $a_f = 0$ | 0.4             | 0.8             |
|              | for $a_f = 1$ | 0.3             | 0.4             |

### 3.2.3.6 Solar zenith angle

Equations to compute the annual variation of the solar constant  $I_0$ , the solar declination  $\delta_s$  and the difference between solar time and official time can be found in Paltridge and Platt (1976). These equations are used to give the cosine of the solar zenith angle.

The mean value of the solar constant  $I_0$  is  $1367 \text{ Wm}^{-2}$  for ECHAM1 and ECHAM2 and  $1365 \text{ Wm}^{-2}$  for ECHAM3.



### 3.3 VERTICAL DIFFUSION

#### 3.3.1 Basic equations

The parameterization scheme represents the turbulent exchanges of heat, momentum, moisture and cloud water at the surface and the turbulent transports of the same quantities in the lowest levels of the model. The top of the turbulent layer is computed using a combination of convective and dynamic criteria. Above this boundary layer the scheme only operates when the air is statically unstable. The equation for the vertical diffusion of any conservative quantity  $X$  is:

$$\frac{\partial X}{\partial t} = \frac{1}{\rho} \frac{\partial}{\partial z} (\rho K_X \frac{\partial X}{\partial z}) = \frac{1}{\rho} \frac{\partial J_X}{\partial z} \quad (3.3.1.1)$$

$K_X$  is the exchange coefficient and  $J_X$  (positive downwards) is the vertical turbulent flux of  $X$ . The following boundary conditions have been assumed:

$$K_X \frac{\partial X}{\partial z} = 0 \quad \text{for } p = p_T \quad (3.3.1.2.a)$$

and

$$K_X \frac{\partial X}{\partial z} \rightarrow C_X |y_h(z)| (X(z) - X_S) \quad \text{for } (z \rightarrow 0) \quad (3.3.1.2.b)$$

where  $p_T$  is the pressure at the top of the boundary layer and  $y_h = (u, v)$  is the horizontal windvector.

The definition of the drag coefficient  $C_X$  depends on the height  $z$  above the ground at which  $y_h$  and  $X$  are taken (the natural choice is the model's lowest level) and on the stability of the layer.  $X_S$  represents a value of  $X$  at the surface.

$X$  may be identified with each of the five variables  $u, v, q_v, q_w$  and  $s$  (dry static energy).  $s$  is defined as:

$$s = C_{pd} (1 + (\delta - 1) q_v) \cdot T + g \cdot z = C_p \cdot T + \phi \quad (3.3.1.3)$$

For the latter the problem is simplified by assuming that  $\phi$  remains constant with respect to time during the evolution process (even if in reality  $T$  variations would modify  $z(p)$ ). A coupling with the vertical diffusion of  $q_v$  is avoided by assuming a constant value of  $C_p(z)$  in time.

Since the thickness of the model layer  $\Delta z$  is small near the ground, when  $(K \cdot 2\Delta t) / (\Delta z)^2 > 1$ , the time-stepping procedure must be implicit in order to avoid numerical instability. The whole interaction with the adiabatic and other processes, however, cannot be treated implicitly. The following procedure has been chosen:

Starting from  $X$  values at  $t - \Delta t$  an implicit treatment of equations (3.3.1.1), (3.3.1.2.a) and (3.3.1.2.b) results in new values  $\tilde{X}(t+1)$ . Dividing the difference  $\tilde{X}(t+1) - X(t-1)$  by the timestep ( $2\Delta t$ , or  $\Delta t$  at the first timestep) the result is added to the adiabatic and radiative tendencies. Thus:

$$\frac{\tilde{X}(t+1) - X(t-1)}{2\Delta t} = \frac{1}{\rho} \frac{\partial}{\partial z} (\rho K_{X(t-1)} \frac{\partial X^*}{\partial z}) \quad (3.3.1.4)$$

and

$$K_{X(t-1)} \frac{\partial X^*}{\partial z} \rightarrow C_{X(t-1)} |v_h(t-1, z)| (X^*(z) - X_S(t-1)) \quad \text{for } (z \rightarrow 0) \quad (3.3.1.5)$$

replace equations (3.3.1.1), (3.3.1.2.a) and (3.3.1.2.b), where

$$X^* = \alpha \cdot \tilde{X}(t+1) + (1 - \alpha) \cdot X(t - \Delta t)$$

In the ECHAM,  $\alpha = 1.5$ .

$X_S$  does not vary in time for the solution of one system. If nothing else was done, this would mean that the surface sensible and latent heat flux and the surface moisture flux might be inconsistent on land with the forecast values for the soil parameter  $T_S$  for  $t + \Delta t$ . This would lead to a numerical instability in  $T_S$  for a too long timestep  $\Delta t$ . One can prevent this instability by storing not only the fluxes but also their derivatives with respect to  $T_S$  and  $W_S$ . The surface routines can then treat the fluxes as linear functions of the soil parameters and a stable (semi-implicit) algorithm can be implemented.

The coefficients  $K_X$  and  $C_X$  are assumed to be the same for  $u, v, q_v, q_w$  and  $s$ . Using  $m$  and  $h$  as subscripts for momentum and heat, the problem is reduced to the determination of  $K_m$  and  $K_h$  (at all atmospheric layers) and  $C_m$  and  $C_h$  at the surface. This has to be done solely from atmospheric values (at  $t - \Delta t$ ) of  $u, v, T, q_v, q_w$  and from the surface conditions.

### 3.3.2 Surface fluxes

The surface fluxes for momentum, dry static energy and cloud water are parameterized as follows:

$$\begin{aligned}
 J_u &= \rho \cdot C_m \cdot |v_h| \cdot u \\
 J_v &= \rho \cdot C_m \cdot |v_h| \cdot v \\
 J_s &= \rho \cdot C_h \cdot |v_h| \cdot (s - s_S) \\
 J_{q_w} &= \rho \cdot C_h \cdot |v_h| \cdot (q_w - q_{wS})
 \end{aligned}
 \tag{3.3.2.1}$$

where  $C_m$  is the drag coefficient,  $C_h$  the transfer coefficient for heat and  $|v_h|$  the absolute value of the horizontal velocity.  $C_m$ ,  $C_h$  and  $|v_h|$  apply to the lowest model level at  $t - \Delta t$ .  $u$ ,  $v$  and  $s$  are the velocity components and the dry static energy to be computed implicitly for the lowest model level.  $s_S$  is the dry static energy at the surface at  $t - \Delta t$ , and  $q_{wS}$  is the cloud water content at the surface (set to zero).

The moisture flux is evaluated distinguishing between sea and land. Over sea

$$J_{q_v} = \rho \cdot C_h \cdot |v_h| \cdot \{q_v - q_s(T_S, p_S)\} \tag{3.3.2.2}$$

where  $q_s$  is the saturation specific humidity at surface temperature  $T_S$  and pressure  $p_S$ .

Over land, each grid square is divided into 4 fractions:

- |               |  |                                      |
|---------------|--|--------------------------------------|
| i. fraction   | $C_{Sn}$                                       | covered with snow                    |
| ii. fraction  | $(1 - C_{Sn}) \cdot C_l$                       | covered with water in skin reservoir |
| iii. fraction | $(1 - C_{Sn}) \cdot (1 - C_l) \cdot (1 - C_v)$ | covered with bare soil               |
| iv. fraction  | $(1 - C_{Sn}) \cdot (1 - C_l) \cdot C_v$       | covered with vegetation              |

The snow cover fraction  $C_{Sn}$  depends on the snow cover  $Sn$  :

$$C_{Sn} = \min\left(1, \frac{Sn}{Sn_{cr}}\right) \tag{3.3.2.3}$$

where  $Sn_{cr}$  is the critical snow cover (= 0.015 m equivalent water depth).

The wet skin fraction  $C_l$  is derived from the skin reservoir water content:

$$C_l = \min\left(1, \frac{W_l}{W_{lmax}}\right) \tag{3.3.2.4}$$

with

$$W_{lmax} = W_{lmax} [(1 - C_v) + C_v \cdot L_t] \tag{3.3.2.5}$$

$W_l$  is the prognostic variable for the skin reservoir content,  $W_{lmax}$  is the maximum skin reservoir con-

tent,  $C_v$  is the vegetation ratio,  $L_t$  is the leaf area index, and  $W_{lmax}$  is the maximum amount of water that can be held on one layer of leaf or bare ground. It is taken to be  $2 \cdot 10^{-4}$  m.

The grid fraction  $C_v$  occupied by vegetation is equal to the climatological field  $C_{vcl}$  except in dry conditions when the vegetation is reduced according to the following empirical expression:

$$C_v = \min \left( C_{vcl}, C_{vcl} \cdot \frac{W_S}{0.4 \cdot W_{Smax}} \right) \quad (3.3.2.6)$$

The quantity  $W_S$  represents the total amount of water available in the root zone and  $W_{Smax}$  is the field capacity (0.2 m water).

Evaporation from snow and the skin reservoir is at the potential rate

$$J_{q_v}(i), (ii) = \rho \cdot C_h \cdot |z_h| \cdot \{q_v - q_s(T_S, p_S)\} \quad (3.3.2.7)$$

For the evaporation from bare soil (no water in skin reservoir) it is assumed that the relative humidity  $h$  at the surface is related to the water content  $W_S$  of the soil:

$$J_{q_v}(iii) = \rho \cdot C_h \cdot |z_h| \cdot \{q_v - h \cdot q_s(T_S, p_S)\} \quad (3.3.2.8)$$

$$h = \max \left[ 0.5 \cdot \left( 1 - \cos \frac{\pi \cdot W_S}{W_{Smax}} \right), \min \left( 1, \frac{q_v}{q_s(T_S, p_S)} \right) \right] \quad (3.3.2.9)$$

The evaporation from dry (no water in skin reservoir) vegetated areas is proportional to the evaporation efficiency  $E$ :

$$J_{q_v}(iv) = \rho \cdot C_h \cdot |z_h| \cdot E \cdot \{q_v - q_s(T_S, p_S)\} \quad (3.3.2.10)$$

Based on Sellers et al. (1986),  $E$  is expressed as:

$$E = \left[ 1 + \frac{C_h \cdot |z_h| \cdot R_{co}(PAR)}{F(W_S)} \right]^{-1} \quad (3.3.2.11)$$

where  $R_{co}/F(W_S)$  is the stomatal resistance of the canopy, with a minimum value  $R_{co}$  dependent on the **Photosynthetically Active Radiation (PAR)**, and an empirical function of the available water in the root zone  $F(W_S)$ .

$$\frac{1}{R_{co}} = \frac{1}{k \cdot c} \left[ \frac{b}{d \cdot PAR} \cdot \ln \left( \frac{d \cdot e^{k \cdot L_t} + 1}{d + 1} \right) - \ln \left( \frac{d + e^{k \cdot L_t}}{d + 1} \right) \right] \quad (3.3.2.12)$$

where

$$d = \frac{a + b \cdot c}{c \cdot PAR}, \quad k = 0.9, \quad L_t = 4, \quad a = 5000 \text{ Jm}^{-3}, \quad b = 10 \text{ Wm}^{-2}, \quad c = 100 \text{ sm}^{-1}$$

and  $PAR$  is 55 % of the net short wave radiation at the surface. In case of dew deposition ( $q_v > q_s$ ) we set

$$E = h = 1 \quad (3.3.2.13)$$

The water stress factor  $F(W_S)$  is

$$F(W_S) = \begin{cases} 1 & \text{if } W_S \geq W_{cr} \\ \frac{W_S - W_{pwp}}{W_{cr} - W_{pwp}} & \text{if } W_{pwp} < W_S < W_{cr} \\ 0 & \text{if } W_S \leq W_{pwp} \end{cases} \quad (3.3.2.14)$$

$W_{cr}$  is a critical value taken as 50% of the field capacity  $W_{Smax}$ , while  $W_{pwp}$  is the permanent wilting point taken as 20% of  $W_{Smax}$ .

The total evaporation in a grid square combines the four fractions:

$$\begin{aligned} J_{q_v} = \rho \cdot C_h \cdot |v_h| \cdot [ & \{ C_{Sn} + (1 - C_{Sn}) \cdot C_l \} \cdot \{ q_v - q_s \} \\ & + (1 - C_{Sn}) \cdot (1 - C_l) \cdot (1 - C_v) \cdot \{ q_v - h \cdot q_s \} \\ & + (1 - C_{Sn}) \cdot (1 - C_l) \cdot C_v \cdot E \cdot \{ q_v - q_s \} ] \end{aligned} \quad (3.3.2.15)$$

### 3.3.3 Definition of the drag coefficients

The method has been described by Louis (1979) and updated subsequently in Louis et al. (1982). Only the main points are mentioned here.

Starting from the Monin-Obukhov similarity theory (using dry air for simplicity), the gradients of wind ( $u$ ) and internal energy ( $s = C_p \cdot T + g \cdot z$ ) are assumed to be universal functions of a stability parameter.

$$\frac{k}{u_*} \cdot z \cdot \frac{\partial u}{\partial z} = \phi_m(z/L) \quad (3.3.3.1.a)$$

$$\frac{k}{s_*} \cdot z \cdot \frac{\partial s}{\partial z} = \phi_h(z/L) \quad (3.3.3.1.b)$$

The stability parameter  $L$  is the Obukhov length:

$$L = \frac{s \cdot u_*^2}{k \cdot g \cdot s_*} \quad (3.3.3.2.a)$$

where  $k$  is von Karman's constant and  $u_*$  and  $s_*$  are scaling parameters derived from the fluxes:

$$\rho \cdot u_*^2 = (J_u)_{z \rightarrow 0} = \rho \cdot C_m \cdot |u|^2 \quad (3.3.3.2.b)$$

$$\rho \cdot u_* \cdot s_* = (J_s)_{z \rightarrow 0} = \rho \cdot C_h \cdot |u| \cdot (s - s_g) \quad (3.3.3.2.c)$$

Equations (3.3.3.1.a) and (3.3.3.1.b) can be integrated over the lowest model layer, and  $L$  eliminated using (3.3.3.2.a) in order to derive  $C_m$  and  $C_h$ . However, such expression cannot be obtained analytically because of the complicated form of  $\phi_m$  and  $\phi_h$ .  $C_m$  and  $C_h$  are approximated by following analytical expressions (Louis, 1979):

$$C_m = \left( \frac{k}{\ln(z/z_0)} \right)^2 \cdot f_m(Ri, z/z_0) \quad (3.3.3.3.a)$$

and

$$C_h = \left( \frac{k}{\ln(z/z_0)} \right)^2 \cdot f_h(Ri, z/z_0) \quad (3.3.3.3.b)$$

here the Richardson number  $Ri$  is defined as:

$$Ri = \frac{g \cdot \Delta z \cdot \Delta s}{C_p \cdot T \cdot |\Delta u|^2} \quad (3.3.3.4)$$

The empirical functions  $f_m$  and  $f_h$  must have the correct behaviour near neutrality and in the asymptotic

cases of high stability or instability.

- a) Near neutrality one obtains  $Ri \rightarrow 0, z/L \rightarrow 0, \phi_m = 1 + b_m \cdot z/L$  and  $\phi_h = 1 + b_h \cdot z/L$ .

We obtain then

$$\begin{aligned} f_m &\cong 1 - 2 \cdot b_m \cdot Ri \\ f_h &\cong 1 - (b_m + b_h) \cdot Ri \end{aligned} \quad (3.3.3.5)$$

Furthermore, there is some evidence (Pandolfo, 1967), that  $Ri \sim z/L$  which implies  $b_h = 2 \cdot b_m$ . Thus we have

$$f_m = 1 - 2 \cdot b \cdot Ri \quad \text{and} \quad f_h = 1 - 3 \cdot b \cdot Ri \quad (3.3.3.6)$$

In ECHAM3  $b = 5$ .

- b) In highly unstable cases only the problem of  $f_h$  in the case of vanishing  $u$  (free convection case) has been considered. To have a non-zero heat flux,  $u$  must vanish from  $(u \cdot f_h)$  for large negative  $(s - s_s)$  (that is for high negative value of  $Ri$ ). So  $f_h$  must behave like  $\sqrt{-Ri}$ .

The analytical expression chosen for the whole unstable case ( $Ri < 0$ ) is:

$$f_h = 1 - \frac{3 \cdot b \cdot Ri}{1 + C_h(z/z_0) \cdot \sqrt{-Ri}} \quad (3.3.3.7)$$

For this free convection case one can write an equation for a new similarity theory, independent of  $J_u$ ,

$$\frac{z}{s_*} \cdot \frac{\partial s}{\partial z} = C \quad (3.3.3.8)$$

with

$$s_* = \left[ \frac{(J_s/\rho)^2}{(g \cdot z)/s} \right]^{1/3}$$

Using Eq. (3.3.3.7) for the limit  $Ri \rightarrow \infty$ ,

$$C_h(z/z_0) = C \cdot 3 \cdot b \left[ \frac{k}{\ln(z/z_0)} \right]^2 [(z/z_0)^{1/3} - 1]^{3/2} \quad (3.3.3.9)$$

One can furthermore replace  $[(z/z_0)^{1/3} - 1]^{3/2}$  by  $\sqrt{(z/z_0)}$  if  $z$  is much greater than  $z_0$ , so that

$$C_h(z/z_0) = C \cdot 3 \cdot b \left[ \frac{k}{\ln(z/z_0)} \right]^2 \sqrt{(z/z_0)} \quad (3.3.3.10)$$

In order to avoid numerical problems for high  $z_0$  values that might suppress  $z$  one replaces  $(z/z_0)$  by  $(z/z_0) + 1$  in (3.3.3.10) and (3.3.3.3.a), (3.3.3.3.b).

In ECHAM3  $C = 5$ .

In the highly unstable case  $f_m$  is not very important since there is little wind shear on which to act. Therefore a similar expression to (3.3.3.7) has been chosen with the same denominator to save computing time

$$f_m = 1 - \frac{2 \cdot b \cdot Ri}{1 + 3 \cdot b \cdot C \left[ \frac{k}{\ln(z/z_0 + 1)} \right]^2 \sqrt{(z/z_0 + 1) (-Ri)}} \quad (3.3.3.11)$$

c) Finally in the highly stable case we follow Ellison (1957) by combining two equations

$$\phi_m^4 - \frac{z}{L} \phi_m^3 - 1 = 0 \quad \text{KEYPS equation} \quad (3.3.3.12)$$

and

$$\frac{\phi_m}{\phi_h} = \frac{1 - (\frac{z}{L}) / \phi_m / R_{crit}}{(1 - [(\frac{z}{L}) / \phi_m])^2} \quad (3.3.3.13)$$

The flux Richardson number  $Ri_f = \frac{z}{L} / \phi_m$  has its critical value  $R_{crit}$  for  $(Ri \rightarrow \infty)$ .

For  $\frac{z}{L} \rightarrow +\infty$  this gives

$$f_m \sim 1 / (\sqrt{Ri}) \quad \text{and} \quad f_h \sim 1 / (Ri^{3/2}) \quad (3.3.3.14)$$

For lack of better information and to minimise the computing time for the whole stable range ( $Ri > 0$ ) the following expressions have been chosen

$$f_m = \frac{1}{1 + (2 \cdot b \cdot Ri) / (\sqrt{1 + d \cdot Ri})} \quad (3.3.3.15)$$

$$f_h = \frac{1}{1 + (3 \cdot b \cdot Ri) \cdot (\sqrt{1 + d \cdot Ri})} \quad (3.3.3.16)$$

$d$  is related to the critical flux Richardson number  $R_{crit}$  by

$$R_{crit} = \frac{2}{3 \cdot d} \quad (3.3.3.17)$$

In ECHAM3  $d = 5$ .



A plot of the drag coefficients for heat and momentum, normalized by their value at neutrality, is shown in Figure 8.

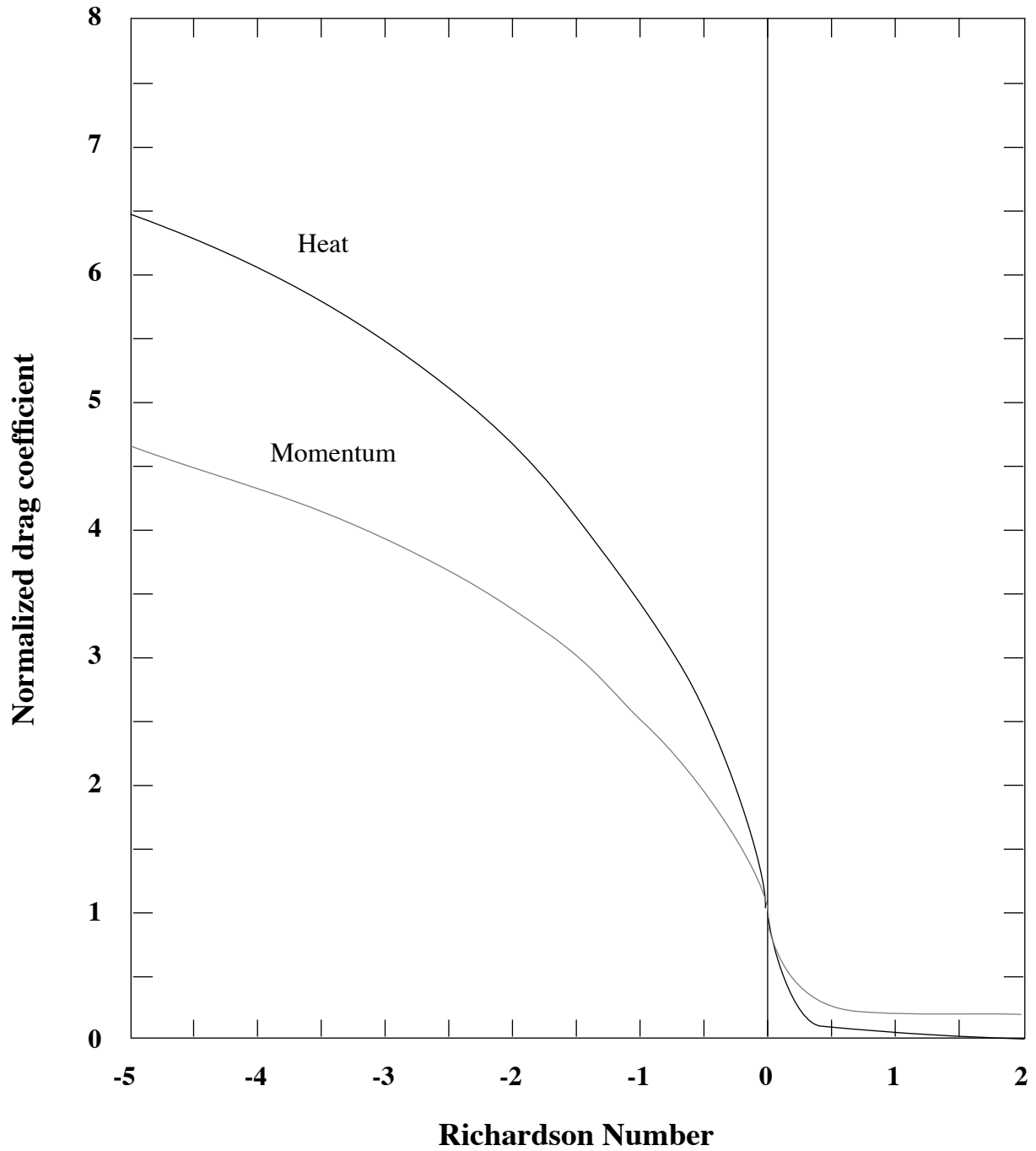


*Figure 8* Drag coefficients for heat (solid) and momentum (dashed) in terms of the Richardson number, normalized by their value at neutrality.

### 3.3.4 Definition of the exchange coefficients

The logical extension of the similarity theory for surface fluxes to the atmosphere is the mixing length approach.

$$K_m = l_m^2 \cdot \left| \frac{\partial v_h}{\partial z} \right| \cdot f_m(Ri) \quad (3.3.4.1)$$

$$K_h = l_h^2 \cdot \left| \frac{\partial v_h}{\partial z} \right| \cdot f_h(Ri) \quad (3.3.4.2)$$

The functional dependencies of  $f_m$  and  $f_h$  on  $Ri$  are the same as for  $C_m$  and  $C_h$  except that the term

$$\left[ \frac{k}{\ln(z/z_0)} \right]^2 [(z/z_0)^{1/3} - 1]^{3/2}$$

in (3.3.3.9) is replaced by its equivalent

$$\frac{l^2}{(\Delta z)^{3/2} \cdot z^{1/2}} \left[ \left( \frac{z + \Delta z}{z} \right)^{1/3} - 1 \right]^{3/2} \quad (3.3.4.3)$$

The intensity of the vertical diffusion in the atmosphere is dependent on the choice of  $l_h$  and  $l_m$ . Here, the solution of Blackadar (1962) is used, that goes smoothly from the asymptotic value  $k \cdot z$  for  $z \rightarrow 0$  to a constant value in the high atmosphere:

$$\frac{1}{l_m} = \frac{1}{k \cdot z} + \frac{1}{\lambda_m}, \quad \frac{1}{l_h} = \frac{1}{k \cdot z} + \frac{1}{\lambda_h} \quad (3.3.4.4)$$

One also has to have a relationship between  $\lambda_m$ ,  $\lambda_h$  and  $d$  so that the critical flux Richardson number in the atmosphere is 1 (e.g. a balance between shear generation and buoyancy destruction).

$$R_{crit}(z \rightarrow \infty) = \frac{2}{3d} \cdot \left( \frac{\lambda_h}{\lambda_m} \right) = 1 \quad (3.3.4.5)$$

gives  $\lambda_h = \lambda_m \sqrt{(3 \cdot d)/2}$ .

In ECHAM3  $\lambda_m = 160$  m.

### 3.3.5 Moisture and cloud effects

In the ECMWF model and also in ECHAM1 and ECHAM2, moisture effects on stability have been included by replacing the temperature  $T$  in the definition in the Richardson number (3.3.3.4) by the virtual temperature  $T_v$ , since it is  $T_v$  that determines the buoyancy in moist (but cloud-free) air. In ECHAM3 cloud effects are considered by reformulating the Richardson number to include the impact of cloud processes on the buoyancy term (Brinkop, 1992). This so-called moist Richardson number can be written according to

$$Ri_m = \frac{g}{\Theta_v} \cdot \frac{A \cdot \Delta\Theta_l + \Theta \cdot B \cdot \Delta q_t}{(\Delta u)^2 + (\Delta v)^2} \cdot \Delta z \quad (3.3.5.1)$$

where  $q_t = q_l + q_i + q_v$  is the total water content,  $\Theta_v$  is the virtual potential temperature,  $\Theta_l = \Theta - (\Theta \cdot L \cdot q_l / T \cdot C_{pd})$  is the liquid water potential temperature which is a conservative quantity in the absence of freezing, precipitation and radiative effects (Betts, 1973), and  $\Theta$  is the potential temperature.

The parameters  $A$  and  $B$  are defined as follows:

Unsaturated case

$$A_{unsat} = 1 + 0.61 \cdot q_t \quad (3.3.5.2)$$

$$B_{unsat} = 0.61 \quad (3.3.5.3)$$

Saturated case

$$A_{sat} = 1 + 0.61 \cdot q_t - \frac{0.622 \cdot \frac{L}{R_d \cdot T} \cdot q_s}{1 + 0.622 \cdot \frac{L^2}{R_d \cdot C_{pd} \cdot T^2}} \cdot \left( \frac{L}{C_{pd} \cdot T} (1 + 0.61 \cdot q_t) \right) \quad (3.3.5.4)$$

$$B_{sat} = \frac{L}{C_{pd} \cdot T} - 1 \quad (3.3.5.5)$$

The coefficients  $A$  and  $B$  in (3.3.5.1) are assumed to depend linearly on cloud cover  $b$ :

$$A = b \cdot A_{sat} + (1 - b) \cdot A_{unsat} \quad (3.3.5.6)$$

$$B = b \cdot B_{sat} + (1 - b) \cdot B_{unsat} \quad (3.3.5.7)$$

In the clear-sky case ( $b = 0$  and  $q_t = q_v$ )  $Ri_m$  as defined by (3.3.5.1) is identical to the more familiar form used in the ECMWF model, for example.

### 3.3.6 Definition of the top of the boundary layer

Two levels are computed.

- a) First level above the dynamical height (Ekman layer height).

$$h_{dyn} = 0.5 \cdot (u_* / f)$$

Equatorwards of  $20^\circ$   $f$  is set to  $5 \cdot 10^{-5} s^{-1}$ .

- b) A dry convective level,  $h_{cny}$ , is defined as the lowest level for which the static stability  $s > s_{NLEV}$ .

The top of the planetary boundary layer is then given by

$$h_{pbl} = \max(h_{dyn}, h_{cny}) \quad (3.3.6.1)$$

The above formulation takes into account early morning cases (where the dry convective boundary layer starts to develop), where considering  $h_{cny} = h_{dyn}$  would give too strong a vertical constraint for the turbulent diffusion.  $p_T$  is then calculated as the pressure of the first model level above  $h_{pbl}$ .

### 3.3.7 Roughness length

Over land the roughness length  $z_0$  is geographically prescribed. Over ice-free sea  $z_0$  is calculated from the Charnock (1955) formula:

$$z_0 = C_{char} \cdot \frac{u_*^2}{g} \quad (3.3.7.1)$$

with a minimum value for  $z_0$  of  $1.5 \cdot 10^{-5} m$ . In ECHAM3 the Charnock constant  $C_{char}$  is set to 0.018 for T21 resolution and to 0.032 for higher resolutions. Over sea ice a constant value of  $z_0 = 0.001 m$  is used.

In unstable conditions over sea an empirical interpolation for heat and moisture is used between the free convection limit and the neutral approximation (Miller et al., 1992):

$$C_h = C_{mn} \cdot (1 + C_R^\gamma)^{1/\gamma} \quad (3.3.7.2)$$

where

$$C_R = \frac{0.0016 \cdot (\Delta\Theta_v)^{1/3}}{C_{mn} \cdot |y_h|}$$

$$C_{mn} = \left( \frac{k}{\ln(z/z_0)} \right)^2$$

and  $\gamma = 1.25$ .

In stable situations the same formulation is used as over land, with  $z_0$  according to (3.3.7.1).

### 3.3.8 Vegetation

Over land, a vegetation ratio  $C_v$  is assigned to each grid box.

### 3.3.9 Kinetic energy dissipation

The kinetic energy lost by the mean flow through the diffusion process is assumed to be directly transformed into internal energy:

$$\delta T_{\text{dissipation}} = \frac{1}{C_p(q)} \cdot \varepsilon = \frac{1}{C_p(q)} \cdot \frac{u^2 + v^2 - (\tilde{u}^2 + \tilde{v}^2)}{2} \quad (3.3.9.1)$$

This procedure by-passes the sub-grid scale energy cascade, but it allows a closed energy cycle in the model.

### 3.3.10 Vertical diffusion at higher levels

Above the planetary boundary layer (cf., section 3.3.6) the vertical diffusion scheme only operates when the air is statically unstable.

### 3.4 GRAVITY WAVE DRAG

#### 3.4.1 Theory

The parameterisation scheme represents the momentum transports due to sub-grid scale gravity waves excited by stably stratified flow over irregular terrain (Miller et al., 1989). The scheme is a modified form of that proposed by Boer et al. (1984) and by Palmer et al. (1986) in which a low-level wave stress is defined together with criteria for the reduction in stress with height as the vertically propagating waves are absorbed and/or reflected.

The influence of these wave stresses in regions of wave momentum flux divergence is as follows:

$$\left(\frac{\partial \underline{v}_h}{\partial t}\right)_{\text{gravity waves}} = -g \left(\frac{\partial \underline{\tau}}{\partial p}\right)_{\text{gravity waves}}$$

where  $\underline{v}_h$  is the horizontal wind vector, and  $\underline{\tau}$  is the wave stress.

#### 3.4.2 The formulation of the scheme

The formulation of the scheme consists of two parts

- (i) The parametric form for  $\underline{\tau}(x, y, t)$
- (ii) The modelling of the dynamical processes which determine the vertical distribution.

(i) The following quantities are defined for use in the scheme:

$\underline{V}_L$  is the wind vector for a suitably defined low-level flow and  $\rho_L$ ,  $N_L$  are the low-level density and the Brunt-Väisälä frequency respectively. The function  $f_1(\underline{x})$  describes the orographic forcing of gravity waves and in the scheme described here  $f_1(\underline{x})$  is prescribed to be a directionally dependent sub-grid scale orographic variance computed from the US Navy dataset containing mean orographic heights for (1/6° lat \* 1/6° lon) areas.  $Fr$  is a form of Froude number for the low-level flow defined as

$$Fr = \frac{N_L \sqrt{f_1(\underline{x})}}{|\underline{V}_L|}$$

where  $\underline{V}_L$  represents a low-level wind vector averaged over the lowest three levels of the model.

$f_2(\underline{x})$  is an orographic anisotropy function measuring the two-dimensionality of the sub-grid scale orography

$$f_2(\underline{x}) = 1 - e^{(1-\alpha)}, \text{ and } \alpha = \max(\alpha_1, \alpha_2) \quad (3.4.2.1)$$

where  $\alpha_1$  and  $\alpha_2$  are computed from the sub-grid scale variances of the four directional components ( $N/S$ ,  $E/W$ ,  $NE/SW$ ,  $NW/SE$ )

$$\begin{aligned}\alpha_1^2 &= \max\left(\frac{\text{var}(N/S)}{\text{var}(E/W)}, \frac{\text{var}(E/W)}{\text{var}(N/S)}\right) \\ \alpha_2^2 &= \max\left(\frac{\text{var}(NE/SW)}{\text{var}(NW/SE)}, \frac{\text{var}(NW/SE)}{\text{var}(NE/SW)}\right)\end{aligned}\quad (3.4.2.2)$$

$z_c$  is the atmospheric depth corresponding to three-quarters of a hydrostatic vertical gravity wavelength and is computed by the solution of the equation

$$\int_0^{z_c} \frac{N(z)}{U(z)} dz = \frac{3\pi}{2} \quad (3.4.2.3)$$

The scheme can then be written as  $\tau_{gw}(p) = \tau_w(p) + \tau_{Fr}(p)$ .

The first term  $\tau_w(p)$  describes a part of the low-level drag and the upper part, dependent on the pressure  $p$

$$\tau_w(p) = \begin{cases} \tau_w(p_S) \cdot (1 - \beta) \cdot \frac{p - p'}{p_S - p'} & \text{for } (p \geq p') \\ \beta \cdot \tau_w(p_S) \cdot f(p) & \text{for } (p < p') \end{cases} \quad (3.4.2.4)$$

where  $f(p)$  describes the vertical stress profile, computed as shown in (ii) below.

The choice of  $p'$  determines the depth for this part of the low-level drag and is currently chosen as  $p' = 0.8 \cdot p_S$ , and  $\beta$  controls the ratio of low to high-level drag (currently equal to 0.3).

$\tau_w(p_S)$  is determined by

$$\tau_w(p_S) = K \cdot V_L \cdot N_L \cdot \text{var}^* \quad , \quad \text{where } \text{var}^* = \min(\text{var}, (Fr_c \cdot |V_L|/N_L)^2)$$

and  $Fr_c$  is the critical value for the low-level Froude number (currently equal to 2).

Analytical results of an isolated bell-shaped mountain give a value for  $K = \pi/(16 \cdot a)$  where  $a$  is the mountain half-width. Hence  $K \sim 2.5 \cdot 10^{-5} m^{-1}$  for typical sub-grid scale orography.

The second term  $\tau_{Fr}(p)$  describes the additional drag which occurs when the low-level flow is supercritical and the dynamical mechanism of resonant trapping of waves occurs leading to high-drag situations (see, for example, Peltier and Clark, 1986). It takes the form

$$\tau_{Fr}(p) = \tau_{Fr}(p_S) \cdot \frac{p - p_{z_c}}{p_S - p_{z_c}} \quad \text{if } (Fr > Fr_c) \quad (3.4.2.5)$$

where

$$\tau_{Fr}(p_S) = \begin{cases} K_L \cdot \rho \cdot \frac{V_L^3}{N_L} \cdot (Fr - Fr_c)^2 \cdot f_2(x) & \text{if } (Fr > Fr_c) \\ 0 & \text{otherwise} \end{cases}$$

$p_{z_c}$  is the pressure corresponding to the height  $z_c$  and  $K_L$  is currently 4 K. Typical values of  $z_c$  are around 3 to 5 km but much larger values do occur.

- (ii) The vertical structure of  $\tau_{gw}$  is calculated by constructing a local wave Richardson number which attempts to describe the onset of turbulence due to the gravity waves becoming convectively unstable or encountering critical layers.

This wave Richardson number can be written in the form  $\tilde{R} = \bar{R} \cdot (1 - \alpha) / (1 + \alpha \cdot \bar{R}^{1/2})^2$  where  $\bar{R}$  is the Richardson number of the basic flow. The parameter  $\alpha = N \cdot |\delta z| / u$  is a form of inverse Froude number in which  $|\delta z|$  represents the amplitude of the wave and  $u$  is the wind speed resolved in the direction of  $\tau_{gw}$ .

By requiring that  $\tilde{R}$  never falls below a critical value  $\tilde{R}_{crit}$  (currently equal to 0.25), values of wave stress are defined progressively from the surface upwards.



### 3.5 CUMULUS CONVECTION

Cumulus convection is parameterized by a mass flux scheme which is described in detail (including numerical aspects) in Tiedtke (1989). The scheme considers penetrative convection, shallow convection and midlevel convection. Clouds are represented by a bulk model and include updraft and downdraft mass fluxes. Momentum transport by convective circulations is also included following the proposal by Schneider and Lindzen (1976).

#### 3.5.1 Large-scale budget equations

The contributions from cumulus convection to the large-scale budget equations of heat, moisture and momentum are:

$$\begin{aligned}
 \left(\frac{\partial \bar{s}}{\partial t}\right)_{cu} &= -\frac{1}{\bar{\rho}} \frac{\partial}{\partial z} [M_u s_u + M_d s_d - (M_u + M_d) \bar{s}] \\
 &\quad + L (c_u - e_d - \tilde{e}_l - \tilde{e}_p) - (L_s - L_v) m \\
 \left(\frac{\partial \bar{q}_v}{\partial t}\right)_{cu} &= -\frac{1}{\bar{\rho}} \frac{\partial}{\partial z} [M_u q_u + M_d q_d - (M_u + M_d) \bar{q}_v] \\
 &\quad + (c_u - e_d - \tilde{e}_l - \tilde{e}_p) \\
 \left(\frac{\partial \bar{u}}{\partial t}\right)_{cu} &= -\frac{1}{\bar{\rho}} \frac{\partial}{\partial z} [M_u u_u + M_d u_d - (M_u + M_d) \bar{u}] \\
 \left(\frac{\partial \bar{v}}{\partial t}\right)_{cu} &= -\frac{1}{\bar{\rho}} \frac{\partial}{\partial z} [M_u v_u + M_d v_d - (M_u + M_d) \bar{v}]
 \end{aligned} \tag{3.5.1.1}$$

where  $M_u$ ,  $M_d$ ,  $c_u$  and  $e_d$  are the net contributions from all clouds to the upward mass flux, downward mass flux, condensation/sublimation and evaporation respectively, and  $s_u$ ,  $s_d$ ,  $q_u$ ,  $q_d$ ,  $u_u$ ,  $u_d$ ,  $v_u$  and  $v_d$  are the weighted averages of  $s$ ,  $q$ ,  $u$  and  $v$  from all updrafts and downdrafts. Here  $\tilde{e}_l$  is the evaporation of cloud water that has been detrained into the environment,  $\tilde{e}_p$  is the evaporation of precipitation in the unsaturated subcloud layer and  $m$  is the melting of snow. In addition to (3.5.1.1) we consider the equations for precipitation

$$\begin{aligned}
 P^w(z) &= \int (G_P^w - e_d^w - \tilde{e}_p^w + m) \bar{\rho} dz \\
 P^l(z) &= \int (G_P^l - e_d^l - \tilde{e}_p^l + m) \bar{\rho} dz
 \end{aligned} \tag{3.5.1.2}$$

where  $P^w(z)$ ,  $P^l(z)$  are the fluxes of rain water and snow at height  $z$  and  $G_P^w$  and  $G_P^l$  are the conversion rates from cloud ice and cloud water into precipitation, respectively.

### 3.5.2 Cloud model equations

The updraft of the cloud ensemble is assumed to be in a steady state. Then the bulk equations for mass, heat, moisture, cloud water content and momentum are

$$\begin{aligned}
 \frac{\partial M_u}{\partial z} &= E_u - D_u \\
 \frac{\partial}{\partial z}(M_u s_u) &= E_u \bar{s} - D_u s_u + L \bar{\rho} c_u \\
 \frac{\partial}{\partial z}(M_u q_u) &= E_u \bar{q}_v - D_u q_u - \bar{\rho} c_u \\
 \frac{\partial}{\partial z}(M_u l) &= D_u l + \bar{\rho} c_u - \bar{\rho} G_P \\
 \frac{\partial}{\partial z}(M_u u_u) &= E_u \bar{u} - D_u u_u \\
 \frac{\partial}{\partial z}(M_u v_u) &= E_u \bar{v} - D_u v_u
 \end{aligned} \tag{3.5.2.1}$$

where  $E$  and  $D$  are the rates of mass entrainment and detrainment per unit length,  $l$  is the cloud water content (water/ice) and  $c_u$  is the net condensation/sublimation in the updrafts.

Cloud air is assumed to be saturated and cloud processes are crudely represented. Freezing and melting processes are not considered and the conversion from cloud droplets to rain/snow is assumed to be proportional to the cloud water content as

$$\bar{\rho} G_P = K(z) \cdot l \cdot M_u$$

where  $K(z)$  is an empirical function that varies with height. This simple parameterization yields rather reasonable vertical distributions of the generation of raindrops (Yanai et al., 1973). Here  $K$  is assumed to be zero near cloud base and constant at higher levels

$$K(z) = \begin{cases} 0, & \text{if } (z \leq Z_B + \Delta z) \\ 2 \cdot 10^{-3} m^{-1}, & \text{if } (z > Z_B + \Delta z) \end{cases} \tag{3.5.2.2}$$

where  $\Delta z$  is 1500 m over sea and 3000 m over land. The choice of  $K = 0$  at lower levels ensures that shallow cumuli do not produce precipitation, noting that a sizeable portion of the liquid water content in nonprecipitating cumuli is of precipitation-sized drops.

We further note that the cloud water detrained into the environmental air is assumed to evaporate there instantaneously. Then

$$\bar{e}_l = \frac{1}{\bar{\rho}} \cdot D_u \cdot l \tag{3.5.2.3}$$

The vertical integration of (3.5.2.1) requires the knowledge of cloud base mass flux and mass entrainment and detrainment. Cloud-base mass flux is determined for the various types of convection from the parameterization assumptions discussed below. Entrainment of mass into convective plumes is assumed to occur through turbulent exchange of mass through the cloud edges and through organized inflow associated with large-scale convergence, detrainment through turbulent exchange and as organized outflow at the top:

$$E_u = E_u^{(1)} + E_u^{(2)}, \quad D_u = D_u^{(1)} + D_u^{(2)} \quad (3.5.2.4)$$

Turbulent entrainment and detrainment are parameterized as

$$E_u^{(1)} = \varepsilon_u M_u, \quad D_u^{(1)} = \delta_u M_u \quad (3.5.2.5)$$

where the fractional entrainment/detrainment rates depend inversely on cloud radii (Simpson and Wigert, 1969; Simpson, 1971):

$$\varepsilon_u = \frac{0.2}{R_u}, \quad \delta_u = \frac{0.2}{R_u} \quad (3.5.2.6)$$

By assuming typical cloud sizes for the various types of convection, average values of entrainment/detrainment rates are defined. In the presence of synoptic scale flow convergence, large clouds which contribute most to the convective heating and moistening are assumed to exist and consequently small values for entrainment/detrainment rates are imposed whereas in the absence of flow convergence clouds of smaller sizes with larger entrainment rates prevail. In order to keep the scheme simple we use fixed values of turbulent entrainment/detrainment rates for each of the various types of convection:

$$\varepsilon_u = \delta_u = \begin{cases} 1 \times 10^{-4} m^{-1} & \text{for penetrative and midlevel} \\ & \text{convection in the presence} \\ & \text{of large-scale flow convergence} \\ 3 \times 10^{-4} m^{-1} & \text{for shallow convection in} \\ & \text{suppressed conditions} \end{cases} \quad (3.5.2.7)$$

For penetrative convection and midlevel convection we deliberately impose a very small value typical for tropical deep convective clouds (Simpson, 1971) so as not to inhibit the penetration of clouds to large heights. For shallow convection we use a value typical for the larger trade wind cumuli (Nitta, 1975), noting that small clouds with much larger entrainment/detrainment rates which detrain immediately above cloud base are not represented in our parameterization.

The parameterization of organized entrainment and detrainment is discussed below.

Below cloud base, the net convective fluxes of heat and moisture due to updraft and compensating subsidence in the environment are assumed to decrease linearly from their values at cloud base towards zero at the surface so as not to alter the vertical structure of the subcloud layer and in particular its well-mixed character.

Downdrafts are considered to be associated with convective precipitation from the updrafts and originate from cloud air influenced by the injection of environmental air. Following Fritsch and Chappell (1980) and Foster (1958), the Level of Free Sinking (LFS) is assumed to be the highest model level where a mixture of equal parts of cloud air and saturated environmental air at wet-bulb temperature becomes negatively buoyant with respect to the environmental air. The downward mass flux is assumed to be directly proportional to the upward mass flux. Following Johnson (1976, 1980) the mass flux at the LFS is specified from the updraft mass flux at cloud base as

$$(M_d)_{LFS} = \gamma (M_u)_{base} \quad \text{with} \quad \gamma = -0.3 \quad (3.5.2.8)$$

The coefficient  $\gamma$  is a disposable parameter.

The vertical distribution of the downdraft mass flux, dry static energy and moisture below the LFS is determined by the equations for mass, dry static energy and moisture content as

$$\begin{aligned} -\frac{\partial M_d}{\partial z} &= E_d - D_d \\ -\frac{\partial}{\partial z} (M_d s_d) &= E_d \bar{s} - D_d s_d + L \bar{\rho} e_d \\ -\frac{\partial}{\partial z} (M_d q_d) &= E_d \bar{q}_v - D_d q_d + \bar{\rho} e_d \\ -\frac{\partial}{\partial z} (M_d u_d) &= E_d \bar{u} - D_d u_d \\ -\frac{\partial}{\partial z} (M_d v_d) &= E_d \bar{v} - D_d v_d \end{aligned} \quad (3.5.2.9)$$

We note that cumulus downdrafts can be viewed as the reverse of updrafts. Entrainment and detrainment in downdrafts are highly uncertain as relevant data are not available. Numerical experiments show, however, that the results are rather insensitive to changes in the entrainment and detrainment rates. We use

$$\varepsilon_d = \delta_d = 2 \times 10^{-4} m^{-1} \quad (3.5.2.10)$$

This gives a mass flux which is independent of height and which effectively detrains into the environment in the subcloud layer. We also note that  $e_d$  is the evaporation of convective rain to maintain a saturated descent and that the moistening and cooling of the environmental air injected at LFS is also due to evaporating rain. As the downdrafts are determined from the updrafts the remaining parameterization task is to specify the updraft. This is done by means of closures defined below for the various types of convection.

### a. Penetrative convection

Many diagnostic studies show that penetrative convection predominantly occurs in disturbed situations and strongly depends on low-level synoptic scale convergence. Various parameterization schemes are based on this relationship one way or another. Here, we apply a moisture convergence hypothesis:

Following Kuo (1965, 1974) and Lindzen (1981), we postulate that when there is a deep layer of conditional instability and large-scale moisture convergence, cumulus clouds exist that entrain environmental air through their base and through their sides directly proportional to the supply of moisture and detrain cloud air at higher levels.

The injection of mass into the clouds through their base is determined by imposing a moisture balance for the subcloud layer such that the moisture content is maintained in the presence of large-scale transports, turbulent transports and convective transports. This balance may be written as

$$[M_u(q_u - \bar{q}_v) + M_d(q_d - \bar{q}_v)]_B = \int_0^B \left[ \bar{y}_h \cdot \nabla \bar{q}_v + \bar{w} \frac{\partial \bar{q}_v}{\partial z} + \frac{1}{\bar{\rho}} \frac{\partial (\bar{\rho} \bar{w}' q'_v)}{\partial z} \right]_{tu} \bar{\rho} dz \quad (3.5.2.11)$$

where  $B$  denotes the cloud base height defined as the condensation level for surface air. The vertical distribution of the updraft mass flux above cloud base is determined using similar arguments as for the subcloud layer, that is, we postulate that there is organized entrainment which is directly proportional to the large-scale moisture convergence as

$$E_u^{(2)} = -\frac{\bar{\rho}}{\bar{q}_v} \left[ \bar{y}_h \cdot \nabla \bar{q}_v + \bar{w} \frac{\partial \bar{q}_v}{\partial z} \right] \quad (3.5.2.12)$$

Organized entrainment is only considered in the lower part of the cloud layer where large-scale convergence is encountered, that is, below the level of strongest vertical ascent. The idea to link the cloud mass flux directly to the large-scale moisture convergence has first been advocated by Lindzen (1981) who indicated that it may provide vertical profiles of mass flux and convective heating in good agreement with observations. The assumption (3.5.2.12) ensures that the vertical distribution of the convective mass flux follows that of the large-scale ascent which is partly supported by diagnostic studies for tropical convection (e.g. Cheng et al., 1980; Johnson, 1980). Equation (3.5.2.12) forms, together with the assumption (3.5.2.11) for the cloud base mass flux, the basic closure and as such is crucial for the performance of the parameterization of penetrative convection. The verification of the scheme during long periods of tropical convection confirms that the closure provides realistic profiles of convective mass fluxes and convective heating (see Tiedtke, 1989).

In addition to organized entrainment we consider turbulent entrainment and detrainment by equations (3.5.2.5) and (3.5.2.6).

Cumulus clouds detrain effectively at levels near to their zero-buoyancy level by means of organized outflow. Therefore, the vertical distribution of the total detrainment from all clouds depends on the spectral cloud distribution. Since spectral cloud distribution is not available, however, organized outflow is assumed to occur only in the model layer which contains the zero-buoyancy level of the deepest clouds. Our detrainment assumption implies an unimodal cloud distribution with large detrainment from the deepest clouds and little detrainment from shallow clouds and medium deep clouds.

The effect from shallow cumuli in the presence of penetrative convection has been neglected because their parameterization is still an unsolved problem. This is because the role of shallow cumuli in connection with penetrative convection is not well understood, particularly when cumulus downdraft occur simultaneously as these compete with shallow convection having similar effects on the environment as shallow cumuli (Johnson, 1976). The results obtained with this scheme indicate, however, that neglecting the contributions from shallow cumuli when penetrative convection is encountered does not introduce large errors in the convective heating and drying.

#### b. Shallow convection

Here we consider cumulus convection, which predominantly occurs in undisturbed flow, that is in the absence of large-scale convergent flow. Typical examples are trade wind cumuli under a subsidence inversion, convection occurring in the ridge region of tropical easterly waves and daytime convection over land. This type of convection seems to be effectively controlled by subcloud layer turbulence. In fact, most of the diagnostic studies carried out for tradewind cumuli show that the net upward moisture flux at cloud base level is nearly equal to the turbulent moisture flux at the surface (Le Mone and Pennell, 1976). As this implies a quasi-steady moisture balance, we shall apply the same moisture budget equation (3.5.2.11) as for penetrative convection. The difference, however, is that the moisture supply to cumulus clouds is now largely through surface evaporation as the contributions from large-scale convergence are either small or even negative, such as in the undisturbed trades where dry air is transported downward to lower levels.

Under typical tradewind conditions the vertical distribution of the total convective fluxes above cloud base is dominated by two types of clouds: very small cumuli, which in large numbers detrain immediately above cloud base, and deeper clouds, which detrain just beneath and above the trade inversion. The intrusion of cumulus clouds into the stable layer above the inversion is through overshooting of cumuli above their level of zero-buoyancy (Nitta, 1975). Because of the coarse resolution employed in large-scale models, where the vertical gridlength is typically 50 to 100 hPa, it is difficult to represent these two types. The scheme presented here ignores the effects of very small cumuli but tentatively accounts for the effects of overshooting cumuli, as we assume that a given fraction of the cloud ensemble penetrates into the inversion layer and detrains there into the environment. Thus, cloud air shall only partly detrain into the environment within the model layer that contains the zero-buoyancy level; the remaining fraction shall intrude into the next layer above and detrain there:

$$\begin{aligned}
 D_u^{(2)} &= \frac{(1 - \beta) (M_u)_{k+1/2}}{\Delta z} && \text{for top layer } k \\
 D_u^{(2)} &= \frac{\beta (M_u)_{k+1/2}}{\Delta z} && \text{for layer } k - 1
 \end{aligned}
 \tag{3.5.2.13}$$

where  $\beta$  is a tunable parameter (currently 0.15)

Although this parameterization is very crude, it clearly reproduces more realistic trade inversions than when the effect from overshooting cumuli is ignored ( $\beta = 0$ ), as then the inversion becomes too strong in the simulation and the cloud layer below the inversion too moist (see Tiedtke, 1989).

### c. Midlevel convection

Midlevel convection, that is, convective cells which have their origin not in the boundary layer but start at levels above the boundary layer, often occur at rainbands at warm fronts and in the warm sector of tropical cyclones (Browning et al., 1973; Houze et al., 1976; Herzegh and Hobbs, 1980). These cells are probably formed by the lifting of low level air until it becomes saturated (Wexler and Atlas, 1959) and the primary moisture source for the clouds is from low-level large-scale convergence (Houze et al., 1976). Often a low-level temperature inversion exists that inhibits convection from starting freely from the surface; therefore convection seems to be initiated by lifting low-level air dynamically to the level of free convection. This occurs often in connection with mesoscale circulations which might be related to conditionally symmetric instability (Bennetts and Hoskins, 1979; Bennetts and Sharp, 1982) or a wave-CISK mechanism (Emanuel, 1982).

Although it is not clear how significant the organization of convection in mesoscale rainbands is for the large-scale flow a parameterization should ideally account for both convective and mesoscale circulations. Such a parameterization, however, is presently not available and we must therefore rely on simplified schemes. Here we use a parameterization which in a simple way considers the findings of the diagnostic studies mentioned above. We assume that convection is activated when there is a large-scale ascent at lower levels, the environmental air is sufficiently moist, i.e., of relative humidity in excess of 90 %, and convectively unstable layer exists above. The free convection level is determined by lifting a parcel of environmental temperature and moisture content

$$T_u = \bar{T}, \quad q_u = \bar{q}_v \tag{3.5.2.14}$$

adiabatically, allowing for condensational heating, and then checking for buoyancy. The upward mass flux is set equal to the vertical mass transport by the large-scale flow at that level:

$$(M_u)_B = \bar{\rho}_B \bar{w}_B \tag{3.5.2.15}$$

which ensures that the amount of moisture which is vertically advected through cloud base by the large-scale ascent is fully available for the generation of convective cells.

In addition to the injection of mass through cloud base, we assume again that cloud air is produced by moisture convergence above cloud base through lateral entrainment in the same way as for penetrative convection given by equation (3.5.2.12).

### 3.5.3 Discretization of the model equations

The flux divergence in the large-scale budget equations (3.5.1.1) and in the cloud equations (3.5.2.1) and (3.5.2.9) are approximated by centered finite differences as

$$\frac{1}{\bar{\rho}} \frac{\partial}{\partial z} (M \cdot a) = g \cdot \frac{M_{k+1/2} \cdot a_{k+1/2} - M_{k-1/2} \cdot a_{k-1/2}}{p_{k+1/2} - p_{k-1/2}} \quad (3.5.3.1)$$

The definition of the large-scale variables at half levels pose a problem, when the half-level values defined by linear interpolation of full-level values (e.g.  $\bar{s}_{k+1/2} = 0.5 (\bar{s}_k + \bar{s}_{k+1})$ ). In this case very noisy profiles evolve in time particularly with regard to humidity. Much smoother profiles are obtained when the half-level values are determined by downward extrapolation from the next full level above along a cloud-ascent through that level:

$$\begin{aligned} \bar{T}_{k+1/2} &= \bar{T}_k + \left( \frac{\partial T}{\partial p} \right)_{h_s} (p_{k+1/2} - p_k) \\ \bar{q}_{k+1/2} &= \bar{q}_k + \left( \frac{\partial q}{\partial p} \right)_{h_s} (p_{k+1/2} - p_k) \end{aligned} \quad (3.5.3.2)$$

where  $h_s = s + L \cdot q_s$  is the saturation moist static energy. Using an extrapolation like (3.5.3.2) for calculating the downward transports is also more consistent with the calculations of the updrafts where cloud air is transported upwards through level  $k + 1/2$  with the thermal state below that level and equally with the downdrafts which depend only on values of  $s$  and  $q_v$  above that level. Similarly, because of (3.5.3.2) the downward transport of environmental air through the same level accounts now only for thermal properties above that level. The choice of a moist adiabat for extrapolation is dictated by the property of the moist static energy which is, by convection in the absence of downdrafts, only changed through the fluxes of moist static energy

$$\left( \frac{\partial \bar{h}}{\partial t} \right)_{cu} = -\frac{1}{\bar{\rho}} \frac{\partial}{\partial z} [M_u (h_u - \bar{h})] \quad (3.5.3.3)$$

As the lines of the saturation moist static energy  $h_s$  through point  $(p_{k+1/2}, \bar{T}_{k-1/2})$  and the updraft moist static energy are almost parallel, apart from entrainment effects, the difference  $h_u - \bar{h}$  is little affected by the vertical discretization.



The ascent in the updrafts is obtained by vertical integration of (3.5.2.1). Starting at the surface the condensation level (= lowest half-level which is saturated or supersaturated and where buoyancy is met) is determined from an adiabatic ascent. The cloud profile above cloud base is determined layer by layer by first doing a dry adiabatic ascent with entrainment and detrainment included and then adjusting temperature and moisture towards a saturated state. The cloud parcel is finally checked for positive buoyancy, that is, for excess of the virtual static energy in the cloud over the environmental value

$$(s_v)_u \geq \bar{s}_v = s + C_p \cdot T \cdot \delta \cdot 0.608 \cdot q_v \quad (3.5.3.4)$$

and cloud top is defined as the level where the parcel loses buoyancy.

Finally, we mention that for numerical reasons the environmental air must not be convectively unstably stratified:

$$\bar{s}_{k-1/2} \geq \bar{s}_{k+1/2} \quad (3.5.3.5)$$

### 3.5.4 Melting of snow

Melting of snow is parameterized as stratiform precipitation (see section 3.6 )

### 3.5.5 Evaporation of rain

The evaporation of convective rain is parameterized following a proposal of Kessler (1969), where the evaporation is assumed to be proportional to the saturation deficit  $q_s - q_v$  and to be dependent on the density of rain  $M_R$  ( $g/m^3$ )

$$E = \alpha_1 \cdot (q_s - q_v) \cdot M_R^{13/20} \quad (3.5.5.1)$$

where  $\alpha_1$  is a constant being zero for  $q_v > q_s$ .

As the density of rain  $M_R$  is not given by the model it is convenient to express it in terms of the rain intensity  $R$  [ $g / (m^2 \text{ sec})$ ] as

$$R = M_R (V_0 + w) \cong M_R \cdot V_0 \quad (3.5.5.2)$$

where  $V_0$  is the mean fall speed of rain drops which again is parameterized following Kessler (1969).

$$V_0 = \frac{\alpha_2 \cdot M_R^{1/8}}{\sqrt{p/p_s}} \quad (3.5.5.3)$$

Thus we have

$$E = \alpha_1 \cdot (q_s - q_v) \left[ \left( \frac{\sqrt{p/p_s}}{\alpha_2} \cdot R \right)^{13/20} \right]^{8/9} \quad (3.5.5.4)$$

Since the convective rain takes place only over a fraction  $C_c$  of the grid area the evaporation rate at level  $k$  becomes

$$E = C_c \cdot \alpha_1 \cdot (q_s - q_v) \left[ \left( \frac{\sqrt{p/p_S}}{\alpha_2} \cdot \frac{R}{C_c} \right) \right]^{\alpha_3} \quad (3.5.5.5)$$

where the constants have the following values (Kessler, 1969)

$$\alpha_1 = 5.44 \cdot 10^{-4}, \quad \alpha_2 = 5.09 \cdot 10^{-3}, \quad \alpha_3 = 0.5777$$

In order to save computing time (with  $\alpha_3 = 1/2$ ) we use slightly different values

$$\alpha_1 = 6.94 \cdot 10^{-4}, \quad \alpha_2 = 7.35 \cdot 10^{-3}, \quad \alpha_3 = 0.5$$

In view of the uncertainty of the fractional area of precipitating clouds a constant value of

$$C_c = 0.05$$

is assumed.

The evaporation rate is calculated implicitly in the model by means of

$$2g \frac{\partial}{\partial p} R^{1/2} = -A \quad (3.5.5.6)$$

which follows from

$$E = A \cdot R^{1/2} \quad A = \alpha_1 (q_s - q_v) \left[ \frac{\sqrt{p/p_S}}{\alpha_2} \cdot \frac{1}{C_c} \right]^{1/2} \quad (3.5.5.7)$$

and

$$E = \frac{1}{\rho} \cdot \frac{\partial R}{\partial z} = -g \cdot \frac{\partial R}{\partial p} \quad (3.5.5.8)$$

### 3.5.6 Stratocumulus

Stratocumulus convection is parameterized by means of a vertical diffusion scheme (Tiedtke et al., 1988). It is only applied in the boundary layer where it provides a net upward transport of moisture and cloud water to avoid the generation of saturated layers within a convective boundary layer.

The net effect of stratocumulus convection is given by the turbulent fluxes of heat, moisture and cloud water, which are parameterized on the basis of the eddy diffusion theory (cf., section 3.3):

$$\left( \frac{\partial s}{\partial t} \right)_{sc} = \frac{1}{\rho} \cdot \frac{\partial}{\partial z} (\rho \cdot K \cdot \frac{\partial s}{\partial z}) \quad (3.5.6.1)$$

$$\left(\frac{\partial q_v}{\partial t}\right)_{sc} = \frac{1}{\rho} \cdot \frac{\partial}{\partial z} (\rho \cdot K \cdot \frac{\partial q_v}{\partial z}) \quad (3.5.6.2)$$

$$\left(\frac{\partial q_w}{\partial t}\right)_{sc} = \frac{1}{\rho} \cdot \frac{\partial}{\partial z} (\rho \cdot K \cdot \frac{\partial q_w}{\partial z}) \quad (3.5.6.3)$$

Equations (3.5.6.1), (3.5.6.2) and (3.5.6.3) are only applied below 900 hPa and when neither the criterion for deep convection nor for shallow convection is fulfilled. Cloud base is the condensation level for surface air. Then (3.5.6.1), (3.5.6.2) and (3.5.6.3) are applied considering the fluxes through cloud base and cloud top using the following parameterization of the eddy diffusion coefficient

$$K [m^2/s] = \begin{cases} K_{max} \cdot \min\left(b \cdot \frac{q_w}{q_{wr}}, 1\right) & \text{cloud layers and cloud base} \\ K_{max} \cdot b \cdot \delta r & \text{cloud top entrainment} \\ 0 & \text{elsewhere} \end{cases}$$

where  $b$  is cloud cover (cf., equation (3.6.1.4)),  $q_{wr}$  is a cloud water threshold (currently  $3 \cdot 10^{-5}$ ),  $\delta r$  is the relative humidity jump at cloud top and  $K_{max}$  is a specified upper limit of  $K$  (currently  $10 \text{ m}^2/s$ ).

### 3.6 STRATIFORM CLOUDS

The equations relevant for the discussion of the stratiform cloud scheme are the budget equations for the mass mixing ratio of water vapour ( $q_v$ ) and cloud water ( $q_w = q_l + q_i$ ), respectively, where  $q_l$  is the liquid fraction and  $q_i$  is the solid fraction. For convenience, the governing equations are given in a compact form according to

$$\frac{\partial q_v}{\partial t} = R(q_v) - C + E \quad (3.6.1)$$

$$\frac{\partial q_w}{\partial t} = R(q_w) + C - P \quad (3.6.2)$$

where  $R(q_v)$  and  $R(q_w)$  denote the sum over all advective and sub-grid scale transports of  $q_v$  and  $q_w$ , respectively. The cloud microphysical terms are the condensation of water vapour ( $C > 0$ ), the evaporation of cloud water  $C < 0$ , the formation of precipitation by coalescence of cloud droplets and sedimentation of ice crystals ( $P > 0$ ), and the evaporation of precipitation in unsaturated air ( $E > 0$ ).

#### 3.6.1 Sub-grid scale cloud formation

Since real clouds are often smaller than the size of a grid box, sub-grid scale cloud formation is taken into account. The formalism has been developed by Sundquist (1978). Assuming that a fractional horizontal area ( $b$ ) of a grid box is covered by clouds while the remaining part ( $1 - b$ ) is cloud-free, the equations (3.6.1) and (3.6.2) are modified according to

$$\frac{\partial q_v}{\partial t} = R(q_v) - b \cdot C_c - (1 - b) \cdot C_o + (1 - b) \cdot E_o \quad (3.6.1.1)$$

$$\frac{\partial q_w}{\partial t} = R(q_w) + b \cdot C_c + (1 - b) \cdot C_o - b \cdot P_c \quad (3.6.1.2)$$

where the subscript ( $c$ ) denotes the respective process in the cloudy part and the subscript ( $o$ ) the process in the cloud-free part of the grid box. The transport terms are assumed to be identical in both parts as well as temperature and wind. Evaporation of precipitation is not allowed in the cloudy part, i.e.  $E_c = 0$ , and there is no precipitation formation outside the cloud, i.e.  $P_o = 0$ . The significance of  $C_o$ , which is formally retained in eqs. (3.6.1.1) and (3.6.1.2) will be discussed below. In the cloudy part, saturation with respect to the grid averaged temperature  $T$  is assumed,  $q_c = q_s(T)$ , while the cloud-free part is unsaturated by definition, i.e.  $q_o < q_s(T)$ . Hence, fractional cloud cover ( $b$ ) and grid-mean water vapour mixing ratio ( $q_v$ ) are related according to

$$q_v = b \cdot q_s + (1 - b) \cdot q_o \quad (3.6.1.3)$$

or, in terms of the relative humidity ( $r = q_v/q_s$ ) and solving for ( $b$ )

$$b = \frac{r - r_o}{1 - r_o} \quad (3.6.1.4)$$

for  $r > r_o$  and  $b = 0$  otherwise. The relative humidity in the cloud-free part ( $r_o$ ) has to be specified or parameterized. The choice of  $r_o$  should depend on factors such as grid resolution and sub-grid scale variance of vertical velocity (Sasamori, 1975). Presently, we specify  $r_o$  as a function of height and stability only: In stable stratification,  $r_o$  decreases linearly from the surface layer ( $r_o = 0.99$ ) to the top of the PBL ( $r_o = 0.85$ ) above which  $r_o$  remains constant. If penetrative convection occurs,  $r_o$  decreases further to a minimum value of 0.5 near the tropopause, as suggested by Xu and Krüger (1991) who showed in a modelling study of a cumulus ensemble that convectively driven stratiform clouds such as cirrus anvils may form already in a relatively dry environment.

### 3.6.2 Condensation and evaporation

Condensational growth of cloud droplets is assumed if the grid-mean relative humidity  $r$  exceeds the threshold  $r_o$ . Oppositely, an existing cloud will be diluted by evaporation if  $r < r_o$ . In the case of cloud formation by moisture convergence or adiabatic cooling, for example, any supersaturation in the cloudy part of the grid box will result in a condensational growth of cloud droplets.

A basic problem is to specify the partitioning of the net moisture convergence between the  $b$ -part and the  $(1 - b)$ -part of the grid box.

According to the definition (3.6.1.3),  $\frac{\partial q_v}{\partial t}$  may be decomposed into three parts,

$$\frac{\partial q_v}{\partial t} = b \cdot \frac{\partial q_s}{\partial t} + (1 - b) \cdot \frac{\partial q_o}{\partial t} + (q_s - q_o) \cdot \frac{\partial b}{\partial t} \quad (3.6.2.1)$$

which represent the changes of  $q_s$ ,  $q_o$  and  $b$  due to temperature changes and moisture convergence. Inserting (3.6.2.1) into (3.6.1.1) and separating the  $b$ -terms, provides the condensation (evaporation) rate  $C_c$  as a function of moisture convergence (divergence) and adiabatic cooling (heating),

$$b \cdot \frac{\partial q_s}{\partial t} = b \cdot R(q_v) - b \cdot C_c \quad (3.6.2.2)$$

According to (3.6.2.2), the  $b$ -fraction of the moisture convergence will be used for condensation while the remaining part,  $(1 - b) \cdot R(q_v)$ , increases the relative humidity in the cloud-free part. The condensation rate is calculated from the moisture convergence into pre-existing clouds only.

Furthermore, we assume that there is always an abundance of cloud condensation nuclei and ice nuclei so that condensational growth is allowed to start as soon as the 100 % relative humidity threshold in the  $b$ -part of the grid box is exceeded. The saturation water vapour pressure is calculated from Tetens formula (Lowe, 1977) with suitable coefficients for the liquid phase and ice phase, respectively.

It remains to calculate the cloud water evaporation rate ( $C_o$ ) in the cloud-free part of the grid box. Cloud water outside the  $b$ -part may be generated by advective or diffusive transports across the boundaries of the grid box while internal mixing by molecular or turbulent diffusion is neglected. Moreover, numerical effects do contribute also as, for example, the representation of cloud water by spherical harmonics in the host model. In these cases we assume that cloud water in the  $(1 - b)$ -part will be evaporated instantaneously,

$$R(q_w) + C_o = 0 \quad (3.6.2.3)$$

Note that all numerical effects are included in the transport term  $R(q_w)$  which may also become negative. In this case,  $C_o$  is positive and actually represents a condensation rate.

### 3.6.3 Precipitation formation

Analogous to equation (3.6.1.3), the grid-mean cloud water mixing ratio is given by

$$q_w = b \cdot q_c \quad (3.6.3.1)$$

assuming that all of the cloud water is confined to the cloudy part of the grid box which implies that the in-cloud mixing ratio is defined as  $q_c = q_w/b$ .

The mechanism of precipitation formation depends crucially on the cloud water phase. Since we apply only one budget equation (3.6.1.2) for the cloud water mixing ratio, the liquid and ice phases are diagnosed as a function of temperature  $T$  according to

$$q_c = q_{cl} + q_{ci} = q_c \cdot f_l(T) + q_c \cdot f_i(T) \quad (3.6.3.2)$$

with  $f_l + f_i = 1$ . The fractions  $f_l$  and  $f_i$  have been obtained from a wealth of aircraft measurements, as compiled by Matveev (1984), by applying an exponential fit to these data (Rockel et al., 1991),

$$f_l(T) = 0.0059 + 0.9941 \cdot e^{-[0.003102(T-273.15)^2]} \quad (3.6.3.3)$$

The growth of cloud droplets to precipitating rain drops by autoconversion is parameterized in a convenient exponential form (Sundquist, 1978). In addition, the collision of cloud droplets with larger rain drops is taken into account (Smith, 1990) so that the total coalescence rate is given by

$$P_{cl} = q_{cl} \left[ C_{r1} \left[ 1 - e^{-(q_{cl}/q_{cr})^2} \right] + C_{r2} \langle P \rangle \right] \quad (3.6.3.4)$$

where  $\langle P \rangle$  is the rain flux density (stratiform and convective) at the top of the respective cloud layer and  $C_{r1}$ ,  $C_{r2}$  and  $q_{cr}$  are microphysical constants which determine the efficiency of rain formation and, thus, the cloud lifetime (in ECHAM3/T42  $C_{r1} = 10^{-4} s^{-1}$ ,  $C_{r2} = 1 m^2 kg^{-1}$  and  $q_{cr} = 3 \cdot 10^{-4}$ ).

Ice crystals settle at a rate which depends on the form and size of the crystals. Both parameters are not available in the model. However, according to an observational study by Heymsfield (1977), the terminal

velocity of the crystals can be parameterized in terms of the ice water mixing ratio which is a model variable,

$$V_t = \alpha \cdot (\rho_a q_{ci})^\beta \quad (3.6.3.5)$$

where  $\rho_a$  is the air density, and the constants  $\alpha$  and  $\beta$  are obtained from a best fit to the data with a slight adjustment (tuning) in the respective model version (in ECHAM3/T42,  $\alpha = 1.77$  and  $\beta = 0.16$ ). The loss of ice crystals due to sedimentation is given by the divergence of the ice flux density,

$$P_{ci} = g \frac{\partial}{\partial p} (V_t \rho_a q_{ci}) \quad (3.6.3.6)$$

where  $p$  is the pressure and  $g$  is the acceleration of gravity. The total rate of precipitation formation is given by

$$P_c = P_{cl} + P_{ci} \quad (3.6.3.7)$$

A crucial assumption in the parameterization (3.6.3.4) - (3.6.3.7) is that the precipitation formation in a mixed phase, i.e. in a temperature range between about 0 °C and -40 °C, can be treated independently for the ice phase and the liquid phase, respectively. A proper treatment of the interaction between both phases, such as the rapid condensational growth of ice crystals at the expense of cloud droplets (Bergeron-Findeisen process), will require a more elaborate scheme which should be based on the budget equations for each phase.

### 3.6.4 Evaporation of precipitation

Precipitation falling into the cloud-free part of a grid box is exposed to evaporation which is parameterized in terms of the saturation deficit according to

$$E_o = -\frac{1}{\Delta t} \cdot \frac{\gamma \cdot (q_o - q_s)}{1 + \frac{L \cdot dq_s/dT}{C_{pd} \cdot (1 + (\delta - 1) q_v)}} \quad (3.6.4.1)$$

where  $\gamma$  is a tunable parameter (currently  $\gamma = 0.1$ ). The evaporation rate in a layer with thickness  $\Delta p$  is limited, however, by the precipitation flux density at the top of the layer, where  $\langle \rangle$  denotes a vertical integral of the respective quantity,

$$\langle E_o(p + \Delta p) \rangle \leq \langle P(p) \rangle \quad (3.6.4.2)$$

with

$$\langle P(p) \rangle = \frac{1}{g} \int_o^p [b P_c - (1 - b) E_o] dp' \quad (3.6.4.3)$$

and

$$\langle E_o(p + \Delta p) \rangle = \frac{1}{g} \int_p^{(p + \Delta p)} E_o dp' \quad (3.6.4.4)$$

### 3.6.5 Melting of snow

Melting of snow is parameterized considering observational data summarized by Mason (1971). Melting occurs in a thin layer of a few 100 m below the freezing level. We therefore assume that the snow can melt in each layer whenever the temperature exceeds 2 °C. The melting is limited not only by the snow amount but also by keeping the included cooling of the layer such that the temperature of the layer after melting is not less than the 2 °C threshold.



## 3.7 SOIL PROCESSES

### 3.7.1 General

The surface parameterization scheme comprises the evolution of a temperature profile in the soil, the soil hydrology and the snow pack over land.

The distribution of gridpoint characteristics is given according to the land-sea mask (Figure 9). The characteristics of sea ice are assumed if the sea surface temperature is below  $-1.8^{\circ}\text{C}$ . An extra mask specifies glacier areas over land covered permanently with ice.

The temperature at the interface between the atmosphere and the surface is always called  $T_S$ . This variable either contains the sea surface temperature, the temperature at the top of the snow pack, or the temperature of the upper soil layer (Figure 10).

$W_S$  is the soil moisture in [m] and  $W_I$  is the water content of the interception reservoir.



*Figure 9* Land-sea mask of the ECHAM3 model for the T42-truncation

### 3.7.2 Soil temperature

The soil is divided into five layers according to Figure 10. The thicknesses of the individual soil layers increase with depth.

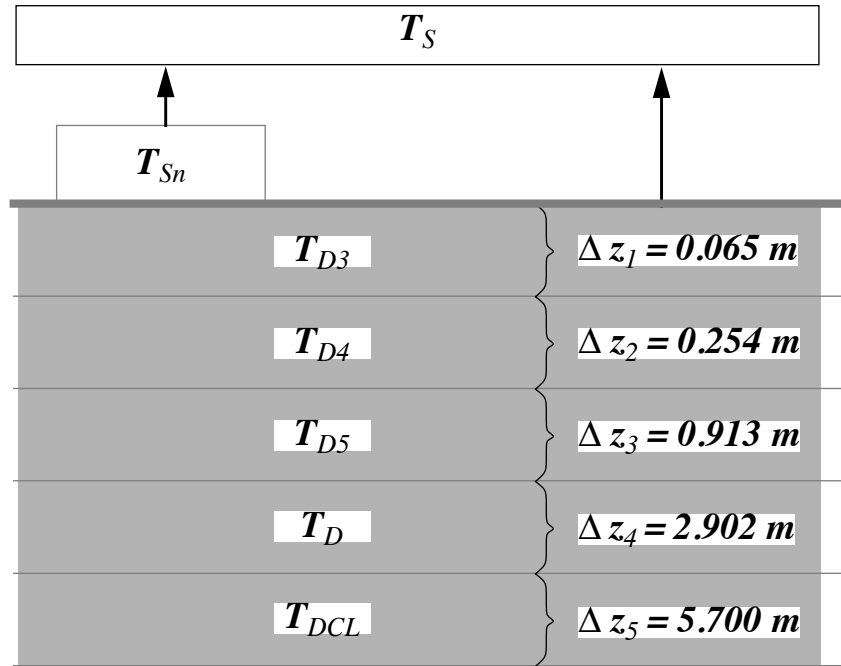


Figure 10 Description of soil temperatures in the ECHAM3 model.<sup>1</sup>

This is an extension of the scheme of Warrilow et al. (1986) to five layers. At the lowest layer boundary a zero heat flux condition is prescribed in order to ensure that no artificial heat sources and sinks may affect the energy balance of the earth-atmosphere system. The heat conduction equation follows from

$$\begin{aligned} \frac{\partial T_1}{\partial t} &= \frac{F_S}{\rho_g C_g \Delta z_1} + \frac{2\kappa(T_2 - T_1)}{\Delta z_1(\Delta z_1 + \Delta z_2)} && \text{(layer 1)} \\ \frac{\partial T_i}{\partial t} &= -\frac{2\kappa(T_i - T_{i-1})}{\Delta z_i(\Delta z_{i-1} + \Delta z_i)} + \frac{2\kappa(T_{i+1} - T_i)}{\Delta z_i(\Delta z_i + \Delta z_{i+1})} && \text{(layers 2 to 5)} \end{aligned} \quad (3.7.2.1)$$

1. Note that for technical reasons the variable  $T_S$  is always the interface temperature to the atmosphere. In snow covered areas it contains the skin temperature of the snow pack extrapolated to the top of the snow pack from  $T_{Sn}$  at the middle of the snow pack. If there is no snow it contains  $T_{D3}$ .

with

|                    |  |   |
|--------------------|--|---|
| $T_1 = T_{D3}$     | temperature for layer 1  | [K]   |
| $T_2 = T_{D4}$     | temperature for layer 2  | [K]   |
| $T_3 = T_{D5}$     | temperature for layer 3  | [K]   |
| $T_4 = T_D$        | temperature for layer 4  | [K]   |
| $T_5 = T_{DCI}$    | temperature for layer 5  | [K]   |
| $\kappa$           | heat diffusivity in the soil   | $7.5 \cdot 10^{-7} \text{ m}^2 \text{ s}^{-1}$    |
| $\rho_g \cdot C_g$ | heat capacity of the soil per unit volume or   | $2.4 \cdot 10^6 \text{ J m}^{-3} \text{ K}^{-1}$  |
|                    | heat capacity of land ice per unit volume  | $2.09 \cdot 10^6 \text{ J m}^{-3} \text{ K}^{-1}$ |
| $F_S$              | sum of the radiative and turbulent fluxes at the surface if there is no snow;<br>heat flux from the snow to the deep soil if the snow depth exceeds 0.025 m. |   |

**NOTE: All soil characteristics are assumed to be the same over all continents.**

### 3.7.3 Snow pack temperature

The scheme accounts for the three different conditions at the surface boundary in the presence of a snow pack over land:

- 1) In the case of permanent ice cover at a grid cell, the soil heat equation Eq.(3.7.2.1) is solved assuming the characteristics of ice. These areas are defined by the glacier mask GLAC.
- 2) For a snow pack of less than 0.025 m water equivalent (3.7.2.1) is solved assuming the characteristics of the bare soil.
- 3) For snow depths deeper than 0.025 m, an extra heat conduction equation (Bauer et al., 1986) evolves according to

$$\frac{\partial T_{Sn}}{\partial t} = \frac{F_S}{\rho_{Sn} \cdot C_{Sn} \cdot Sn} \quad (3.7.3.1)$$

with

|                    |  |   |
|--------------------|--|---|
| $T_{Sn}$           | temperature in the middle of the snow pack               |   |
| $F_S$              | sum of the radiative and turbulent fluxes at the surface |   |
| $\rho_{Sn} C_{Sn}$ | heat capacity of the snow per unit volume                | $0.6345 \cdot 10^6 \text{ J m}^{-3} \text{ K}^{-1}$ |
|                    | computed using a density of snow $\rho_{Sn}$ of          | $300 \text{ kg m}^{-3}$                             |
| $Sn$               | depth of the snow pack                                   |   |

### 3.7.4 Snow melt

The temperature  $T_{Sn}$  is used to define a temperature  $T_S$  at the top of the snow pack by extrapolation.  $T_S$  serves as an interface to the atmosphere. This temperature may not exceed the snow melt temperature  $T_{melt}$ . If sufficient energy is available to raise the temperature  $T_{Sn}$  above  $T_{melt}$ , this energy is used to warm the soil underneath. Only if both  $T_{D3}$  and  $T_{Sn}$  reach the value of  $T_{melt}$ , further energy input will be used to melt the snow. Snow that is less deep than 0.025 m may melt if  $T_{D3}$  equals  $T_{melt}$ .

### 3.7.5 Sea-ice temperature

The ice-surface temperature  $T_{ice}$  is calculated from the energy balance at the ice surface. To avoid problems due to a large time step it is assumed that  $T_{ice}$  represents the uppermost 10 cm of the ice sheet. The energy balance equation for this layer can be written as

$$C_{pi} \left( \frac{dT_{ice}}{dt} \right) = F_{atm} + F_{oce} \quad (3.7.5.1)$$

where  $C_{pi}$  is the heat capacity of a 10 cm ice layer.  $F_{atm}$  is the atmospheric heat flux consisting of the solar and thermal radiation and the sensible and latent heat flux. The oceanic heat flux  $F_{oce}$  is parameterized as

$$F_{oce} = \frac{\alpha}{h_{ice}} \cdot (T_{oce} - T_{ice}) \quad (3.7.5.2)$$

where  $\alpha$  is a heat transfer coefficient (2 W/mK),  $h_{ice}$  is the ice thickness and  $T_{oce}$  is the temperature of the underlying ocean.

To solve equation (3.7.5.1) the atmospheric heat flux is linearized with respect to the surface temperature at the previous time step  $T_S^{old}$

$$F_{atm}(T_{ice}) = F_{atm}(T_S^{old}) + \frac{\partial}{\partial T} F_{atm}(T_{ice} - T_S^{old}) \quad (3.7.5.3)$$

This leads to a linear equation for the new ice-surface temperature  $T_S^{new}$

$$T_S^{new} = \frac{F_{atm} - \frac{\partial}{\partial T} F_{atm} T_S^{old} + \frac{\alpha}{h_{ice}} \cdot T_{oce} + \frac{C_{pi}}{\Delta t} \cdot T_{ice}^{old}}{\frac{C_{pi}}{\Delta t} + \frac{\alpha}{h_{ice}} - \frac{\partial F_{atm}}{\partial T}} \quad (3.7.5.4)$$

### 3.7.6 Soil hydrology

The parameterisation of soil hydrology comprises three budget equations for

- i. snow amount  $S_n$  (m water equivalent) accumulated at the surface,
- ii. water amount  $W_l$  intercepted by the vegetation during rain or snow melt episodes (the so-called skin reservoir),
- iii. soil water amount  $W_s$ .

The water equivalent of the snow layer is computed over land and glacier areas from

$$\frac{\partial S_n}{\partial t} = \frac{J_{q_{Sn}} + P_{Sn} - M_{Sn}}{\rho_w} \quad (3.7.6.1)$$

with

|              |   |
|--------------|---|
| $J_{q_{Sn}}$ | evaporation rate per unit area over the snow pack |
| $P_{Sn}$     | snow fall rate per unit area                      |
| $M_{Sn}$     | snow melt rate per unit area                      |
| $\rho_w$     | density of water                                  |

Rain water and melting snow on the leaves is intercepted by the vegetation until its water holding capacity  $W_{l_{mx}}$  (cf. equation (3.3.2.5)) is exceeded. The corresponding budget equation is given by

$$\frac{\partial W_l}{\partial t} = \frac{J_{q_{vi}} + C_{ip} \cdot C_v \cdot (C_a \cdot P_R + M_{Sn})}{\rho_w} \quad (3.7.6.2)$$

with

|              |  |
|--------------|--|
| $J_{q_{vi}}$ | evaporation rate from the skin reservoir (cf., section 3.3.2)  |
| $P_R$        | rainfall rate per unit area  |
| $C_v$        | fraction of the grid box covered with vegetation (cf., (3.3.2.6))  |
| $C_{ip}$     | coefficient of efficiency of rain and snow melt interception (currently 50 %)  |
| $C_a$        | fractional area wetted by rain during a time step<br>(currently 100 % for large-scale rain and 50 % for convective rain) |

The amount of rain and snow melt which does not enter the skin reservoir is used to calculate the amount of soil infiltration and surface runoff. The soil water reservoir evolves according to

$$\frac{\partial W_s}{\partial t} = \frac{J_{q_v} - J_{q_{vi}} + P_R - P_{Ri} + M_{Sn} - M_{Sni} - R_R - R_D}{\rho_w} \quad (3.7.6.3)$$

with

|           |   |
|-----------|---|
| $J_{qv}$  | grid-mean evaporation rate per unit area according to (3.3.2.15)          |
| $P_{Ri}$  | rainfall rate per unit area intercepted by the skin reservoir             |
| $M_{Sni}$ | snow melt rate per unit area intercepted by the skin reservoir            |
| $R_R$     | surface runoff rate per unit area from precipitation events and snow melt |
| $R_D$     | runoff rate per unit area from drainage processes                         |

The computation of  $R_D$  and  $R_R$  follows the scheme by Dümenil and Todini (1992) which is based on catchment considerations. The scheme accounts for the heterogeneity of a grid area by assuming that the total field capacity  $W_{Smax}$  for the grid area results from the integral of the local field capacities which are distributed over the grid area in a non-linear way. The resulting fractional saturated area  $s/S$  is a function of the degree of the grid-mean relative soil wetness  $W_S/W_{Smax}$  and a structure parameter  $b$  that defines the sub-grid scale characteristics of the basin or grid box:

$$\frac{s}{S} = 1 - \left(1 - \frac{W_S}{W_{Smax}}\right)^b \quad (3.7.6.4)$$

Equation (3.7.6.4) defines a fractional saturated area  $s/S$  of a grid box where runoff would occur for a certain rainfall (or snow melt) event, while in the area  $1 - (s/S)$  the rainfall would infiltrate (cf., Figure 11). The surface runoff rate  $R_R$  is computed from the area integral of rain and snow melt that arrives in the saturated part  $s/S$  of the grid area. The amount of surface runoff resulting from a rainfall (or snow melt) event during a time interval  $\Delta t$  (e.g. the model time step) is computed from

$$\frac{1}{\rho_w} \int_{t_0}^{t_0 + \Delta t} R_R dt = Q - (W_{Smax} - W_S) + W_{Smax} \left[ \left(1 - \frac{W_S}{W_{Smax}}\right)^{\frac{1}{1+b}} - \frac{Q}{(1+b) \cdot W_{Smax}} \right]^{1+b} \quad (3.7.6.5)$$

if [...] > 0 or

$$\frac{1}{\rho_w} \int_{t_0}^{t_0 + \Delta t} R_R dt = Q - (W_{Smax} - W_S) \quad (3.7.6.6)$$

if [...] ≤ 0 and  $Q + W_S > W_{Smax}$

where

$$Q = \int_{t_0}^{t_0 + \Delta t} \frac{(P_R - P_{Ri} + M_{Sn} - M_{Sni})}{\rho_w} dt \quad (3.7.6.7)$$

is the total water available for infiltration and runoff after possible interception in the skin reservoir (cf., equation (3.7.6.2)).

Equation (3.7.6.6) represents the well-known “bucket model” (Manabe, 1969) where runoff is computed if the precipitation event would cause an oversaturation of the whole grid box (i.e.,  $W_S + Q > W_{Smax}$ ). Note also, that the scheme (3.7.6.5) converges to the bucket model for  $b \rightarrow 0$ .

In the ECHAM model, the structure parameter  $b$  is parameterized in terms of the sub-grid scale height distribution which is taken as a measure of the typical steepness of the terrain in the respective grid box:

$$b = \max \left[ \frac{\sigma_h - \sigma_o}{\sigma_h + \sigma_{max}}; 0.01 \right] \quad (3.7.6.8)$$

where  $\sigma_h$  is the standard deviation of the terrain height and  $\sigma_o$  and  $\sigma_{max}$  are prescribed minimum and maximum values of  $\sigma_h$  depending on the model resolution (currently,  $\sigma_o = 100$  m and  $\sigma_{max} = 1000$  (1500) m for T21 (T42) resolution).

According to the runoff parameterization (3.7.6.5) - (3.7.6.8), surface runoff is extremely efficient in steep terrain ( $b$  approaching 0.5 for  $\sigma_h \rightarrow \sigma_{max}$ ) while most of the precipitation is allowed to infiltrate the soil if the terrain is relatively flat ( $b \rightarrow 0.01$ ).

The infiltration rate per unit area  $I_R$  is defined as

$$\frac{1}{\rho_w} \int_{t_0}^{t_0 + \Delta t} I_R dt = Q - \frac{1}{\rho_w} \int_{t_0}^{t_0 + \Delta t} R_R dt \quad (3.7.6.9)$$

For frozen soil, however, we assume zero infiltration so that the surface runoff results as

$$\frac{1}{\rho_w} \int_{t_0}^{t_0 + \Delta t} R_R dt = Q \quad (3.7.6.10)$$

Runoff due to drainage processes occurs independently of the water input  $Q$  if the soil wetness is between 5 % and 90 % of the field capacity (slow drainage) or larger than 90 % (fast drainage):

$$\frac{R_D}{\rho_w} = \begin{cases} d_{min} \cdot \frac{W_S}{W_{Smax}} & \text{if } (W_{Smin} < W_S < W_{dr}) \\ d_{min} \cdot \frac{W_S}{W_{Smax}} + (d_{max} - d_{min}) \left( \frac{W_S - W_{dr}}{W_{Smax} - W_{dr}} \right)^d & \text{if } (W_S \geq W_{dr}) \end{cases} \quad (3.7.6.11)$$

with

$$d_{min} = 2.8 \cdot 10^{-10} \text{ m/s}$$

$$d_{max} = 2.8 \cdot 10^{-8} \text{ m/s}$$

$$d = 1.5$$

$$W_{Smin} = 0.05 \cdot W_{Smax}$$

$$W_{dr} = 0.9 \cdot W_{Smax}$$

The amount of evaporation is computed from the atmospheric demand (cf., section 3.3.2) but is limited by the soil moisture availability over bare soil and due to vegetation.

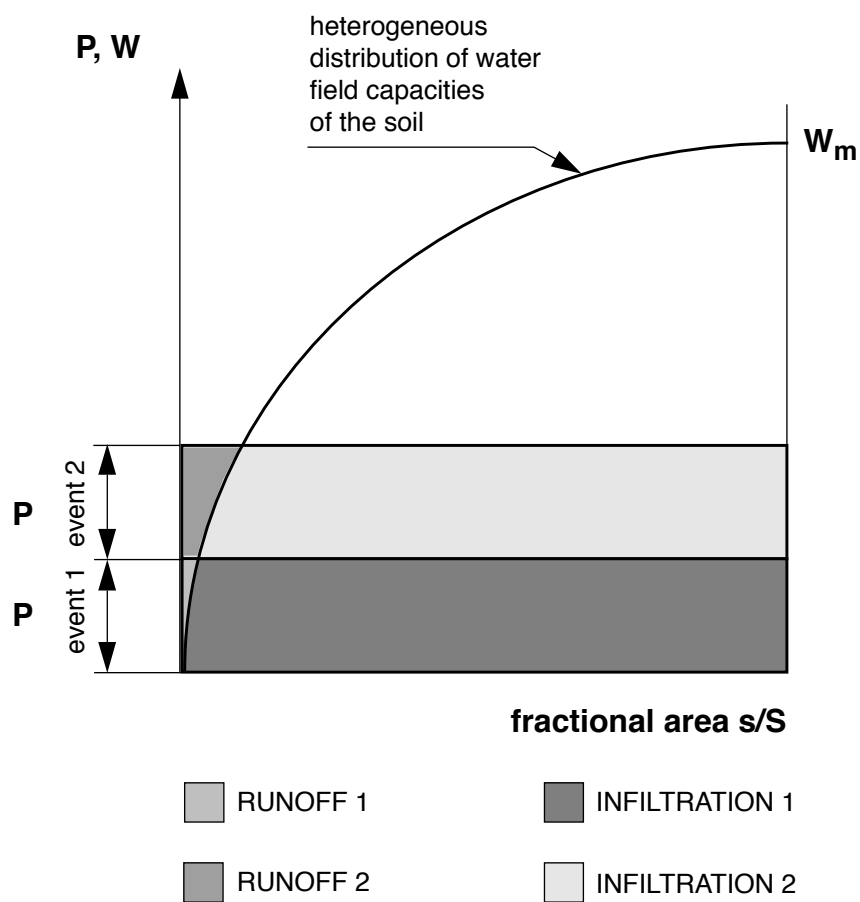


*Figure 11* Surface runoff and infiltration from precipitation events.



## 4. SYSTEM DESCRIPTION

### 4.1 OVERVIEW AND THE CONTROL ROUTINES

Figure 12 is a diagram of the ECHAM3 climate model. It shows the main sections of the model as well as the name of the control routines. The main program is called MASTER. Its function is to start the whole system by calling subroutine CONTROL.

Routine CONTROL first calls several subroutines to set up constants, default values and logical switches. The first subroutine called is INILOC, which initialises the memory manager. Then subroutine MAKESD is called to read and initialize namelist SDSCTL and store it in common block COMSDS. Subroutine INCOM which calls various subroutines to set up constants in most of the common blocks, and subroutine INILEG is called to compute Legendre coefficients needed for the Legendre transforms.

Depending on whether the run is the continuation of a previous run or a new run, CONTROL then calls either RESTART or START. The main function of these subroutines is to read the initial data and to set up the work files. The initial data exists as spherical harmonics for the atmosphere (prognostic variables) and as gridpoint data for the surface.

After labelling the run's output (subroutine LABRUN), CONTROL finally calls subroutine STEPON which supervises the actual running of the model. Essentially, STEPON organizes the scanning through the data (Figure 13). STEPON also calls the subroutines which perform calculations in spectral space (part of the semi-implicit adjustment and horizontal diffusion), it increments the timestep and checks for the completion of the run.

The computation is divided into two scans through the latitude lines. The two scan structure is shown in Figure 13. During the first scan (shown in Figure 14), all the calculations in Fourier and grid-point space are done, then direct Legendre transforms produce spherical harmonics coefficients. After performing the end of the semi-implicit adjustment and the horizontal diffusion in spectral space, a second scan (shown in Figure 15) is used to go back to Fourier space by inverse Legendre transform.

All the physical parameterisation is done in grid point space. As shown in Figure 16, it is controlled by routine PHYSC, called by GPC. The routine which computes the radiative heating rates uses a forward timestep, from  $t - \Delta t$  to  $t + \Delta t$ , using some input computed at less frequent interval, as described in section 2.5. The vertical diffusion also uses a forward timestep, but it is performed implicitly in order to keep it numerically stable despite the fine vertical resolution near the ground. The moist convection modifies the tendencies previously computed, and the stratiform precipitation routine adjusts the  $t + \Delta t$  moisture, cloud water and temperature fields.

The computations of the geopotential height and the pressure of the model levels are self-explanatory and not described here.

Overall the model computations may be divided into five main categories.

- Grid point computations.

These include the computations of non linear dynamical terms, the parametrization of diabatic processes and the treatment of linear terms which could be calculated in spectral space but only at the expense of extra storage (time filtering, linear-combinations of  $t$  and  $t - \Delta t$  values of the variables associated with the semi-implicit schemes).

- Fourier transforms.

These use a fast transform technique according to Temperton (1983) to convert from grid point to Fourier space and vice versa.

- Fourier space computations.

These include computations of zonal derivatives and of some quantities related to the semi-implicit treatment of vorticity and humidity.

- Legendre transforms.

These carry out conversion from Fourier to spectral space and vice versa. They include the computations of the meridional derivatives and of the Laplacian operator.

- Spectral computations.

These comprise the final solution of equation (2.5.43) and the spectral forms of (2.5.31) and (2.5.32), that is the completion of the semi implicit scheme. Horizontal diffusion is also computed in spectral space.

4.2 FLOW DIAGRAM

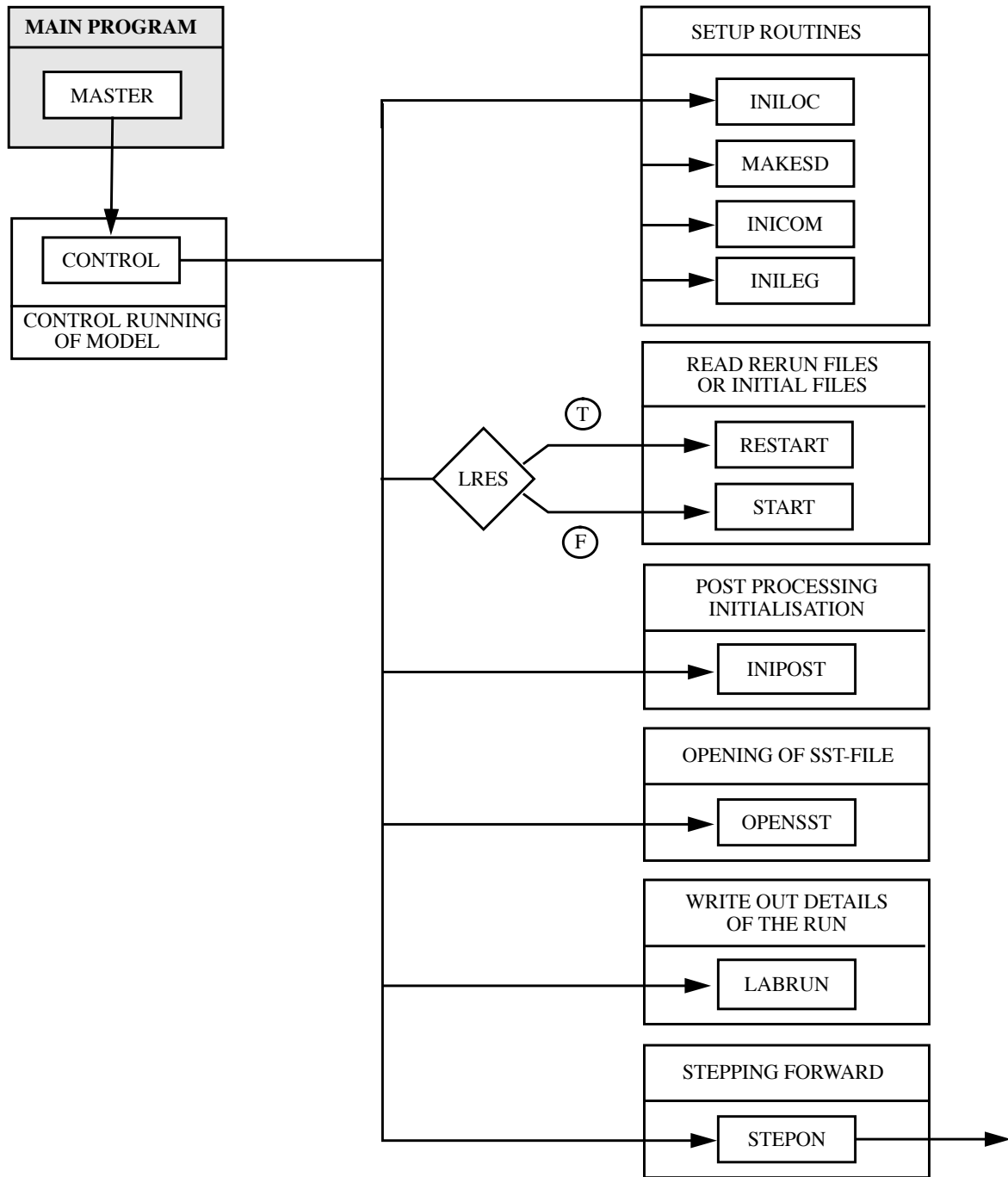


Figure 12 Flow diagram showing the initialization and control subroutines, which are managed by subroutine CONTROL.

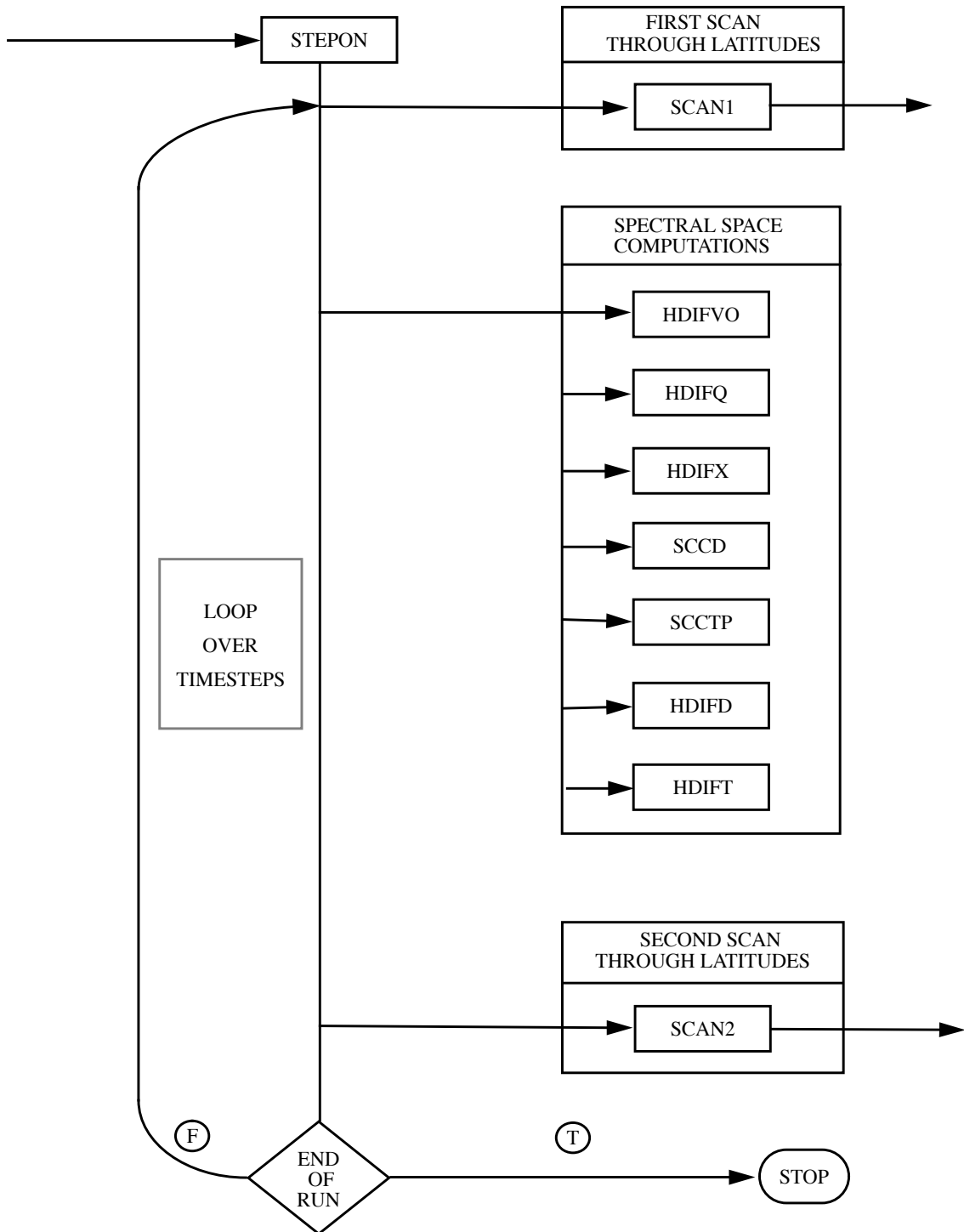


Figure 13 Flow diagram showing the two scan structure of the model, which is controlled by subroutine STEPON.

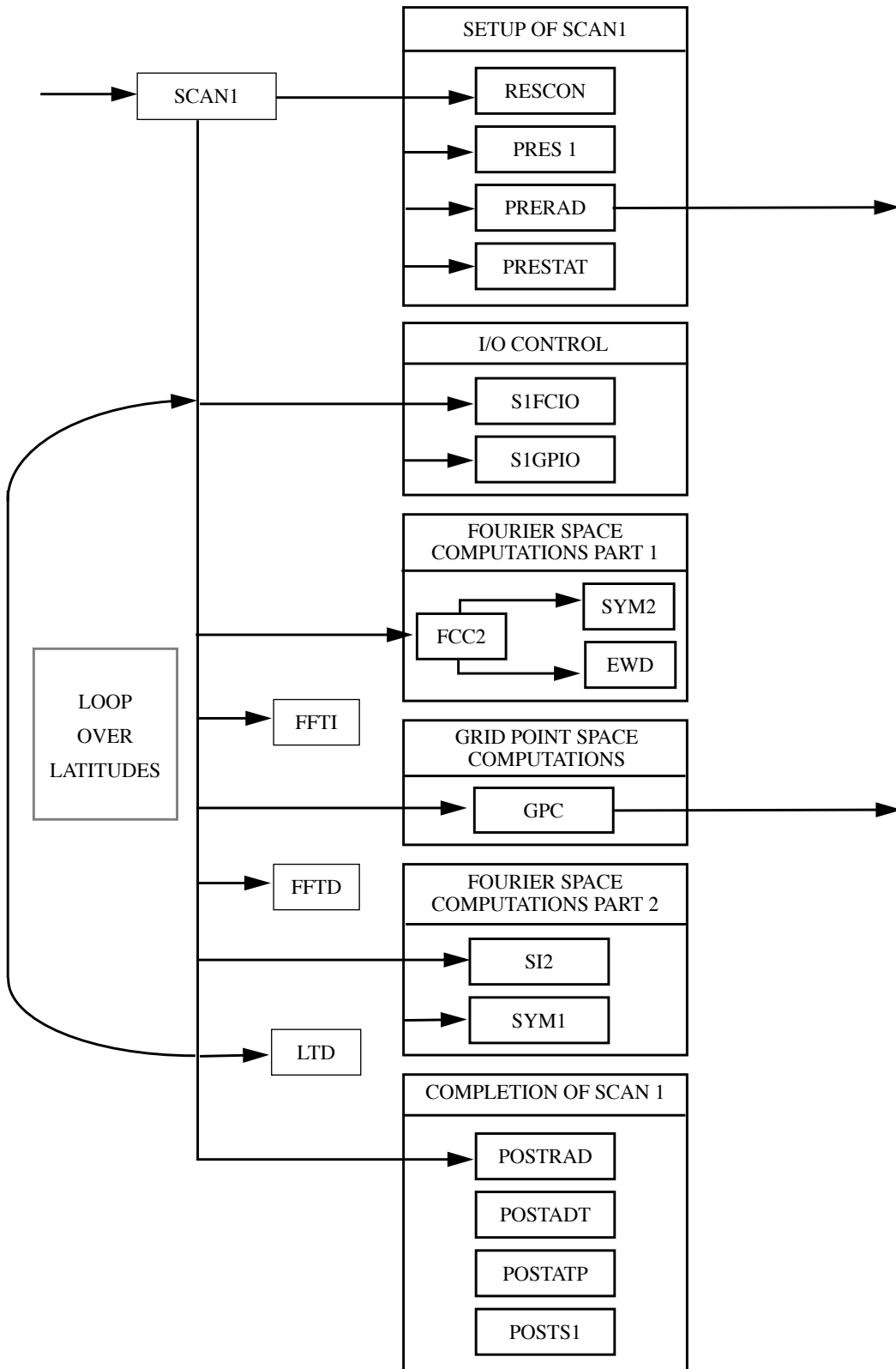
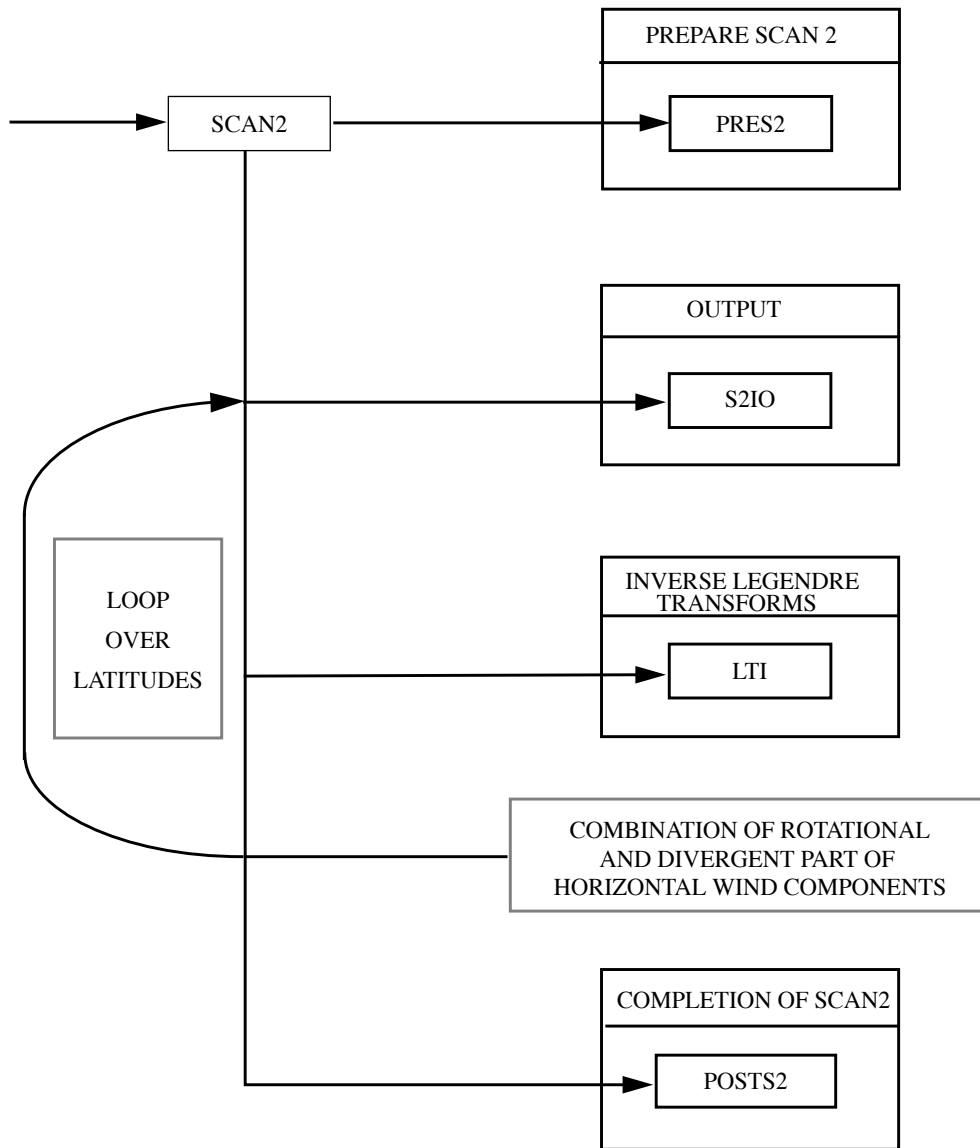


Figure 14 Flow diagram showing the detailed structure of the computations done in the first scan, which is controlled by subroutine SCAN1.



*Figure 15* Simplified flow diagram showing the main computations done in the second scan, which is controlled by subroutine SCAN2.

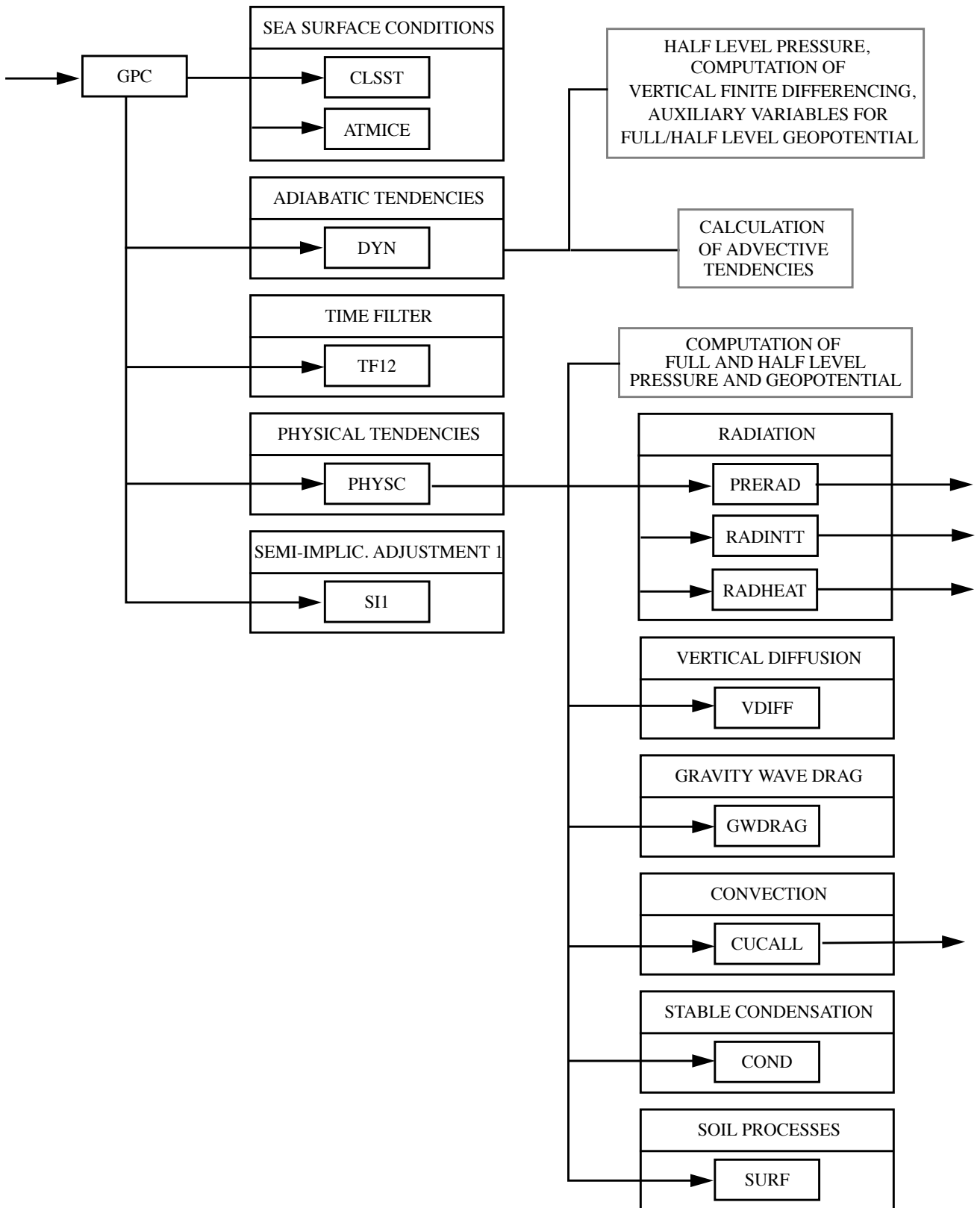
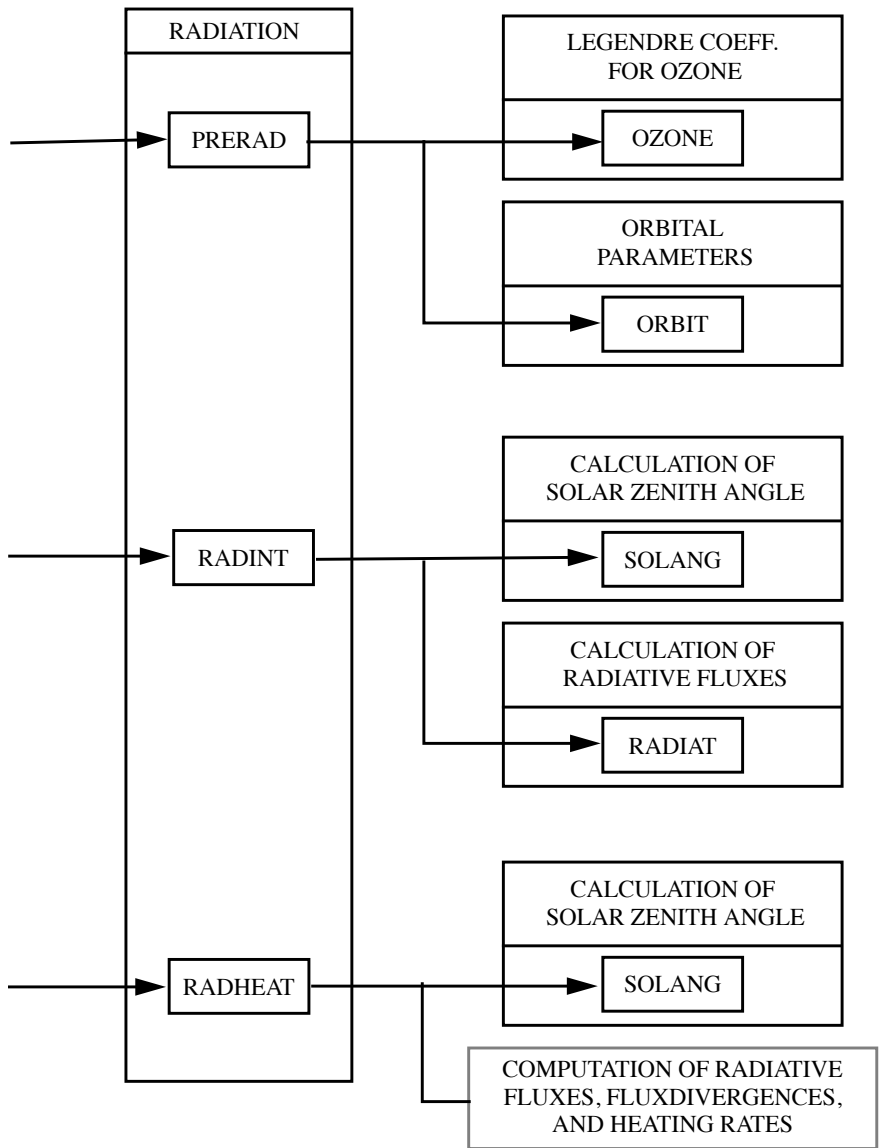


Figure 16 Flow diagram showing the grid point space computations done in the first scan controlled by subroutine GPC.



*Figure 17* Simplified flow diagram showing the structure of the radiation scheme, which is called by subroutine GPC and controlled by subroutines PRERAD, RADINT and RADHEAT.



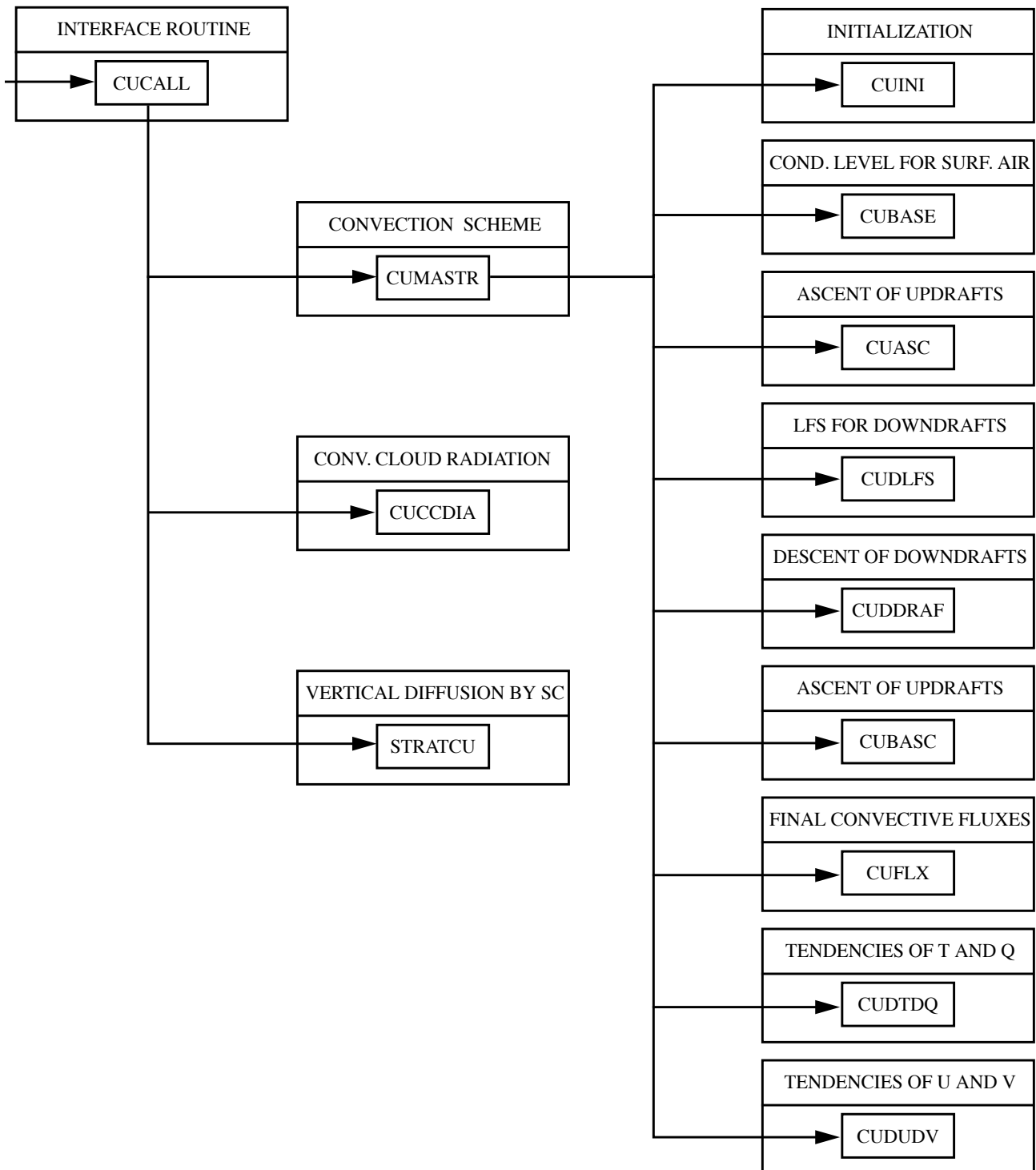


Figure 18 Flow diagram showing the structure of cumulus convection and stratocumulus schemes controlled by subroutine CUCALL.

## 4.3 COMPUTER CODE ORGANIZATION

### 4.3.1 The two scans

To save memory storage, it is necessary to store data on disk and scan through it in order only to keep in the central memory what is needed. For low resolution versions of the model (< T106) memory storage is not a problem. In this case an optional in-core version of the model can be used (LCORE=T in namelist RUNCTL). In this version the principle scanning structure of the model is the same but instead of writing to disk the data is copied into global memory buffers.

Grid point and Fourier space computations proceed one latitude row at a time. Therefore it is natural to store slices on disk or in the global memory buffer accordingly. However, when the data is represented in terms of spherical harmonics (what we also call the spectral space), the computations need a global set of spectral coefficients. These are kept in the central memory.

Subroutine SCAN1 reads through the data latitude row by latitude row. As shown in Figure 14, SCAN1 handles the computations in grid-point and Fourier space. Then it performs the direct Legendre transforms to accumulate the spectral coefficients. In order to perform the Legendre transforms efficiently it is necessary to compute the symmetric and antisymmetric parts of the Fourier components with respect to the equator. As a consequence the latitude lines are scanned alternately in the Northern and Southern hemispheres. Hence odd numbered lines go from the North pole to the equator, while even numbered lines go from the South pole to the equator.

In addition SCAN1 calls some diagnostic subroutines, as well as some subroutines to prepare the computation of radiation (PRERAD) and statistics (PRESTAT), and to print some output (POSTRAD, POSTATP, POSTATD, POSTS1).

After the computations in spectral space are finished, subroutine SCAN2 then performs the inverse Legendre transforms and stores the Fourier coefficients latitude row by latitude row, in the alternate fashion as described above. The part of the flow diagram, which is subject to the computations in subroutine SCAN2, is shown in Figure 15.

### 4.3.2 Dynamic subroutines

In this section we give some details about each subroutine involved in the adiabatic computation. The physical parametrization is controlled by subroutine PHYSC.

#### GPC

This subroutine controls all the grid-point computations, i.e. the adiabatic and physical tendencies (DYN and PHYSC), the time filtering (TF12) and the contribution of the current and previous time levels to the semi-implicit scheme (SI1). In addition, some global statistics for the dynamics and the physics are computed and printed (STATD and STATP). A schematic of the computations done in subroutine GPC is shown in Figure 16.

Some specialised subroutines are called by DYN and SI1: PRES computes the pressure at all half-levels, knowing the surface pressure. AUXHYB computes some auxiliary variables such as the pressure difference across the model layers and the logarithm of the ratio of the pressures at the half levels; GEOPOT integrates the hydrostatic equation to get the geopotential at all levels; PGRAD computes the geopotential and pressure gradient terms for the semi-implicit scheme; and CONTEQ calculates the temperature and surface pressure increments for the semi-implicit scheme.

#### FFTD and FFTI

Direct and inverse fast Fourier transforms respectively.

#### SI2

Computes the contributions to the semi-implicit scheme which can be performed using Fourier components. They are mainly related to the semi-implicit treatment of vorticity and humidity.

#### SYM1

Computes the symmetric and antisymmetric parts of the Fourier components in order to take full advantage of the symmetry properties of the Legendre polynomials in the Legendre transforms.

#### FCC2

This corresponds to the computations involving Fourier components done before the inverse Fourier transforms (FFTI). It consists of two blocks:

#### SYM2

Recomputes real Fourier components from their symmetric and antisymmetric parts.

#### EWD

Computes Fourier components of the zonal derivatives (since  $\left(\frac{\partial F}{\partial \lambda}\right)_m = im(F_m)$ ) and also Fourier components of the winds from their rotational and divergent parts.

LTD

This subroutine performs direct Legendre transforms, of which there are three types:

$$a) \quad \text{The basic ones:} \quad F_m \rightarrow F_n^m = \sum_{k=1}^K F_m(\mu_k) P_n^m(\mu_k) w(\mu_k) \quad (4.3.2.1)$$

where

$k$  scans over latitude lines,

$m$  is the zonal wave number (refer to Figure 2 on page 12),

$n$  is the meridional index (refer to Figure 2 on page 12),

$F_m$  represents Fourier components,

$P_n^m(\mu_k)$  are values of the Legendre polynomials for the corresponding latitude line,

$w(\mu_k)$  are quadrature weights (Gaussian weights),

$\mu = \cos\phi$ , the cosine of the latitude.

Equation (4.3.2.1) can also be written

$$F_n^m = \sum_{k=1}^{K/2} \{ F_m(\mu_k) P_n^m(\mu_k) w(\mu_k) + F_m(-\mu_k) P_n^m(-\mu_k) w(-\mu_k) \} \quad (4.3.2.2)$$

An important property of the Legendre polynomials is that

$$P_n^m(-\mu) = P_n^m(\mu), \quad \text{if } (n+m) \text{ even}$$

$$P_n^m(-\mu) = -P_n^m(\mu), \quad \text{if } (n+m) \text{ odd}$$

We have also  $w(-\mu) = w(\mu)$ , thus

$$F_n^m = \sum_{k=1}^{K/2} \{ F_m(\mu_k) + F_m(-\mu_k) \} P_n^m(\mu_k) w(\mu_k), \quad \text{if } (n+m) \text{ even} \quad (4.3.2.3)$$

$$F_n^m = \sum_{k=1}^{K/2} \{ F_m(\mu_k) - F_m(-\mu_k) \} P_n^m(\mu_k) w(\mu_k), \quad \text{if } (n+m) \text{ odd}$$

Using symmetric ( $F_m(\mu) + F_m(-\mu)$ ) or antisymmetric ( $F_m(\mu) - F_m(-\mu)$ ) parts of the Fourier components in this way results in a significant computational saving compared with direct use of form (4.3.2.1).

b) The meridional derivatives of the Legendre transform:

$$F_m \rightarrow \left( \frac{\partial F}{\partial \mu} \right)_n^m = - \sum_k F_m(\mu_k) A_n^m(\mu_k) w(\mu_k) \quad (4.3.2.4)$$

where

$$A_n^m(\mu_k) = \frac{\partial}{\partial \mu} P_n^m(\mu_k)$$

The negative sign corresponds to an integration by parts.

For these we also make use of symmetry properties i.e.

$$A_n^m(-\mu) = -A_n^m(\mu), \text{ for } (n+m) \text{ even}$$

$$A_n^m(-\mu) = A_n^m(\mu), \text{ for } (n+m) \text{ odd}$$

c) Laplacian operator of the Legendre transform:

$$F_m \rightarrow (\nabla^2 F)_n^m = \sum_k F_m(\mu_k) R_n^m(\mu_k) w(\mu_k)$$

with

$$R_n^m(\mu_k) = -\frac{n(n+1)}{a^2} P_n^m(\mu) \quad (4.3.2.5)$$

using the fact that spherical harmonics are eigenfunctions of the Laplacian operator on the sphere. The  $R_n^m(\mu)$  have the same symmetry properties as the  $P_n^m(\mu)$ .

### LTI

This subroutine performs inverse Legendre transforms and makes use of the same symmetric properties as the direct transforms. It computes symmetric and antisymmetric parts of Fourier components for the main fields and their meridional derivatives. Specifically,

$$\begin{aligned} & Q_m \text{ and } \left( \frac{1}{a} \frac{\partial Q}{\partial \mu} \right)_m \\ & T_m \text{ and } \left( \frac{1}{a} \frac{\partial T}{\partial \mu} \right)_m \\ & (\ln p_s)_m \text{ and } \left( \frac{1}{a} \frac{\partial}{\partial \mu} \ln p_s \right)_m. \end{aligned}$$

For vorticity and divergence LTI computes also the rotational and divergent symmetric and antisymmetric parts of the Fourier components of the wind, i.e. for  $\xi_m$ :

$$\begin{aligned} U_{\xi_m} &= \sum_n \frac{a(1-\mu)^2}{n(n+1)} \xi_n^m \frac{\partial}{\partial \mu} P_n^m \\ iV_{\xi_m} &= \sum_n \frac{am}{n(n+1)} \xi_n^m P_n^m \end{aligned}$$

and for  $D_m$

$$iU_{D_m} = \sum_n \frac{am}{n(n+1)} D_n^m P_n^m$$

$$V_{D_m} = -\sum_n \frac{a(1-\mu)^2}{n(n+1)} D_n^m \frac{\partial}{\partial \mu} P_n^m$$

These rotational and divergent parts are recombined in SYM2.

### SCCx

These subroutines perform computations in spectral space to complete the semi-implicit scheme:

- SCCD      inverts the Helmholtz equation (cf equation (2.5.43)).
- SCCTP    computes the implicit contribution of divergence (as computed in SCCD) to the surface pressure and temperature (cf equations (2.5.31) and (2.5.32)).

#### 4.4 SUBROUTINES IN ALPHABETICAL ORDER

The code of the ECHAM3 model includes much more routines, but they are not called.

The list of called routines consists of:

|                |   |
|----------------|---|
| <b>AERO</b>    | for the aerosol distribution.   |
| <b>ALLOCA</b>  | memory manager routine to allocate array space.   |
| <b>ALLOCB</b>  | memory manager routine to allocate buffer array space.  |
| <b>ATMICE</b>  | computes seaice cover and depth for uncoupled runs.   |
| <b>AUXHYB</b>  | calculates auxiliary variables connected with the vertical finite differencing scheme.  |
| <b>BSSLZR</b>  | routine to return zeros of the j0 Bessel function.  |
| <b>BUFF4A</b>  | routine to allocate buffers for the symmetric/antisymmetric Fourier-coefficients read in <b>SCAN1</b> and written in <b>SCAN2</b> . |
| <b>BUFGRD</b>  | input/output routine to allocate gridpoint buffers.   |
| <b>BUFIN</b>   | reads a buffer from disk.   |
| <b>BUFNL1</b>  | input/output routine to allocate Legendre buffer <b>L1</b>  |
| <b>BUFNL2</b>  | input/output routine to allocate Legendre buffer <b>L2</b>  |
| <b>BUFNL3</b>  | input/output routine to allocate Legendre buffer <b>L3</b>  |
| <b>BUFOUT</b>  | writes a buffer to disk.  |
| <b>CLSST</b>   | reads climate sea-surface-temperatures to atmosphere.   |
| <b>CONTEQ</b>  | computes temperature and surface pressure increments for the semi-implicit scheme.  |
| <b>CONTROL</b> | main control routine for the model.   |
| <b>COPYBFI</b> | copies a buffer from global array to row array.   |
| <b>COPYBFO</b> | copies a buffer from row array to global array.   |
| <b>COPYI</b>   | copies one integer array into another.  |
| <b>COPYRE</b>  | copies real values from 1. argument to 2. argument.   |
| <b>COTOEC</b>  | organizes the output from the cologne radiation scheme.   |
| <b>CUADJTQ</b> | adjusts T and q due to condensation in cloud ascent.  |
| <b>CUASC</b>   | calculates profiles of T, q, l, u and v, corresponding fluxes and precipitation rates during cloud ascent.                          |
| <b>CUBASE</b>  | calculates cloud base values for cumulus-parameterization.  |
| <b>CUBASMC</b> | calculates cloud base values for midlevel convection.   |
| <b>CUCALL</b>  | receives updated tendencies, precipitation and convective cloud parameters for radiation.   |
| <b>CUCCDIA</b> | updates precipitation, cloud base and top for diagnostic scheme of cumulus parameterization.  |
| <b>CUDDRAF</b> | calculates vertical profiles for cumulus downdrafts.  |
| <b>CUDLFS</b>  | calculates level of free sinking for cumulus downdrafts.  |
| <b>CUDTDQ</b>  | updates precipitation rates and tendencies of T and q.  |
| <b>CUDUDV</b>  | updates tendencies of u and v.  |

|                |  |
|----------------|--|
| <b>CUENTR</b>  | calculates en-/detrainment rates for updrafts in cumuli.                       |
| <b>CUFLX</b>   | final calculation of convective fluxes in the cloud and in the subcloud layer. |
| <b>CUMASTR</b> | master routine for massflux-scheme.  |
| <b>CUPARAM</b> | defines disposable parameters for massflux-scheme.                             |
| <b>DATEFM</b>  | calculates initial and forecast data time.                                     |
| <b>DATIM</b>   | returns date and time in ECMWF format.   |
| <b>DYN</b>     | computes adiabatic tendencies and auxilliary hybrid.                           |
| <b>ECTOCO</b>  | organises input to the cologne radiation scheme.                               |
| <b>EWD</b>     | computes east west derivatives.  |
| <b>EXPAND</b>  | expands compressed <b>G3</b> -fields.  |
| <b>FCC2</b>    | 2nd part of the computations in Fourier space.                                 |
| <b>FFTD</b>    | direct Fourier transforms.   |
| <b>FFTI</b>    | inverse Fourier transforms.  |
| <b>FLUSS</b>   | calculates long-wave radiative flux densities.                                 |
| <b>FMDDR3</b>  | routine to create model grid descriptor record(DDR3).                          |
| <b>FORMDDR</b> | routine to format data description records.                                    |
| <b>FREEALL</b> | memory manager routine to free all managed memory space.                       |
| <b>GAUAW</b>   | computes abscissas and weights for gaussian integration.                       |
| <b>GEOPOT</b>  | calculates full- or half-level geopotentials.                                  |
| <b>GETDDR</b>  | routine to read data description records.                                      |
| <b>GPC</b>     | controls grid point computations.  |
| <b>GWDRAG</b>  | does the gravity wave parameterisation.  |
| <b>GWPACK</b>  | packs directional orographic variances.  |
| <b>GWUNPK</b>  | unpacks directional orographic variances.                                      |
| <b>HARRAY</b>  | prints name and value of hollerith array.                                      |
| <b>HDIFD</b>   | horizontal diffusion on divergence.  |
| <b>HDIFQ</b>   | horizontal diffusion on humidity.  |
| <b>HDIFT</b>   | horizontal diffusion on temperature.   |
| <b>HDIFVO</b>  | horizontal diffusion on vorticity.   |
| <b>HDIFX</b>   | horizontal diffusion on extra variable.  |
| <b>HELMO</b>   | computes matrix needed to invert Helmholtz equation.                           |
| <b>HVAR</b>    | prints name and value of character variable.                                   |
| <b>IARRAY</b>  | prints name and value of integer array.  |
| <b>INHYSI</b>  | initializes constants for the vertical part of the semi-implicit scheme.       |
| <b>INICOM</b>  | sets up constants in various common blocks.                                    |
| <b>INICON</b>  | presets constants in <b>COMCON</b> .   |
| <b>INICTL</b>  | presets constants in <b>COMCTL</b> .   |
| <b>INIDIA</b>  | presets constants in <b>COMDIA</b> .   |
| <b>INIDOC</b>  | presets constants in <b>COMDOC</b> .   |
| <b>INIFFT</b>  | presets constants in <b>COMFFT</b> .   |



|                |  |
|----------------|--|
| <b>INIGAU</b>  | presets constants in <b>COMGAU</b> .   |
| <b>INIHYP</b>  | initializes constants for vertical coordinate calculations.  |
| <b>INILEG</b>  | sets up polynomials needed for the Legendre transforms.  |
| <b>INILOC</b>  | initializes memory manager tables.   |
| <b>ININMI</b>  | presets variables in <b>COMNMI</b> .   |
| <b>INIPHY</b>  | initializes physical constants of uncertain value.   |
| <b>INISOIL</b> | initiates soil temperatures at five levels.  |
| <b>INISU0</b>  | computes initial spectral components for the zonal mean wind used in linearization of vort. and hum. equation. |
| <b>INITASK</b> | sets up task control.  |
| <b>IOPOSI</b>  | routine to position data sets for an initial run.  |
| <b>IOPOSR</b>  | routine to position data sets for an resumed run.  |
| <b>IQTASK</b>  | retrieves the number of the current task.  |
| <b>IRRAD</b>   | organizes computation of long-wave radiative flux densities.   |
| <b>IVAR</b>    | print name and value of integer variable.  |
| <b>KU00</b>    | computes T and q tendencies by deep convection (ECHAM1 and 2 only).  |
| <b>LABRUN</b>  | labels a forecast run.   |
| <b>LARRAY</b>  | prints name and value of logical array.  |
| <b>LEGINV</b>  | calculates modified Legendre polynomials for inverse transform using Legendre-polynomials.                     |
| <b>LEGMOD</b>  | calculates modified Legendre polynomials for direct transform using Legendre-polynomials.                      |
| <b>LEGTRI</b>  | Legendre functions for a triangular truncation.  |
| <b>LOCATE</b>  | memory manager routine to request data.  |
| <b>LTD</b>     | direct Legendre transforms needed for all except the mean wind.  |
| <b>LTI</b>     | inverse Legendre transforms for all except the mean wind.  |
| <b>LVAR</b>    | prints name and value of logical variable.   |
| <b>LWCOND</b>  | computes large-scale water phase changes and cloud cover.  |
| <b>MAKEDDR</b> | routine to create data description records.  |
| <b>MAKESD</b>  | makes a start data set.  |
| <b>MASTER</b>  | main program.  |
| <b>MESSAGE</b> | prints 48 characters message on channel nout.  |
| <b>MMERROR</b> | memory manager error reporting routine.  |
| <b>MMGETL</b>  | memory manager routine to retrieve the table length.   |
| <b>MMGETN</b>  | memory manager routine to retrieve from the name table.  |
| <b>MMLIST</b>  | memory manager routine to trace back subroutines.  |
| <b>MMPUTN</b>  | memory manager routine to enter into the name table.   |
| <b>MMSWAPN</b> | memory manager routine to swap names in the name table.  |
| <b>MODDDR</b>  | routine to modify data description records.  |
| <b>OFFTR</b>   | memory manager routine to switch trace off.  |
| <b>ONLOCK</b>  | allows code to be protected in a multi-tasking environment.  |

|                |  |
|----------------|--|
| <b>ONTR</b>    | memory manager routine to switch trace on.   |
| <b>OPENR</b>   | opens a data set.  |
| <b>OPENSST</b> | opens SST-file.  |
| <b>OPTI</b>    | calculates long-wave optical depths.   |
| <b>OPTS</b>    | computes optical depths for solar radiation.   |
| <b>ORBIT</b>   | compute solar orbital parameters.  |
| <b>OUTGP</b>   | controls postprocessing of gridpoint fields (disk version).  |
| <b>OUTGPI</b>  | controls postprocessing of gridpoint fields (incore version).  |
| <b>OUTSP</b>   | controls postprocessing of spectral fields.  |
| <b>OZONE</b>   | compute annual cycle of the ozone distribution.  |
| <b>PACKVEG</b> | packs vegetation parameters.   |
| <b>PGRAD</b>   | computes sum of geopotential and pressure gradient terms for semi-implicit scheme.                   |
| <b>PHCS</b>    | computes the values of the Legendre polynomials and their meridional derivations.                    |
| <b>PHYSC</b>   | organises calculation of physical tendencies.  |
| <b>POSTATD</b> | completes statistics for dynamics.   |
| <b>POSTATP</b> | completes budgets for physics.   |
| <b>POSTRAD</b> | reallocates space for the matrix for the Helmholtz equation and recompute it after a radiation step. |
| <b>POSTS1</b>  | routine to complete <b>SCAN1</b> input/output.   |
| <b>POSTS2</b>  | routine to complete <b>SCAN2</b> input/output.   |
| <b>PRERAD</b>  | presets some constants for radiation before first line of latitude.                                  |
| <b>PRES</b>    | calculates half-level pressures.   |
| <b>PRES1</b>   | routine to initialise <b>SCAN1</b> input/output.   |
| <b>PRES2</b>   | routine to initialise <b>SCAN2</b> input/output.   |
| <b>PRESF</b>   | computes full-level pressures.   |
| <b>PRESTAT</b> | sets up logical switches and blank statistics at beginning of timestep.                              |
| <b>PUSHMEM</b> | memory manager routine to compress managed memory space.   |
| <b>PUTDDR</b>  | routine to process data description records.   |
| <b>QMEM</b>    | determines how much additional memory can be requested by a job.                                     |
| <b>QNEGAT</b>  | avoids negative values for specific humidity.  |
| <b>RADHEAT</b> | computes temperature changes due to radiation.   |
| <b>RADIAT</b>  | calculates long- and short-wave radiative flux densities.  |
| <b>RADINT</b>  | organizes the radiation full computations.   |
| <b>RARRAY</b>  | prints name and value of real array.   |
| <b>READR</b>   | reads a record from disk.  |
| <b>RELBUF</b>  | routine to release buffers.  |
| <b>RENAM</b>   | memory manager routine to rename data.   |
| <b>REORD</b>   | reorders Legendre polynomials.   |
| <b>RESCON</b>  | resets some constants to zero at the start of <b>SCAN1</b> .   |

|                 |   |
|-----------------|---|
| <b>RESETH</b>   | resets array hpa(kdim) to hpvalue.  |
| <b>RESETI</b>   | resets array ka(kdim) to kvalue.  |
| <b>RESETL</b>   | resets array lpa(kdim) to lpvalue.  |
| <b>RESETP</b>   | resets parameterisation scheme data.  |
| <b>RESETR</b>   | resets real array pa(kdim) to pval.   |
| <b>RESTART</b>  | routine to control the restart of an experiment.  |
| <b>RVAR</b>     | prints name and value of real variable.   |
| <b>SAVEHIS3</b> | saves history files.  |
| <b>S1FCIO</b>   | control routine for <b>SCAN1</b> Fourier coefficient input/output.                          |
| <b>S1GPIO</b>   | control routine for <b>SCAN1</b> grid point input/output.                                   |
| <b>S2IO</b>     | control routine for <b>SCAN2</b> input/output.  |
| <b>SCALEI</b>   | scales integer array by constant.   |
| <b>SCALER</b>   | scales real array by constant.  |
| <b>SCAN1</b>    | 1st scan over the latitude lines.   |
| <b>SCAN2</b>    | 2nd scan over the latitude lines.   |
| <b>SCCD</b>     | calculates final solution of the divergence equation.                                       |
| <b>SCCTP</b>    | adds the implicit contribution of divergence to temperature- and surface-pressure-equation. |
| <b>SCPAR</b>    | computes parameters used for computations in spectral space.                                |
| <b>SETBUF</b>   | routine to allocate buffers.  |
| <b>SETDDR</b>   | routine to process data description records.  |
| <b>SETDIG</b>   | presets constants for zonal mean and mask diagnostics.                                      |
| <b>SETDYN</b>   | presets and modify constants in dynamics,initialisation of commonblocks.                    |
| <b>SETPHYS</b>  | presets constants in physical common blocks.  |
| <b>SETPRES</b>  | set surface pressure to a constant value.   |
| <b>SETRAD</b>   | presets and modify constants in radiation common blocks.                                    |
| <b>SETZERO</b>  | resets accumulated diagnostic variables (disk version).                                     |
| <b>SETZEROI</b> | resets accumulated diagnostic variables (incore version).                                   |
| <b>SI1</b>      | 1st part of the semi-implicit scheme(done in grid point space).                             |
| <b>SI2</b>      | 2nd part of the semi-implicit scheme(done in Fourier space).                                |
| <b>SIGNI</b>    | scales real array by constant.  |
| <b>SIGNR</b>    | scales real array by constant.  |
| <b>SKINTEM</b>  | calculates sea-ice skin temperature.  |
| <b>SOLANG</b>   | for solar zenith angle and relative daylength.  |
| <b>SOLRAD</b>   | organizes calculation of short-wave radiative flux densities.                               |
| <b>START</b>    | routine to control the initial start-up of the experiment.                                  |
| <b>STATD</b>    | computes statistics on prognostics variables.   |
| <b>STATP</b>    | computes diagnostics of physical variables.   |
| <b>STEPON</b>   | controls the time stepping.   |
| <b>SUBJOB</b>   | submits a job at the end of a run.  |

|                |   |
|----------------|---|
| <b>SURF</b>    | updates land values of temperature, moisture and snow.  |
| <b>SW2DDR</b>  | creates a model switch data description record.   |
| <b>SW4DDR</b>  | routine to create model switch for <b>G4</b> file.  |
| <b>SYM1</b>    | computes symmetric and antisymmetric parts of Fourier components.                                       |
| <b>SYM2</b>    | computes Fourier components from their symmetric-asymmetric parts.                                      |
| <b>TF12</b>    | 1st and 2nd part of time filtering.   |
| <b>TTRACE</b>  | memory manager backtracing routine.   |
| <b>UNLOC</b>   | memory manager routine to release an array.   |
| <b>UNPKVEG</b> | unpacks vegetation parameters.  |
| <b>VARIA</b>   | computes temperature profiles, heights of ozone maximum and absorber amounts for radiation calculation. |
| <b>VDIFF</b>   | does the vertical exchange of u,v,T,q by turbulence.  |
| <b>WAITR</b>   | waits for completion of an I/O process.   |
| <b>WRITER</b>  | writes a record to disk.  |

## 4.5 TECHNICAL DETAILS

### 4.5.1 Internal data flow of the model

Figure 19 is a simplified diagram of the data flow in the model. As an example, the various memory buffers, data transformations and I/O processes are shown for the prognostic variable  $X$  (cloud water).

As described in section 2.5 two time levels of prognostic variables are required. They are stored in two global buffers. The data for the  $t - 1$  level are stored as grid point values in the global grid point buffer and the  $t$  level is stored as Fourier coefficients in the global Fourier buffer. A third global buffer is provided for Legendre constants. In the in-core version of the model the global buffers are stored in memory and in the disk version they reside on work files.

At the beginning of SCAN1  $t - 1$  and  $t$ -values are copied from global buffers via SIGPIO and S1FCIO into their respective latitude slice buffers.

Symmetric and antisymmetric Fourier components of cloud water (FSX, FAX) and their meridional derivatives (FSXM, FAXM) of time level  $t$  are recombined in SYM2 and are stored in arrays X and DXM respectively. Routine EWD computes Fourier components of the zonal derivatives (DXL). The Fourier components of the main field and their horizontal derivatives are transformed to grid point space via the inverse Fourier transformation FFTI. In DYN the derivatives are used to compute horizontal advection which is part of the adiabatic tendency stored in array XE. In TF12 the first part of the time-filter is applied to the main field (equation (2.5.11)). The result is stored in array XF and is copied to the global grid point buffer via SIGPIO.

Grid point values of time level  $t - 1$  are stored in array XM1. In TF12 the second part of the time filter is applied (equation (2.5.12)) which gives fully filtered values XM1. XM1 and the adiabatic tendency XE contribute to the diabatic tendency which is calculated in PHYSC. The first part of the semi implicit time integration is performed in SI1 where the accumulated adiabatic and diabatic tendency XE is added. The result is transformed to Fourier space via the direct Fourier transformation FFTD. In the second part of the semi implicit scheme SI2 some implicit contributions are added. In SYM1 the result is split into symmetric and antisymmetric components which are stored in arrays FSX1 and FAX1. The accumulation of spectral coefficients SX is performed via the direct Legendre transform LTD using Legendre constants from the third global buffer. After the first scan through the latitudes is completed a global set of spectral coefficients is provided in array SX. In spectral space the semi implicit scheme is completed and horizontal diffusion is computed. In the second scan inverse Legendre transforms are performed in routine LTI which computes symmetric and antisymmetric parts of Fourier components for the main field (FSX, FAX) and their meridional derivatives (FSXM, FAXM).

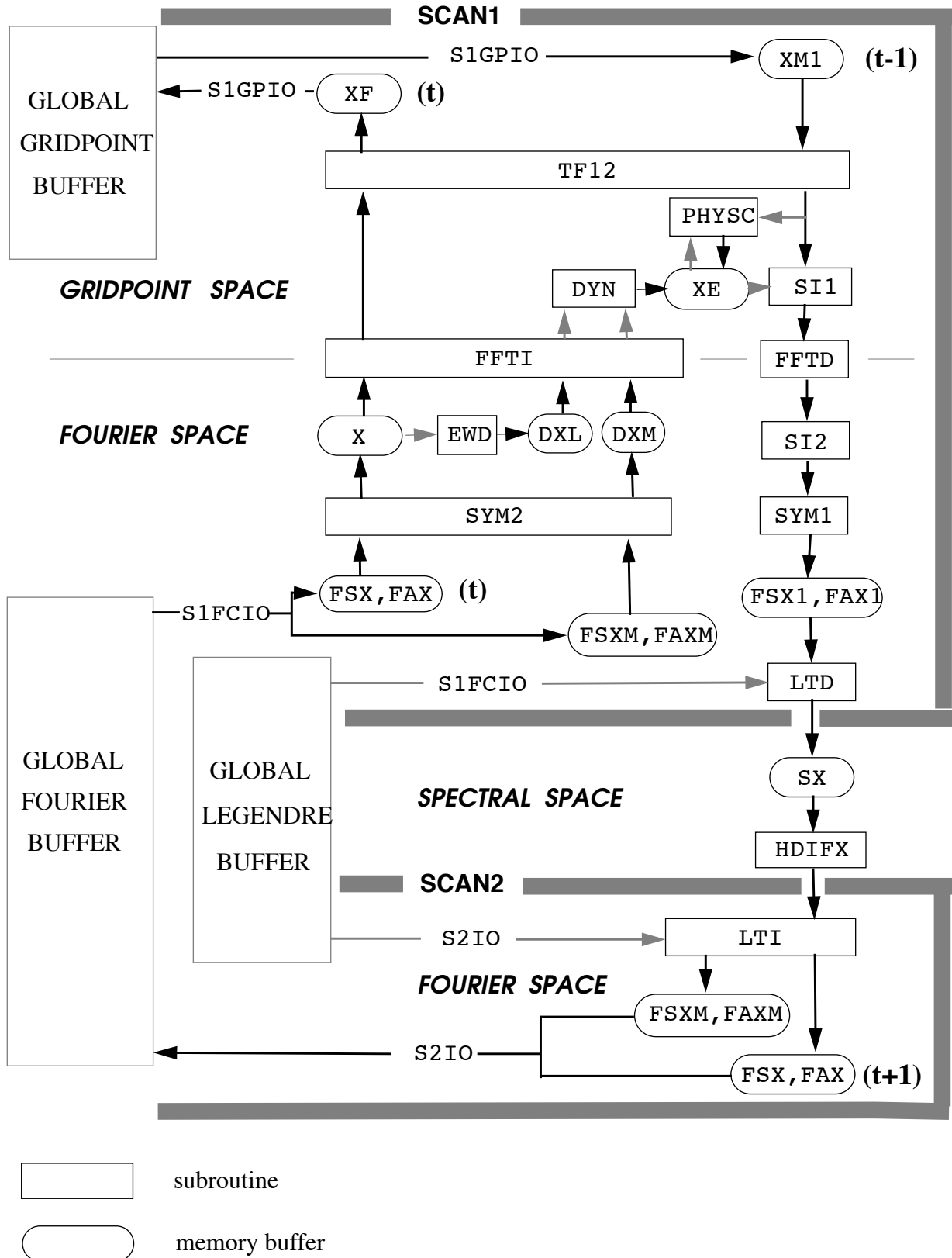


Figure 19 Data flow for the prognostic variable  $X$  (cloud water) in the ECHAM3 spectral model

4.5.2 Connection between buffers, work- and history-files

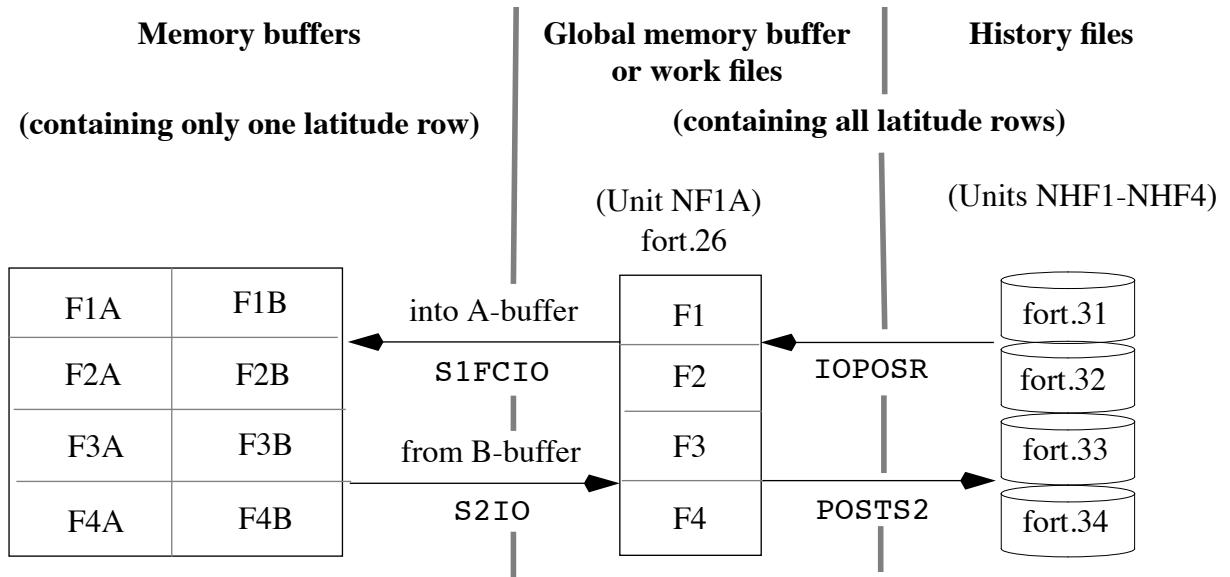


Figure 20 Associated memory buffers, work- and history files for Fourier components.

The F-buffers are allocated in subroutine BUFF4A. FA and FB buffers both have the same memory addresses, because they are not used at the same time. FA buffers are used in the first scan (SCAN1) and contain fields and their meridional derivatives of prognostic variables and wind components at time  $t$ , while FB buffers are used in the second scan (SCAN2) for variables at time  $t + 1$ .

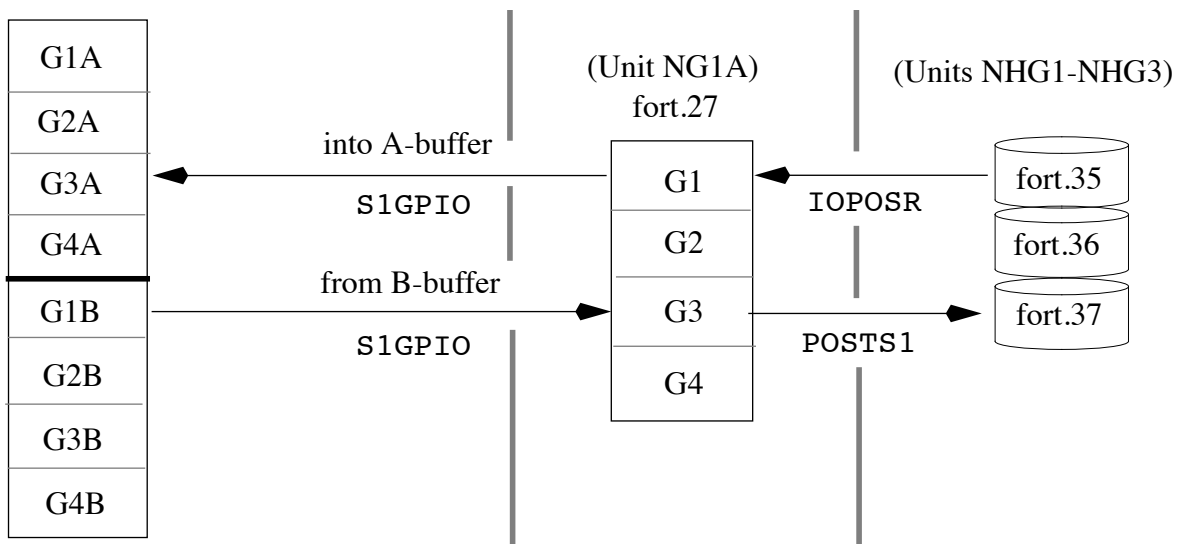


Figure 21 Associated memory buffers, work- and history files for grid point data.

The G-buffers are allocated in subroutine BUFGRD. G1 and G2-buffers contain all prognostic variables and also the wind components at time  $t - 1$  in grid point space. G3 contains the so called **uninterpolated fields**, e.g. surface fields, which are needed continuously. The G4 buffer is never used.

Addresses and lengths of buffers are stored in COMMON /COMBUF/. For example:

address of buffer F2A : NPTRB(NF2ABK),  
length of buffer G3B : NLENB(NG3BBK)



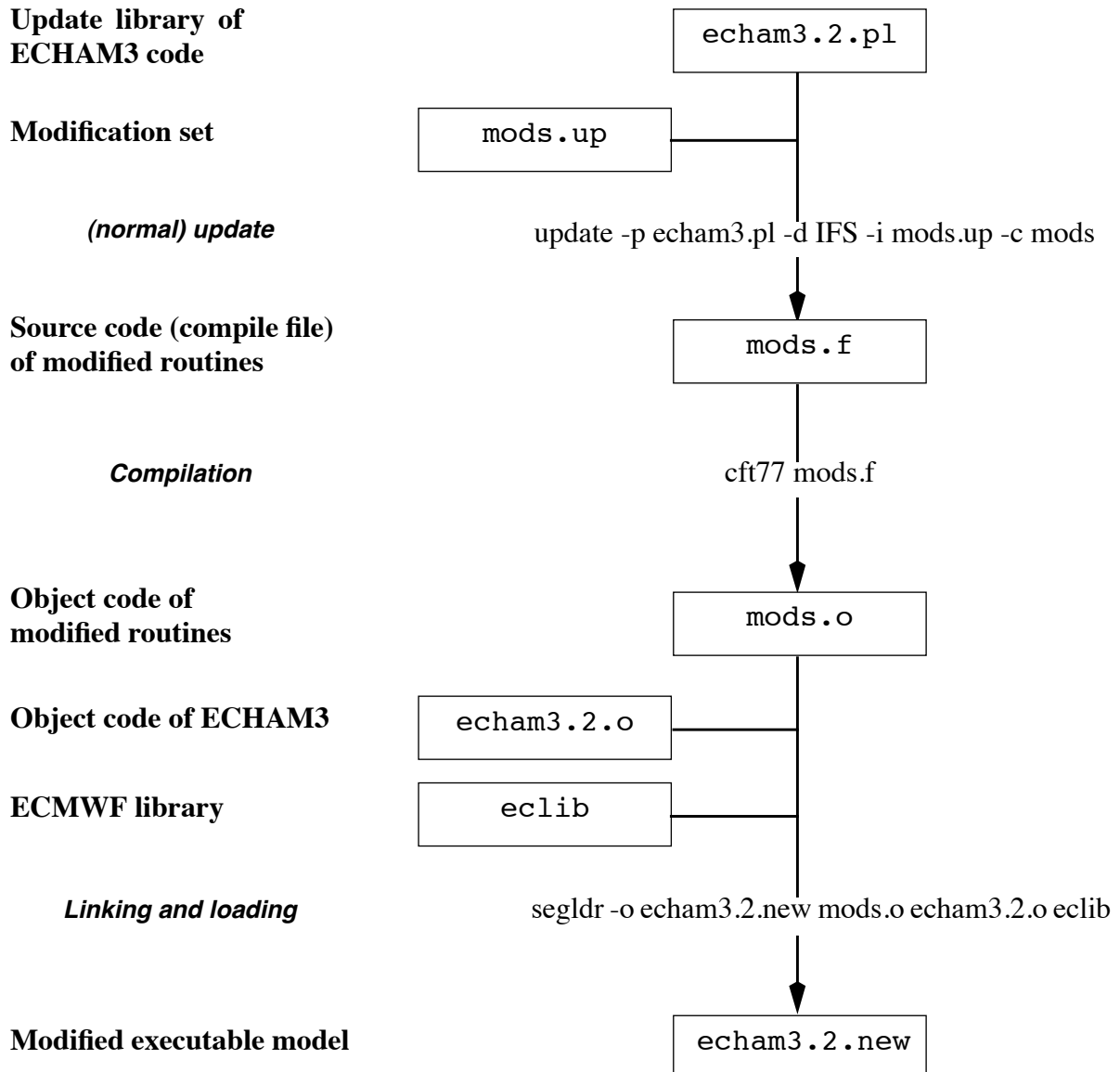
## 5. USER'S MANUAL

### 5.1 MODIFICATION OF THE SOURCE CODE

#### 5.1.1 General

Modification of the model source code is done using the CRAY UNICOS UPDATE utility. First of all a modification set has to be created (edited). UPDATE uses the modification set and the update library to build the source code of the modified routines. The source code is compiled creating the object code of the modified routines, which then has to be linked together with the ECHAM3 object code and the ECMWF library to create the modified executable model.

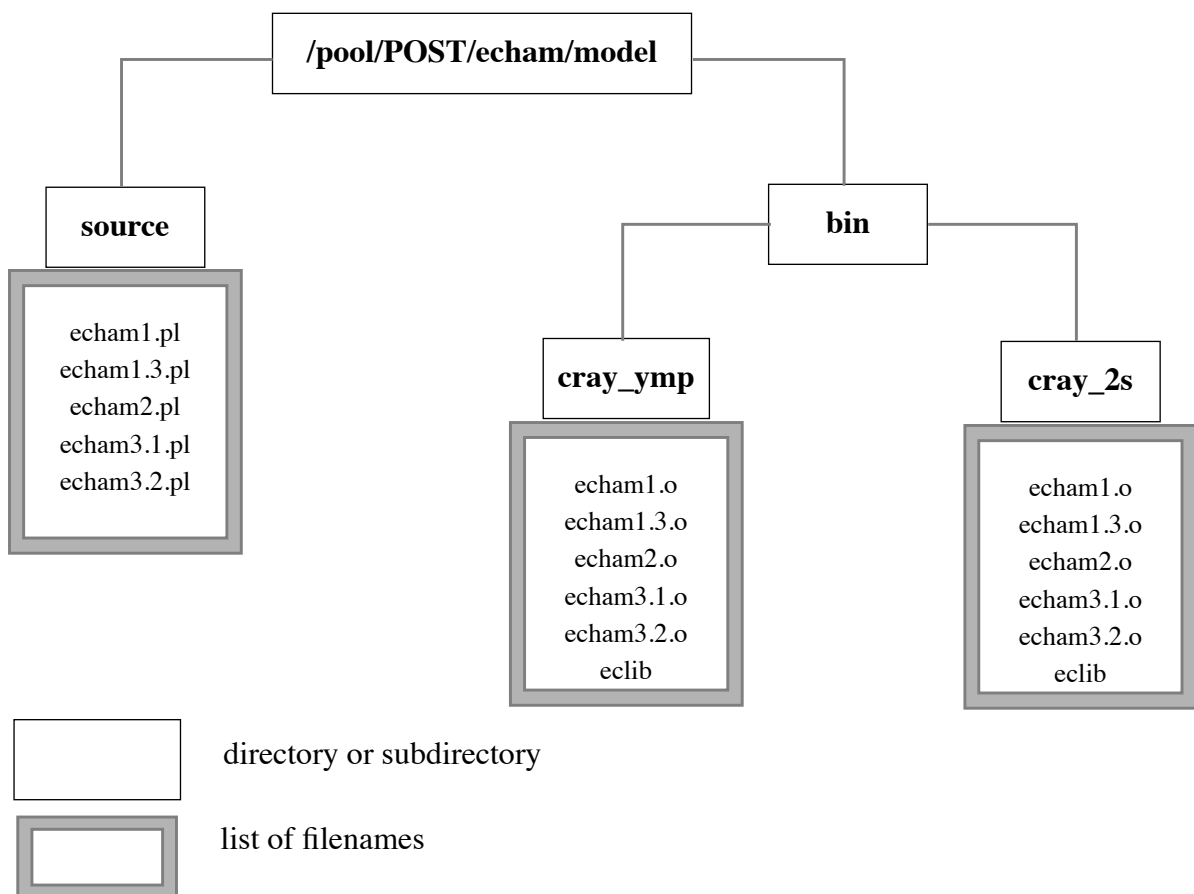
#### 5.1.2 Modification tree



### 5.1.3 Location of libraries

On the CRAY-2S the ECMWF library (eclib), the object code of ECHAM3 (echam3\*.o) and the update libraries of several model versions (echam3\*.pl) reside in global accessible directories. The path names are shown in the diagram following.

Unfortunately disk space on the CRAY-YMP is very low, so a similar structure of global accessible directories could not be installed up to now. Using the model on the YMP requires to transfer the files needed from the CRAY-2S to the CRAY-YMP via FTP.



On the CRAY-YMP, global accessible ECHAM3 libraries reside at the following path's, until the same structure as on the CRAY-2S can be installed there:

```

/pf/k/k204003/ham3dir/echam3.1.pl
/pf/k/k204003/ham3dir/echam3.1.o
/pf/k/k204003/ham3dir/echam3.2.pl
/pf/k/k204003/ham3dir/echam3.2.o
/pf/k/k204003/eclib
  
```

### 5.1.4 Example script for model modification

```

#QSUB
set -e
# example script for model modifications
LIB=/pool/POST/echam/model
#-----
# 1. update-input-file (=modification set) with modifications for
#   for subroutines VDIFF and SURF
#
cat > mods.up << EOR
*ID US141289
*/
*/ MODS IN SUBROUTINE VDIFF
*C VDIFF
*I VDIFF.123
      ZTP1(JL, JK)=TM1(JL, JK)+ZTIMST*TE(JL, JK)
*/
*/ MODS IN SUBROUTINE SURF
*C SURF
*D SURF.456
EOR
#-----
# 2. make source code (=compile file) of modified subroutines
#
update -p $LIB/source/echam3.2.pl -d IFS -i mods.up -c mods
#-----
# 3. compile modified subroutine
#
cft77 mods.f
#-----
# 4. load modified model
#
segldr -o echam3.2.new \
mods.o \
$LIB/bin/cray_2s/echam3.2.o \
$LIB/bin/cray_2s/eclib
#-----
exit

```

The output of this job will contain the following messages:

```

*Caution* Duplicate entry point 'SURF' encountered;
  Entry in module 'SURF' from file 'mods.o' is used
  Entry in module 'SURF' from file '/pool/POST/echam/model/bin/cray_2s/echam3.2.o' is ignored
*Caution* Duplicate entry point 'VDIFF' encountered;
  Entry in module 'VDIFF' from file 'mods.o' is used
  Entry in module 'VDIFF' from file '/pool/POST/echam/model/bin/cray_2s/echam3.2.o' is ignored
*Caution* Duplicate entry point 'IC2YMD' encountered;
  Entry in module 'IC2YMD' from file 'mods.o' is used
  Entry in module 'IC2YMD' from file '/pool/POST/echam/model/bin/cray_2s/echam3.2.o' is ignored
*Caution* Duplicate entry point 'CD2DAT' encountered;
  Entry in module 'CD2DAT' from file 'mods.o' is used
  Entry in module 'CD2DAT' from file '/pool/POST/echam/model/bin/cray_2s/echam3.2.o' is ignored
*Caution* Duplicate entry point 'IDAT2C' encountered;
  Entry in module 'IDAT2C' from file 'mods.o' is used
  Entry in module 'IDAT2C' from file '/pool/POST/echam/model/bin/cray_2s/echam3.2.o' is ignored

```

Note that the last three caution messages are default.

The source code of this script can be found at:

/pool/POST/echam/example\_scripts/ham3load

## 5.2 I/O

### 5.2.1 Diagnostic output

Output is written in GRIB format to a file connected to unit 29. The output interval is controlled by NPTIME in namelist RUNCTL (default: 12 hours).

Prognostic variables at time  $t + 1$  are written out as spherical harmonics by subroutine OUTSP. They are taken from the spectral buffers containing SD, SVO, STP, SQ and SX (see Appendix E, Table 9). The content of the spectral output is controlled by namelist POSTCTL (see section 5.3.2). SX is not written out by default.

Grid point variables from the **G3B** buffer are written out by subroutines OUTGPI for the in-core version and OUTGP for the disk version respectively. The content of the output is controlled by the code table of the input file stdin (see Appendix F, Table 10).

For details refer to section 5.3(example job).

### 5.2.2 Newstart

Two initial files are needed:

A file connected to **unit 23** (NISP) containing prognostic variables as spectral coefficients.

A file connected to **unit 24** (NIGP) containing some fields used in the **G3** buffer.

Spectral coefficients are read from **unit 23** by routine IOPOSI. During a fictive time step NSTEP = -1 they are transferred into fourier coefficients (buffer **F1-F4**) by an inverse legendre transform (done by subroutine LTI in SCAN2), which are then written to the global memory buffer containing Fourier coefficients or to the workfile connected to **unit 26** (done by subroutine S2IO in SCAN2) latitude row by latitude row.

Grid point fields are read from **unit 24** via subroutine IOPOSI. Fields, that are needed to fill up the **G3** buffer, but not read from **unit 24** (mostly accumulated diagnostic fields), are preset by subroutine RESETP (usually set to 0.). The whole **G3** buffer is then written to the global memory buffer containing grid point data or to the workfile connected to **unit 27**.

**G1** and **G2** buffers normally contain forecast variables in grid point space at time  $(t - 1)$ , which are not yet available, because the model is starting to run.  $(t - 1)$ -values are obtained by copying the actual values (time  $t$ ) into the **G1** and **G2** buffers in the first scan ( subroutine SCAN1) at timestep NSTEP = 0. This first timestep is only a forward timestep and not a leap-frog-step, because of the equality of  $t$ - and  $(t - 1)$ -values.

Actual values (time  $t$ ) are the spectral coefficients read and transformed to Fourier coefficients in SCAN2 during time step NSTEP = -1. In SCAN1 they are transformed to grid point values via subroutine FFTI (inverse Fourier transform).

### 5.2.3 Rerun

History files of a previous run are read into the connected memory buffers and are copied to the respective global memory buffers or workfiles (done by subroutine IOPOSR).

At the end of the run the same is done vice versa by subroutines POSTS1 and POSTS2.

### 5.2.4 Input of sea surface temperature

The sea-surface temperature (SST) is read each time step from the file connected to **unit 20** by subroutine CLSST.

## 5.2.5 Files used for a model run

Table 5 Files used for a model run

| file type      | file name                       | unit name | unit no. | input routine       | output routine  | file content                                     |
|----------------|---------------------------------|-----------|----------|---------------------|-----------------|--|
| <b>INITIAL</b> | tNNXXX.73 <sup>a</sup>          | NISP      | 23       | IOPOSI              | -               | spectr. atmospheric field (prognostic variables) |
|                | XXXNNm.new <sup>b</sup>         | NIGP      | 24       | IOPOSI              | -               | gridpoint surface fields                         |
|                | yearNNm.new <sup>c</sup>        | -         | 20       | CLSST<br>INISOIL    | -               | 12 month climatology of surface temperature      |
| <b>CONTROL</b> | stdin                           | NIN       | 5        | INlccc <sup>d</sup> | -               | namelists, code table                            |
| <b>WORK</b>    | l1a                             | NL1A      | 25       | S1FCIO              | S1FCIO          | Legendre constants                               |
|                | f1a                             | NF1A      | 26       | S1FCIO              | S1FCIO          | Fourier coefficients                             |
|                | g1a                             | NG1A      | 27       | S1GPI0              | S1GPI0          | gridpoint fields                                 |
| <b>HISTORY</b> | \${EXP}.31 <sup>e</sup>         | NHF1      | 31       | IOPOSR              | POSTS2          | Fourier F1 buffer                                |
|                | \${EXP}.32 <sup>e</sup>         | NHF2      | 32       | IOPOSR              | POSTS2          | Fourier F2 buffer                                |
|                | \${EXP}.33 <sup>e</sup>         | NHF3      | 33       | IOPOSR              | POSTS2          | Fourier F3 buffer                                |
|                | \${EXP}.34 <sup>e</sup>         | NHF4      | 34       | IOPOSR              | POSTS2          | Fourier F4 buffer                                |
|                | \${EXP}.35 <sup>e</sup>         | NHG1      | 35       | IOPOSR              | POSTS1          | gridpoint G1 buffer                              |
|                | \${EXP}.36 <sup>e</sup>         | NHG2      | 36       | IOPOSR              | POSTS1          | gridpoint G2 buffer                              |
|                | \${EXP}.37 <sup>e</sup>         | NHG3      | 37       | IOPOSR              | POSTS1          | gridpoint G3 buffer                              |
| <b>OUTPUT</b>  | \${EXP}_yyymm <sup>f</sup>      | NUNITSP   | 29       | -                   | OUTSP           | spectral fields on hybrid levels                 |
|                |                                 | NUNITUN   | 29       | -                   | OUTGP<br>OUTGPI | gridpoint fields<br>uninterpolated fields        |
|                | stdout                          | NOUT      | 6        | -                   | various         | quick diagnostics, parameters, switches          |
|                | \${EXPNO}HDIF_yymm <sup>g</sup> | -         | 4        | -                   | HDIFD           | diagnostics of horizontal diffusion              |

a. NN : Resolution (21, 42, 63 or 106)

XXX : Month (jan, apr, jul, oct)

Example : t21jan.73

b. NN : Resolution (21, 42, 63 or 106)

XXX : Month (jan, apr, jul, oct)

Example : jul42m.new

c. NN : Resolution (21, 42, 63 or 106)

Example : year42m.new

d. ccc : Prefix of COMMON-Blocks ( CON, CTL, DIA, FFT, etc.)

Example : INICTL for COMCTL

e. EXP : User-defined filename-prefix (Shell-variable)

f. EXP : same as in <sup>e</sup>

yy : Year (01, 02,...)

mm : Month (01, 02, ...,12)

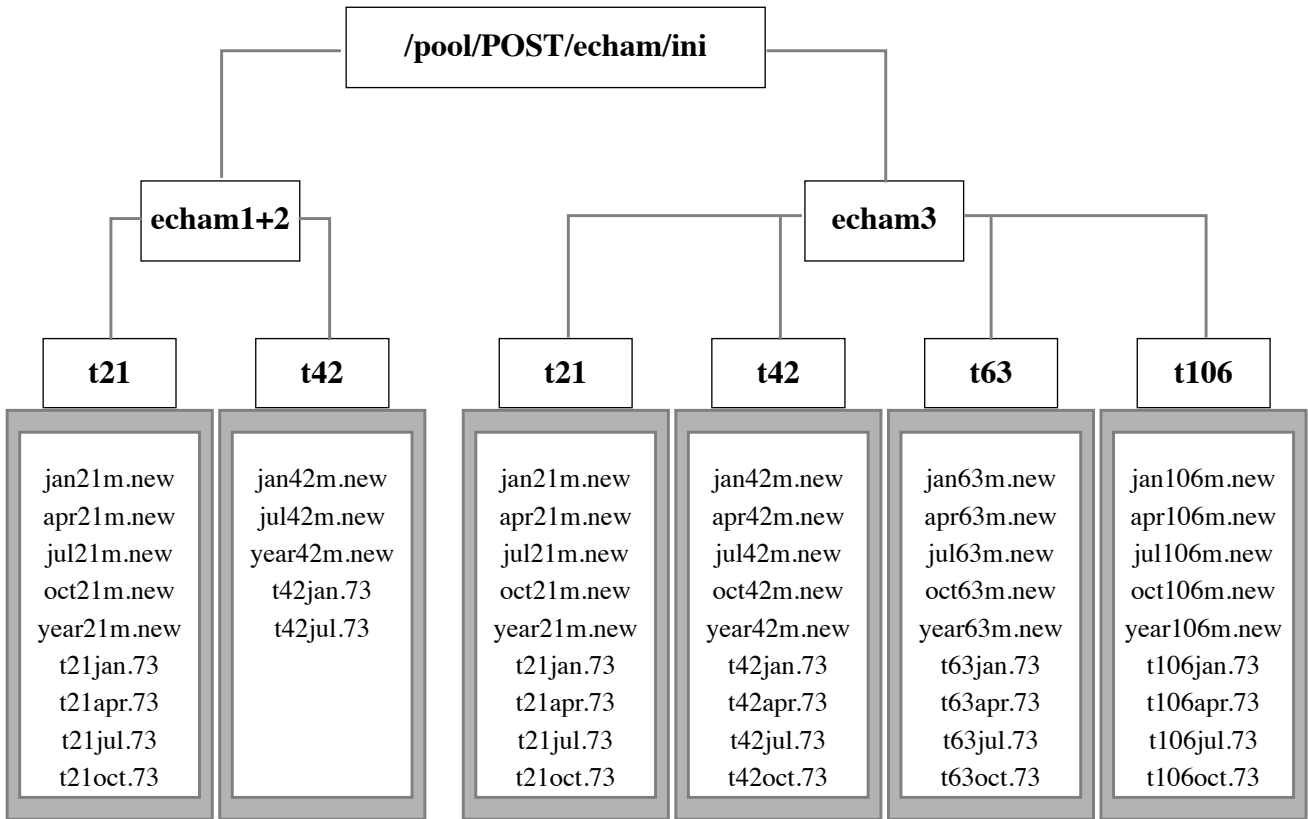
g. EXPNO: first five characters of EXP

yy : Year (01, 02,...)

mm : Month (01, 02, ...,12)

### 5.2.6 Location of initial files

As the libraries, the initial files reside in global accessible directories on the CRAY-2S. The initial files are divided into categories. The two main categories distinguish the model versions (echam1/2 and echam3). Further subdivision is necessary to distinguish the initial files for different horizontal resolutions (T21/T42/T63/T106). For path's refer to the diagram following.



directory or subdirectory



list of filenames

## 5.3 RUNNING THE MODEL

### 5.3.1 Example script for running the T21-model (Bourne shell)

```

#QSUB -lT 2500
#QSUB -lM 3 Mw
#QSUB -eo
#QSUB
#
cd $MFHOME
set -e
#####
#set variables: #
#
EXP=01120ctrl # <-- experiment identifier
#
MODEL=echam3 # <-- name of executable model
#
RERUN=F # <-- rerun switch
# (set TRUE after initial
# run is submitted to
# enable rerun chain !)
#
DPATH=$MFHOME/ # <-- output file directory
# #####
INI=/pool/POST/echam/ini/echam3/t21 # <-- paths to initial files
#####
#
# specification of file structures (activate/deactivate respective blocks)
#
##### CRAY-2 #####
assign -s pure -a $INI/t21jan.73 u:23 # <-- atmosphere initial file
assign -s pure -a $INI/jan21m.new u:24 # <-- surface initial file
assign -s pure -a $INI/year21m.new u:20 # <-- sst climate file
#
assign -s pure -a $TMPDIR/l1a u:25 # <
assign -s pure -a $TMPDIR/fla u:26 # <-- work files (scratch)
assign -s pure -a $TMPDIR/gla u:27 # <
#
assign -s pure u:29 # <-- output file (GRIB format)
# filename: ${EXP}_yymm
assign -s pure -a $DPATH${EXP}.31 u:31 # <
assign -s pure -a $DPATH${EXP}.32 u:32 # <
assign -s pure -a $DPATH${EXP}.33 u:33 # <
assign -s pure -a $DPATH${EXP}.34 u:34 # <-- rerun files
assign -s pure -a $DPATH${EXP}.35 u:35 # <
assign -s pure -a $DPATH${EXP}.36 u:36 # <
assign -s pure -a $DPATH${EXP}.37 u:37 # <
#
##### CRAY-YMP #####
#assign -s unblocked -a $INI/t21jan.73 u:23 # <-- atmosphere initial file
#assign -s unblocked -a $INI/jan21m.new u:24 # <-- surface initial file
#assign -s unblocked -a $INI/year21m.new u:20 # <-- sst climate file
#
#assign -s u -a $TMPDIR/l1a u:25 # <
#assign -s u -a $TMPDIR/fla u:26 # <-- work files (scratch)
#assign -s u -a $TMPDIR/gla u:27 # <
#
#assign -s unblocked u:29 # <-- output file (GRIB format)
# filename: ${EXP}_yymm
#assign -s unblocked -a $DPATH${EXP}.31 u:31 # <
#assign -s unblocked -a $DPATH${EXP}.32 u:32 # <
#assign -s unblocked -a $DPATH${EXP}.33 u:33 # <
#assign -s unblocked -a $DPATH${EXP}.34 u:34 # <-- rerun files
#assign -s unblocked -a $DPATH${EXP}.35 u:35 # <
#assign -s unblocked -a $DPATH${EXP}.36 u:36 # <
#assign -s unblocked -a $DPATH${EXP}.37 u:37 # <

```



```
#####
#
# stdin file: control parameter namelists, output path, experiment name
# and code table as "here document"
#
cat > namelist << EOR
&SDSCTL
  LRES=$RERUN
&END
&RUNCTL
  NSTOP=20,
&END
&DYNCTL
&END
&NMICTL &END
&PHYSCTL
&END
&RADCTL
&END
&POSTCTL
&END
$DPATH
$EXP
129 GEOSP
134 APS
139 TS
140 WS
141 SN
142 APRL
143 APRC
144 APRS
145 VDIS
146 AHFS
147 AHFL
159 USTAR3
160 RUNOFF
163 ACLCV
164 ACLCOV
165 U10
166 V10
167 TEMP2
168 DEW2
169 TSURF
170 TD
171 WIND10
172 SLM
173 AZ0
175 ALBEDO
176 SRADS
177 TRADS
178 SRAD0
179 TRAD0
180 USTR
181 VSTR
182 EVAP
183 TDCL
194 WLM1
201 T2MAX
202 T2MIN
203 SRAD0U
204 SRADSU
205 TRADSU
206 TSN
207 TD3
208 TD4
209 TD5
210 SEAICE
214 TSMAX
```

```

215 TSMIN
216 WIMAX
217 TOPMAX
218 SNMEL
220 TSLIN
221 DSNAC
222 ALWCAC
223 ACLCAC
224 SRAD0F
225 TRAD0F
226 ACCNTF
227 SRAD0C
228 TRAD0C
229 ACCNTC
230 QVI
231 ALWCVI
999 END
EOR
#
#
ja                                     # <-- start job accounting
#
$MFHOME/$MODEL < namelist           # <-- execute model
#
ja -lsc                               # <-- print job accounting
ja -t                                 # <-- terminate job accounting
#
qsub ham3run                          # <-- submit next job
#                                     # (rerun chain)
#
chmod a+r $DPATH${EXP}_*             # <-- make output file public

```

The source code of this script can be found in:

`/pool/POST/echam/example_scripts/ham3run`

### 5.3.2 Selectable model parameters

#### **SDSCTL - information necessary to start or resume the experiment**

| <u>Name</u> | <u>Type</u> | <u>Purpose</u>   | <u>Default</u> |
|-------------|-------------|--|----------------|
| LRES        | LOGICAL     | Rerun switch:<br>TRUE: Restart from rerun files (fort.31...37)<br>FALSE: Start from initial files (fort.23, fort.24) | TRUE           |

#### **RUNCTL - run control variables**

| <u>Name</u> | <u>Type</u>      | <u>Purpose</u>   | <u>Default</u>                                      |
|-------------|------------------|--|---|
| NSTOP       | INTEGER          | Time step to stop the experiment<br>NSTOP > 0 : stop after NSTOP timesteps<br>NSTOP < 0 : stop after -NSTOP days                               | 10 timesteps  |
| NPTIME      | INTEGER          | Frequency of post processing<br>(= output data write out)<br>NPTIME > 0 : every NPTIME timesteps<br>NPTIME < 0 : every -NPTIME days            | 12 hours  |
| NWTIME      | INTEGER          | Frequency of rerun files write-up<br>(causes interrupt of model run)<br>NWTIME > 0 : every NWTIME timesteps<br>NWTIME < 0 : every -NWTIME days | 30 days   |
| LWMONTH     | LOGICAL          | Interrupt a run at the end of a month<br>including write-up of rerun files<br>(set to FALSE if the default value is not used)                  | TRUE  |
| NWLAG       | INTEGER          | Frequency for saving rerun files<br>in months (inhibits overwriting)   | 13 (i.e.<br>no saving)                              |
| LABORT      | LOGICAL          | True for exit at end of the experiment<br>(timestep=NSTOP) to stop rerun chain   | TRUE  |
| DTIME       | REAL             | Time step in seconds   | T21: 2400.<br>T42: 1440.<br>T63: 900.<br>T106: 720. |
| NSPACE1     | INTEGER          | Size of space managed by memory manager  | auto-adjustment                                     |
| LCORE       | LOGICAL          | True for incore version of model which<br>reduces i/o overhead   | TRUE  |
| NG3XP       | INTEGER          | Number of extra G3-fields (G3Xnn)  | 0   |
| NG3XL       | INTEGER<br>ARRAY | Number of levels of extra G3-fields  | 99*1  |
| LXACCU      | LOGICAL<br>ARRAY | Switches for accumulation (= mean over<br>postprocessing interval) of extra G3-fields  | 99*F  |
| NXPBITS     | INTEGER          | Number of GRIB code bits for extra G3-fields   | 99*16   |

**DYNCTL - control options for the dynamics and general control**

| <u>Name</u> | <u>Type</u> | <u>Purpose</u>   | <u>Default</u>  |
|-------------|-------------|--|---|
| NDIADFR     | INTEGER     | Frequency of diagnostic printout<br>NDIADFR > 0 : every NDIADFR time step<br>NDIADFR = 0 : no diagnostics<br>NDIADFR < 0 : every -NDIADFR hour                 | 5 days  |
| NDIAVFR     | INTEGER     | Frequency of dynamical diagnostics for each level<br>NDIAVFR > 0 : every NDIAVFR time step<br>NDIAVFR = 0 : no diagnostic<br>NDIAVFR < 0 : every -NDIAVFR hour | 0 (no diagn.)   |
| LZONDIA     | LOGICAL     | Zonal diagnostics in NDIADFR interval  | FALSE   |
| LUMAX       | LOGICAL     | Print information on maximum wind<br>in NDIADFR interval   | FALSE   |
| APSURF      | REAL        | Global mean surface pressure [Pa]<br>(depends on orography)  | 98200.  |
| DIFVO       | REAL        | Coefficient for horizontal<br>diffusion of vorticity   | <u>T21</u> 1.0 E7 <u>T42</u> 11.E16 <u>T63</u> 8.5E6 <u>T106</u> 5.E6 |
| DIFD        | REAL        | Same for divergence  | 5.0 E7    55. E16    42.5E6    25.E6                                  |
| DIFT        | REAL        | Same for temperature   | 0.2 E7    4.4 E16    1.7E6    1.E6                                    |
| DIFQ        | REAL        | Same for specific humidity   | 0.2 E7    4.4 E16    1.7E6    1.E6                                    |
| DIFX        | REAL        | Same for liquid water  | 0.2 E7    4.4 E16    1.7E6    1.E6                                    |
| LDIAHDF     | LOGICAL     | Diagnostics of horizontal diffusion  | FALSE   |

**PHYSCTL - control options for diabatic processes**

| <u>Name</u> | <u>Type</u> | <u>Purpose</u>   | <u>Default</u>     |
|-------------|-------------|--|--------------------|
| LPHYS       | LOGICAL     | True for parameterization of diabatic processes  | TRUE               |
| LVDIFF      | LOGICAL     | True for turbulent vertical diffusion  | TRUE               |
| LMFPEN      | LOGICAL     | True for cumulus convection (mass flux)  | TRUE               |
| LKU00       | LOGICAL     | True for zero order Kuo convection   | TRUE               |
| LSCV        | LOGICAL     | True for shallow convection  | TRUE               |
| LGWDRAG     | LOGICAL     | True for gravity wave drag scheme  | TRUE<br>T21: FALSE |
| LCOND       | LOGICAL     | True for large scale condensation scheme   | TRUE               |
| LSURF       | LOGICAL     | True for soil model  | TRUE               |
| LQNEGAT     | LOGICAL     | True for correction of negative specific humidity  | FALSE              |
| NDIAPFR     | INTEGER     | Frequency of physics budget diagnostics<br>NDIAPFR > 0 : every NDIAPFR timesteps<br>NDIAPFR < 0 : every -NDIAPFR hours | 10 days            |

**RADCTL - control options for the radiation scheme**

| <u>Name</u> | <u>Type</u> | <u>Purpose</u>  | <u>Default</u>   |
|-------------|-------------|---|--|
| LRAD        | LOGICAL     | True for radiation  | TRUE   |
| LDIUR       | LOGICAL     | True for diurnal cycle  | TRUE   |
| NMONTH      | INTEGER     | Month for perpetual month experiments<br>NMONTH = 1...12 : number of month (Jan...Dec)<br>( <b>choose appropriate initial data !</b> )<br>NMONTH = 0 : annual cycle | 0  |
| NRADFR      | INTEGER     | Frequency of full radiation computations<br>NRADFR > 0 : every NRADFR timesteps<br>NRADFR < 0 : every -NRADFR hours   | 2 hours  |
| NRADPFR     | INTEGER     | Print frequency for radiation statistics<br>in number of radiation steps  | 126  |
| NRADPLA     | INTEGER     | Print radiation statistics every NRADPLA<br>latitude line   | 10   |
| CO2FAC      | REAL        | Factor for CO <sub>2</sub> concentration  | <u>ECHAM1/2</u><br>1. (330 ppm) <u>ECHAM3</u><br>1.045 (345 ppm) |

**POSTCTL- control of spectral variables write out**

| <u>Name</u> | <u>Type</u> | <u>Purpose</u>   | <u>Default</u> |
|-------------|-------------|--|----------------|
| LPPSPE      | LOGICAL     | True for write out of all spectral<br>variables except liquid water SX | TRUE           |
| LPPD        | LOGICAL     | True for write out of divergence                                       | TRUE           |
| LPPVO       | LOGICAL     | Same for vorticity   | TRUE           |
| LPPT        | LOGICAL     | Same for temperature   | TRUE           |
| LPPP        | LOGICAL     | Same for surface pressure  | TRUE           |
| LPPQ        | LOGICAL     | Same for specific humidity   | TRUE           |
| LPPX        | LOGICAL     | Same for liquid water content  | FALSE          |

Note: Write out of grid point variables is controlled by the code table as shown in the example job in section 5.3.1 (for definition of codes and code numbers refer to Appendix F, Table 10).

**5.3.3 Output examples**

to be made by anyone with procedure  
/pool/POST/t21.post

## 5.4 STRUCTURE OF DATASETS

All files except **stdin** and **stdout** are pure data files, i.e. no control words or record terminators are used. BUFFER IN/OUT is used for I/O and SETPOS for file positioning. Use the following **assign** commands for specification of file structure:

### **CRAY-2:**

|                |                      |      |
|----------------|----------------------|------|
| assign -s pure | -a \$INI/t21jan.73   | u:23 |
| assign -s pure | -a \$INI/jan21m.new  | u:24 |
| assign -s pure | -a \$INI/year21m.new | u:20 |
| assign -s pure | -a \$TMPDIR/l1a      | u:25 |
| assign -s pure | -a \$TMPDIR/f1a      | u:26 |
| assign -s pure | -a \$TMPDIR/g1a      | u:27 |
| assign -s pure |                      | u:29 |
| assign -s pure | -a \$DPATH\${EXP}.31 | u:31 |
| assign -s pure | -a \$DPATH\${EXP}.32 | u:32 |
| assign -s pure | -a \$DPATH\${EXP}.33 | u:33 |
| assign -s pure | -a \$DPATH\${EXP}.34 | u:34 |
| assign -s pure | -a \$DPATH\${EXP}.35 | u:35 |
| assign -s pure | -a \$DPATH\${EXP}.36 | u:36 |
| assign -s pure | -a \$DPATH\${EXP}.37 | u:37 |

### **CRAY-YMP:**

|                     |                      |      |
|---------------------|----------------------|------|
| assign -s unblocked | -a \$INI/t21jan.73   | u:23 |
| assign -s unblocked | -a \$INI/jan21m.new  | u:24 |
| assign -s unblocked | -a \$INI/year21m.new | u:20 |
| assign -s u         | -a \$TMPDIR/l1a      | u:25 |
| assign -s u         | -a \$TMPDIR/f1a      | u:26 |
| assign -s u         | -a \$TMPDIR/g1a      | u:27 |
| assign -s unblocked |                      | u:29 |
| assign -s unblocked | -a \$DPATH\${EXP}.31 | u:31 |
| assign -s unblocked | -a \$DPATH\${EXP}.32 | u:32 |
| assign -s unblocked | -a \$DPATH\${EXP}.33 | u:33 |
| assign -s unblocked | -a \$DPATH\${EXP}.34 | u:34 |
| assign -s unblocked | -a \$DPATH\${EXP}.35 | u:35 |
| assign -s unblocked | -a \$DPATH\${EXP}.36 | u:36 |
| assign -s unblocked | -a \$DPATH\${EXP}.37 | u:37 |

The data written to the output file (unit 29, name: \${EXP}\_yymm) is in GRIB format.

For processing these data a variety of utility routines are available:

|                                   |  |
|-----------------------------------|--|
| " <i>Afterburner</i> "            | <b>mod21, mod42, mod63, and mod106</b> |
| " <i>Tape accessing scripts</i> " | <b>extract and extrakt</b>             |
| " <i>grib moduls</i> "            |  |

Documentation on this postprocessing routines can be found in

**Description of programs handling files in WMO GRIB and EXTRA format,  
DKRZ Report, to be published;**

The output files produced on CRAY-2 can be processed on CRAY-YMP and vice versa. For details see corresponding documentation.

As with the pure file structure, “private” utilities reading the output data must be aware of how the file was written in order to read it properly. For reading in a FORTRAN program use the **assign** command to specify the file structure:

```
assign -s pure "filename"      on CRAY-2S  
assign -s unblocked "filename" on CRAY-YMP
```





## 6. REFERENCES

Alexander, R.C. and Mobley, R.L., 1976:

Monthly average sea-surface temperatures and ice-pack limits on a global grid;  
*Mon. Wea. Rev.*, 104, 143-148.

Asselin, R., 1972:

Frequency filter for time integrations;  
*Mon. Wea. Rev.*, 100, 487-490.

Baede, A.P.M., M. Jarraud and U. Cubasch, 1979:

Adiabatic formulation and organization of ECMWF's spectral model;  
*ECMWF Tech. Rep.*, 15, 40 pp.

Bauer, H., E. Heise, J. Pfaendtner and V. Renner, 1985:

Development of an economical soil model for climate simulation.

In: A. Ghazi and R. Fantechi (Eds.)

*Current Issues in Climate Research*, Proceedings of EC Climatology Programme Symposium, Sophia Antipolis, France, 2-5 Oct. 1984, D. Reidel, Dordrecht, 219-226.

Bennetts, A., and B.J. Hoskins, 1979:

Conditional symmetric instability - a possible explanation for frontal rainbands;  
*Quart. J. Roy. Meteor. Soc.*, 105, 945-962.

Bennetts, A., and J.C. Sharp, 1982:

The relevance of conditional symmetric instability to the prediction of meso-scale frontal rainbands;

*Quart. J. Roy. Meteor. Soc.*, 108, 595-602.

Betts, A.K., 1973:

Non-precipitating cumulus convection and its parameterization;  
*Quart. J. Roy. Meteor. Soc.*, 99, 178-196.

Blackadar, A.K., 1962:

The vertical distribution of wind and turbulent exchange in a neutral atmosphere;  
*J. Geophys. Res.*, 67, 3095-3102.

Blondin, C., 1989:

Research on land surface parameterization schemes at ECMWF;

*Proceedings of the workshop on "Parameterization of fluxes over land surface"*, ECMWF, Reading, UK.

Blondin, C. and H. Böttger, 1987:

The surface and sub-surface parameterisation scheme in the ECMWF forecasting system. Revision and operational assessment of weather elements;

*ECMWF Tech. Memo.*, 135, 48 pp.

- Boer, G.J., N.A. McFarlane, R. Laprise, J.D. Henderson, and J.-P. Blanchet, 1984:  
The Canadian Climate Centre spectral atmospheric general circulation model;  
*Atmos.-Ocean*, 22, 397-429.
- Bourke, W., 1972:  
An efficient one level primitive-equation spectral model;  
*Mon. Wea. Rev.*, 100, 683-689.
- Bourke, W., 1974:  
A multi-level spectral model: Formulation and hemispheric integrations;  
*Mon. Wea. Rev.*, 102, 688-701.
- Brinkop, S., 1991:  
Inclusion of cloud processes in the ECHAM PBL parameterization;  
In: R. Sausen (Ed.)  
*Studying Climate with the ECHAM Atmospheric Model*.  
Large Scale Atmospheric Modelling, Report No. 9, 5-14,  
Meteorologisches Institut der Universität Hamburg.
- Brinkop, S., 1992:  
Parameterisierung von Grenzschichtwolken für Zirkulationsmodelle;  
*Berichte aus dem Zentrum für Meeres- und Klimaforschung*, Reihe A: Meteorologie,  
Nr. 2, Meteorologisches Institut der Universität Hamburg, 77 pp.
- Browning, K.A., M.E. Hardman, T.W. Harrold and C.W. Pardoc, 1973:  
The structure of rainbands within a mid-latitude depression;  
*Quart. J. Roy. Meteor. Soc.*, 99, 215-231.
- Burridge, D.M. and J. Haseler, 1977:  
A model for medium range weather forecasting - Adiabatic formulation;  
*ECMWF Tech. Rep.* No 4, 46 pp.
- Cess, R.D. and G.L. Potter, 1987:  
Explanatory studies of cloud radiative forcing with a General Circulation Model;  
*Tellus*, 39A, 460-473.
- Cess, R.D. and G.L. Potter, 1988:  
A methodology for understanding and intercomparing atmospheric climate  
feedback processes in General Circulation Models;  
*J. Geophys. Res.*, 93, 8305-8314.
- Charnock, M., 1955:  
Wind stress on a water surface;  
*Quart. J. Roy. Meteor. Soc.*, 81, 639-640.
- Cheng, L., T.-C. Yip and H.-R. Cho, 1980:  
Determination of mean cumulus cloud vorticity from GATE A/B-scale potential  
vorticity budget;  
*J. Atm. Sci.*, 37, 797-811.

Dorman, J.L. and P.J. Sellers, 1989:

A global climatology of albedo, roughness length and stomatal resistance for atmospheric general circulation models as represented by the Simple Biosphere Model (SiB);

*J. Appl. Meteor.*, 28, 833-855.

Dufour, L. and J. van Mieghem, 1975:

Thermodynamic de l'Atmosphere;

*Institut Royal Météorologique de Belgique*, 278 pp.

Dümenil, L. and E. Todini, 1992:

GCM parameterization of soil hydrology using a catchment scheme;  
*in preparation*.

Eickerling, H., 1989:

Parameterisierung des infraroten Strahlungstransports für Kohlendioxid, Wasserdampf und Ozon in einem breitbandigen Strahlungstransportmodell;  
*Diplomarbeit*, Institut für Meteorologie und Geophysik, Univ. Köln, FRG.

Eliassen, E., B. Machenhauer and E. Rasmussen, 1970:

On a numerical method for integration of the hydrodynamical equations with a spectral representation of the horizontal fields;

*Inst. of Theor. Met.*, Univ. of Copenhagen, No. 2.

Ellison, T.H., 1957:

Turbulent transfer of heat and momentum from an infinite rough plane;

*J. Fluid. Mech.*, 2, 456-466.

Emanuel, K.A., 1982:

Inertial instability and mesoscale convective systems,

Part II: Symmetric CISK in a baroclinic flow;

*J. Atm. Sci.*, 39, 1080-1097.

Foster, D.S., 1958:

Thunderstorm gusts compared with computed downdraft speeds;

*Mon. Wea. Rev.*, 86, 91-94.

Fritsch, J. M. and C. G. Chapell, 1980:

Numerical prediction of convectively driven mesoscale pressure systems,

Part I: Convective parameterization;

*J. Atm. Sci.*, 37, 1722-1733.

Geleyn, J.F. and H.J. Preuss, 1983:

A new data set of satellite-derived surface albedo values for operational use at ECMWF;

*Arch. Meteor. Geophys. Bioclim.*, Ser. A, 32, 353-359.

Girard, C. and M. Jarraud, 1982:

Short and medium range forecast differences between a spectral and a grid-point model: An extensive quasi-operational comparison;  
*ECMWF Tech. Rep. No. 32*, 178pp.

Hense, A., M. Kerschgens and E. Raschke, 1982:

An economical method for computing radiative transfer in circulation models;  
*Quart. J. Roy. Meteor. Soc.*, 108, 231-252.

Herzogh, P.H. and P.V. Hobbs, 1980:

The mesoscale and microscale structure and organization of clouds and precipitation in mid-latitude cyclones, Part II: Warm frontal clouds;  
*J. Atm. Sci.*, 37, 597-611.

Heymsfield, A.J., 1977:

Precipitation development in stratiform ice clouds: A microphysical and dynamical study;  
*J. Atm. Sci.*, 34, 367-381.

Hoskins, B.J. and Simmons, A.J., 1975:

A multi-layer spectral model and the semi-implicit method;  
*Quart. J. Roy. Meteor. Soc.*, 101, 637-655.

Houze, R.A., J.D. Locatelli and P.V. Hobbs, 1976:

Dynamics and cloud microphysics of the rainbands in an occluded frontal system;  
*J. Atm. Sci.*, 35, 1921-1936.

ICAO, 1964:

Manual of the ICAO Standard Atmosphere;  
*U.S. Government Printing Office, Washington, D.C.*

Jarraud, M., C. Girard, and U. Cubasch, 1981:

Comparison of medium-range forecasts made with the models using spectral or finite-difference techniques in the horizontal;  
*ECMWF Tech. Rep. No. 23*, 96 pp.

Jarraud, M., C. Girard, and J.-F. Geleyn, 1982:

Note on a possible linearization of the vorticity equation in a primitive equations spectral model;  
 Research Activities in Atmospheric and Oceanic Modelling, Report No. 3, pp 4.2-4.4

Johnson, R.H., 1976:

The role of convective-scale precipitation downdrafts in cumulus and synoptic scale interactions;  
*J. Atm. Sci.*, 33, 1890-1910.

- Johnson, R.H., 1980:  
Diagnosis of convective and mesoscale motions during Phase III of GATE;  
*J. Atm. Sci.*, 37, 733-753.
- Kasahara, A., 1974:  
Various vertical coordinate systems used for numerical weather prediction;  
*Mon. Wea. Rev.*, 102, 509-522.
- Kerschgens, M., U. Pilz, E. Raschke, 1978:  
A modified two-stream approximation for computations of the solar radiation budget in a cloudy atmosphere;  
*Tellus*, 30, 429-435.
- Kessler, E., 1969:  
On the distribution and continuity of water substance in atmospheric circulation;  
*Meteorological Monographs*, 10, Americ. Meteor. Soc., Boston, MA.
- Krylov, V.I., 1962:  
Approximate calculation of integrals;  
*Macmillan*, New York, 357 pp.
- Kukla, G. and D. Robinson, 1980:  
Annual cycle of surface albedo;  
*Mon. Wea. Rev.*, 108, 56-58.
- Kuo, H. L., 1965:  
On formation and intensification of tropical cyclones through latent heat release by cumulus convection;  
*J. Atm. Sci.*, 22, 40-63.
- Kuo, H. L., 1974:  
Further studies of the parameterization of the influence of cumulus convection on large-scale flow;  
*J. Atm. Sci.*, 31, 1232-1240.
- Laursen, L. and E. Eliassen, 1989:  
On the effects of the damping mechanisms in an atmospheric general circulation model;  
*Tellus*, 41A, 385-400.
- Le Mone, M. A. and W. T. Pennell, 1976:  
The relationship of trade wind cumulus distribution to subcloud layer fluxes and structure;  
*Mon. Wea. Rev.*, 104, 524-539.
- Lindzen, R. S., 1981:  
Some remarks on cumulus parameterization;  
*Rep. on NASA-GISS Workshop "Clouds in Climate": Modelling and Satellite Observational Studies*, 42-51.

Louis, J. F., 1979:

A parametric model of vertical eddy fluxes in the atmosphere;  
*Boundary Layer Meteorology*, 17, 187-202.

Louis, J. F., Tiedtke, M., Geleyn, J.-F., 1982:

A short history of the PBL parameterisation at ECMWF;  
*Proceedings, ECMWF workshop on planetary boundary layer parameterization*,  
Reading, 25-27 Nov. 81, 59-80.

London, J., Bojkov, R. D., Oltmans, S., Kelley, J. I., 1976:

Atlas of the global distribution of total ozone, July 1957 - June 1967;  
*NCAR Technical Note*, 113+STR.

Lowe, P.R., 1977:

An approximating polynomial for the computation of saturation vapor pressure;  
*J. Appl. Meteor.*, 16, 100-103.

Machenhauer, B. and E. Rasmussen, 1972:

On the integration of the spectral hydrodynamical equations by a transform  
method;  
*Inst. of Theor. Met.*, Univ. of Kopenhagen, Report No. 4.

Manabe, S., 1969:

Climate and the ocean circulation  
1. The atmospheric circulation and the hydrology of the earth's surface;  
*Mon. Wea. Rev.*, 97, 739-774.

Mason, B.J., 1971:

The physics of clouds  
*Clarendon Press*, Oxford, 671 pp.

Matthews, E., 1983:

Global vegetation and land use: New high-resolution data bases for climate  
studies;  
*J. Clim. Appl. Meteor.*, 22, 474-487.

Matveev, L. T., 1984:

Cloud dynamics;  
*Atm. Sci. Library*, D. Reidel Publishing Company, Dordrecht, 340 pp.

Miller, M. J., T. N. Palmer and R. Swinbank, 1989:

Parameterization and influence of sub-grid scale orography in general circulation  
and numerical weather prediction models;  
*Met. Atm. Phys.*, 40, 84-109.

Miller, M. J., A. Beljaars and T. N. Palmer, 1992:

The sensitivity of the ECMWF model to the parameterization of evaporation from  
the tropical oceans;  
*J. Clim.*, in press.

- Nitta, T., 1975:  
Observational determination of cloud mass flux distributions;  
*J. Atm. Sci.*, 32, 73-91.
- Orszag, S.A., 1970:  
Transform method for calculation of vector coupled sums;  
*J. Atm. Sci.*, 27, 890-895.
- Palmer, T. N., G. J. Shutts and R. Swinbank, 1986:  
Alleviation of a systematic westerly bias in general circulation and numerical weather prediction models through an orographic gravity wave drag parameterization;  
*Quart. J. Roy. Meteor. Soc.*, 112, 1001-1031.
- Paltridge, G. W. and C. M. R. Platt, 1976:  
Radiative processes in Meteorology and Climatology;  
*Developments in Atmospheric Science*, Vol. 5, Elsevier Scientific Publ. Co., Amsterdam etc., 318 pp.
- Pandolfo, J.P., 1967:  
Wind and temperature profiles for constant-flux boundary layer in lapse rate conditions with a variable eddy conductivity to eddy viscosity ratio;  
*J. Atm. Sci.*, 23, 495-502.
- Peltier, W.R. and T.L. Clark, 1987:  
Nonlinear mountain waves and wave-mean flow interaction: elements of a drag parameterization;  
*ECMWF Seminar/Workshop on Observation, Theory and Modelling of Orographic Effects*, ECMWF, Reading, 15-20 Sep. 1986, Vol 1, 223-249.
- Phillips, N.A., 1957:  
A coordinate system having some special advantages for numerical forecasting;  
*J. Met.*, 14, 184-185.
- Reynolds, R. W., 1988:  
A real-time global sea surface temperature analysis;  
*J. of Climate*, 1, 75-86.
- Robert, A. J., 1981:  
A stable numerical integration scheme for the primitive meteorological equations;  
*Atmos. Ocean*, 19, 35-46.
- Robert, A. J., 1982:  
A semi-Lagrangian and semi-implicit numerical integration scheme for the primitive meteorological equations;  
*J. Met. Soc. Japan*, 60, 319-325.

- Robert, A. J., J. Henderson and C. Turnbull, 1972:  
An implicit time integration scheme for baroclinic models in the atmosphere;  
*Mon. Wea. Rev.*, 100, 329-335.
- Robock, A., 1980:  
The seasonal cycle of snow cover, sea-ice and surface albedo;  
*Mon. Wea. Rev.*, 108, 267-285.
- Rockel, B., E. Raschke and B. Weyres, 1991:  
A parameterization of broad band radiative transfer properties of water, ice and mixed clouds;  
*Beitr. Phys. Atmosph.*, 64, 1-12.
- Roeckner, E. and U. Schlese, 1985:  
January simulation of clouds with a prognostic cloud cover scheme;  
*ECMWF Workshop on "Cloud cover in numerical models"*, 26-28 Nov. 1984, 87-108, ECMWF, Reading, UK.
- Roeckner, E., M. Rieland and E. Keup, 1991:  
Modelling of cloud and radiation in the ECHAM model;  
*ECMWF/WCRP Workshop on "clouds, radiative transfer and the hydrological cycle"*, 12-15 Nov. 1990, 199-222, ECMWF, Reading, UK.
- Roeckner, E., K. Arpe, L. Bengtsson, S. Brinkop, L. Dümenil, M. Esch, E. Kirk, F. Lunkeit, M. Ponater, B. Rockel, R. Sausen, U. Schlese, S. Schubert and M. Windelband, 1992:  
Simulation of the present-day climate with the ECHAM model:  
Impact of model physics and resolution;  
*Max-Planck-Institut für Meteorologie, Report No. 93*.
- Sasamori, T., 1975:  
A statistical model for stationary atmospheric cloudiness, liquid water content and rate of precipitation;  
*Mon. Wea. Rev.*, 103, 1037-1049.
- Schneider, E.K. and R.S. Lindzen, 1976:  
A discussion of the parameterization of momentum exchange of cumulus convection;  
*J. Geophys. Res.*, 81, 3158-3160.
- Sellers, P.J., Y. Mintz, Y.C. Sud and A. Dalcher, 1986:  
A simple biosphere model (Sib) for use within general circulation models;  
*J. Atm. Sci.*, 43, 505-531.
- Shettle, E.P. and R. Fenn, 1976:  
Models of the atmospheric aerosols and their optical properties;  
*AGARD Conference Proceedings, No. 183*, AGARD-CP-183.



Simmons, A.J. and D.M. Burridge, 1981:

An energy and angular-momentum conserving vertical finite difference scheme and hybrid vertical coordinates;  
*Mon. Wea. Rev.*, 109, 758-766.

Simmons, A.J. and R. Strüfing, 1981:

An energy and angular-momentum conserving finite difference scheme, hybrid coordinates and medium-range weather prediction;  
*ECMWF Tech. Rep. No. 28*, 68 pp.

Simmons, A.J., B.J. Hoskins and D.M. Burridge, 1978:

Stability of the semi-implicit time scheme;  
*Mon. Wea. Rev.*, 106, 405-412.

Simmons, A.J. and J. Chen, 1991:

The calculation of geopotential and pressure-gradient in the ECMWF atmospheric model: Influence on the simulation of the polar atmosphere and on temperature analyses;  
*Quart. J. Roy. Meteor. Soc.*, 117, 29-58.

Simpson, J., 1971:

On cumulus entrainment and one-dimensional models;  
*J. Atm. Sci.*, 28, 449-455.

Simpson, J. and V. Wiggert, 1969:

Models of precipitating cumulus towers;  
*Mon. Wea. Rev.*, 97, 471-489.

Smith, R.N.B., 1990:

A scheme for predicting layer clouds and their water content in a general circulation model;  
*Quart. J. Roy. Meteor. Soc.*, 116, 435-460.

Stephens, G.L., 1978:

Radiation profiles in extended water clouds: 2. parameterization schemes;  
*J. Atm. Sci.*, 35, 2123-2132.

Sundquist, H., 1978:

A parameterization scheme for non-convective condensation including prediction of cloud water content;  
*Quart. J. Roy. Meteor. Soc.*, 104, 677-690.

Temperton, C., 1983:

Fast mixed-radix real Fourier transforms;  
*ECMWF Tech. Memo.*, 71, 18 pp.

Tiedtke, M., 1989:

A comprehensive mass flux scheme for cumulus parameterization in large-scale models;

*Mon. Wea. Rev.*, 117, 1779-1800.

Tiedtke, M., W.A. Heckley, and J. Slingo, 1988:

Tropical forecasting at ECMWF: On the influence of physical parameterization on the mean structure of forecasts and analyses;

*Quart. J. Roy. Meteor. Soc.*, 114, 639-664.

Warrilow, D.A., A.B. Sangster and A. Slingo, 1986:

Modelling of land surface processes and their influence on European climate;

*Meteorological Office*, Met O 20 Tech. Note DCTN 38, Bracknell, U.K.

Wexler, R., and D. Atlas, 1959:

Precipitation generating cells;

*J. Meteor.*, 16, 327-332.

Wilcox, R. W. and A. D. Belmont, 1977:

Ozone concentration by latitude, altitude and month, near 80°W;

*Report, Control Data Corporation*, Contract No. DOT-FA77WA-3999.

Wilson, M.F. and A. Henderson-Sellers, 1985:

A global archive of land cover and soil data sets for use in general circulation climate models;

*J. Climat.*, 5, 119-143.

Xu, K.M., and S.K. Krueger, 1991:

Evaluation of cloudiness parameterizations using a cumulus ensemble model;

*Mon. Wea. Rev.*, 119, 342-367.

Yanai, M., S. Esbensen and J.-H. Chu, 1973:

Determination of bulk properties of tropical cloud clusters from large-scale heat and moisture budgets;

*J. Atm. Sci.*, 30, 611-627.

Zdunkowski, W.G., R.M. Welch, G. Korb, 1980:

An investigation of the structure of typical two-stream methods for the calculation of solar fluxes and heating rates in clouds;

*Beitr. Phys. Atm.*, 53, 147-166.

## Appendix A THE UNPARAMETRIZED EQUATIONS

### A.1 INTRODUCTION

To derive the governing equations given by (2.2.1) - (2.2.7) and (2.2.12) - (2.2.15), we take start from the unparametrized equations for a mixture of dry air, water vapour, liquid water and ice, and work for convenience in a Cartesian coordinate system. An individual component is denoted by a subscript "k", where  $k = d, v, l$  or  $i$  for dry air, water vapour, liquid water or ice, respectively. The specific mass of component  $k$ , denoted by  $q_k$ , is defined by

$$q_k = \frac{m_k}{m} = \frac{\rho_k}{\rho} \quad (\text{A.1.1})$$

where

$m_k$  is the mass of component  $k$  in a small material volume moving with the local velocity of the atmosphere,  
 $m = \sum m_k$  is the total mass of the material volume,  
 $\rho_k$  is the density of component  $k$ , and  
 $\rho = \sum \rho_k$  is the density of the atmosphere.

The rate of change of  $m_k$  is denoted by  $\dot{m}_k$ . This change occurs because of

- (a) internal phase changes
- (b) rainfall, snowfall, and surface exchanges.

The rate of change due to (a) alone is denoted by  $\dot{m}_{ki}$ , and that due to (b) by  $\dot{m}_{ke}$ . Then

$$\dot{m}_k = \dot{m}_{ki} + \dot{m}_{ke} \quad (\text{A.1.2})$$

$$\dot{m}_{di} = \dot{m}_{de} = 0 \quad (\text{A.1.3})$$

$$\sum_k \dot{m}_{ki} = 0 \quad (\text{A.1.4})$$

The rate of change of total mass is given by

$$\dot{m} = \sum_k \dot{m}_k = \sum_k \dot{m}_{ke} \quad (\text{A.1.5})$$

The rate of change of density of component  $k$  satisfies the equation

$$\dot{\rho}_k = \frac{\rho}{m} \dot{m}_k \quad (\text{A.1.6})$$

provided (as is reasonable) volume changes due to precipitation or phase changes are neglected. The net rate of change of density,  $\dot{\rho}$ , is then given by

$$\dot{\rho} = \frac{\rho}{m} \sum_k \dot{m}_k = \frac{\rho}{m} \dot{m} \quad (\text{A.1.7})$$

## A.2 THE ADVECTIVE FORM OF THE UNPARAMETRIZED EQUATIONS

### A.2.1 The material derivative

The material derivative is denoted by  $\frac{d}{dt}$ . Its definition is

$$\frac{d}{dt} \equiv \frac{\partial}{\partial t} + \underline{v} \cdot \nabla \quad (\text{A.2.1.1})$$

where  $\underline{v}$  here denotes the three-dimensional velocity vector, and  $\nabla$  the usual three-dimensional vector operator. Horizontal vectors and operators will subsequently be denoted by a subscript "h".

### A.2.2 The equation of state

We consider a volume  $V$  of atmosphere, of which dry air and water vapour occupy a volume  $V_{d+v}$ . The equations of state for dry air and water vapour are

$$p_d V_{d+v} = m_d R_d T \quad (\text{A.2.2.1})$$

and

$$p_v V_{d+v} = m_v R_v T \quad (\text{A.2.2.2})$$

where  $p_d$  and  $p_v$  are partial pressures. Dalton's Law then shows that the total pressure  $p$  is given from (A.2.2.2) by

$$p = \frac{m_d R_d T + m_v R_v T}{V_{d+v}} \quad (\text{A.2.2.3})$$

Introducing the specific volumes of liquid water  $v_l$ , and ice  $v_i$ ,

$$\begin{aligned} V_{d+v} &= V - m_l v_l - m_i v_i \\ &= \frac{m}{\rho} (1 - \rho (q_l v_l + q_i v_i)) \end{aligned} \quad (\text{A.2.2.4})$$

and (A.2.2.3) becomes

$$p = \rho T \frac{R_d q_d + R_v q_v}{1 - \rho (q_l v_l + q_i v_i)} \quad (\text{A.2.2.5})$$

or

$$p = \rho T R_d \frac{1 + (\frac{1}{\varepsilon} - 1) q_v - q_l - q_i}{1 - \rho (q_l v_l + q_i v_i)} \quad (\text{A.2.2.6})$$

where

$$\varepsilon = R_d / R_v \quad (\text{A.2.2.7})$$

### A.2.3 Mass conservation

Conservation of mass for element  $k$  leads to the equation

$$\frac{d\rho_k}{dt} + \rho_k (\nabla \cdot \mathbf{y}) = \dot{\rho}_k = \frac{\rho \dot{m}_k}{m} \quad (\text{A.2.3.1})$$

Summing over  $k$  then gives

$$\frac{d\rho}{dt} + \rho (\nabla \cdot \mathbf{y}) = \frac{\rho \dot{m}}{m} = \dot{\rho} \quad (\text{A.2.3.2})$$

In addition, by definition

$$\frac{dm_k}{dt} = \dot{m}_k \quad (\text{A.2.3.3})$$

which gives

$$\frac{dq_k}{dt} = \frac{\dot{m}_k}{m} - \frac{m_k \dot{m}}{m^2} = \frac{1}{m} (\dot{m}_k - q_k \dot{m}) \quad (\text{A.2.3.4})$$

### A.2.4 The velocity equation

The advective form of the equations for the horizontal components of velocity is unaltered by mass changes. The horizontal velocity components thus satisfy the equation

$$\frac{d\mathbf{y}_h}{dt} = -\frac{1}{\rho} \nabla_h p - 2 (\boldsymbol{\Omega} \times \mathbf{y}_h)_h \quad (\text{A.2.4.1})$$

where  $\boldsymbol{\Omega}$  is the earth's rotation vector. Changes due to molecular stresses are neglected.

### A.2.5 The thermodynamic equation

As discussed by Dufour and Van Mieghem (1975, Eq. 5.21), the first law of thermodynamics may be written

$$\delta Q + \alpha dp = d_i H = d_i \left( \sum m_k h_k \right) \quad (\text{A.2.5.1})$$

where the  $h_k$  are specific enthalpies,  $\alpha = 1/\rho$  is the specific volume and the subscript  $i$  denotes changes independent of the mass changes due to precipitation. As molecular diffusion is neglected,  $\delta Q$  represents the heat received by the atmospheric element due to radiation and to heat exchange with falling rain or snow.

Under the usual assumptions of perfect gas behaviour for dry air and water vapour, and neglect of variations of the specific enthalpies of water and ice with pressure, we can write

$$h_k = h_k^0 + C_{pk} T \quad (\text{A.2.5.2})$$

and (A.2.5.1) becomes

$$m C_p dT = \alpha dp + \delta Q - \sum_k h_k d_i m_k \quad (\text{A.2.5.3})$$

where

$$C_p = \sum_k C_{pk} q_k \quad (\text{A.2.5.4})$$

Thus considering a material volume of the atmosphere, we obtain the thermodynamic equation

$$C_p \frac{dT}{dt} = \frac{1}{\rho} \frac{dp}{dt} + Q_R + Q_M - \sum_k h_k \frac{\dot{m}_{ki}}{m} \quad (\text{A.2.5.5})$$

where  $Q_R$  and  $Q_M$  are the heating rates due to respectively radiation and the heat transferred from falling rain or snow.

### A.3 THE FLUX FORMS OF THE EQUATIONS

It is convenient to define the differential operator  $\frac{D}{Dt}$  by

$$\frac{DX}{Dt} = \frac{dX}{dt} + X(\nabla \cdot \underline{v}) = \frac{\partial X}{\partial t} + \nabla \cdot (X\underline{v}) \quad (\text{A.3.1})$$

Note that

$$\rho = \frac{dx}{dt} = \frac{D\rho x}{Dt} \text{ if } \dot{\rho} = 0 \quad . \quad (\text{A.3.2})$$

Equations (A.2.3.4), (A.2.4.1) and (A.2.5.5) may then be written

$$\frac{D\rho}{Dt} = \frac{\rho}{m}\dot{m} = \dot{\rho} \quad (\text{A.3.3})$$

$$\frac{D\rho q_k}{Dt} = \frac{\rho}{m}\dot{m}_k = \dot{\rho}_k \quad (\text{A.3.4})$$

$$\frac{D\rho \underline{v}_h}{Dt} = \dot{\rho} \underline{v}_h - \nabla_h p - 2\rho (\underline{\Omega} \times \underline{v}_h)_h \quad (\text{A.3.5})$$

$$C_p \frac{D\rho T}{Dt} = C_p \dot{\rho} T + \frac{dp}{dt} + \rho (Q_R + Q_M) - \rho \sum_k h_k \frac{\dot{m}_{ki}}{m} \quad (\text{A.3.6})$$

From the definition (A.2.5.4) of  $C_p$  we obtain

$$\frac{DC_p \rho T}{Dt} = C_p \frac{D\rho T}{Dt} + \rho T \frac{d}{dt} \sum_k C_{pk} q_k \quad (\text{A.3.7})$$

and using (A.2.5.4) and (A.3.6) gives

$$\begin{aligned} \frac{DC_p \rho T}{Dt} &= C_p \dot{\rho} T + \frac{dp}{dt} + \rho (Q_R + Q_M) - \rho \sum_k (h_k^0 + C_{pk} T) \frac{\dot{m}_{ki}}{m} \\ &\quad + \rho T \sum_k C_{pk} \left( \frac{\dot{m}_k}{m} - \frac{q_k \dot{m}}{m} \right) \end{aligned} \quad (\text{A.3.8})$$

Using (A.1.2), (A.1.7) and (A.2.5.4), we obtain from (A.3.8):

$$\frac{DC_p \rho T}{Dt} = \frac{dp}{dt} + \rho (Q_R + Q_M) - \rho \sum_k h_k^0 \frac{\dot{m}_{ki}}{m} + \rho T \sum_k C_{pk} \frac{\dot{m}_{ke}}{m} \quad (\text{A.3.9})$$

#### A.4 THE INTRODUCTION OF DIFFUSIVE FLUXES

We now introduce a separation of dependent variables into components that will be explicitly resolved in the model and components the effect of which will require parametrization.

If the operator ( $\bar{\quad}$ ) represents an average over unresolved scales in space and time, then we write:

$$\begin{aligned} X &= \bar{X} + X' \quad \text{with } \bar{X}' = 0 \\ \text{and} \quad X &= \bar{\bar{X}} + X'' \quad \text{with } \bar{\bar{X}}'' = 0, \\ \text{where} \quad \bar{\bar{X}} &= \frac{\bar{\rho} \bar{X}}{\bar{\rho}} \quad \text{is a mass weighted average.} \end{aligned}$$

It follows that

$$\begin{aligned} \frac{\bar{D}\bar{\rho}\bar{X}}{Dt} &= \frac{D\bar{\rho}\bar{X}}{Dt} - (\nabla \cdot \overline{\rho y'' X''}) \\ \frac{d\bar{X}}{dt} &= \frac{d\bar{X}}{dt} - (\overline{y'' \cdot \nabla \bar{X}}) \\ \bar{\rho} X Y &= \overline{\rho X Y} = \bar{\rho} \bar{\bar{X}} \bar{Y} + \overline{\rho X'' Y''} \end{aligned}$$

Using these results, equations (A.3.2) - (A.3.4) and (A.3.8) become

$$\frac{\bar{D}\bar{\rho}}{Dt} = \bar{\dot{\rho}} = \bar{\rho} \left( \frac{\bar{\dot{m}}}{m} \right) \quad (\text{A.4.1})$$

$$\frac{\bar{D}\bar{\rho} \bar{q}_k}{Dt} = \bar{\rho}_k - (\nabla \cdot \overline{\rho y'' q''_k}) = \bar{\rho} \left( \frac{\bar{\dot{m}}_k}{m} \right) - (\nabla \cdot \overline{\rho y'' q''_k}) \quad (\text{A.4.2})$$

$$\begin{aligned} \frac{\bar{D}\bar{\rho} \bar{y}_h}{Dt} &= \bar{\rho} \bar{y}_h - \nabla_h \bar{p} - 2\bar{\rho} (\bar{\Omega} \times \bar{y}_h)_h - (\nabla \cdot \overline{\rho y'' y''_h}) \\ &= \bar{\rho} \left( \frac{\bar{\dot{m}}}{m} \right) \bar{y}_h - \nabla_h \bar{p} - 2\bar{\rho} (\bar{\Omega} \times \bar{y}_h)_h - (\nabla \cdot \overline{\rho y'' y''_h}) - \overline{\rho \left( \frac{\dot{m}}{m} \right) y''_h} \end{aligned} \quad (\text{A.4.3})$$

and

$$\begin{aligned} \frac{\bar{D}}{Dt} (\bar{\rho} \bar{C}_p \bar{T} + \overline{\rho C''_p T''}) &= \frac{d\bar{p}}{dt} + \bar{\rho} (\bar{Q}_R + \bar{Q}_M) - \bar{\rho} \sum_k h_k^0 \left( \frac{\bar{\dot{m}}_{ki}}{m} \right) \\ &\quad + \bar{\rho} \bar{T} \sum_k C_{pk} \left( \frac{\bar{\dot{m}}_{ke}}{m} \right) + \overline{y'' \cdot \nabla p} - (\nabla \cdot \overline{\rho y'' C_p T''}) \\ &\quad + \sum_k \overline{C_{pk} \rho T'' \left( \frac{\dot{m}_{ke}}{m} \right)} \end{aligned} \quad (\text{A.4.4})$$



The equation of state (A.2.2.5) gives

$$p = \rho RT \quad (\text{A.4.5})$$

where  $R = (R_d q_d + R_v q_v) / \{1 - \rho (q_l v_l + q_i v_i)\}$

whence

$$\bar{p} = \overline{\rho RT} = \overline{\bar{\rho} \bar{R} \bar{T}} + \overline{\rho R'' T''} \quad (\text{A.4.6})$$

Using  $\overline{C_p} = \sum C_{pk} \bar{q}_k$ , (A.4.2) and (A.4.4) may be written

$$\begin{aligned} \overline{C_p \frac{D\bar{p}}{Dt}} &= \frac{d\bar{p}}{dt} + \bar{\rho} (\overline{Q_R} + \overline{Q_M}) - \bar{\rho} \sum_k \bar{h}_k \left( \frac{\overline{\dot{m}_{ki}}}{m} \right) + \overline{\bar{\rho} C_p \bar{T} \left( \frac{\overline{\dot{m}}}{m} \right)} \\ &+ \overline{v'' \nabla p} - \nabla \cdot \overline{\rho v'' (C_p T)''} + \overline{\bar{T} \sum_k C_{pk} \nabla \cdot \rho v'' q''_k} \\ &- \frac{\overline{D}}{Dt} (\overline{\rho C_p'' T''}) + \sum_k \overline{C_{pk} \rho T'' \left( \frac{\overline{\dot{m}_{ke}}}{m} \right)} \end{aligned} \quad (\text{A.4.7})$$

## A.5 APPROXIMATIONS AND DEFINITIONS

At this stage, we make two approximations. The first is to neglect the higher-order correlations

$$\overline{\rho T'' \left( \frac{\overline{\dot{m}_{ke}}}{m} \right)'}, \frac{\overline{D}}{Dt} (\overline{\rho C_p'' T''}), \overline{\rho T'' R''} \text{ and } \overline{\rho \left( \frac{\overline{\dot{m}}}{m} \right)'' v''_h}.$$

This is equivalent to assuming higher-order terms are important only when eddy velocities and derivatives are involved. The second is to neglect the term  $\rho (q_l \cdot v_l + q_i \cdot v_i)$  in the equation of state, or equivalently to neglect the volume occupied by liquid water and ice compared with that occupied by dry air and water vapour.

In addition we introduce the following notation:

a) The vertical flux of a variable  $X$ ,  $\overline{\rho w'' X''}$ , is denoted by  $J_X$ . Here  $w$  is the vertical velocity component.

b) The term  $\overline{v'' \cdot \nabla p}$  is added to the term  $\frac{\partial}{\partial z} \overline{\rho w'' (C_p T)''}$  and the resulting sum is

expressed as the derivative  $\frac{\partial J_S}{\partial z}$  of the vertical flux of dry static energy, plus a term

which is written  $\overline{\bar{\rho} Q_D}$  and regarded as representing unorganized transfers between enthalpy and sub-grid scale kinetic energy. The latter is parametrized by the heating implied by the dissipation of kinetic energy due to the parametrized vertical momentum fluxes  $J_{v_h}$ .

c) The net effect of horizontal fluxes is represented only by their contribution  $K_X$  to the tendency of variable  $X$ .

d) The term  $-\bar{\rho} \sum_k \bar{h}_k \left( \frac{\overline{\dot{m}_{ki}}}{m} \right)$  representing the latent heat release associated with internal phase changes is written  $\bar{\rho} \overline{Q_L}$ .

## A.6 RETURN TO THE ADVECTIVE FORM

With the above approximations and definitions, we obtain from the equations of Appendix A.4, on dropping the  $(\bar{\quad})$  and  $(\overline{\quad})$  signs,

$$\frac{d\rho}{dt} + \rho \nabla \cdot \underline{v} = \rho \frac{\dot{m}}{m} \quad (\text{A.6.1})$$

$$\frac{dq_k}{dt} = S_{q_k} - \frac{1}{\rho} \frac{\partial J_{q_k}}{\partial z} + K_{q_k} \quad (\text{A.6.2})$$

$$\frac{d\underline{v}_h}{dt} = -\frac{1}{\rho} \nabla_h p - 2 (\underline{\Omega} \times \underline{v}_h)_h - \frac{1}{\rho} \frac{\partial J_{\underline{v}_h}}{\partial z} + K_{\underline{v}_h} \quad (\text{A.6.3})$$

$$\frac{dT}{dt} = \frac{1}{\rho C_p} \frac{dp}{dt} + \frac{1}{C_p} \left( Q_R + Q_L + Q_M + Q_D - \frac{1}{\rho} \left[ \frac{\partial J_S}{\partial z} - T \sum_k C_{pk} \frac{\partial J_{q_k}}{\partial z} \right] \right) + K_T \quad (\text{A.6.4})$$

where

$$S_{q_k} = \frac{\dot{m}_k}{m} - q_k \frac{\dot{m}}{m} \quad (\text{A.6.5})$$

In addition we have the equation of state

$$p = \rho T (R_d q_d + R_v q_v) \quad (\text{A.6.6})$$

and the hydrostatic equation

$$\frac{\partial p}{\partial z} = -g\rho \quad (\text{A.6.7})$$

## A.7 THE MODEL EQUATIONS

The model equations (2.2.1) - (2.2.7) and (2.2.12) - (2.2.15) are finally obtained by neglecting density changes due to precipitation or evaporation, setting  $\dot{m} = 0$  in (A.6.1). This approximation is traditionally made, although it is open to question.

In addition,  $Q_M$  is set to zero, an approximation of the same order as the assumption of no variation of latent heat with temperature that is made in the parametrizations.

The governing equations are

$$\frac{dy_h}{dt} = -\frac{1}{\rho} \nabla_h p - 2 (\underline{\Omega} \times y_h)_h - \frac{1}{\rho} \frac{\partial J_{y_h}}{\partial z} + K_{y_h} \quad (\text{A.7.1})$$

$$\frac{dT}{dt} = \frac{R_d T_v}{p C_p} \frac{dp}{dt} + \frac{1}{C_p} \left( Q_R + Q_L + Q_D - \frac{1}{\rho} \left[ \frac{\partial J_S}{\partial z} - C_{pd} T (\delta - 1) \frac{\partial J_{q_v}}{\partial z} \right] \right) + K_T \quad (\text{A.7.2})$$

$$\frac{dq_v}{dt} = S_{q_v} - \frac{1}{\rho} \frac{\partial J_{q_v}}{\partial z} \quad (\text{A.7.3})$$

$$\frac{dq_w}{dt} = S_{q_w} - \frac{1}{\rho} \frac{\partial J_{q_w}}{\partial z} \quad (\text{A.7.4})$$

$$p = \rho R_d T_v \quad (\text{A.7.5})$$

$$\frac{\partial p}{\partial z} = -g\rho \quad (\text{A.7.6})$$

with

$$T_v = T \left( 1 + \left( \frac{1}{\epsilon} - 1 \right) q_v \right) \quad (\text{A.7.7})$$

In this case

$$C_p = C_{pd} (1 - q_v) + C_{pv} q$$

which is written

$$C_p = C_{pd} (1 + (\delta - 1) q_v) \quad (\text{A.7.8})$$

where  $\delta = \frac{C_{pv}}{C_{pd}}$ .

The model equations then follow from a change from  $z$ - to  $\eta$ -coordinates, the formalism for which is given by Kasahara (1974), and from rewriting the adiabatic terms in their usual form for a spherical geometry.



**Appendix B LISTS OF CONSTANTS AND SYMBOLS**

| <u>Symbol</u> | <u>Definition</u>  | <u>Value</u>                   | <u>Unit</u>                            |
|---------------|--|--------------------------------|--|
| $a$           | radius of the earth  | $6.371 \times 10^6$            | m                                      |
| $A_k$         | constant defining the vertical coordinate  |                                | Pa                                     |
| $B$           | Planck function  |                                | $\text{Wm}^{-2}$                       |
| $B_k$         | constant defining the vertical coordinate  |                                | -                                      |
| $C_m, C_h$    | drag coefficient for momentum and heat   |                                | -                                      |
| $C_p$         | $= C_{pd} [1 + (\delta - 1) q_v]$ := specific heat of moist air at constant pressure   |                                | $\text{J kg}^{-1} \text{K}^{-1}$       |
| $C_{pd}$      | specific heat of dry air at constant pressure  | 1005.46                        | $\text{J kg}^{-1} \text{K}^{-1}$       |
| $C_{pv}$      | specific heat of water vapour at constant pressure   | 1869.46                        | $\text{J kg}^{-1} \text{K}^{-1}$       |
| $D$           | $= \frac{1}{a} \left( \frac{1}{1 - \mu^2} \frac{\partial U}{\partial \lambda} + \frac{\partial V}{\partial \mu} \right)$ := divergence |                                | $\text{s}^{-1}$                        |
| $E$           | $= \frac{1}{2} \cdot (U^2 + V^2) / (1 - \mu^2)$ := kinetic energy/unit mass  |                                | $\text{m}^2 \text{s}^{-2}$             |
| $f$           | $= 2\Omega \sin \theta$ := Coriolis parameter  |                                | $\text{s}^{-1}$                        |
| $g$           | acceleration of gravity  | 9.80665                        | $\text{m s}^{-2}$                      |
| $G$           | $= \phi + E$ := total dry energy per unit mass   |                                | $\text{m}^2 \text{s}^{-2}$             |
| $I_0$         | solar constant   | ECHAM1/2: 1365<br>ECHAM3: 1367 | $\text{W m}^{-2}$<br>$\text{W m}^{-2}$ |
| $J_X$         | vertical eddy flux of variable $X$   |                                | $[X] \text{kg m}^{-2} \text{s}^{-1}$   |
| $k$           | von Karman constant  | 0.4                            | -                                      |
| $K_m, K_h$    | vertical eddy diffusion coefficient for momentum and heat  |                                | $\text{m}^2 \text{s}^{-1}$             |
| $K_x$         | tendency of variable $X$ due to horizontal diffusion   |                                | $[X] \text{s}^{-1}$                    |
| $l_m, l_h$    | mixing lengths for momentum and heat   |                                | m                                      |
| $L$           | Monin-Obukhov length   |                                | m                                      |
| $L_s$         | latent heat of sublimation   | $2.8345 \times 10^6$           | $\text{J kg}^{-1}$                     |
| $L_t$         | leaf area index  | 4                              | -                                      |
| $L_v$         | latent heat of vapourisation   | $2.5008 \times 10^6$           | $\text{J kg}^{-1}$                     |
| $m$           | zonal wave number  |                                | -                                      |
| $M_+$         | upward radiative flux density  |                                | $\text{Wm}^{-2}$                       |
| $M_-$         | downward radiative flux density  |                                | $\text{Wm}^{-2}$                       |
| $n$           | meridional index   |                                | -                                      |
| $N_G$         | number of Gaussian latitudes   |                                | -                                      |

|                   |   |        |                      |
|-------------------|---|--------|----------------------|
| $p$               | pressure  |        | Pa                   |
| $p_0$             | reference pressure for vertical coordinate                        |        | Pa                   |
| $p_S$             | surface pressure  |        | Pa                   |
| $P_x$             | parameterized tendency of variable $x$                            |        | $[x]s^{-1}$          |
| $P_n^m(\mu)$      | associated Legendre function of the first kind                    |        | -                    |
| $q_i$             | ice mixing ratio  |        | $kg\ kg^{-1}$        |
| $q_l$             | liquid water mixing ratio   |        | $kg\ kg^{-1}$        |
| $q_s$             | saturation water vapour mixing ratio                              |        | $kg\ kg^{-1}$        |
| $q_v$             | water vapour mixing ratio   |        | $kg\ kg^{-1}$        |
| $q_w$             | cloud water mixing ratio ( $q_w = q_i + q_l$ )                    |        | $kg\ kg^{-1}$        |
| $Q_Y$             | heating rate due to physical process $Y$                          |        | $K\ s^{-1}$          |
| $R$               | precipitation rate  |        | $kg\ m^{-2}\ s^{-1}$ |
| $R_d$             | gas constant for dry air  | 287.05 | $J\ kg^{-1}K^{-1}$   |
| $R_v$             | gas constant for water vapour                                     | 461.51 | $J\ kg^{-1}K^{-1}$   |
| $Ri$              | Richardson number   |        | -                    |
| $Ri_{crit}$       | critical Richardson number  |        | -                    |
| $Ri_m$            | moist Richardson number   |        | -                    |
| $s$               | dry static energy   |        | $m^2\ s^{-2}$        |
| $s_*$             | scaling dry static energy   |        | $m^2\ s^{-2}$        |
| $S_{q_v}$         | change of $q_v$ due to condensation or evaporation                |        | $s^{-1}$             |
| $S_{q_w}$         | change of $q_w$ due to condensation, evaporation or precipitation |        | $s^{-1}$             |
| $Sn$              | snow depth (liquid water equivalent)                              |        | m                    |
| $Sn_{cr}$         | critical snow depth (liquid water equivalent)                     |        | m                    |
| $t$               | time  |        | s                    |
| $T$               | temperature   |        | K                    |
| $T_m$             | ice melting temperature   | 273.16 | K                    |
| $T_S$             | surface temperature   |        | K                    |
| $T_{Sn}$          | temperature of the snow pack                                      |        | K                    |
| $T_v$             | $= T [1 + (1/\epsilon - 1) q_v]$ := virtual temperature           |        | K                    |
| $u$               | zonal wind  |        | $m\ s^{-1}$          |
| $u_*$             | scaling velocity  |        | $m\ s^{-1}$          |
| $U$               | $= u \cdot \cos\theta$ := scaled zonal wind                       |        | $m\ s^{-1}$          |
| $v$               | meridional wind   |        | $m\ s^{-1}$          |
| $\underline{v}_h$ | $= (u, v)$ := horizontal wind vector                              |        | $m\ s^{-1}$          |

|                        |   |                      |                                |
|------------------------|---|----------------------|--------------------------------|
| $V$                    | $= v \cdot \cos\theta$ := scaled meridional wind  |                      | $\text{m s}^{-1}$              |
| $w(\mu)$               | quadrature (or Gaussian) weight   |                      | -                              |
| $W_l$                  | skin reservoir content  |                      | m                              |
| $W_{lmax}$             | maximum skin reservoir content  | $2 \cdot 10^{-4}$    | m                              |
| $W_{lmx}$              | local maximum skin reservoir  |                      | m                              |
| $W_S$                  | soil moisture   |                      | m                              |
| $W_{Smax}$             | field capacity  | 0.2                  | m                              |
| $z$                    | height  |                      | m                              |
| $z_0$                  | roughness length  |                      | m                              |
| $\delta$               | $= C_{pv}/C_{pd}$   |                      | -                              |
| $\delta_s$             | solar declination   |                      | -                              |
| $\epsilon$             | $R_d/R_v$   |                      | -                              |
| $\eta$                 | $\eta_k = A_k/p_0 + B_k$ := generalized vertical coordinate   |                      | -                              |
| $\dot{\eta}$           | $= d\eta/dt = \eta$ -coordinate vertical velocity   |                      | $\text{s}^{-1}$                |
| $\theta$               | latitude  |                      | -                              |
| $\Theta$               | potential temperature   |                      | K                              |
| $\Theta_l$             | liquid water potential temperature  |                      | K                              |
| $\Theta_v$             | virtual potential temperature   |                      | K                              |
| $\phi$                 | $g \cdot z$ , geopotential  |                      | $\text{m}^2\text{s}^{-2}$      |
| $\phi_m, \phi_h$       | universal flux profile functions for momentum and heat  |                      | -                              |
| $\kappa$               | $= R_d/C_{pd}$  |                      | -                              |
| $\lambda$              | longitude   |                      | -                              |
| $\lambda_m, \lambda_h$ | asymptotic mixing length for momentum and heat  |                      | -                              |
| $\mu$                  | $= \sin\theta$  |                      | -                              |
| $\xi$                  | $= \frac{1}{a} \left( \frac{1}{1-\mu^2} \frac{\partial V}{\partial \lambda} - \frac{\partial U}{\partial \mu} \right)$ : relative vorticity |                      | $\text{s}^{-1}$                |
| $\rho$                 | air density   |                      | $\text{kg m}^{-3}$             |
| $\rho_w$               | density of liquid water   | 1000                 | $\text{kg m}^{-3}$             |
| $\rho_{Sn}$            | density of snow   |                      | $\text{kg m}^{-3}$             |
| $\sigma$               | $= p/p_s$   |                      | -                              |
| $\sigma$               | Stefan-Boltzmann constant   | $5.67 \cdot 10^{-8}$ | $\text{W m}^{-2}\text{K}^{-4}$ |
| $\phi$                 | $= g \cdot z$ := geopotential height  |                      | $\text{m}^2\text{s}^{-2}$      |
| $\phi_s$               | surface geopotential height   |                      | $\text{m}^2\text{s}^{-2}$      |
| $\chi$                 | velocity potential  |                      | $\text{m}^2\text{s}^{-1}$      |

|                  |  |                       |                           |
|------------------|--|-----------------------|---------------------------|
| $\psi$           | stream function                              |                       | $\text{m}^2\text{s}^{-1}$ |
| $\omega$         | $= dp/dt := p$ -coordinate vertical velocity |                       | $\text{Pa s}^{-1}$        |
| $\tilde{\omega}$ | single scattering albedo                     |                       | -                         |
| $\Omega$         | angular velocity of earth                    | $7.292 \cdot 10^{-5}$ | $\text{s}^{-1}$           |



## Appendix C GAUSSIAN LATITUDES FOR ECHAM3-TRUNCATIONS

**NOTE: The Gaussian latitudes are symmetrical to the equator !**

**Therefore only the values from the North pole to the equator are printed.**

The Gaussian latitudes are scanned by subroutine SCAN1. To get the current numbers of ILAT, the number count from the North pole, and IROW, the number count in the model, write

```
ITASK=IQTASK()
ILAT=NLAT(ITASK+1)
IROW=NROW(ITASK+1)
```

NLAT and NROW belong to the commonblock COMCTL.

### C.1 THE "GAUSSIAN" LATITUDES FOR T21-TRUNCATION

| No. from North pole (ILAT) | No. in the model (IROW) | Latitude (°) | No. from North pole (ILAT) | No. in the model (IROW) | Latitude (°) |
|----------------------------|-------------------------|--------------|----------------------------|-------------------------|--------------|
| 1                          | 1                       | 85.760       | 9                          | 17                      | 41.532       |
| 2                          | 3                       | 80.268       | 10                         | 19                      | 35.995       |
| 3                          | 5                       | 74.744       | 11                         | 21                      | 30.457       |
| 4                          | 7                       | 69.212       | 12                         | 23                      | 24.919       |
| 5                          | 9                       | 63.678       | 13                         | 25                      | 19.382       |
| 6                          | 11                      | 58.142       | 14                         | 27                      | 13.844       |
| 7                          | 13                      | 52.606       | 15                         | 29                      | 8.306        |
| 8                          | 15                      | 47.069       | 16                         | 31                      | 2.768        |

C.2 THE "GAUSSIAN" LATITUDES FOR T42-TRUNCATION

| <b>No. from<br/>North pole<br/>(ILAT)</b> | <b>No.<br/>in the model<br/>(IROW)</b> | <b>Latitude (°)</b> | <b>No. from<br/>North pole<br/>(ILAT)</b> | <b>No.<br/>in the model<br/>(IROW)</b> | <b>Latitude (°)</b> |
|---|--|---------------------|---|--|---------------------|
| 1   | 1                                      | 87.863              | 17  | 33                                     | 43.254              |
| 2   | 3                                      | 85.096              | 18  | 35                                     | 40.463              |
| 3   | 5                                      | 82.312              | 19  | 37                                     | 37.673              |
| 4   | 7                                      | 79.525              | 20  | 39                                     | 34.882              |
| 5   | 9                                      | 76.736              | 21  | 41                                     | 32.091              |
| 6   | 11                                     | 73.947              | 22  | 43                                     | 29.301              |
| 7   | 13                                     | 71.157              | 23  | 45                                     | 26.510              |
| 8   | 15                                     | 68.367              | 24  | 47                                     | 23.720              |
| 9   | 17                                     | 65.577              | 25  | 49                                     | 20.929              |
| 10  | 19                                     | 62.787              | 26  | 51                                     | 18.138              |
| 11  | 21                                     | 59.997              | 27  | 53                                     | 15.348              |
| 12  | 23                                     | 57.206              | 28  | 55                                     | 12.557              |
| 13  | 25                                     | 54.416              | 29  | 57                                     | 9.767               |
| 14  | 27                                     | 51.625              | 30  | 59                                     | 6.976               |
| 15  | 29                                     | 48.835              | 31  | 61                                     | 4.185               |
| 16  | 31                                     | 46.044              | 32  | 63                                     | 1.395               |

C.3 THE "GAUSSIAN" LATITUDES FOR T63-TRUNCATION

| <b>No. from<br/>North pole<br/>(ILAT)</b> | <b>No.<br/>in the model<br/>(IROW)</b> | <b>Latitude (°)</b> | <b>No. from<br/>North pole<br/>(ILAT)</b> | <b>No.<br/>in the model<br/>(IROW)</b> | <b>Latitude (°)</b> |
|---|--|---------------------|---|--|---------------------|
| 1   | 1                                      | 88.572              | 25  | 49                                     | 43.833              |
| 2   | 3                                      | 86.722              | 26  | 51                                     | 41.968              |
| 3   | 5                                      | 84.861              | 27  | 53                                     | 40.102              |
| 4   | 7                                      | 82.998              | 28  | 55                                     | 38.237              |
| 5   | 9                                      | 81.134              | 29  | 57                                     | 36.372              |
| 6   | 11                                     | 79.270              | 30  | 59                                     | 34.507              |
| 7   | 13                                     | 77.405              | 31  | 61                                     | 32.641              |
| 8   | 15                                     | 75.541              | 32  | 63                                     | 30.776              |
| 9   | 17                                     | 73.676              | 33  | 65                                     | 28.911              |
| 10  | 19                                     | 71.811              | 34  | 67                                     | 27.046              |
| 11  | 21                                     | 69.946              | 35  | 69                                     | 25.180              |
| 12  | 23                                     | 68.080              | 36  | 71                                     | 23.315              |
| 13  | 25                                     | 66.215              | 37  | 73                                     | 21.450              |
| 14  | 27                                     | 64.350              | 38  | 75                                     | 19.585              |
| 15  | 29                                     | 62.485              | 39  | 77                                     | 17.719              |
| 16  | 31                                     | 60.620              | 40  | 79                                     | 15.854              |
| 17  | 33                                     | 58.755              | 41  | 81                                     | 13.989              |
| 18  | 35                                     | 56.890              | 42  | 83                                     | 12.124              |
| 19  | 37                                     | 55.024              | 43  | 85                                     | 10.258              |
| 20  | 39                                     | 53.159              | 44  | 87                                     | 8.393               |
| 21  | 41                                     | 51.294              | 45  | 89                                     | 6.528               |
| 22  | 43                                     | 49.429              | 46  | 91                                     | 4.663               |
| 23  | 45                                     | 47.563              | 47  | 93                                     | 2.797               |
| 24  | 47                                     | 45.698              | 48  | 95                                     | 0.932               |

C.4 THE "GAUSSIAN" LATITUDES FOR T106-TRUNCATION

| <b>No. from<br/>North pole<br/>(ILAT)</b> | <b>No.<br/>in the model<br/>(IROW)</b> | <b>Latitude (°)</b> | <b>No. from<br/>North pole<br/>(ILAT)</b> | <b>No.<br/>in the model<br/>(IROW)</b> | <b>Latitude (°)</b> |
|---|--|---------------------|---|--|---------------------|
| 1   | 1                                      | 89.141              | 41  | 81                                     | 44.298              |
| 2   | 3                                      | 88.029              | 42  | 83                                     | 43.177              |
| 3   | 5                                      | 86.910              | 43  | 85                                     | 42.055              |
| 4   | 7                                      | 85.790              | 44  | 87                                     | 40.934              |
| 5   | 9                                      | 84.669              | 45  | 89                                     | 39.812              |
| 6   | 11                                     | 83.548              | 46  | 91                                     | 38.691              |
| 7   | 13                                     | 82.427              | 47  | 93                                     | 37.569              |
| 8   | 15                                     | 81.306              | 48  | 95                                     | 36.448              |
| 9   | 17                                     | 80.185              | 49  | 97                                     | 35.326              |
| 10  | 19                                     | 79.063              | 50  | 99                                     | 34.205              |
| 11  | 21                                     | 77.942              | 51  | 101                                    | 33.083              |
| 12  | 23                                     | 76.821              | 52  | 103                                    | 31.962              |
| 13  | 25                                     | 75.699              | 53  | 105                                    | 30.840              |
| 14  | 27                                     | 74.578              | 54  | 107                                    | 29.719              |
| 15  | 29                                     | 73.457              | 55  | 109                                    | 28.597              |
| 16  | 31                                     | 72.335              | 56  | 111                                    | 27.476              |
| 17  | 33                                     | 71.214              | 57  | 113                                    | 26.355              |
| 18  | 35                                     | 70.092              | 58  | 115                                    | 25.233              |
| 19  | 37                                     | 68.971              | 59  | 117                                    | 24.112              |
| 20  | 39                                     | 67.849              | 60  | 119                                    | 22.990              |
| 21  | 41                                     | 66.728              | 61  | 121                                    | 21.869              |
| 22  | 43                                     | 65.606              | 62  | 123                                    | 20.747              |
| 23  | 45                                     | 64.485              | 63  | 125                                    | 19.626              |
| 24  | 47                                     | 63.363              | 64  | 127                                    | 18.504              |
| 25  | 49                                     | 62.242              | 65  | 129                                    | 17.383              |
| 26  | 51                                     | 61.120              | 66  | 131                                    | 16.261              |
| 27  | 53                                     | 59.999              | 67  | 133                                    | 15.140              |
| 28  | 55                                     | 58.878              | 68  | 135                                    | 14.018              |
| 29  | 57                                     | 57.756              | 69  | 137                                    | 12.897              |

| <b>No. from<br/>North pole<br/>(ILAT)</b> | <b>No.<br/>in the model<br/>(IROW)</b> | <b>Latitude (°)</b> | <b>No. from<br/>North pole<br/>(ILAT)</b> | <b>No.<br/>in the model<br/>(IROW)</b> | <b>Latitude (°)</b> |
|---|--|---------------------|---|--|---------------------|
| 30  | 59                                     | 56.635              | 70  | 139                                    | 11.775              |
| 31  | 61                                     | 55.513              | 71  | 141                                    | 10.654              |
| 32  | 63                                     | 54.392              | 72  | 143                                    | 9.532               |
| 33  | 65                                     | 53.270              | 73  | 145                                    | 8.411               |
| 34  | 67                                     | 52.149              | 74  | 147                                    | 7.289               |
| 35  | 69                                     | 51.027              | 75  | 149                                    | 6.168               |
| 36  | 71                                     | 49.906              | 76  | 151                                    | 5.046               |
| 37  | 73                                     | 48.784              | 77  | 153                                    | 3.925               |
| 38  | 75                                     | 47.663              | 78  | 155                                    | 2.803               |
| 39  | 77                                     | 46.541              | 79  | 157                                    | 1.682               |
| 40  | 79                                     | 45.420              | 80  | 159                                    | 0.560               |



## Appendix D LAND-SEA MASKS FOR ECHAM3-TRUNCATIONS

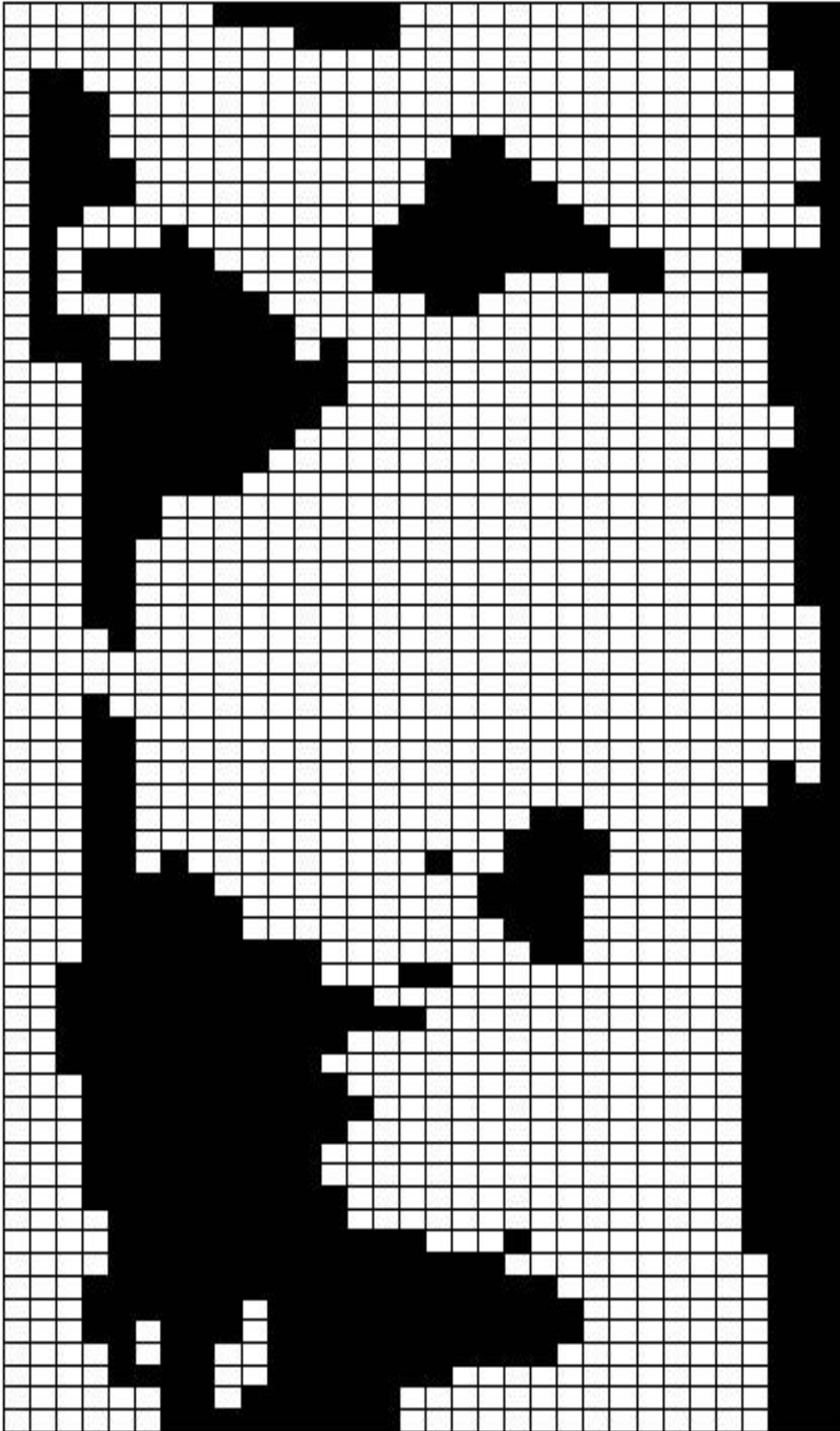
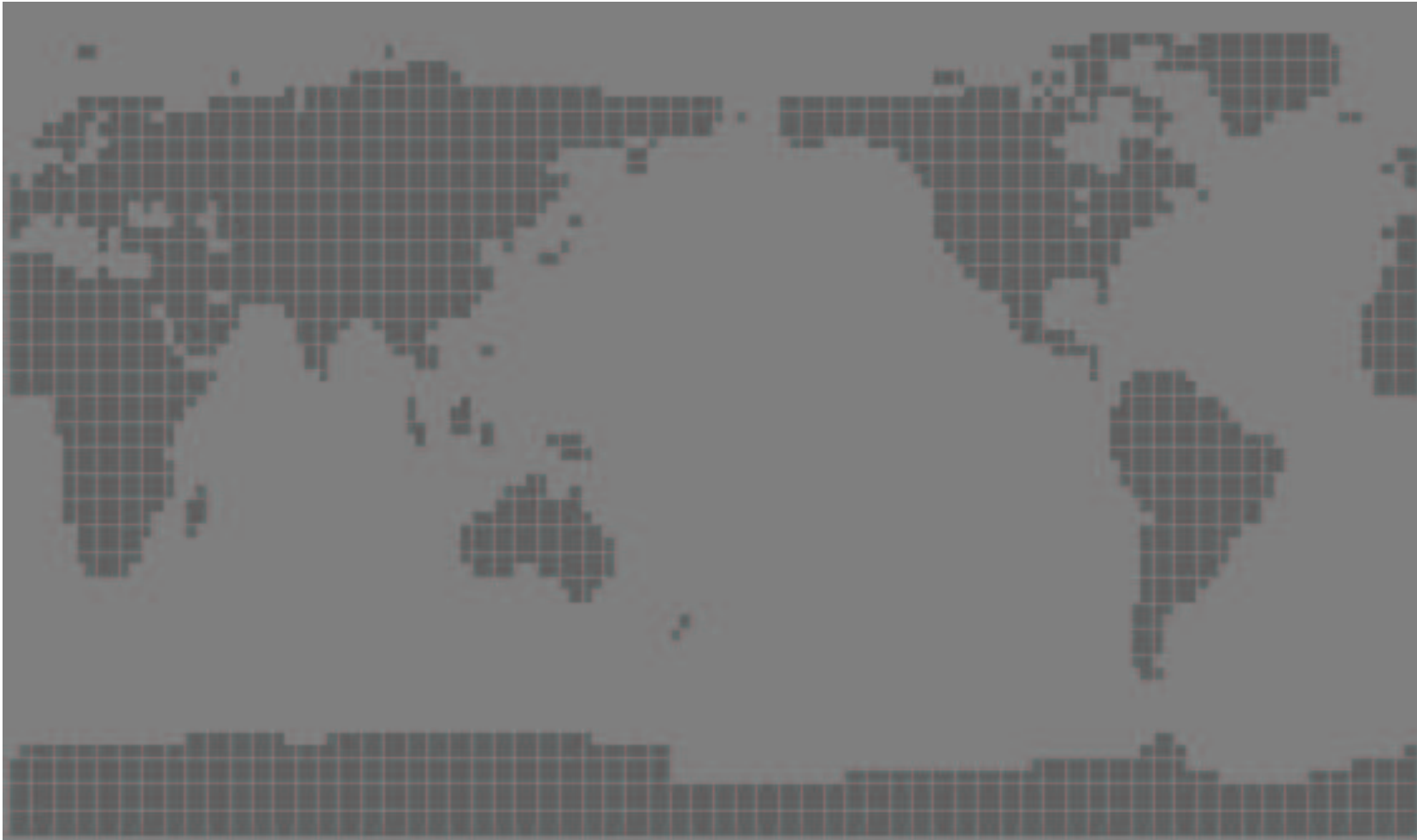


Figure 22 Land-sea mask for T21 model truncation



*Figure 23* Land-sea mask for T42 model truncation





*Figure 24* Land-sea mask for T63 model truncation



*Figure 25* Land-sea mask for T106 model truncation

## **Appendix E PROGRAMMING CONVENTIONS**

### E.1 INTRODUCTION

The programming standard on which the following conventions are based was derived from the OLYMPUS system , and is called DOCTOR.

### E.2 PROGRAM STRUCTURE

#### E.2.1 Subtasks

Systems developed using this standard are, where reasonable, organised into a hierarchical, tree-like structure. The climate simulation is divided into major subtasks, each with a distinct purpose. Subtasks consist of a control routine together with a set of computational routines. The subtask is always entered by calling the control routine. The control routine need not always be called from the same location within the code, but is always called to control the calling of some or all of the set of computational routines comprising the subtask. In this way subtasks can be self contained units, and alternative subtasks can be substituted when desired.

Subtasks may extend over a wide range of logically connected processes, such as radiation, dynamics, parameterization, etc., or may be of more limited scope, such as horizontal diffusion, etc.

#### E.2.2 Utility routines

A set of utility routines is available. These are taken from the set of OLYMPUS utility routines. They are used to output messages, list values of variables, reset values, etc. . Table 6 gives a list of the utility routines available, and the functions they perform.

**Table 6 Utility routines**

| <b>NAME</b> | <b>PARAMETERS</b>        | <b>PURPOSE</b>   |
|-------------|--------------------------|--|
| RVAR        | KNAME, PVALUE            | Print name and value of real variable                  |
| IVAR        | KNAME, KVALUE            | Print name and value of integer variable               |
| HVAR        | KNAME, HPVALUE           | Print name and value of Hollerith variable             |
| LVAR        | KNAME, LPVAL             | Print name and value of logical variable               |
| RARRAY      | KNAME, PA, KDIM          | Print name and values of real array                    |
| IARRAY      | KNAME, KA, KDIM          | Print name and values of integer array                 |
| HARRAY      | KNAME, HPA, KDIM         | Print name and values of Hollerith array               |
| LARRAY      | KNAME, LPA, KDIM         | Print name and values of logical array                 |
| RARRAY2     | KNAME, PA, KDIMX, KX, KY | Print name and values of doubly subscripted real array |
| RESETR      | PA, KDIM, PVALUE         | Reset real array to specified value                    |
| RESETI      | KA, KDIM, KVALUE         | Reset integer array to specified value                 |
| RESETH      | HPA, KDIM, HPVALUE       | Reset Hollerith array to specified value               |
| RESETL      | LPA, KDIM, KLVAL         | Reset logical array to specified value                 |
| SCALER      | PA, KDIM, PC             | Scale real array by a real value                       |
| SCALEI      | KA, KDIM, KC             | Scale integer array by an integer value                |
| SIGNR       | PA, KDIM                 | Change the sign of a real array                        |
| SIGNI       | KA, KDIM                 | Change the sign of an integer array                    |
| COPYR       | PA1, PA2, KDIM           | Copy one real array into another                       |
| COPYI       | KA1, KA2, KDIM           | Copy one integer array into another                    |

### E.3 SUBROUTINE STRUCTURE

Subroutines should perform a single well defined task. The first section of each subroutine should contain a documentation of the following form:

- a) A C\*\*\*\* statement with the title beginning with the subroutine name.
- b) The author's name and the date written.
- c) Modification details (name and date).
- d) Headed sections, giving the following information:
  - 1) PURPOSE                the function of the routine,
  - 2) INTERFACE            how the routine receives its data and returns its results,
  - 3) METHOD                how the results are obtained,
  - 4) EXTERNALS            what external routines are required,
  - 5) REFERENCE            references to external documentation, if any,
  - 6) MODIFICATIONS      date and nature of any modification made to the routine.

This section of the subroutine should be regarded as the documentation that would be supplied to an external user of the routine. It should contain information which can stand alone as a separate document, and sufficient information to enable an external user to decide whether the routine is suitable for his/her purpose, and to enable him/her to use it.

The computational part of each subroutine should be divided into sections and sub-sections. These should be numbered for cross reference purposes. Subsection n of section m should be numbered "m.n". Sections should be ruled off from one another by a comment containing C in column 1 and "-----" in columns 7 to 71. Each section should begin with a title, which should be underlined by the next statement. Sections should begin with a CONTINUE statement of the form

```
m00  CONTINUE
```

enabling branches to be made to the beginning of the section. A sub-section should begin with a title, followed by a CONTINUE statement of the form

```
mn0  CONTINUE
```

enabling branches to be made to the sub-section. Sub-section titles should not be underlined, and may be intended with respect to section titles to produce well formatted documentation when listed.

## E.4 COMMON BLOCK STRUCTURE

COMMON blocks contain a documentation defining the variables they contain in tabular form:

- a) A C\*\* statement beginning with the COMMON block name and indicating its purpose.
- b) The following table headings:
 

| <u>NAME</u> | <u>TYPE</u> | <u>PURPOSE</u> |
|-------------|-------------|----------------|
|-------------|-------------|----------------|
- c) A table entry for each variable in the COMMON block.

To avoid duplication of these comments in each routine calling the COMMON block, some or all of the comments may be enclosed in UPDATE \*DEFINE brackets, using

```
*IF DEF,DOC
and
*ENDIF
```

Sequences of comments of the form

```
C
C -----
C
```

should be used where appropriate to improve the layout.

## E.5 FORMAT STATEMENTS

FORMAT statements are used where several READ/WRITE use the same format, or where long FORMAT definitions would make a READ or WRITE statement long, complicated, or difficult to read. In general, use should be made of the ability to code format specifications within the READ or WRITE statement. This ability is especially useful for printing messages.

Where used, FORMAT statements should be numbered within the range of 9901 to 9999, and gathered together at the end of the routine in which they are referenced.

## E.6 BLOCK STRUCTURE

Statement numbers should not be associated with executable statements. With the exception of FOR-MAT statements, the only numbered statement should be CONTINUE statements. Each DO loop should end on a separate CONTINUE statement.

IF-THEN-ELSE sequences should make use of indentation to illustrate the scope of each conditional block. ENDIF should always be coded as a single word.

E. g.:

```
IF (NROW.EQ.MAXROW) THEN
  JJ=JJ+1
  CALL SPOLE
  IF (JJ.GT.JTEST) THEN
    JJ2=JJ-ILIM
    CALL SSPOLE
  ENDIF
ELSE CALL NOTSPOL
ENDIF
```

E.7 VARIABLE NAMES

Variable names begin with significant prefix letters. These prefix letters not only indicate the type of variable (real, integer, etc.) but also the status of the variable (local, common, etc.).

## 1) Variable type

LOGICAL variables begin with L.  
 INTEGER variables begin with I, J, K, M, or N.  
 HOLLERITH variables begin with H.  
 CHARACTER variables begin with Y and are defined \*8.  
 All other variables are of type REAL

## 2) Variable status

The status of variables is indicated in the following way:

## a) Dummy arguments:

Dummy arguments begin with

|    |              |
|----|--------------|
| LP | if LOGICAL   |
| K  | if INTEGER   |
| P  | if REAL      |
| HP | if HOLLERITH |
| YP | if CHARACTER |

## b) Local variables:

variables local to a routine begin with

|    |              |
|----|--------------|
| LO | if LOGICAL   |
| I  | if INTEGER   |
| Z  | if REAL      |
| HO | if HOLLERITH |
| YO | if CHARACTER |

## c) Loop control variables:

All loop control variables begin with J.

## d) Variables in COMMON blocks:

All remaining prefixes are available for variables located in COMMON blocks.

Typing of variables should be achieved by using:

IMPLICIT LOGICAL(L), INTEGER(H), CHARACTER\*8(Y)



## E.8 MEMORY MANAGEMENT

### E.8.1 General

The memory manager is application independent. The remainder of this section describes the way in which the model uses it.

### E.8.2 Method of use

The memory manager recognizes two types of storage - long term storage of arrays required by several routines, and temporary storage used for work space within a routine.

A list of memory manager routines used by the model is given in Table 7.

Arrays are allocated by calling ALLOCA. Contiguous memory locations may be obtained by repeated calls to the alternative allocation routine ALLOCB. Arrays allocated in one routine may be located in a subsequent routine by calling LOCATE. Storage no longer required is returned to the manager for possible future allocation by calling UNLOC.

**Table 7 Memory manager routines**

| <b>ROUTINE</b> | <b>PURPOSE</b>            |
|----------------|---------------------------|
| ALLOCA         | Allocate space            |
| ALLOCB         | Allocate contiguous space |
| LOCATE         | Locate allocated space    |
| UNLOC          | Release allocated space   |

### E.8.3 Example

A simple example for a subroutine using the memory manager is given below.

Four arrays are involved in this example:

1. Long term arrays which are already allocated but not local to this subroutine:  
 TM1(NLP2,NLEV), and  
 TE(NLP2,NLEV).
2. Short term arrays (only for use in this subroutine):  
 ZTP1(NLON,NLEV), and  
 ZTEX(NLON,NLEV).

## SUBROUTINE EXAMPLE

```

C
C**** *EXAMPLE* - DEMONSTRATES PROGRAMMING CONVENTIONS
C
C      U. SCHLESE          DKRZ - HAMBURG    JUL-92
C
C      PURPOSE.
C      -----
C
C      THIS ROUTINE DEMONSTRATES THE *DOCTOR* PROGRAMMING CONVENTIONS
C      AND THE USE OF THE MEMORY MANAGER.
C
C      INTERFACE.
C      -----
C
C      *EXAMPLE* IS CALLED FROM *MAIN*.
C      IT TAKES ITS INPUT FROM THE LONG TERM STORAGE:
C      TM1 : TEMPERATURE AT FULL LEVELS
C      TE  : TENDENCY OF TEMPERATURE
C
C      IT RETURNS ITS OUTPUT TO THE SAME SPACE:
C      TE: UPDATED BY PROCESSES CALCULATED IN *SUB1*
C
C      METHOD.
C      -----
C
C      STRAIGHTFORWARD.
C
C      EXTERNALS.
C      -----
C
C      *LOCATE*   LOCATE LONG TERM STORAGE
C      *ALLOCA*  ALLOCATE TEMPORARY STORAGE
C      *SUB1*    UPDATES TENDENCIES
C
C      REFERENCE.
C      -----
C
C      NONE.
C
C      MODIFICATIONS.
C      -----
C
C      NONE.
C
C*   *COMMON* *COMCTL* - CONTROL VARIABLES FOR MODEL HOUSEKEEPING.
C
C      NAME      TYPE      PURPOSE
C      ----      -
C
C      *NLEV*    *INTEGER*  NUMBER OF VERTICAL LEVELS.
C      *NLON*    *INTEGER*  NUMBER OF POINTS ON EACH LATITUDE LINE.
C      *NLP2*    *INTEGER*  NUMBER OF POINTS ON EACH LATITUDE LINE + 2.
C
C      COMMON /COMCTL/
C      I          NLEV,NLON,NLP2

```

```

C
C -----
C
C   POINTER   (ITM1, TM1(NLP2, NLEV)),           ! Declare managed arrays
*             (ITE, TE(NLP2, NLEV)),           ! by means of
*             (IZTP1, ZTP1(NLON, NLEV)),       ! POINTER statements
*             (IZTEX, ZTEX(NLON, NLEV))
C
C -----
C*  1. LOCATE AND POSITION SPACE.
C     -----
C
100  CONTINUE
      ITASK=IQTASK()                             ! Get current task number.
      IGPTYPE=ITASK+3                             ! Set type of data
C
      CALL LOCATE(ITM1, 'TM1', IGPTYPE)          ! Get addresses (=POINTER
      CALL LOCATE(ITE, 'TE', IGPTYPE)          ! values) of TM1 and TE
C
      CALL ALLOCA(IBASE, 2*NLON*NLEV, 'EXAMPLE', 99) ! Allocate temporary storage
      IZTP1=IBASE                                ! for ZTP1 and ZTEX and
      IZTEX=IZTP1+NLON*NLEV                     ! calculate addresses (alter-
                                              ! native: automatic arrays)
C
C -----
C*  2. PREPARE INPUT FOR *SUB1*.
C     -----
C
200  CONTINUE
      DO 202 JK=1, NLEV
      DO 201 JL=1, NLON
      ZTP1(JL, JK)=TM1(JL, JK)+ZTMST*TE(JL, JK) ! Use arrays within the
      ZTEX(JL, JK)=EXP(ZTP1(JL, JK))           ! code as usual
201  CONTINUE
202  CONTINUE
C
C -----
C*  3. UPDATE TENDENCIES.
C     -----
C
300  CONTINUE
      CALL SUB1(ZTP1, ZTEX, TE)
C
C -----
C*  4. RELEASE SPACE.
C     -----
C
400  CONTINUE
      CALL UNLOC('EXAMPLE', 99)                ! Release temporary space
C
C -----
C
      RETURN
      END

```

### E.8.4 Managed arrays

Long term arrays are identified by the memory manager by means of a name and a code. Throughout the climate simulation routines code are allocated according to grid type or sub-system, as indicated in Table 8, while the actual array name is used where possible. The purpose of this dual identification is to ensure uniqueness even if the same name is used for different storage areas in different subsystems.

Short-term arrays are identified by means of a name and a specific code of 99. By convention, the name used is that of the calling routine. A routine may repeatedly request temporary array space in this way, and releases all of the allocated space by a single call to UNLOC.

Managed arrays are declared by means of POINTER statements. The pointer values are assigned by the memory manager.

**Table 8 Grid code used with the Memory Manager**

| <b>GRID CODE</b> | <b>CODE TYPE</b> | <b>TYPE OF DATA</b>                     |
|------------------|------------------|---|
| 1                | ISY              | Basic control blocks (SDS, DDR's, etc.) |
| 3                | IGP              | Grid point data                         |
| 20               | ILC              | Transformation constants                |
| 30               | ISP              | Spectral coefficients                   |
| 40               | IFC              | Fourier coefficients                    |
| 60               | IDI              | Other diagnostics                       |
| 70               | IRD              | Radiation workspace                     |
| 99               | none             | Temporary storage                       |

Table 9 gives a list of managed arrays used by the ECHAM3 climate model and the name of the subroutines in which allocation (ALLOC) and release (UNLOC) of the arrays is done. Refer to the footnotes to obtain the higher level calling subroutines.

**Table 9 List of managed arrays, ALLOCS and UNLOCS  
(Sheet 1 of 11)**

| NAME              | TYPE | ALLOC               | UNLOC               | VARIABLE   |
|-------------------|------|---------------------|---------------------|--|
| ACLC<br>ACLCM     | IGP  | BUFGRD <sup>1</sup> | RELBUF <sup>2</sup> | cloud cover [fract.]   |
| ACLCAC<br>ACLCACM | IGP  | BUFGRD <sup>1</sup> | RELBUF <sup>2</sup> | cloud cover [fract.*s]<br>(accumulated) <sup>9</sup>                                   |
| ACLCOV<br>ACLCOVM | IGP  | BUFGRD <sup>1</sup> | RELBUF <sup>2</sup> | total cloud cover [fract.*s]<br>(accumulated) <sup>9</sup>                             |
| AHFL<br>AHFLM     | IGP  | BUFGRD <sup>1</sup> | RELBUF <sup>2</sup> | surface latent heat flux [J/m**2]<br>(accumulated) <sup>9</sup>                        |
| AHFS<br>AHFSM     | IGP  | BUFGRD <sup>1</sup> | RELBUF <sup>2</sup> | surface sensible heat flux [J/m**2]<br>(accumulated) <sup>9</sup>                      |
| ALB<br>ALBM       | IGP  | BUFGRD <sup>1</sup> | RELBUF <sup>2</sup> | surface background albedo [fract.]   |
| ALBEDO<br>ALBEDOM | IGP  | BUFGRD <sup>1</sup> | RELBUF <sup>2</sup> | surface albedo [fract.]  |
| ALNPR             | IGP  | SCAN1               | PHYSC               | logarithm of pressure ratios   |
| ALPHA             | IGP  | SCAN1               | PHYSC               | $\alpha_k$ (see equation (2.4.2.12) in section 2.4.2 )                                 |
| ALPS              | IGP  | SCAN1               | SCAN1               | logarithm of surface pressure  |
| ALPSE             | IGP  | SCAN1               | SCAN1               | tendency of logarithm of surface pressure  |
| ALPSF             | IGP  | BUFGRD <sup>1</sup> | RELBUF <sup>2</sup> | logarithm of surface pressure (semi filtered) <sup>6</sup>                             |
| ALPSM1            | IGP  | BUFGRD <sup>1</sup> | RELBUF <sup>2</sup> | logarithm of surface pressure at t - $\Delta t$  |
| ALWC<br>ALWCM     | IGP  | BUFGRD <sup>1</sup> | RELBUF <sup>2</sup> | liquid water content [kg/kg]   |
| ALWCAC<br>ALWCACM | IGP  | BUFGRD <sup>1</sup> | RELBUF <sup>2</sup> | liquid water content [(kg/kg)*s]<br>(accumulated) <sup>9</sup>                         |
| ALWCVI<br>ALWCVIM | IGP  | BUFGRD <sup>1</sup> | RELBUF <sup>2</sup> | vertically integrated liquid water content [(kg/m**2)*s]<br>(accumulated) <sup>9</sup> |
| AMU0              | IGP  | RADHEAT<br>RADINT   | RADINT<br>RADHEAT   | cosine of solar zenith angle   |
| ANMD              | ILC  | BUFNL1 <sup>3</sup> | RELBUF <sup>2</sup> | constants for Legendre transforms  |
| ANMI              | ILC  | BUFNL2 <sup>4</sup> | RELBUF <sup>5</sup> | constants for Legendre transforms  |
| ANMIUV            | ILC  | BUFNL3 <sup>4</sup> | RELBUF <sup>5</sup> | constants for Legendre transforms  |
| APH               | IGP  | SCAN1               | STAT                | half level pressure [Pa]   |
| APHM1             | IGP  | PHYSC               | SCAN1               | half level pressure at t - $\Delta t$ [Pa]   |
| APHP1             | IGP  | PHYSC               | PHYSC               | half level pressure at t + $\Delta t$ [Pa]   |

**Table 9 List of managed arrays, ALLOCS and UNLOCS  
(Sheet 2 of 11)**

| NAME            | TYPE | ALLOC               | UNLOC               | VARIABLE  |
|-----------------|------|---------------------|---------------------|---|
| APM1            | IGP  | PHYSC               | SCAN1               | full level pressure at $t - \Delta t$ [Pa]                                  |
| APP1            | IGP  | PHYSC               | PHYSC               | full level pressure at $t + \Delta t$ [Pa]                                  |
| APRC<br>APRCM   | IGP  | BUFGRD <sup>1</sup> | RELBUF <sup>2</sup> | convective precipitation [(m/s)*s]<br>(accumulated) <sup>9</sup>            |
| APRL<br>APRLM   | IGP  | BUFGRD <sup>1</sup> | RELBUF <sup>2</sup> | large scale precipitation [(m/s)*s]<br>(accumulated) <sup>9</sup>           |
| APRS<br>APRSM   | IGP  | BUFGRD <sup>1</sup> | RELBUF <sup>2</sup> | snow fall [(m/s)*s]<br>(convective + large scale, accumulated) <sup>9</sup> |
| APS<br>APSM     | IGP  | BUFGRD <sup>1</sup> | RELBUF <sup>2</sup> | surface pressure [Pa]   |
| ARPRC<br>ARPRCM | IGP  | BUFGRD <sup>1</sup> | RELBUF <sup>2</sup> | cloud parameters for radiation<br>(not used)                                |
| AZ0<br>AZ0M     | IGP  | BUFGRD <sup>1</sup> | RELBUF <sup>2</sup> | surface roughness [m]   |
| CN              | ISP  | POSTRAD<br>SETDYN   | SCAN1               | matrix used to invert the divergence equation                               |
| CVGHL           | IGP  | VDIFF               | SURF                | ratio of moisture fluxes  |
| D               | IGP  | SCAN1               | SCAN1               | divergence [1/s]  |
| DALPSL          | IGP  | SCAN1               | DYN                 | zonal derivative of logarithm of surface pressure                           |
| DALPSM          | IGP  | SCAN1               | DYN                 | meridional derivative of logarithm of surface pressure                      |
| DELP            | IGP  | SCAN1               | DYN                 | pressure thickness of layers [Pa]   |
| DEW2<br>DEW2M   | IGP  | BUFGRD <sup>1</sup> | RELBUF <sup>2</sup> | 2m dew point temperature [K*s]<br>(accumulated) <sup>9</sup>                |
| DF              | IGP  | BUFGRD <sup>1</sup> | RELBUF <sup>2</sup> | divergence (semi filtered) <sup>6</sup> [1/s]                               |
| DHFQ            | IGP  | VDIFF               | SURF                | derivative of moisture flux with respect to soil moisture<br>(not used)     |
| DHFQW           | IGP  | VDIFF               | SURF                | derivative of moisture flux with respect to skin reservoir                  |
| DHFQS           | IGP  | VDIFF               | SURF                | derivative of moisture flux over snow with respect to<br>snow depth         |
| DHFT            | IGP  | VDIFF               | SKINTEM             | derivative of sensible heat flux with respect to surface<br>temperature     |
| DIA             | IGP  | PRESTAT             | POSTATP             | memory buffer for physical diagnostics                                      |
| DIA1            | IDI  | SETRAD              |                     | memory buffer for radiation diagnostics                                     |
| DL              | IGP  | S12                 | SCAN1               | $\tilde{D}_\lambda$ (see equation (2.5.38) in section 2.5)                  |
| DM              | IGP  | SI1                 | SCAN1               | $\tilde{D}_\mu$ (see equation (2.5.39) in section 2.5)                      |

**Table 9 List of managed arrays, ALLOCS and UNLOCS  
(Sheet 3 of 11)**

| NAME            | TYPE | ALLOC                 | UNLOC                 | VARIABLE  |
|-----------------|------|-----------------------|-----------------------|---|
| DM1             | IGP  | BUFGRD <sup>1</sup>   | RELBUF <sup>2</sup>   | divergence at $t - \Delta t$ [1/s]  |
| DQL             | IGP  | SCAN1                 | DYN                   | zonal derivative of specific humidity   |
| DQM             | IGP  | SCAN1                 | DYN                   | meridional derivative of specific humidity  |
| DSNAC<br>DSNACM | IGP  | BUFGRD <sup>1</sup>   | RELBUF <sup>2</sup>   | snow depth change [m/s]   |
| DTL             | IGP  | SCAN1                 | DYN                   | zonal derivative of temperature   |
| DTM             | IGP  | SCAN1                 | DYN                   | meridional derivative of temperature  |
| DU0             | IGP  | SCAN1                 | SCAN1                 | derivative of zonal reference wind  |
| DXL             | IGP  | SCAN1                 | DYN                   | zonal derivative of cloud water   |
| DXM             | IGP  | SCAN1                 | DYN                   | meridional derivative of cloud water  |
| EMTER<br>EMTERM | IGP  | BUFGRD <sup>1</sup>   | RELBUF <sup>2</sup>   | effective emissivity  |
| EVAP<br>EVAPM   | IGP  | BUFGRD <sup>1</sup>   | RELBUF <sup>2</sup>   | evaporation from the surface [(m/s)*s]<br>(accumulated) <sup>9</sup>                            |
| FAD             | IFC  | BUFF4A <sup>3,4</sup> | RELBUF <sup>2,5</sup> | antisymmetric part of divergence  |
| FADL            | IFC  | SCAN1                 | SCAN1                 | antisymmetric part of $\tilde{D}_\lambda$<br>(see equation (2.5.38) in section 2.5)             |
| FADM            | IFC  | SCAN1                 | SCAN1                 | antisymmetric part of $\tilde{D}_\mu$<br>(see equation (2.5.39) in section 2.5)                 |
| FADU0           | IFC  | BUFF4A <sup>3,4</sup> | RELBUF <sup>2,5</sup> | antisymmetric part of meridional derivative of zonal<br>reference wind at $t - \Delta t$        |
| FAQ             | IFC  | BUFF4A <sup>3,4</sup> | RELBUF <sup>2,5</sup> | antisymmetric part of specific humidity   |
| FAQ1            | IFC  | SCAN1                 | SCAN1                 | antisymmetric part of specific humidity at $t + \Delta t$                                       |
| FAQM            | IFC  | BUFF4A <sup>3,4</sup> | RELBUF <sup>5</sup>   | antisymmetric part of meridional derivative of specific<br>humidity                             |
| FAR             | IFC  | SCAN1                 | SCAN1                 | antisymmetric part of $R$<br>(see equation (2.5.40) in section 2.5)                             |
| FATP            | IFC  | BUFF4A <sup>3,4</sup> | RELBUF <sup>2,5</sup> | antisymmetric part of temperature and<br>surface pressure <sup>7</sup>                          |
| FATP1           | IFC  | SCAN1                 | SCAN1                 | antisymmetric part of temperature and surface pressure<br>at $t + \Delta t$ <sup>7</sup>        |
| FATPM           | IFC  | BUFF4A <sup>3,4</sup> | RELBUF <sup>2,5</sup> | antisymmetric part of meridional derivative of<br>temperature and surface pressure <sup>7</sup> |
| FAU             | IFC  | BUFF4A <sup>3,4</sup> | RELBUF <sup>2,5</sup> | antisymmetric part of zonal wind  |
| FAU0            | IFC  | BUFNF4 <sup>3,4</sup> | RELBUF <sup>2,5</sup> | antisymmetric part of zonal reference wind at $t - \Delta t$                                    |

**Table 9 List of managed arrays, ALLOCS and UNLOCS  
(Sheet 4 of 11)**

| NAME              | TYPE | ALLOC                 | UNLOC                 | VARIABLE  |
|-------------------|------|-----------------------|-----------------------|---|
| FAUD              | IFC  | SCAN2                 | SCAN2                 | antisymmetric part of divergent zonal wind  |
| FAUL              | IFC  | SCAN1                 | SCAN1                 | antisymmetric part of zonal reference wind  |
| FAUR              | IFC  | SCAN2                 | SCAN2                 | antisymmetric part of rotational zonal wind   |
| FAV               | IFC  | BUFF4A <sup>3,4</sup> | RELBUF <sup>2,5</sup> | antisymmetric part of meridional wind   |
| FAVD              | IFC  | SCAN2                 | SCAN2                 | antisymmetric part of divergent meridional wind   |
| FAVO              | IFC  | BUFF4A <sup>3,4</sup> | RELBUF <sup>2,5</sup> | antisymmetric part of vorticity   |
| FAVR              | IFC  | SCAN2                 | SCAN2                 | antisymmetric part of rotational meridional wind  |
| FAX               | IFC  | BUFF4A <sup>3,4</sup> | RELBUF <sup>2,5</sup> | antisymmetric part of cloud water   |
| FAX1              | IFC  | SCAN1                 | SCAN1                 | antisymmetric part of cloud water at $t + \Delta t$   |
| FAXM              | IFC  | BUFF4A                | RELBUF <sup>5</sup>   | antisymmetric part of meridional derivative of cloud water                                  |
| FAZL              | IFC  | SCAN1                 | SCAN1                 | antisymmetric part of $\tilde{Z}_{\lambda m}$<br>(see equation (2.5.24) in section 2.5)     |
| FAZM              | IFC  | SCAN1                 | SCAN1                 | antisymmetric part of $\tilde{Z}_{\mu m}$<br>(see equation (2.5.25) in section 2.5)         |
| FOREST<br>FORESTM | IGP  | BUFGD <sup>1</sup>    | RELBUF <sup>2</sup>   | forest cover [fract.]   |
| FSD               | IFC  | BUFF4A <sup>3,4</sup> | RELBUF <sup>2,5</sup> | symmetric part of divergence  |
| FSDL              | IFC  | SCAN1                 | SCAN1                 | symmetric part of $\tilde{D}_{\lambda}$<br>(see equation (2.5.38) in section 2.5)           |
| FSDM              | IFC  | SCAN1                 | SCAN1                 | symmetric part of $\tilde{D}_{\mu}$<br>(see equation (2.5.39) in section 2.5)               |
| FSDU0             | IFC  | BUFF4A <sup>3,4</sup> | RELBUF <sup>2,5</sup> | symmetric part of derivative of zonal reference wind<br>at $t - \Delta t$                   |
| FSQ               | IFC  | BUFF4A <sup>3,4</sup> | RELBUF <sup>2,5</sup> | symmetric part of specific humidity   |
| FSQ1              | IFC  | SCAN1                 | SCAN1                 | symmetric part of specific humidity at $t + \Delta t$                                       |
| FSQM              | IFC  | BUFF4A <sup>3,4</sup> | RELBUF <sup>2,5</sup> | symmetric part of meridional derivative of specific<br>humidity                             |
| FSR               | IFC  | SCAN1                 | SCAN1                 | symmetric part of $R$<br>(see equation (2.5.40) in section 2.5)                             |
| FSTP              | IFC  | BUFF4A <sup>3,4</sup> | RELBUF <sup>2,5</sup> | symmetric part of temperature and surface pressure <sup>7</sup>                             |
| FSTP1             | IFC  | SCAN1                 | SCAN1                 | symmetric part of temperature and surface pressure<br>at $t + \Delta t$ <sup>7</sup>        |
| FSTPM             | IFC  | BUFF4A <sup>3,4</sup> | RELBUF <sup>2,5</sup> | symmetric part of meridional derivative of temperature<br>and surface pressure <sup>7</sup> |



**Table 9 List of managed arrays, ALLOCS and UNLOCS  
(Sheet 5 of 11)**

| NAME                                      | TYPE | ALLOC                 | UNLOC                                | VARIABLE  |
|---|------|-----------------------|--------------------------------------|---|
| FSU                                       | IFC  | BUFF4A <sup>3,4</sup> | RELBUF <sup>2,5</sup>                | symmetric part of zonal wind  |
| FSU0                                      | IFC  | BUFF4A <sup>3,4</sup> | RELBUF <sup>2,5</sup>                | symmetric part of zonal reference wind at $t - \Delta t$                            |
| FSUD                                      | IFC  | SCAN2                 | SCAN2                                | symmetric part of divergent zonal wind  |
| FSUL                                      | IFC  | SCAN1                 | SCAN1                                | symmetric part of zonal reference wind  |
| FSUR                                      | IFC  | SCAN2                 | SCAN2                                | symmetric part of rotational zonal wind   |
| FSV                                       | IFC  | BUFF4A <sup>3,4</sup> | RELBUF <sup>2,5</sup>                | symmetric part of meridional wind   |
| FSVD                                      | IFC  | SCAN2                 | SCAN2                                | symmetric part of divergent meridional wind   |
| FSVO                                      | IFC  | BUFF4A <sup>3,4</sup> | RELBUF <sup>2,5</sup>                | symmetric part of vorticity   |
| FSVR                                      | IFC  | SCAN2                 | SCAN2                                | symmetric part of rotational meridional wind  |
| FSX                                       | IFC  | BUFF4A <sup>3,4</sup> | RELBUF <sup>2,5</sup>                | symmetric part of cloud water   |
| FSX1                                      | IFC  | SCAN1                 | SCAN1                                | symmetric part of cloud water at $t + \Delta t$                                     |
| FSXM                                      | IFC  | BUFF4A <sup>3,4</sup> | RELBUF <sup>2,5</sup>                | symmetric part of meridional derivative of cloud water                              |
| FSZL                                      | IFC  | SCAN1                 | SCAN1                                | symmetric part of $\tilde{Z}_{\lambda m}$<br>(see equation (2.5.24) in section 2.5) |
| FSZM                                      | IFC  | SCAN1                 | SCAN1                                | symmetric part of $\tilde{Z}_{\mu m}$<br>(see equation (2.5.25) in section 2.5)     |
| GEOM1                                     | IGP  | PHYSC                 | SCAN1                                | geopotential relative to surface [ $m^{**2}/s^{**2}$ ]                              |
| GEOSP<br>GEOSPM                           | IGP  | BUFGRD <sup>1</sup>   | RELBUF <sup>2</sup>                  | surface geopotential (orography) [ $m^{**2}/s^{**2}$ ]                              |
| GLAC<br>CLACM                             | IGP  | BUFGRD <sup>1</sup>   | RELBUF <sup>2</sup>                  | glacier mask [0:no/1:yes]   |
| IDDR1<br>IDDR2<br>IDDR3<br>IDDR4<br>IDDR5 | ISY  | GETDDR<br>MAKEDDR     | POSTS1<br>POSTS2<br>IOPOSI<br>IOPOSR | data description records  |
| ILAB                                      | IGP  | PHYSC                 | COND                                 | flag for convective event   |
| ISDS                                      | ISY  | MAKESD<br>INICTL      |                                      | start data set information  |
| KE  | IGP  | DYN                   | PHYSC                                | change of kinetic energy [ $m^{**2}/s^{**3}$ ]                                      |
| LOLAND                                    | IGP  | PHYSC                 | PHYSC                                | flag for land/sea mask (true: land, false: sea)                                     |
| NBASEC<br>NBASECM                         | IGP  | BUFGRD <sup>1</sup>   | RELBUF <sup>2</sup>                  | cloud parameter for radiation<br>(not used)   |

**Table 9 List of managed arrays, ALLOCS and UNLOCS  
(Sheet 6 of 11)**

| NAME   | TYPE | ALLOC                 | UNLOC                 | VARIABLE   |
|--|------|-----------------------|-----------------------|--|
| NF1A<br>NF2A<br>NF3A<br>NF4A                                 | IFC  | BUFF4A <sup>3,4</sup> | RELBUF <sup>2,5</sup> | padding space for Fourier buffers  |
| NG1A<br>NG2A<br>NG3A<br>NG4A<br>NG1B<br>NG2B<br>NG3B<br>NG4B | IGP  | BUFGRD <sup>1</sup>   | RELBUF <sup>2</sup>   | padding space for grid point buffers   |
| NTOPC<br>NTOPCM  | IGP  | BUFGRD <sup>1</sup>   | RELBUF <sup>2</sup>   | cloud parameter for radiation<br>(not used)                                      |
| PNMD   | ILC  | BUFNL1 <sup>3</sup>   | RELBUF <sup>2</sup>   | constants for Legendre transform   |
| PNMI   | ILC  | BUFNL2 <sup>4</sup>   | RELBUF <sup>5</sup>   | constants for Legendre transform   |
| PNMIUV   | ILC  | BUFNL3 <sup>4</sup>   | RELBUF <sup>5</sup>   | constants for Legendre transform   |
| Q  | IGP  | SCAN1                 | SCAN1                 | specific humidity [kg/kg]  |
| QE   | IGP  | SCAN1                 | SCAN1                 | tendency of specific humidity [1/s]  |
| QF   | IGP  | BUFGRD <sup>1</sup>   | RELBUF <sup>2</sup>   | specific humidity (semi filtered) <sup>6</sup> [kg/kg]                           |
| QHFL   | IGP  | VDIFF                 | SURF                  | moisture flux at the surface [kg/(m**2*s)]                                       |
| QM1  | IGP  | BUFGRD <sup>1</sup>   | RELBUF <sup>2</sup>   | specific humidity at t - Δt [kg/kg]  |
| QSF  | IGP  | SI1                   | SI2                   | $\tilde{\Delta}_t Q$ for specific humidity (see equation (2.5.8) in section 2.5) |
| QVI<br>QVIM  | IGP  | BUFGRD <sup>1</sup>   | RELBUF <sup>2</sup>   | vertically integrated specific humidity [kg/m**2]<br>(accumulated) <sup>9</sup>  |
| RAD1<br>RAD2<br>RAD3<br>RAD4                                 | IRD  | RADINT                | RADINT                | memory buffers for radiative calculations  |
| RDAYL  | IGP  | RADHEAT<br>RADINT     | RADHEAT<br>RADINT     | relative daylength<br>(= 1 for diurnal cycle on)                                 |
| RH   | IGP  | SCAN1                 | SCAN1                 | R (see equation (2.5.40) in section 2.5)   |
| RNMD   | ILC  | BUFNL1 <sup>3</sup>   | SCAN1                 | constants for Legendre transform   |
| RSFC   | IGP  | PHYSC                 | SURF                  | convective rain flux at the surface  |
| RSFL   | IGP  | PHYSC                 | SURF                  | large scale rain flux at the surface   |
| RUNOFF<br>RUNOFFM  | IGP  | BUFGRD <sup>1</sup>   | RELBUF <sup>2</sup>   | surface runoff [(m/s)*s]<br>(accumulated) <sup>9</sup>                           |

**Table 9 List of managed arrays, ALLOCS and UNLOCS  
(Sheet 7 of 11)**

| NAME              | TYPE | ALLOC               | UNLOC               | VARIABLE  |
|-------------------|------|---------------------|---------------------|---|
| SD                | ISP  | SCAN1<br>IOPOSI     |                     | divergence [1/s]  |
| SEAICE<br>SEAICEM | IGP  | BUFGRD <sup>1</sup> | RELBUF <sup>2</sup> | sea-ice cover [fract.]  |
| SICED<br>SICEDM   | IGP  | BUFGRD <sup>1</sup> | RELBUF <sup>2</sup> | sea-ice depth [m]   |
| SLM<br>SLMM       | IGP  | BUFGRD <sup>1</sup> | RELBUF <sup>2</sup> | land sea mask [0:sea/1:land]  |
| SN<br>SNM         | IGP  | BUFGRD <sup>1</sup> | RELBUF <sup>2</sup> | snow depth [m]  |
| SNM1<br>SNM1M     | IGP  | BUFGRD <sup>1</sup> | RELBUF <sup>2</sup> | snow depth at t - Δt [m]  |
| SNMEL<br>SNMELM   | IGP  | BUFGRD <sup>1</sup> | RELBUF <sup>2</sup> | snow melt [(m/s)*s]<br>(accumulated) <sup>9</sup>                     |
| SQ                | ISP  | SCAN1<br>IOPOSI     |                     | specific humidity [kg/kg]   |
| SRAD0<br>SRAD0M   | IGP  | BUFGRD <sup>1</sup> | RELBUF <sup>2</sup> | top solar radiation [J/m**2]<br>(accumulated) <sup>9</sup>            |
| SRAD0U<br>SRAD0UM | IGP  | BUFGRD <sup>1</sup> | RELBUF <sup>2</sup> | top solar radiation upward [J/m**2]<br>(accumulated) <sup>9</sup>     |
| SRADS<br>SRADSM   | IGP  | BUFGRD <sup>1</sup> | RELBUF <sup>2</sup> | surface solar radiation [J/m**2]<br>(accumulated) <sup>9</sup>        |
| SRADSU<br>SRADSUM | IGP  | BUFGRD <sup>1</sup> | RELBUF <sup>2</sup> | surface solar radiation upward [J/m**2]<br>(accumulated) <sup>9</sup> |
| SRFL              | IGP  | RADHEAT             | SKINTEM             | net solar radiative flux at the surface                               |
| SSFC              | IGP  | PHYSC               | SURF                | convective snow flux at the surface [kg/(m**2*s)]                     |
| SSFL              | IGP  | PHYSC               | SURF                | large scale snow flux at the surface [kg/(m**2*s)]                    |
| STP               | ISP  | SCAN1<br>IOPOSI     |                     | temperature [K] and<br>logarithm of surface pressure                  |
| SU0               | ISP  | SCAN1<br>IOPOSI     |                     | zonal reference wind [m/s]  |
| SVO               | ISP  | SCAN1<br>IOPOSI     |                     | vorticity [1/s]   |
| SX                | ISP  | SCAN1<br>IOPOSI     |                     | liquid water content [kg/kg]  |
| T                 | IGP  | SCAN1               | SCAN1               | temperature [K]   |
| T2MAX<br>T2MAXM   | IGP  | BUFGRD <sup>1</sup> | RELBUF <sup>2</sup> | maximum 2m temperature [K]<br>(during output interval)                |

**Table 9 List of managed arrays, ALLOCS and UNLOCS  
(Sheet 8 of 11)**

| NAME  | TYPE | ALLOC               | UNLOC               | VARIABLE   |
|---|------|---------------------|---------------------|--|
| T2MIN<br>T2MINM   | IGP  | BUFGRD <sup>1</sup> | RELBUF <sup>2</sup> | minimum 2m temperature [K]<br>(during output interval)   |
| TD<br>TDM<br>TD3<br>TD3M<br>TD4<br>TD4M<br>TD5<br>TD5M<br>TDCL<br>TDCLM                     | IGP  | BUFGRD <sup>1</sup> | RELBUF <sup>2</sup> | soil temperatures [K]<br>(see description of soil temperatures in<br>section 3.7 (SOIL PROCESSES))                           |
| TDM1<br>TDM1M<br>TD3M1<br>TD3M1M<br>TD4M1<br>TD4M1M<br>TD5M1<br>TD5M1M<br>TDCLM1<br>TDCLM1M | IGP  | BUFGRD <sup>1</sup> | RELBUF <sup>2</sup> | soil temperatures at $t - \Delta t$ [K]<br>(see description of soil temperatures in<br>section 3.7 (SOIL PROCESSES))         |
| TE  | IGP  | SCAN1               | SCAN1               | tendency of temperature [K/s]  |
| TEFF<br>TEFFM   | IGP  | BUFGRD <sup>1</sup> | RELBUF <sup>2</sup> | (effective) sea-ice skin temperature [K]   |
| TEMP2<br>TEMP2M   | IGP  | BUFGRD <sup>1</sup> | RELBUF <sup>2</sup> | 2m temperature [K*s]<br>(accumulated) <sup>9</sup>   |
| TF  | IGP  | BUFGRD <sup>1</sup> | RELBUF <sup>2</sup> | temperature (semi filtered) <sup>6</sup> [K]   |
| THFL  | IGP  | VDIFF               | SKINTEM             | VDIFF: sensible heat flux at the surface [W/m**2]<br>SURF: sum of sensible and latent heat flux at the sur-<br>face [W/m**2] |
| TM1   | IGP  | BUFGRD <sup>1</sup> | RELBUF <sup>2</sup> | temperature at $t - \Delta t$ [K]  |
| TOPMAX<br>TOPMAXM   | IGP  | BUFGRD <sup>1</sup> | RELBUF <sup>2</sup> | maximum height of convective cloud tops [m]<br>(during output interval)  |
| TRAD0<br>TRAD0M   | IGP  | BUFGRD <sup>1</sup> | RELBUF <sup>2</sup> | top thermal radiation [J/m**2]<br>(accumulated) <sup>9</sup>   |
| TRADS<br>TRADSM   | IGP  | BUFGRD <sup>1</sup> | RELBUF <sup>2</sup> | surface thermal radiation [J/m**2]<br>(accumulated) <sup>9</sup>   |
| TRADSU<br>TRADSUM   | IGP  | BUFGRD <sup>1</sup> | RELBUF <sup>2</sup> | surface thermal radiation upward [J/m**2]<br>(accumulated) <sup>9</sup>  |
| TRSOL<br>TRSOLM   | IGP  | BUFGRD <sup>1</sup> | RELBUF <sup>2</sup> | effective transmissivity   |

**Table 9 List of managed arrays, ALLOCS and UNLOCS  
(Sheet 9 of 11)**

| NAME              | TYPE | ALLOC               | UNLOC               | VARIABLE  |
|-------------------|------|---------------------|---------------------|---|
| TS<br>TSM         | IGP  | BUFGRD <sup>1</sup> | RELBUF <sup>2</sup> | surface temperature [K]   |
| TSLIN<br>TSLINM   | IGP  | BUFGRD <sup>1</sup> | RELBUF <sup>2</sup> | land: residual surface heat budget [W/m**2]<br>sea-ice: conductive heat flux [W/m**2] |
| TSM1<br>TSM1M     | IGP  | BUFGRD <sup>1</sup> | RELBUF <sup>2</sup> | surface temperature at t - Δt [K]   |
| TSURF<br>TSURFM   | IGP  | BUFGRD <sup>1</sup> | RELBUF <sup>2</sup> | surface temperature [K*s]<br>(accumulated) <sup>9</sup>                               |
| TSMAX<br>TSMAXM   | IGP  | BUFGRD <sup>1</sup> | RELBUF <sup>2</sup> | maximum surface temperature [K]<br>(during output interval)                           |
| TSMIN<br>TSMINM   | IGP  | BUFGRD <sup>1</sup> | RELBUF <sup>2</sup> | minimum surface temperature [K]<br>(during output interval)                           |
| U                 | IGP  | SCAN1               | STAT                | zonal wind [m/s]  |
| U0                | IGP  | SCAN1               | SCAN1               | reference zonal wind at t - Δt [m/s]  |
| U10<br>U10M       | IGP  | BUFGRD <sup>1</sup> | RELBUF <sup>2</sup> | 10m u-velocity [(m/s)*s]<br>(accumulated) <sup>9</sup>                                |
| UF                | IGP  | BUFGRD <sup>1</sup> | RELBUF <sup>2</sup> | zonal wind (semi filtered) <sup>6</sup> [m/s]   |
| UL                | IGP  | SCAN1               | SCAN1               | zonal reference wind [m/s]  |
| UM1               | IGP  | BUFGRD <sup>1</sup> | RELBUF <sup>2</sup> | zonal wind at t - Δt [m/s] <sup>8</sup>   |
| USTAR3<br>USTAR3M | IGP  | BUFGRD <sup>1</sup> | RELBUF <sup>2</sup> | TKE for ocean mixed layer [(m**3/s**3)*s]<br>(accumulated) <sup>9</sup>               |
| USTR<br>USTRM     | IGP  | BUFGRD <sup>1</sup> | RELBUF <sup>2</sup> | u-stress [Pa*s]<br>(accumulated) <sup>9</sup>   |
| USTRGW<br>USTRGWM | IGP  | BUFGRD <sup>1</sup> | RELBUF <sup>2</sup> | u-gravity wave stress [Pa*s]<br>(accumulated) <sup>9</sup>                            |
| V                 | IGP  | SCAN1               | STAT                | meridional wind [m/s]   |
| V10<br>V10M       | IGP  | BUFGRD <sup>1</sup> | RELBUF <sup>2</sup> | 10m v-velocity [(m/s)*s]<br>(accumulated) <sup>9</sup>                                |
| VAROR             | IGP  | DYN                 | SURF                | orographic variance   |
| VARP<br>VARPM     | IGP  | BURGRD <sup>1</sup> | RELBUF <sup>2</sup> | directional orographic variance<br>(packed)   |
| VDIS<br>VDISM     | IGP  | BUFGRD <sup>1</sup> | RELBUF <sup>2</sup> | boundary layer dissipation [J/m**2]<br>(accumulated) <sup>9</sup>                     |
| VDISGW<br>VDISGWM | IGP  | BUFGRD <sup>1</sup> | RELBUF <sup>2</sup> | dissipation by gravity wave drag [J/m**2]<br>(accumulated) <sup>9</sup>               |
| VEGRAT<br>VEGRATM | IGP  | BUFGRD <sup>1</sup> | RELBUF <sup>2</sup> | packed array containing orographic variance, skin reservoir and vegetation ratio      |

**Table 9 List of managed arrays, ALLOCS and UNLOCS  
(Sheet 10 of 11)**

| NAME              | TYPE | ALLOC               | UNLOC               | VARIABLE  |
|-------------------|------|---------------------|---------------------|---|
| VERVEL            | IGP  | DYN                 | PHYSC               | vertical velocity [Pa/s]  |
| VF                | IGP  | BUFGRD <sup>1</sup> | RELBUF <sup>2</sup> | meridional wind (semi filtered) <sup>6</sup> [m/s]                |
| VGRAT             | IGP  | DYN                 | SURF                | vegetation ratio  |
| VM1               | IGP  | BUFGRD <sup>1</sup> | RELBUF <sup>2</sup> | meridional wind at t - Δt [m/s] <sup>8</sup>                      |
| VO                | IGP  | SCAN1               | SCAN1               | vorticity [1/s]   |
| VOF               | IGP  | BUFGRD <sup>1</sup> | RELBUF <sup>2</sup> | vorticity (semi filtered) <sup>6</sup> [1/s]                      |
| VOL               | IGP  | SCAN1               | SCAN1               | tendency of zonal wind [m/s**2] <sup>8</sup>                      |
| VOM               | IGP  | SCAN1               | SCAN1               | tendency of meridional wind [m/s**2] <sup>8</sup>                 |
| VOM1              | IGP  | BUFGRD <sup>1</sup> | RELBUF <sup>2</sup> | vorticity at t - Δt [1/s]   |
| VSTR<br>VSTRM     | IGP  | BUFGRD <sup>1</sup> | RELBUF <sup>2</sup> | v-stress [Pa*s]<br>(accumulated) <sup>9</sup>                     |
| VSTRGW<br>VSTRGWM | IGP  | BUFGRD <sup>1</sup> | RELBUF <sup>2</sup> | v-gravity wave stress [Pa*s]<br>(accumulated) <sup>9</sup>        |
| WDCL<br>WDCLM     | IGP  | BUFGRD <sup>1</sup> | RELBUF <sup>2</sup> | not used  |
| WDM1<br>WDM1M     | IGP  | BUFGRD <sup>1</sup> | RELBUF <sup>2</sup> | not used  |
| WIMAX<br>WIMAXM   | IGP  | BUFGRD <sup>1</sup> | RELBUF <sup>2</sup> | maximum 2m windspeed [m/s]<br>(during output interval)            |
| WIND10<br>WIND10M | IGP  | BUFGRD <sup>1</sup> | RELBUF <sup>2</sup> | 10m windspeed [(m/s)*s]<br>(accumulated) <sup>9</sup>             |
| WLM               | IGP  | DYN                 | SURF                | skin reservoir content of plants [m]                              |
| WLM1<br>WLM1M     | IGP  | BUFGRD <sup>1</sup> | RELBUF <sup>2</sup> | skin reservoir content of plants at t - Δt [m]                    |
| WS<br>WSM         | IGP  | BUFGRD <sup>1</sup> | RELBUF <sup>2</sup> | soil wetness [m]  |
| WSM1<br>WSM1M     | IGP  | BUFGRD <sup>1</sup> | RELBUF <sup>2</sup> | soil wetness at t - Δt [m]  |
| X                 | IGP  | SCAN1               | SCAN1               | cloud water [kg/kg]   |
| XE                | IGP  | SCAN1               | SCAN1               | tendency of cloud water [1/s]                                     |
| XF                | IGP  | BUFGRD <sup>1</sup> | RELBUF <sup>2</sup> | cloud water (semi filtered) <sup>6</sup> [kg/kg]                  |
| XHFL              | IGP  | PHYSC               | PHYSC               | cloud water flux at the surface [kg/(m**2*s)]<br>(fog deposition) |
| XM1               | IGP  | BUFGRD <sup>1</sup> | RELBUF <sup>2</sup> | cloud water at t - Δt [kg/kg]                                     |

**Table 9 List of managed arrays, ALLOCS and UNLOCS  
(Sheet 11 of 11)**

| NAME | TYPE | ALLOC | UNLOC | VARIABLE  |
|------|------|-------|-------|---|
| XSF  | IGP  | SI1   | SI2   | $\tilde{\Delta}_t X$ for cloud water<br>(see equation (2.5.8) in section 2.5) |

1. Called by PRES1 at the beginning of SCAN1.
2. Called by POSTS1 at the end of SCAN1.
3. Called by SETBUF called by PRES1 at the beginning of SCAN1.
4. Called by SETBUF called by PRES2 at the beginning of SCAN2.
5. Called by POSTS2 at the end of SCAN2.
6. See equation (2.5.11) in section 2.5 (TIME INTEGRATION SCHEME)
7. Temperature at full levels and logarithm of surface pressure are stored in one array of 20 levels with logarithm of surface pressure stored in level 20.
8. Winds in the model are scaled  $U = u \cdot \cos\Theta$ . For practical purposes the winds and their tendencies are divided by  $\cos\Theta$  at the beginning of PHYSC and are rescaled at the end of PHYSC.
9. Accumulated variables are weighted by the time step interval during accumulation. Before write out they are divided by the time of the output interval. For example the unit  $J/m^{**2}$  of the surface fluxes during accumulation is converted to  $W/m^{**2}$  before write out. The units of all postprocessed variables are listed in the code table (Table 10 in Appendix F).





## Appendix F ECHAM3 CODE-LIST OF VARIABLES

The following code-list is available from /pool/POST/echam/doc/codes.

All grid variables with an internal name can be requested as model output. All spectral variables (except SX, the liquid water content) are written out by default (see description of namelist POSTCTL in Table 11). Use code 222 for output of liquid water content. All variables without an internal name are derived variables, which can be computed by the *afterburner*<sup>1</sup> postprocessing package (DKRZ Technical Report: Description of programs handling files in WMO GRIB and EXTRA Format, to be published). The *afterburner* also computes grid point versions of spectral variables.

Two methods for the calculation of clear sky diagnostics and cloud forcing exist:

1. **Method I**, applied to the standard model, calls the radiation code once. It diagnoses clear sky or overcast events, counts them and accumulates radiative properties for the two cases. It outputs the accumulated radiative properties and the number of events separately in an output interval (6 or 12 hours, depending on the model version).
2. **Method II** calls the radiation code twice each radiation time step, first with true cloudiness and then with simulated clear sky, and averages both separately over the output interval.

For details of the two methods see Cess and Potter (1987, 1988).

type: g=grid, s=spectral, m=mean over output interval, p=packed

**Table 10 Code numbers of the ECHAM-Models (Sheet 1 of 6)**

| code  | levels | internal name | type | variable                         | unit                 |
|---|--------|---------------|------|----------------------------------|----------------------|
| -----   |        |               |      |                                  |                      |
| <b>clear sky diagnostics (method II), not available in standard model</b> |        |               |      |                                  |                      |
| 101   | 1      | SRAFS         | g m  | net surface solar radiation      | (clear sky) [W/m**2] |
| 102   | 1      | TRAFS         | g m  | net surface thermal radiation    | (clear sky) [W/m**2] |
| 103   | 1      | SRAF0         | g m  | net top solar radiation          | (clear sky) [W/m**2] |
| 104   | 1      | TRAF0         | g m  | net top thermal radiation        | (clear sky) [W/m**2] |
| 105   | 1      | SRAF0U        | g m  | top solar radiation upward       | (clear sky) [W/m**2] |
| 106   | 1      | SRAFSU        | g m  | surface solar radiation upward   | (clear sky) [W/m**2] |
| 107   | 1      | TRAFSU        | g m  | surface thermal radiation upward | (clear sky) [W/m**2] |
| -----   |        |               |      |                                  |                      |

1. To compute multi level derived variables and for interpolation to pressure levels the *afterburner* package needs all spectral variables and the surface geopotential (code 129). Therefore altering of namelist POSTCTL is not recommended. The output of code 129 is forced internally.

**Table 10 Code numbers of the ECHAM-Models (Sheet 2 of 6)**

| code | levels | internal name | type | variable  | unit                   |
|------|--------|---------------|------|---|------------------------|
| 129  | 1      | GEOSP         | g    | surface geopotential (orography)                      | [m**2/s**2]            |
| 130  | 19     | STP           | s    | temperature   | [K]                    |
| 131  | 19     |               | g    | u-velocity  | [m/s]                  |
| 132  | 19     |               | g    | v-velocity  | [m/s]                  |
| 133  | 19     | SQ            | s    | specific humidity                                     | [kg/kg]                |
| 134  | 1      | APS           | g    | surface pressure                                      | [Pa]                   |
| 135  | 19     |               | g    | vertical velocity                                     | [Pa/s]                 |
| 138  | 19     | SVO           | s    | vorticity   | [1/s]                  |
| 139  | 1      | TS            | g    | surface temperature                                   | [K] (see also 169)     |
| 140  | 1      | WS            | g    | soil wetness  | [m]                    |
| 141  | 1      | SN            | g    | snow depth <sup>I</sup>                               | [m]                    |
| 142  | 1      | APRL          | g m  | large scale precipitation                             | [m/s]                  |
| 143  | 1      | APRC          | g m  | convective precipitation                              | [m/s]                  |
| 144  | 1      | APRS          | g m  | snow fall   | [m/s]                  |
| 145  | 1      | VDIS          | g m  | boundary layer dissipation                            | [W/m**2]               |
| 146  | 1      | AHFS          | g m  | surface sensible heat flux                            | [W/m**2]               |
| 147  | 1      | AHFL          | g m  | surface latent heat flux                              | [W/m**2]               |
| 148  | 19     |               | g    | streamfunction  | [m**2/s]               |
| 149  | 19     |               | g    | velocity potential                                    | [m**2/s]               |
|      |        |               |      |   |                        |
| 151  | 1      |               | g    | mean sea level pressure                               | [Pa]                   |
| 152  | 1      | STP(20)       | s    | log surface pressure                                  |                        |
| 153  | 19     | SX            | s    | liquid water content                                  | [kg/kg] (see 161, 222) |
| 154  |        |               |      |   |                        |
| 155  | 19     | SD            | s    | divergence  | [1/s]                  |
| 156  | 19     |               | g    | geopotential height                                   | [gpm]                  |
| 157  | 19     |               | g    | relative humidity <sup>II</sup>                       | [fract.]               |
| 158  | 1      |               | g    | tendency of surface pressure <sup>II</sup>            | [Pa/s]                 |
| 159  | 1      | USTAR3        | g m  | ustar**3  | [m**3/s**3]            |
| 160  | 1      | RUNOFF        | g m  | surface runoff ( <b>not ECHAM1 !</b> ) <sup>III</sup> | [m/s] (see also 271)   |
| 161  | 19     | ALWC          | g    | liquid water content                                  | [kg/kg] (see also 222) |

**Table 10 Code numbers of the ECHAM-Models (Sheet 3 of 6)**

| code | levels | internal name | type | variable                            | unit                    |
|------|--------|---------------|------|-------------------------------------|-------------------------|
| 162  | 19     | ACLC          | g    | cloud cover                         | [fract.] (see also 223) |
| 163  | 1      | ACLCV         | g    | total cloud cover                   | [fract.] (see also 164) |
| 164  | 1      | ACLCOV        | g m  | total cloud cover                   | [fract.]                |
| 165  | 1      | U10           | g m  | 10m u-velocity                      | [m/s]                   |
| 166  | 1      | V10           | g m  | 10m v-velocity                      | [m/s]                   |
| 167  | 1      | TEMP2         | g m  | 2m temperature                      | [K]                     |
| 168  | 1      | DEW2          | g m  | 2m dew point temperature            | [K]                     |
| 169  | 1      | TSURF         | g m  | surface temperature                 | [K] (see also 139)      |
| 170  | 1      | TD            | g    | deep soil temperature <sup>IV</sup> | [K]                     |
| 171  | 1      | WIND10        | g m  | 10m windspeed                       | [m/s]                   |
| 172  | 1      | SLM           | g    | land sea mask                       | [0: sea, 1: land]       |
| 173  | 1      | AZ0           | g    | surface roughness                   | [m]                     |
| 174  | 1      | ALB           | g    | surface background albedo           | [fract.]                |
| 175  | 1      | ALBEDO        | g    | surface albedo                      | [fract.]                |
| 176  | 1      | SRADS         | g m  | surface solar radiation             | [W/m**2]                |
| 177  | 1      | TRADS         | g m  | surface thermal radiation           | [W/m**2]                |
| 178  | 1      | SRAD0         | g m  | top solar radiation                 | [W/m**2]                |
| 179  | 1      | TRAD0         | g m  | top thermal radiation               | [W/m**2]                |
| 180  | 1      | USTR          | g m  | u-stress                            | [Pa]                    |
| 181  | 1      | VSTR          | g m  | v-stress                            | [Pa]                    |
| 182  | 1      | EVAP          | g m  | evaporation                         | [m/s]                   |
| 183  | 1      | TDCL          | g    | soil temperature <sup>IV</sup>      | [K]                     |
|      |        |               |      |                                     |                         |
| 194  | 1      | WLM1          | g    | skin reservoir content of plants    | [m]                     |
| 195  | 1      | USTRGW        | g m  | u-gravity wave stress               | [Pa]                    |
| 196  | 1      | VSTRGW        | g m  | v-gravity wave stress               | [Pa]                    |
| 197  | 1      | VDISGW        | g m  | gravity wave dissipation            | [W/m**2]                |
|      |        |               |      |                                     |                         |
| 201  | 1      | T2MAX         | g    | maximum 2m-temperature              | [K]                     |
| 202  | 1      | T2MIN         | g    | minimum 2m-temperature              | [K]                     |
| 203  | 1      | SRAD0U        | g m  | top solar radiation upward          | [W/m**2]                |

**Table 10 Code numbers of the ECHAM-Models (Sheet 4 of 6)**

| code  | levels | internal name                                    | type | variable  | unit                 |
|-------|--------|--|------|---|----------------------|
| 204   | 1      | SRADSU   | g m  | surface solar radiation upward                                      | [W/m**2]             |
| 205   | 1      | TRADSU   | g m  | surface thermal radiation upward                                    | [W/m**2]             |
| 206   | 1      | TSN  | g    | snow temperature <sup>IV</sup>                                      | [K]                  |
| 207   | 1      | TD3  | g    | soil temperature <sup>IV</sup>                                      | [K]                  |
| 208   | 1      | TD4  | g    | soil temperature <sup>IV</sup>                                      | [K]                  |
| 209   | 1      | TD5  | g    | soil temperature <sup>IV</sup>                                      | [K]                  |
| 210   | 1      | SEAICE   | g    | sea ice cover   | [fract.]             |
| 211   | 1      | SICED  | g    | sea ice depth   | [m]                  |
| 212   | 1      | FOREST   | g    | forest cover  | [fract.]             |
| 213   | 1      | TEFF   | g    | (effective) sea-ice skin temperature                                | [K]                  |
| 214   | 1      | TSMAX  | g    | maximum surface temperature   | [K]                  |
| 215   | 1      | TSMIN  | g    | minimum surface temperature   | [K]                  |
| 216   | 1      | WIMAX  | g    | maximum 2m-wind speed   | [m/s]                |
| 217   | 1      | TOPMAX   | g    | maximum convective cloud tops                                       | [m]                  |
| 218   | 1      | SNMEL  | g m  | snow melt   | [m/s]                |
|       |        |  |      |   |                      |
| 220   | 1      | TSLIN  | g m  | land: residual surface heat budget<br>sea-ice: conductive heat flux | [W/m**2]<br>[W/m**2] |
| 221   | 1      | DSNAC  | g m  | snow depth change   | [m/s]                |
| 222   | 19     | ALWCAC   | g m  | liquid water content  | [kg/kg]              |
| 223   | 19     | ACLCAC   | g m  | cloud cover   | [fract.]             |
| ----- |        | <b>clear/overcast sky diagnostics (method I)</b> |      |   | -----                |
| 224   | 1      | SRAD0F   | g m  | top solar radiation in clear-sky areas                              | [W/m**2]             |
| 225   | 1      | TRAD0F   | g m  | top thermal radiation in clear-sky areas                            | [W/m**2]             |
| 226   | 1      | ACCNTF   | g    | number of clear-sky events  |                      |
| 227   | 1      | SRAD0C   | g m  | top solar radiation in overcast areas                               | [W/m**2]             |
| 228   | 1      | TRAD0C   | g m  | top thermal radiation in overcast areas                             | [W/m**2]             |
| 229   | 1      | ACCNTC   | g    | number of overcast events   |                      |
| ----- |        |  |      |   |                      |
| 230   | 1      | QVI  | g m  | vertically integrated specific humidity                             | [kg/m**2]            |
| 231   | 1      | ALWCVI   | g m  | vertically integrated liquid water cont.                            | [kg/m**2]            |

**Table 10 Code numbers of the ECHAM-Models (Sheet 5 of 6)**

| code  | levels | internal name   | type | variable  | unit            |
|-------|--------|---|------|---|-----------------|
| 232   | 1      | GLAC  | g    | glacier mask  | [0: no, 1: yes] |
| 241   | 19     | XT(1)   | s    | tracer gas  |                 |
| ..    |        |   |      |   |                 |
| 255   | 19     | XT(15)  | s    | tracer gas  |                 |
| 259   | 19     |   | g    | windspeed $((u^{*2}+v^{*2})^{1/2})$   |                 |
| 260   | 1      |   | g m  | total precipitation (142+143)   |                 |
| 261   | 1      |   | g m  | total top radiation (178+179)   |                 |
| 262   | 1      |   | g m  | total surface radiation (176+177)   |                 |
| 263   | 1      |   | g m  | net surface heat flux (146+147+176+177-220-C*218)<br>where C = (Latent heat of fusion) * (density of water) |                 |
| 264   | 1      |   | g m  | total surface water (142+143+182-160-221)   |                 |
| 265   | 1      |   | g m  | top solar cloud forcing ( <b>method I</b> ) (178-224)   |                 |
| 266   | 1      |   | g m  | top thermal cloud forcing ( <b>method I</b> ) (179-225)   |                 |
| 267   | 1      |   | g m  | total top cloud forcing ( <b>method I</b> ) (178+179-224-225)   |                 |
| 268   | 1      |   | g m  | atmospheric solar radiation (178-176)   |                 |
| 269   | 1      |   | g m  | atmospheric thermal radiation (179-177)   |                 |
| 270   | 1      |   | g m  | total atmospheric radiation (178+179-176-177)   |                 |
| 271   | 1      |   | g m  | surface runoff ( <b>only ECHAM1 !</b> ) (142+143+182-221)   |                 |
| 272   | 19     |   | g    | mass stream function  |                 |
| 273   | 1      |   | g    | $dp_s/d\lambda$ zonal derivative of surface pressure  |                 |
| 274   | 1      |   | g    | $dp_s/d\phi$ meridional derivative of surface pressure  |                 |
| 275   | 1      |   | g m  | precipitation - evaporation (142+143+182)   |                 |
| ----- |        | <b>cloud forcing (method II), not available in the standard model</b> |      |   | -----           |
| 364   |        |   | g m  | top solar cloud forcing (178-103)   |                 |
| 365   |        |   | g m  | top thermal cloud forcing (179-104)   |                 |
| 366   |        |   | g m  | top net cloud forcing (364+365)   |                 |
|       |        |   |      |   |                 |
| 370   |        |   | g m  | surface solar cloud forcing (176-101)   |                 |
| 371   |        |   | g m  | surface thermal cloud forcing (177-102)   |                 |
| 372   |        |   | g m  | surface net cloud forcing (370+371)   |                 |

**Table 10 Code numbers of the ECHAM-Models (Sheet 6 of 6)**

| code  | levels | internal name | type | variable  | unit                |
|-------|--------|---------------|------|---|---------------------|
| 373   |        |               | g m  | atmospheric solar cloud forcing (364-370)             |                     |
| 374   |        |               | g m  | atmospheric thermal cloud forcing (365-371)           |                     |
| 375   |        |               | g m  | atmospheric net cloud forcing (373+374)               |                     |
| 376   |        |               | g m  | surface net radiation (clear sky) (101+102)           |                     |
| 377   |        |               | g m  | atmospheric solar radiation (clear sky) (103-101)     |                     |
| 378   | 1      |               | g m  | atmospheric thermal radiation (clear sky) (104-102)   |                     |
| 379   | 1      |               | g m  | atmospheric net radiation (clear sky) (377+378)       |                     |
| ----- |        |               |      |   |                     |
| 380   | 1      |               | g m  | planetary albedo <sup>V</sup> $-(203/(178-203))*100.$ | [perc.]             |
| 381   | 1      |               | g m  | planetary albedo <sup>V</sup> $-(105/(103-105))*100.$ | [perc.] (clear sky) |
| 382   | 1      |               | g m  | surface albedo $-(204/(176-204))*100.$                | [[perc.]            |

## I. ECHAM1:

Over land ice (SN > 9.5 m or GLAC = 1) the snow melt is not calculated i.e. the snow gradually accumulates. In long term integrations with coupled models a suitable ice flow to the ocean (glacier calving) has to be introduced for maintaining the water budget.

II. Codes 157 (relative humidity) and 158 (tendency of surface pressure) are predefined but not calculated by the *afterburner* package.

## III. ECHAM2/ECHAM3:

Due to a coding error the runoff (code 160) should not be used.

A "residual runoff" (code 271) may be applied for long term water budget studies instead.

IV. For description of soil temperatures see section 3.7.2

V. The planetary albedo (code 380 and 381, respectively for clear sky) equals zero, if the numerator is zero.

Calculate albedos only from temporal or eventually spatial mean fluxes.

The global mean results from the global mean of fluxes !

**Table 11 Namelist POSTCTL  
(control of spectral variable write out)**

| Name   | Type    | Purpose  | Default |
|--------|---------|--|---------|
| LPPSPE | LOGICAL | True for write out all spectral variables except liquid water SX   | TRUE    |
| LPPD   | LOGICAL | True for write out divergence SD   | TRUE    |
| LPPVO  | LOGICAL | True for write out vorticity SVO   | TRUE    |
| LPPT   | LOGICAL | True for write out temperature STP   | TRUE    |
| LPPP   | LOGICAL | True for write out surface pressure STP(20)  | TRUE    |
| LPPQ   | LOGICAL | True for write out specific humidity SQ  | TRUE    |
| LPPX   | LOGICAL | True for write out liquid water content SX (For output of liquid water content request of code 222 is recommended) | FALSE   |

## INDEX OF KEYWORDS

### A

|  |               |
|--|---------------|
| absorption coefficient . . . . .             | 38            |
| adiabatic . . . . .                          | 5, 21, 35, 93 |
| adiabatic ascent . . . . .                   | 65, 67        |
| adiabatic computation . . . . .              | 93            |
| adiabatic cooling . . . . .                  | 71            |
| adiabatic heating . . . . .                  | 71            |
| adiabatic processes . . . . .                | 43            |
| adiabatic tendency . . . . .                 | 44            |
| advective transport of cloud water . . . . . | 72            |
| aerosol . . . . .                            | 40            |
| afterburner . . . . .                        | 179           |
| albedo . . . . .                             | 2, 37, 41     |
| ALLOCA . . . . .                             | 163           |
| ALLOCB . . . . .                             | 163           |
| angular momentum . . . . .                   | 19, 20        |

### B

|                                       |       |
|---------------------------------------|-------|
| backscattering coefficients . . . . . | 38    |
| Bergeron-Findeisen process . . . . .  | 73    |
| boundary layer . . . . .              | 8, 43 |
| broad-band formulation . . . . .      | 36    |
| Brunt-Vaisala frequency . . . . .     | 56    |
| bucket model . . . . .                | 81    |

### C

|                                     |                  |
|-------------------------------------|------------------|
| carbon dioxide . . . . .            | 40               |
| CFL-criterion . . . . .             | 31               |
| Charnock constant . . . . .         | 54               |
| clear sky diagnostics . . . . .     | 179              |
| cloud base height . . . . .         | 63               |
| cloud base mass flux . . . . .      | 61, 63           |
| cloud condensation nuclei . . . . . | 71               |
| cloud cover . . . . .               | 35               |
| cloud droplets . . . . .            | 60               |
| cloud ensemble . . . . .            | 60               |
| cloud forcing . . . . .             | 179              |
| cloud formation . . . . .           | 70               |
| cloud lifetime . . . . .            | 72               |
| cloud liquid water . . . . .        | 40               |
| cloud overlap . . . . .             | 40               |
| cloud profile . . . . .             | 67               |
| cloud top . . . . .                 | 67               |
| cloud water . . . . .               | 1, 6, 20, 29, 70 |

|   |                  |
|---|------------------|
| cloud water content . . . . .                     | 60               |
| CLSST . . . . .                                   | 111              |
| coalescence . . . . .                             | 70               |
| coalescence rate . . . . .                        | 72               |
| code documentation . . . . .                      | 159, 160         |
| computational modes . . . . .                     | 23               |
| COMSDS . . . . .                                  | 83               |
| condensation level . . . . .                      | 63, 67           |
| condensational growth of cloud droplets . . . . . | 71               |
| CONTEQ . . . . .                                  | 93               |
| continuity equation . . . . .                     | 6, 19            |
| CONTROL . . . . .                                 | 83, 85           |
| convection . . . . .                              | 2, 8, 35, 59, 61 |
| convective boundary layer . . . . .               | 54               |
| convective cells . . . . .                        | 65, 66           |
| convective drying . . . . .                       | 64               |
| convective flux . . . . .                         | 64               |
| convective heating . . . . .                      | 64               |
| convective precipitation . . . . .                | 62               |
| convective rain . . . . .                         | 68               |
| convective transport . . . . .                    | 63               |
| critical flux Richardson number . . . . .         | 50, 52           |
| CUCALL . . . . .                                  | 91               |
| cumulus convection . . . . .                      | 59, 91           |
| cumulus ensemble . . . . .                        | 71               |
| cut-off wave number . . . . .                     | 29               |

### D

|   |                      |
|---|----------------------|
| Dalton's Law . . . . .                          | 134                  |
| damping time for horizontal diffusion . . . . . | 29                   |
| data flow . . . . .                             | 103, 104             |
| dew deposition . . . . .                        | 47                   |
| diabatic processes . . . . .                    | 118                  |
| diffuse radiation . . . . .                     | 38                   |
| diffusion . . . . .                             | 23, 29, 30, 43       |
| diffusion coefficient . . . . .                 | 29, 35               |
| diffusive transport of cloud water . . . . .    | 72                   |
| diffusivity factor . . . . .                    | 37                   |
| dissipation . . . . .                           | 8                    |
| dissipation of kinetic energy . . . . .         | 139                  |
| divergence . . . . .                            | 1, 8, 14, 23, 26, 29 |
| DOCTOR standard . . . . .                       | 157                  |
| downdraft . . . . .                             | 59                   |
| drag coefficient . . . . .                      | 43, 45, 48, 51       |
| dry static energy . . . . .                     | 8, 43, 62            |

|   |                        |   |              |
|---|------------------------|---|--------------|
| dry static energy at the surface . . . . .      | 45                     | Gaussian weights . . . . .                        | 94           |
| dry static energy flux at the surface . . . . . | 45                     | G-buffers . . . . .                               | 105          |
| DYN . . . . .                                   | 93, 103                | GEOPOT . . . . .                                  | 93           |
| DYNCTL . . . . .                                | 118                    | geopotential . . . . .                            | 20, 21, 83   |
| <b>E</b>  |                        | glacier areas over land . . . . .                 | 75           |
| ECHAM . . . . .                                 | 1, 4, 5                | global memory buffer . . . . .                    | 92           |
| ECHAM3 . . . . .                                | 29, 83, 104, 166       | GPC . . . . .                                     | 83, 89, 93   |
| ECMWF . . . . .                                 | 1, 4, 7, 19, 29, 31    | gravity wave . . . . .                            | .5, 26       |
| ECMWF library . . . . .                         | 107                    | gravity wave drag . . . . .                       | .3, 35, 56   |
| effective absorber mass . . . . .               | 37                     | grid point buffer . . . . .                       | 103          |
| efficiency of rain formation . . . . .          | 72                     | grid point fields . . . . .                       | 111          |
| Ekman layer height . . . . .                    | 54                     | grid point space . . . . .                        | 105          |
| emissivity . . . . .                            | 36                     | grid size . . . . .                               | 33           |
| emissivity of clouds . . . . .                  | 39                     | gridpoint fields . . . . .                        | 112          |
| energy-conversion . . . . .                     | 21                     | <b>H</b>  |              |
| enthalpy . . . . .                              | 136, 139               | half levels . . . . .                             | 16           |
| equation of state . . . . .                     | 134, 139               | half-level pressure . . . . .                     | 16, 21       |
| evaporation efficiency . . . . .                | 46                     | heat . . . . .                                    | 44, 51, 60   |
| evaporation of precipitation . . . . .          | 70, 74                 | heat budget equation . . . . .                    | 59           |
| evaporation of rain . . . . .                   | 67                     | heat conduction equation . . . . .                | 76, 77       |
| evaporation rate . . . . .                      | 68                     | Helmholtz equation . . . . .                      | 96           |
| executable model . . . . .                      | 107                    | high-level drag . . . . .                         | 57           |
| explicit . . . . .                              | 24, 26                 | history file . . . . .                            | 105          |
| <b>F</b>  |                        | horizontal diffusion . . . . .                    | 3, 5, 23, 25 |
| fast Fourier transform . . . . .                | 84, 93                 | humidity . . . . .                                | 29, 84, 93   |
| F-buffers . . . . .                             | 105                    | hybrid coordinate . . . . .                       | 1, 5, 16, 19 |
| FFTD . . . . .                                  | 103                    | hydrostatic equation . . . . .                    | .6, 21       |
| FFTI . . . . .                                  | 103, 111               | hydrostatic vertical gravity wavelength . . . . . | 57           |
| file structure . . . . .                        | 120                    | <b>I</b>  |              |
| finite differences . . . . .                    | 1                      | ICAO standard atmosphere . . . . .                | 30           |
| flux divergence . . . . .                       | 66                     | ice crystals . . . . .                            | 72           |
| flux Richardson number . . . . .                | 50                     | ice phase . . . . .                               | 71           |
| Fourier buffer . . . . .                        | 103                    | implicit time stepping . . . . .                  | 26, 43, 44   |
| Fourier coefficients . . . . .                  | 9, 10                  | INCOM . . . . .                                   | 83           |
| Fourier space . . . . .                         | 24                     | in-core version . . . . .                         | 92, 103      |
| free convection . . . . .                       | 49                     | INILEG . . . . .                                  | 83           |
| free convection level . . . . .                 | 65                     | INILOC . . . . .                                  | 83           |
| Froude number . . . . .                         | 56, 57, 58             | internal energy . . . . .                         | 55           |
| full-level pressure . . . . .                   | 16, 18                 | inversion layer . . . . .                         | 64           |
| <b>G</b>  |                        | IOPOSI . . . . .                                  | 110          |
| gas absorption . . . . .                        | 38                     | IOOSR . . . . .                                   | 111          |
| Gaussian grid . . . . .                         | 27                     | <b>K</b>  |              |
| Gaussian integration . . . . .                  | 15, 25                 | Karman's constant . . . . .                       | 48           |
| Gaussian latitudes . . . . .                    | 15, 147, 148, 149, 150 | kinetic energy . . . . .                          | .8, 20, 55   |
| Gaussian quadrature . . . . .                   | 15, 25                 | kinetic energy dissipation . . . . .              | 55           |



**L**

|  |              |
|--|--------------|
| land-sea mask . . . . .                    | 75           |
| land-surface processes . . . . .           | 3            |
| Laplacian operator . . . . .               | 95           |
| large-scale budget equations . . . . .     | 66           |
| large-scale moisture convergence . . . . . | 63           |
| large-scale transport . . . . .            | 63           |
| latent heat . . . . .                      | 141          |
| latent heat flux at the surface . . . . .  | 44           |
| leap frog . . . . .                        | 1, 110       |
| Legendre buffer . . . . .                  | 103          |
| Legendre Functions . . . . .               | 9, 10, 15    |
| Legendre functions . . . . .               | 83           |
| Legendre polynomials . . . . .             | 93           |
| Legendre transforms . . . . .              | 83, 92, 93   |
| level of free convection . . . . .         | 65           |
| Level of Free Sinking . . . . .            | 62           |
| liquid phase . . . . .                     | 71           |
| liquid water . . . . .                     | 60           |
| LOCATE . . . . .                           | 163          |
| low-level drag . . . . .                   | 57           |
| low-level wave stress . . . . .            | 56           |
| LTD . . . . .                              | 103          |
| LTI . . . . .                              | 95, 103, 110 |

**M**

|  |                                  |
|--|----------------------------------|
| MAKESD . . . . .                       | 83                               |
| mass detrainment . . . . .             | 60, 61                           |
| mass entrainment . . . . .             | 60, 61                           |
| mass flux . . . . .                    | 59                               |
| mass flux scheme . . . . .             | 35                               |
| melting of snow . . . . .              | 67                               |
| memory buffer . . . . .                | 103                              |
| memory manager . . . . .               | 83, 163, 166                     |
| meridional derivatives . . . . .       | 94                               |
| mesoscale circulation . . . . .        | 65                               |
| midlevel convection . . . . .          | 59, 61, 65                       |
| mixing length approach . . . . .       | 52                               |
| moist convection . . . . .             | 83                               |
| moist static energy . . . . .          | 66                               |
| moisture . . . . .                     | 6, 8, 13, 20, 23, 24, 43, 60, 62 |
| moisture budget equation . . . . .     | 59                               |
| moisture convergence . . . . .         | 35, 71                           |
| momentum . . . . .                     | 6, 7, 35, 43, 44, 51, 60         |
| momentum budget equation . . . . .     | 59                               |
| momentum flux . . . . .                | 139                              |
| momentum flux at the surface . . . . . | 45                               |
| momentum transport . . . . .           | 56, 59                           |

|   |    |
|---|----|
| Monin-Obukhov similarity theory . . . . . | 48 |
| multiple scattering . . . . .             | 35 |

**N**

|                                   |    |
|-----------------------------------|----|
| nonprecipitating cumuli . . . . . | 60 |
|-----------------------------------|----|

**O**

|                               |       |
|-------------------------------|-------|
| Obukhov length . . . . .      | 48    |
| optical thickness . . . . .   | 38    |
| orography . . . . .           | 1, 56 |
| OUTGP . . . . .               | 110   |
| OUTGPI . . . . .              | 110   |
| OUTSP . . . . .               | 110   |
| overshooting cumuli . . . . . | 65    |
| ozone . . . . .               | 40    |

**P**

|   |                    |
|---|--------------------|
| penetrative convection . . . . .              | 59, 61, 63, 66, 71 |
| pentagonal truncation . . . . .               | 11                 |
| PGRAD . . . . .                               | 93                 |
| phase changes . . . . .                       | 133                |
| Photosynthetically Active Radiation . . . . . | 46                 |
| PHYSC . . . . .                               | 83, 93, 103        |
| PHYSCTL . . . . .                             | 118                |
| Planck function . . . . .                     | 37                 |
| planetary boundary layer . . . . .            | 3, 54              |
| POINTER statement . . . . .                   | 166                |
| polar regions . . . . .                       | 15                 |
| POSTCTL . . . . .                             | 119                |
| postprocessing routines . . . . .             | 120                |
| potential energy . . . . .                    | 20                 |
| precipitating clouds . . . . .                | 68                 |
| precipitation . . . . .                       | 59                 |
| precipitation flux density . . . . .          | 74                 |
| precipitation formation . . . . .             | 72                 |
| PRERAD . . . . .                              | 90, 92             |
| PRES . . . . .                                | 93                 |
| pressure gradient . . . . .                   | 20                 |
| Product truncation . . . . .                  | 12                 |

**R**

|                                       |        |
|---------------------------------------|--------|
| RADCTL . . . . .                      | 119    |
| RADHEAT . . . . .                     | 90     |
| radiation . . . . .                   | 2, 8   |
| radiation scheme . . . . .            | 90     |
| radiative heating rate . . . . .      | 36, 83 |
| radiative tendency . . . . .          | 44     |
| radiative transfer equation . . . . . | 36     |

|  |         |
|--|---------|
| RADINT . . . . .                       | 90      |
| rain flux . . . . .                    | 59      |
| Rayleigh scattering . . . . .          | 38      |
| reference sea-level pressure . . . . . | 17      |
| relative humidity . . . . .            | 70, 71  |
| RESETP . . . . .                       | 110     |
| RESTART . . . . .                      | 83      |
| Richardson number . . . . .            | 48      |
| roughness length . . . . .             | 1, 54   |
| run control variables . . . . .        | 117     |
| RUNCTL . . . . .                       | 92, 117 |

**S**

|   |                    |
|---|--------------------|
| S2IO . . . . .                              | 110                |
| saturation deficit . . . . .                | 67                 |
| saturation moist static energy . . . . .    | 66                 |
| saturation specific humidity . . . . .      | 45                 |
| scale-selective diffusion . . . . .         | .8                 |
| SCAN1 . . . . .                             | 87, 92, 103, 105   |
| SCAN2 . . . . .                             | 88, 92, 105, 110   |
| scattering . . . . .                        | 37                 |
| scattering coefficient . . . . .            | 38                 |
| SDSCTL . . . . .                            | 83, 117            |
| sea surface temperature . . . . .           | 75                 |
| sea-ice . . . . .                           | .1                 |
| sedimentation of ice crystals . . . . .     | 70                 |
| semi-implicit . . . . .                     | 1, 5, 24, 26       |
| semi-implicit scheme . . . . .              | 23, 26, 29, 93     |
| sensible heat flux at the surface . . . . . | 44                 |
| shallow convection . . . . .                | 59, 61, 64         |
| shallow water equation . . . . .            | 23                 |
| SI1 . . . . .                               | 93, 103            |
| SI2 . . . . .                               | 103                |
| sigma coordinate . . . . .                  | 5, 7, 16           |
| single scattering albedo . . . . .          | 37, 38             |
| skin reservoir water content . . . . .      | 45                 |
| snow cover . . . . .                        | 45                 |
| snow coverage . . . . .                     | 35                 |
| snow flux . . . . .                         | 59                 |
| snow melt . . . . .                         | 78                 |
| snow pack over land . . . . .               | 75                 |
| soil hydrology . . . . .                    | 75, 79             |
| soil layers . . . . .                       | 76                 |
| solar constant . . . . .                    | 42                 |
| solar declination . . . . .                 | 42                 |
| solar spectrum . . . . .                    | 37                 |
| solar zenith angle . . . . .                | 36, 37, 42         |
| spectral coefficients . . . . .             | 10, 13, 24, 28, 92 |

|  |                          |
|--|--------------------------|
| spectral discretization . . . . .            | .5                       |
| spectral fields . . . . .                    | 112                      |
| spectral kinetic energy . . . . .            | 31                       |
| spectral model . . . . .                     | 13, 104                  |
| spectral space . . . . .                     | 83, 92, 103              |
| spectral tendencies . . . . .                | 13                       |
| spectral transform . . . . .                 | .1                       |
| spectral truncation . . . . .                | 14                       |
| spherical harmonics . . . . .                | 5, 9                     |
| SST . . . . .                                | .1                       |
| stability parameter . . . . .                | 48                       |
| START . . . . .                              | 83                       |
| STEPON . . . . .                             | 83, 86                   |
| stomatal resistance of the canopy . . . . .  | 46                       |
| stratiform precipitation . . . . .           | 67, 83                   |
| stratosphere . . . . .                       | .5                       |
| streamfunction . . . . .                     | .8                       |
| subcloud layer . . . . .                     | 59, 61, 63               |
| sub-grid scale cloud formation . . . . .     | 70                       |
| sub-grid scale orographic variance . . . . . | 56                       |
| sub-grid scale transport . . . . .           | 70                       |
| surface flux . . . . .                       | 35                       |
| surface fluxes . . . . .                     | 45                       |
| surface geopotential . . . . .               | .9                       |
| surface parameterization . . . . .           | 75                       |
| surface pressure . . . . .                   | 1, 7, 16, 23, 26, 93, 96 |
| surface runoff . . . . .                     | 80                       |
| surface-pressure tendency . . . . .          | 19                       |

**T**

|                                  |                            |
|----------------------------------|----------------------------|
| T106 . . . . .                   | 92, 150                    |
| T21 . . . . .                    | 29, 31, 147                |
| T42 . . . . .                    | 1, 29, 31, 148             |
| T63 . . . . .                    | 149                        |
| temperature . . . . .            | .1, 13, 23, 26, 29, 93, 96 |
| temperature inversion . . . . .  | 65                         |
| terrestrial spectrum . . . . .   | 37                         |
| Tetens formula . . . . .         | 71                         |
| thermodynamic . . . . .          | .6                         |
| thermodynamic equation . . . . . | 136                        |
| time filter . . . . .            | 24                         |
| timestep . . . . .               | 24                         |
| time-step criterion . . . . .    | 23                         |
| total energy . . . . .           | 21                         |
| trade wind cumuli . . . . .      | 61, 64                     |
| transmissivity . . . . .         | 36                         |
| triangular truncation . . . . .  | .1, 11, 15                 |
| tropical convection . . . . .    | 63                         |

|   |    |
|---|----|
| tropical cyclones . . . . .                   | 65 |
| tropical thunder clouds . . . . .             | 61 |
| turbulent exchange . . . . .                  | 43 |
| turbulent transport . . . . .                 | 63 |
| two scan spectral space computation . . . . . | 83 |
| two scan structure . . . . .                  | 86 |
| two-stream approximation . . . . .            | 36 |

**U**

|                                       |          |
|---------------------------------------|----------|
| unimodal cloud distribution . . . . . | 64       |
| UNLOC . . . . .                       | 163, 166 |
| update library . . . . .              | 107      |
| updraft . . . . .                     | 59       |
| US Navy . . . . .                     | 1        |
| US Navy dataset . . . . .             | 56       |

**V**

|   |                                 |
|---|---------------------------------|
| vegetation . . . . .                        | 1                               |
| vegetation ratio . . . . .                  | 46, 55                          |
| velocity equation . . . . .                 | 135                             |
| velocity potential . . . . .                | 8                               |
| vertical advection . . . . .                | 20                              |
| vertical diffusion . . . . .                | 43, 52, 83                      |
| vertical finite difference scheme . . . . . | 5                               |
| vertical fluxes . . . . .                   | 7                               |
| vertical stress profile . . . . .           | 57                              |
| vertical velocity . . . . .                 | 6                               |
| vertical-coordinate parameters . . . . .    | 17                              |
| virtual static energy . . . . .             | 67                              |
| virtual temperature . . . . .               | 7                               |
| vorticity . . . . .                         | 1, 5, 8, 14, 23, 25, 29, 84, 93 |

**W**

|   |          |
|---|----------|
| water stress factor . . . . .           | 47       |
| water vapour . . . . .                  | 1, 6, 70 |
| wave momentum flux divergence . . . . . | 56       |
| wave Richardson number . . . . .        | 3, 58    |
| wave-CISK mechanism . . . . .           | 65       |

**Z**

|                                    |    |
|------------------------------------|----|
| zero heat flux condition . . . . . | 76 |
| zero-buoyancy level . . . . .      | 64 |
| zonal advection . . . . .          | 23 |
| zonal derivative . . . . .         | 93 |
| zonal velocity . . . . .           | 24 |
| zonal wave number . . . . .        | 15 |